

ICPAC MONGOLIA



<https://icpacmongolia2024.org/>

HOLIDAY INN ULAANBAATAR & CONFERENCE CENTER

28 Aug – 1 Sept 2024

International Congress on Pure & Applied Chemistry Ulaanbaatar, Mongolia

Book of Abstracts



“Promoting Excellence in Chemical Research and Innovation”



Organized by:



Institut Kimia Malaysia

In Collaboration with:



Mongolian Chemical Society

ACC

Asia Chem Corporation, Japan

ICPAC MONGOLIA 2024 ORGANIZING COMMITTEE

Datuk ChM Dr. Soon Ting Kueh (Chairman)	<i>President, Institut Kimia Malaysia</i>
Prof Dr Avid Budeebazar (Co-Chair)	<i>President, Mongolian Chemical Society</i>
ChM Dr. Yang Farina Abdul Aziz	<i>Institut Kimia Malaysia</i>
ChM Chang Hon Fong	<i>Institut Kimia Malaysia</i>
ChM Dr. Malarvili Ramalingam	<i>Institut Kimia Malaysia</i>
Prof. ChM Dr. Juan Joon Ching	<i>Institut Kimia Malaysia</i>
DCP(R) Dato' ChM Dr. Yew Chong Hooi	<i>Institut Kimia Malaysia</i>

INSTITUT KIMIA MALAYSIA COUNCIL 2024/2025

<i>President</i>	Datuk ChM Dr Soon Ting Kueh
<i>Vice President</i>	ChM Dr Yang Farina binti Abdul Aziz
<i>Registrar</i>	ChM Marhayani binti Md. Saad
<i>Hon. Secretary</i>	ChM Chang Hon Fong
<i>Hon. Treasurer</i>	ChM Dr Malarvili Ramalingam
<i>Hon. Asst. Secretary</i>	Prof. ChM Dr Juan Joon Ching
<i>Hon. Asst. Treasurer</i>	DCP(R) Assoc. Prof. Dato' ChM Dr Yew Chong Hooi
<i>Council Members</i>	Datin ChM Dr Zuriati Zakaria, Dato' ChM Dr Hj Mas Rosemal Hakim bin Mas Haris, ChM Dr Li Hui Ling, Asst. Prof ChM Dr Yvonne Choo Shuen Lann, ChM Dr. Lee Yook Heng, ChM Ts Damien Khoo Yiyuan, Academician ChM Dr Ho Chee Cheong, Prof ChM Dr Rusli Daik, ChM Dr Nurul Huda binti Abd Karim
<i>Co-opted Members</i>	Prof. ChM Dr. Phang Sook Wai, Assoc. Prof. ChM Dr. Fatimah Salim
<i>Co-opted Members - Chairperson of IKM Branches</i>	Northern branch – Dato' ChM Dr Hj Mas Rosemal Hakim bin Mas Haris Southern branch – ChM Yap Fei Ching Sarawak branch – Prof ChM Dr Sim Siong Fong Sabah & FT Labuan branch – ChM Dr Jenny Lee Nyuk Len Perak branch – Asst Prof ChM Dr Wong Lai Peng Terengganu branch – ChM Teo Chook Kiong Pahang branch – Assoc Prof ChM Dr Awis Sukarni bin Mohmad Sabere

INSTITUT KIMIA MALAYSIA

127B, Jalan Aminuddin Baki, Taman Tun Dr Ismail, 60000 Kuala Lumpur, MALAYSIA
Email: ikmhq@ikm.org.my Website: <https://ikm.org.my/>
Phone: +603-77283272 / +603-77283858 / +603-77269029

The Abstracts

All abstracts printed in this Book of Abstracts were produced directly from the soft copies submitted by the authors, some with some minor editorial amendments. Although all efforts were made to ensure the accuracy and correctness of the abstracts, Institut Kimia Malaysia, as the Publisher, will not be responsible or liable for any unintentional errors made during the publication of this book.

Datuk ChM Dr Soon Ting Kueh

on behalf of the ICPAC Mongolia 2024 Organising Committee

Date : 15 August 2024

Solvation Environment of solute molecules dissolved in a single levitated microdroplet revealed by fluorescence microscopy

Kenji Sakota*

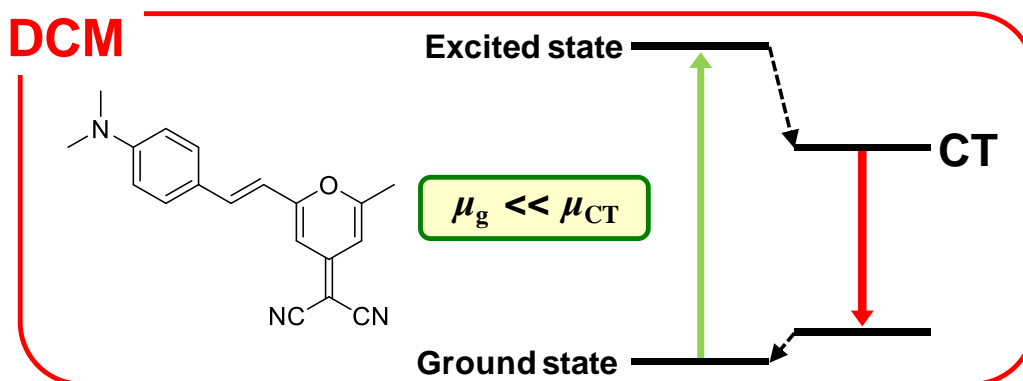
Department of Chemistry, Faculty of Science, Osaka Metropolitan University, Japan

*Corresponding author: sakota@omu.ac.jp

Abstract

Numerous reports indicate that chemical reactions proceeding in microdroplets occur several orders of magnitude faster than in bulk solutions[1]. When solute molecules involved in the reaction are preferentially localized at the droplet surface, they are only partially solvated by solvent molecules. If the reaction barrier decreases due to the partial solvation of solute molecules localized at the surface, it is expected that in microdroplets, where the surface area to volume ratio is large, the reduction in the reaction barrier due to partial solvation and the associated increase in reaction rate become more pronounced. Most previous studies have evaluated the reactivity within droplets by introducing numerous droplets into a mass spectrometer and detecting the final reaction products. However, using mass spectrometry alone cannot elucidate the solvation environment of solute molecules dissolved in microdroplets, and it remains unclear whether solute molecules are partially solvated within these droplets. In this study, we compared the fluorescence spectra of solute molecules dissolved in a single levitated microdroplet and in bulk solutions to investigate the solvation environment of solute molecules in a single microdroplet. We focused on DCM and Rhodamine B (RhB) as solute molecules. Compared to bulk solutions, the fluorescence spectra of DCM dissolved in a droplet showed a blue shift. This blue shift can be attributed to the partial solvation of DCM at the droplet surface. In contrast, no such blue shift was observed for RhB. The difference between DCM and RhB may be due to the difference in the magnitude of the electric dipole moment in the electronic excited state.

Keywords: microdroplet, partial solvation, fluorescence microscopy, reaction acceleration



References

1. Wei, Z.; Li, Y.; Cooks, G.; Yan, X. *Annu. Rev. Phys. Chem.* 2020, 71, 31-51.

UREA REMOVAL FROM AQUEOUS SOLUTION BY ADSORPTION ON ALKALINE SLUDGE FROM SOLAR PHOTOVOLTAIC INDUSTRY

Nur Hidayah Deeleanie^a, Nur Imanina Farhana Japar^b, Azizul Hakim Lahuri^{c,*}, Syawal Mohd Yusof^d, Siti Sarahah Sulhadi^e, Ainil Hafiza Abdul Aziz^f, Mohd Azlan Kassim^g,
^{a,b,c,d,e,f}*Department of Science and Technology, Universiti Putra Malaysia Bintulu Campus, Nyabau Road, P.O. Box 396, 97008 Bintulu, Sarawak, Malaysia.*

^g*Research Centre for Carbon Dioxide Capture and Utilisation (CCDCU), School of Engineering and Technology, Sunway University, No. 5 Jalan Universiti, Bandar Sunway, 47500 Petaling Jaya, Selangor, Malaysia.*

**Corresponding author: azizulhakim@upm.edu.my*

Abstract

This study focuses on addressing environmental concerns arising from the growth of the agricultural sector, especially those related to the inadequate treatment of wastewater from agricultural effluent. Urea is a prevalent component in agricultural wastewater due to its widespread use as a fertilizer, contributing to issues related to nutrient runoff. The imperative to advance waste reduction through the principles of reusability and sustainability is a pivotal endeavor in the modern industrial landscape. The primary objective is to explore the utilization of industrial solid waste as an adsorbent for the removal of urea from an aqueous solution with parameters including initial concentration, adsorbent dosage, temperature and adsorption time. The alkaline sludge was obtained from the solar photovoltaic industry. The standard urea aqueous solution was prepared to obtain the standard curve. Ultraviolet-Visible (UV-Vis) spectrometer was used to analyze the urea aqueous solution. The study's findings indicate that the most efficient adsorbent for urea removal is calcined alkaline sludge at 900°C (CAS), using initial urea concentration of 30 mg/L, an adsorbent loading of 0.2 g, a temperature of 40°C and an adsorption period of 6 hours. These parameters exhibited that the removal percentage of CAS was 82.50% while the removal efficiency was 4.95 mg/g. A slightly higher adsorption temperature of 40°C increases kinetic energy of the molecules within the adsorption systems. This research presents a sustainable and practical solution to address the challenges associated with agricultural wastewater management.

Keywords: Adsorption, agricultural wastewater, solid sorbent, solid waste, urea

References

1. El-Lateef, H. M. A.; Al-Omair, M. A.; Touny, A. H.; Saleh, M. M. *J. Environ. Chem. Eng.* 2019, 7, 102939.
2. Kurniawati, D.; Bahrizal, Sari, T. K.; Adella, F.; Salmariza, S. *J. Phys. Conf. Ser.* 2021, 1788, 012008.
3. Pillai, M. G., Simha, P.; Gugalia, A. *J. Environ. Chem. Eng.* 2014, 2, 46-55.
4. Pirzadeh, B. *Physical Wastewater Treatment in Wastewater Treatment. Intechopen.* 2022. 104324.

DEVELOPMENT OF PHOTOCATALYSTS FOR ENVIRONMENTAL WATER PURIFICATION BY HIGH-THROUGHPUT EXPERIMENTATION

Kyo Yanagiyama^a, Toshiaki Taniike^{a*}

^aJapan Advanced Institute of Science and Technology

*Corresponding author: taniike@jaist.ac.jp

Abstract

Photocatalysis has emerged as a promising method for achieving water purification through the complete mineralization of organic pollutants using sustainable solar energy.¹ However, for practical applications, it is essential to consider not only photocatalysts but also various contaminants in environmental water.² High-throughput experimentation is a promising technique for screening the vast search space created by multiple factors such as photocatalysts, pollutants, and operating environments. We have developed a high-throughput screening instrument for photocatalytic water purification, enabling the simultaneous testing of 132 photocatalytic reactions under uniform visible light irradiation, temperature control, and stirring (Figure 1A).³ Using this instrument, the impact of photocatalysts (TiO₂, ZnO, α -Fe₂O₃) and environmental water (seawater, urban wastewater, industrial wastewater) on dye (methylene blue, methyl orange, congo red, rhodamine B) degradation was investigated. The photocatalytic activities were reduced in environmental water compared to pure water due to the inhibition of adsorption by environmental ions such as carbonate and phosphate. In addition, to develop catalysts with high activity in environmental water, metal nanoparticles were supported. The results showed that Au and Pt enhanced activity in both of pure and environmental water (Figure 1B).

Keywords: photocatalysis, high-throughput screening, water purification, environmental water

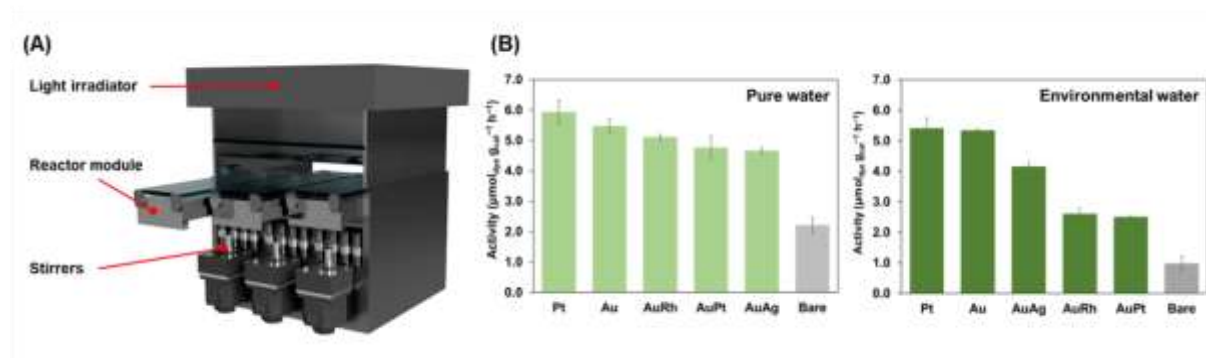


Figure 1. A) Developed high-throughput instrument and B) the photocatalytic activity of top 5 metal modified catalysts.

Acknowledgement: This work is supported by JST-Mirai Program (JPMJMI22G4). The work of K.Y. is supported by JST SPRING (JPMJSP2102).

References

1. Konstantinou, I. K.; Albanis, T. A. *Appl. Catal. B*, **2004**, *49*, 1–14.
2. Joorabi, F. T.; Kamali, M.; Sheibani, S. *Mater. Sci. Semicond. Process.*, **2022**, *139*, 106335.
3. Yanagiyama, K.; Takimoto, K.; Le, S. D.; Ton, N. N. T.; Taniike, T. *Environ. Pollut.*, **2024**, *342*, 122974.

Evaluation of soil quality in the industrial area and reduce of copper polluted soil by electrokinetic remediation

Bolormaa Oyuntsetseg^{1*}, Jajinjav Yondonjamts¹, Ochirkhuyag Bayanjargal³

¹Department of Chemistry, School of Arts and Sciences, National University of Mongolia, 14201 Ulaanbaatar, Mongolia

²Department of Chemical and Biological Engineering, School of Engineering and Applied Sciences, National University of Mongolia, 14201, Ulaanbaatar Mongolia

**Corresponding author email: bolormaa@num.edu.mn*

Abstract

The soil contamination mostly caused by urban activities such as traffic, waste disposal, and mining industries. The aims of this research are to investigate the contents of the selected heavy metals including Cu in topsoil of the residential, industrial, tailing dam and control area in Erdenet, Mongolia and to evaluate their chemical speciation using sequential extraction, and then finally to reduce heavy metal contents from contaminated industrial soil using the electrokinetic (EK) remediation.

Fifteen soil samples were collected from the Erdenet mining area in winter, spring, summer, and fall. The heavy metals removal from the obtained soil samples were conducted by EK remediation with electrolytic solution of sodium chloride.

Cu, As, and Mo concentrations in soil samples of the industrial area were higher than Mongolian Soil Quality Standards, while the concentrations of Pb and Zn were lower than the standard. The optimal conditions of EK remediation were at 15 V for 156 hours in electrolytic solution and reactor with an anolyte and a catholyte chamber. The copper content of topsoil sample was decreased about 90%.

Keywords: electrokinetic remediation, mining, topsoil, industry, sequential extraction

Decontamination - Standardize Procedure and Environmental Protection

M Hisham Ibrahim^{a,*}, Norzaimi Azam^a, M Zakaria Osman^a,

^aGroup Technical Solution, Petronas.

*Corresponding author: hishamc@petronas.com.my

Abstract

The "Development and Establishment of Sustainable Decontamination Chemical" initiative leverages the Technology Challenge and Strategic technological collaborations to enhance decontamination processes within the organization. This project aligns with company vision, aiming to foster innovation and sustainability. The initiative seeks to explore and expand new technological ventures, addressing the company's decontamination needs more effectively while optimizing on third-party services. A critical issue faced by the organization is the non-standardization of decontamination procedures and chemical testing. Currently, the lack of standardized protocols results in inconsistent outcomes and inefficiencies in decontamination activities. By standardizing these procedures, we aim to streamline operations, ensuring consistent and effective decontamination across all operational units. This standardization also involves rigorous testing and validation of chemicals to ensure their efficacy and safety, contributing to overall process optimization. This initiative addresses several key pain points encountered during decontamination services. Firstly, the ineffectiveness of existing chemicals often prolongs decontamination activities, adversely impacting Plant Mechanical days and operational efficiency. Additionally, the absence of decontamination procedures for various process units poses significant operational challenges. Particularly concerning is the environmental impact of high Chemical Oxygen Demand (COD) levels in waste disposal, which necessitates additional, often costly, wastewater treatment activities in Effluent Treatment Plants (ETPs). Innovative solutions are thus essential. The initiative aims to develop biodegradable chemicals that facilitate the proper separation of emulsions and water layers, enabling direct disposal without further treatment. This innovation not only reduces environmental impact but also cuts down on unnecessary wastewater treatment costs. Furthermore, the project seeks to minimize operational disruptions, such as foaming at the Acid Gas Removal Unit (AGRU), by addressing chemical and material incompatibilities through comprehensive blending studies. These studies will explore the impact of various factors, including foaming agent reduction, chemical introduction pressure, and nitrogen (N₂) blinding procedures. By addressing these multifaceted challenges, the initiative aims to provide a comprehensive, environmentally sustainable solution for decontamination services within the organization. This will enhance operational efficiency, reduce environmental impact, and achieve significant cost savings, ultimately supporting organization strategic goals.

Keywords: Insert maximum of 5 keywords

Sustainability

Decontamination

Chemical Oxygen Demand

Graphic / Image (Optional)

Size Effect of Pt Cocatalysts on Carbon Nitride for Photocatalytic Hydrogen Evolution

Yuki Yamamazaki^a, Yuki Tomoyasu^a, Tokuhisa Kawawaki^a,

Kenji Yamazaki^b, Akira Yamakata^c, Yuichi Negishi^{a,d,*},

^a Graduate School of Science, Tokyo University of Science, Japan

^b Division of Applied Physics, Faculty of Engineering, Hokkaido University, Japan

^c Graduate School of Natural Science and Technology, Okayama University, Japan

^d Institute of Multidisciplinary Research for Advanced Materials, Tohoku University, Japan

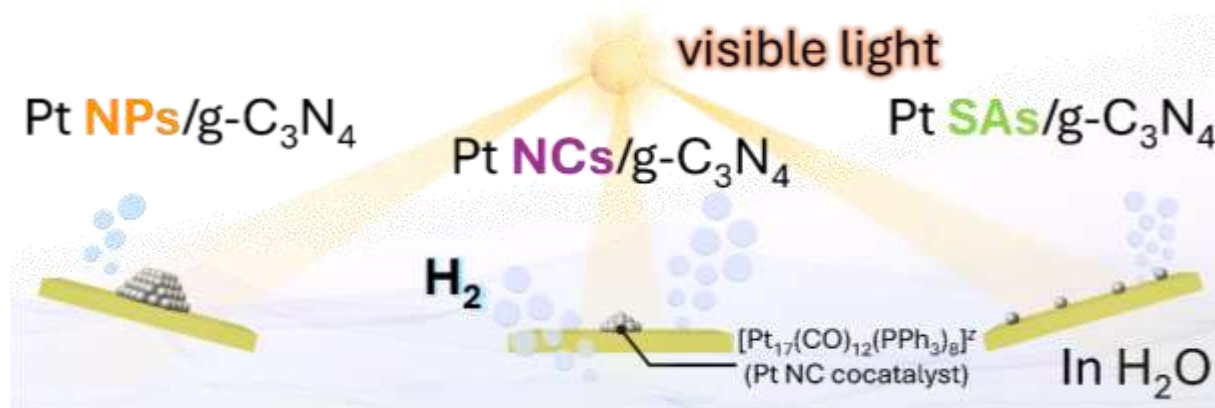
*Corresponding author: yuichi.negishi.a8@tohoku.ac.jp

Abstract

Hydrogen (H₂) is expected to be a clean energy source in a sustainable society. Water-splitting photocatalysts that can produce H₂ from water and sunlight are attracting attention.¹ In recent years, the enhancement of H₂-evolution reaction (HER) efficiency has been reported by loading the metal nanoparticles (NPs), nanoclusters (NCs), and single-atoms (SAs) on photocatalyst.^{2,3}

In this study, we aimed to find the optimal size of platinum (Pt) cocatalyst, which is the effective metal species for water-splitting HER. We loaded Pt NPs, NCs, and SAs on graphitic carbon-nitride (g-C₃N₄) photocatalyst, respectively, and evaluated their photocatalytic HER activity. As a result, Pt NCs showed ~1.7 and ~2.5 times higher H₂ evolution rates than Pt SAs and Pt NPs, respectively. The reasons for this result are assumed to be that 1) the increase in the ratio of surface atoms enhances HER activity and 2) the discretization of the electronic state in Pt promotes a decrease in HER activity. Therefore, we clarified that Pt NCs is a highly active HER cocatalyst for photocatalytic HER, because Pt NCs have a metallic electronic state and fine particle size.⁴

Keywords: water-splitting photocatalyst, size effect, cocatalyst, metal nanocluster, single atom



References

1. Kawawaki, T.; Mori, Y.; Wakamatsu, K.; Ozaki, S.; Kawachi, M.; Hossain, S.; Negishi, Y. *J. Mater. Chem. A* 2020, 8, 16081-16113.
2. Yazaki, D.; Kawawaki, T.; Hirayama, D.; Kawachi, M.; Kosaku, K.; Oguchi, S.; Yamaguchi, Y.; Kikkawa, S.; Ueki, Y.; Hossain, S.; Osborn, D. J.; Ozaki, F.; Tanaka, S.; Yoshinobu, J.; Metha, Gregory. F.; Yamazoe, S.; Kudo, A.; Yamakata, A.; Negishi, Y. *Small* 2023, 19, 2208287.
3. Akinaga, Y.; Kawawaki, T.; Kameko, H.; Yamazaki, Y.; Yamazaki, K.; Nakayasu, Y.; Kato, K.; Tanaka, Y.; Hanindriyo, A. T.; Takagi, M.; Shimazaki, T.; Tachikawa, M.; Yamakata, A.; Negishi, Y. *Adv. Funct. Mater.* 2023, 33, 2303321.
4. Yamazaki, Y.; Tomoyasu, Y.; Kawawaki, T.; Negishi, Y. *in preparation*.

Effects of Cellular Exposure to Atmospheric Dust on the Suppression of Exosome Secretion

Daisuke Onoshima

Institutes of Innovation for Future Society, Nagoya University, Japan

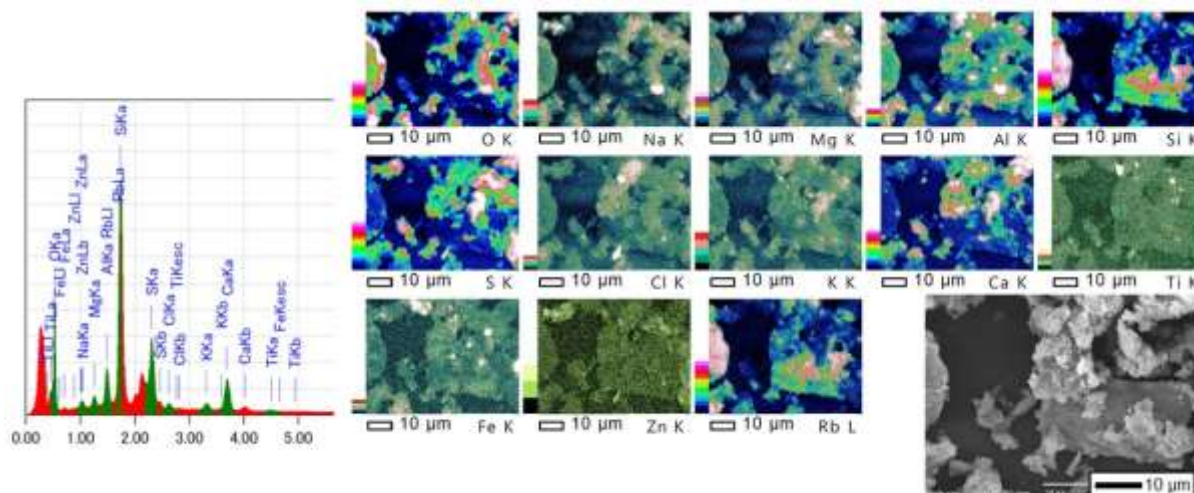
**Corresponding author: onoshima-d@nanobio.nagoya-u.ac.jp*

Abstract

Particulate matter (PM) poses a health hazard to the respiratory tract and other organs as a carcinogen. For example, the accelerating effect of PM_{2.5} on cancer formation has been reported [1]. Transition metals in PM cause oxidative stress to living organisms [2]. This oxidative stress may inhibit the secretion of extracellular vesicles. In the present study, the secretion of exosomes and intracellular ROS were measured by cellular exposure to atmospheric dust in the analysis of tumor promotion processes.

Urban air dust collected in the St Louis area of Missouri, USA, was used to measure exosome secretion following administration to lung cancer cells A549. Luciferase Nano-Luc luminescence measurements were used for the secretion experiments. Oxidative stress was also detected using cell-permeable fluorescent probes. Changes in the fluorescence intensity of the fluorescent probe were used to measure intracellular ROS. Atmospheric dust components were analyzed by SEM-EDS. Exosome secretion was reduced by about 40% with the use of 20 µg/mL of atmospheric dust. Cell numbers did not change significantly. Intracellular ROS levels increased with the administration of atmospheric dust. Polystyrene latex particles functioned successfully as a negative control, suggesting that dust components containing Fe and Mn had an inhibitory effect on exosome secretion. As a result, the correlation between exosome secretion and oxidative stress was successfully analyzed. In the future, we will measure intracellular pH and MVB to further investigate the mechanism of exosome secretion in cancer cells.

Keywords: PM_{2.5}, exosome, cancer cell, ROS, oxidative stress



References

1. Balmain, A. *Nature* 2023, 616, 35-36.
2. Kajino, M.; Hagino, H.; Fujitani Y.; Morikawa, T.; Fukui, T.; Onishi, K.; Okuda T.; Igarashi, Y. *Sci. Rep.* 2021, 11, 6550.

Highly selective single cell introduction system into ICP-AES/MS using cell sorter

Akane Yaida^{a*}, Syu Yamaji^a, Kai Fukuchi^a, Yuya Shimizu^a, Yuki Maemoto^b,
Motohide Aoki^b, Tomonari Umemura^b and Akitoshi Okino^a

^a FIRST, Tokyo Institute of Technology,

^b School of Life Sciences, Tokyo University of Pharmacy and Life Sciences

*Corresponding author: yaida@plasma.es.titech.ac.jp

Abstract

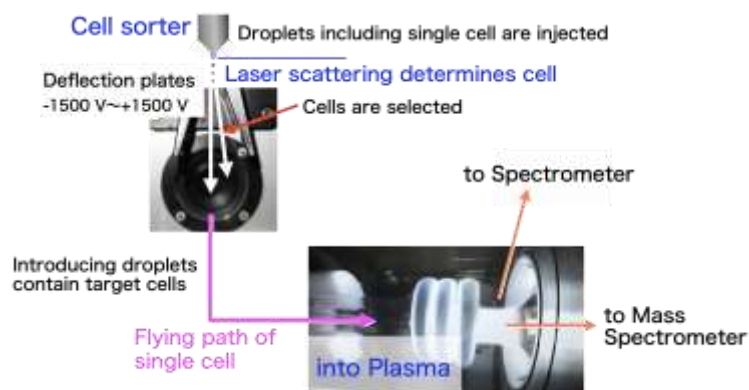
Elemental analysis in single cells is expected to contribute to the progress of various fields, such as regenerative medicine and drug discovery. We have developed a single cell elemental analysis system in which a single cell is continuously introduced into Inductively Coupled Plasma (ICP) devices ¹. However, in a previous system, cells in a cell suspension sample were unselectively introduced. In this study, a highly selective single cell introduction system was developed using flow cytometer with a cell sorter to introduce target cells into an ICP-atomic emission spectrometer (AES)/mass spectrometer (MS).

In this system, cells in cell suspension are injected as micro droplets by a cell sorter (FENIX, Allied Flow) equipped with a laser to measure the presence, size, and type of cells. Each droplet is given a charge ranging from positive to negative depending on the laser measurement result before being injected.

By changing the voltage applied to the droplets from -330 V to +330 V based on the laser measurement results, the droplets were distributed into five different pathways. Of these, only droplets containing the target cells were introduced into the plasma in a straight flight by not providing them a charge. On the other hand, the frequency of droplets ejected by the cell sorter is very fast, about 38 kHz. Since the mass signal from a single cell is about 1 ms, the cell introduction frequency must be less than 1000 Hz to avoid duplication of this signal. If the next target cell was injected at an early timing, to limit the introduction frequency to less than the limit, a non-zero voltage was applied to the droplet to control it from being introduced into the plasma. This introduction timing can be changed by software. As a result, stable introduction of single cells into the plasma was achieved. This setup realizes selective introduction of only target single cells into the ICP-AES/MS.

In the presentation, the details of the function and some data of the highly selective single cell introduction system using a cell sorter will be presented.

Keywords: Single cell analysis, Cell sorter, Sample introduction, ICP-AES, ICP-MS



References

1. Shigeta, K.; Köllensperger, G.; Rampler, E.; Traub, H.; Rottmann, L.; Panne, U.; Okino, A.; Jakubowski, N. *J. Anal. At. Spectrom.*, 2013, 28, 637-645.

SPECTROPHOTOMETRY OF NANOPARTICLES BY USING POLARIZED LIGHTS

Hitoshi Watarai

R3 Institute for Newly-Emerging Science Design, Osaka University, Toyonaka, Japan

*Corresponding author: watarai@chem.sci.osaka-u.ac.jp

Abstract

Linear dichroism (LD) is observed as the difference between the absorbances for a horizontally polarized light (H) and a vertically polarized light (V), $LD = A(H) - A(V)$. Recently, the powerful analytical potential of the LD spectra was demonstrated for the detection of the critical aggregation concentration of iron oxide magnetic nanoparticles (MNPs) in water in the presence of metal ions and surfactants.¹ When a magnetic field less than 40 mT was applied with a Voigt configuration (horizontally) to a quartz cell containing MNPs, the LD spectrum was observed clearly showing a broad maximum at around 350 nm. This phenomenon is called the magnetic orientational linear dichroism (MOLD) of the magnetic nanoparticles. On the other hand, circular dichroism (CD) can be observed as the difference between the absorbances for a left-circularly polarized light (R) and a right-circularly polarized light (L), $CD = A(L) - A(R)$. The CD can be observed for any molecules having asymmetric carbon atoms and has been widely used for the identification of the structure and conformation of the chiral molecules in isotropic samples. Chiral molecule-induced CD (ICD) of achiral dye molecules has also been used for a sensitive analytical method.² In this talk, some new applications of LD and CD spectrometry will be presented for the liquid and film samples containing MNPs^{3,4} and cellulose nanofibers (CNF). The most interesting result, which shows the high sensitivity of the LD method, will be the detection of the geomagnetic orientation of MNPs by using LD spectrometry. The magnetic orientation of MNPs by a very weak geomagnetic field of 36 μ T could be observed in a dried film sample containing MNPs (Fig. 1).

Keywords: Linear dichroism, circular dichroism, magnetic nanoparticles, geomagnetic field, cellulose nanofibers

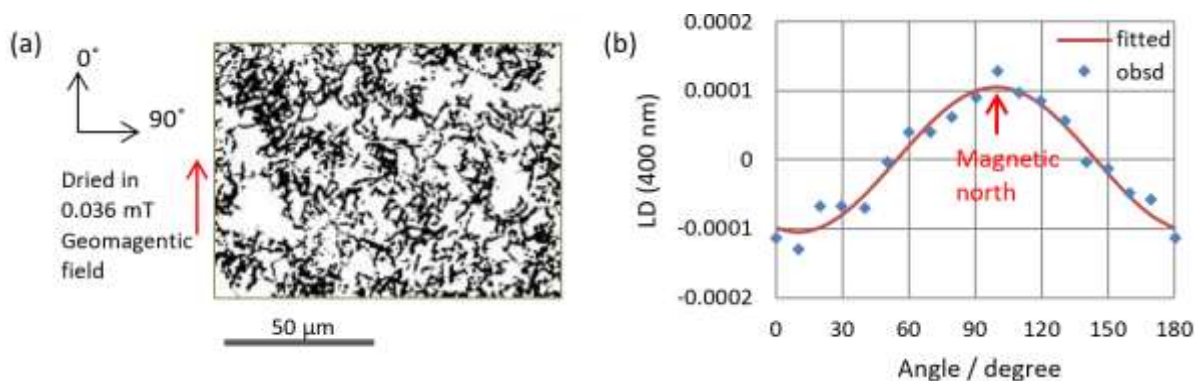


Fig. 1 (a) Microscope image of the dried film under the geomagnetic field shown by the binary mode. (b) Angle dependence of the LD values of the dried film; 0.016 wt% MNPs, 0.001M TX-100, 0.001M HCl in 200 μ L.

1. Watarai, H.; Sakurai, S. S. M. *Langmuir* **2020**, *36*, 12414-12422.
2. Watanabe, S.; Watarai, H. *Bull. Chem. Soc. Jpn.* **2015**, *88*, 955-962.
3. Watarai, H.; Takechi, H. *J. Phys. Chem. C*, **2023**, *127*, 5479-5490.
4. Watarai, H. *Bull. Chem. Soc. Jpn.* **2024**, *97*, <https://doi.org/10.1093/bulcsj/uoad026>.

Phytochemicals Identification from Rice-Infused *Eleusine Indica* and Their Anti-Inflammatory Effect in RAW 264.7 Cell Through Tandem LCMS Molecular Networking Technique

Fatimah Salim^{a,*}, Zikry Hamizan Md Zakri^b, Monica Suleiman^b, Ibrahim Jantan^c,

^a3Atta-ur-Rahman Institute for Natural Product Discovery (AuRIns), Universiti Teknologi MARA Selangor Branch, Puncak Alam Campus, 42300 Bandar Puncak Alam, Selangor, Malaysia; Faculty of Applied Sciences, Universiti Teknologi MARA, 40450 Shah Alam, Selangor, Malaysia.

^b Institute for Tropical Biology and Conservation, Universiti Malaysia Sabah, 88400 Kota Kinabalu, Sabah, Malaysia.

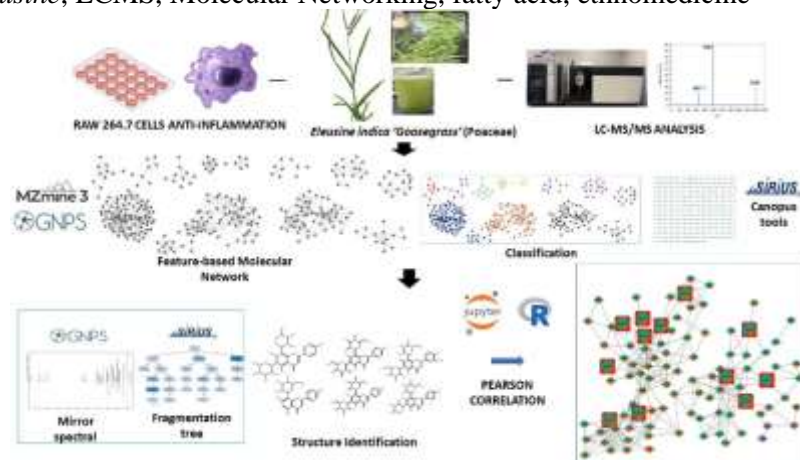
^c Institute of Systems Biology (INBIOSIS), Universiti Kebangsaan Malaysia, 43600 Bangi, Selangor, Malaysia.

*Corresponding author: fatimah2940@uitm.edu.my

Abstract

Eleusine indica (Poaceae) is a perennial herb, locally known as ‘rumput sambau’. The aerial part of the plant infused with rice has been used traditionally by the local people of Kadazandusun in Sabah to treat flu-related ailments such as inflammation. However, no scientific study has been done to support this claim. This study aims to unravel the anti-inflammatory potential of the phytochemicals in the aerial aqueous extracts of *E. indica* with and without rice infusion to justify the traditional practice. The anti-inflammatory activity was evaluated through nitric oxide (NO) production inhibition in RAW 264.7 macrophage cells. While, the chemical compositions of the extracts, their variation, and their correlation with the activities were determined through tandem LCMS molecular networking data analyses. The IC₅₀ value of NO production for infused plant extract ($90.875 \pm 1.215 \mu\text{g/mL}$) was lower than plant extract ($179.15 \pm 14.05 \mu\text{g/mL}$) and rice extract ($150.5 \pm 3.0 \mu\text{g/mL}$). A total of 112 phytochemicals were identified through the molecular networking technique from 11 clusters of phytochemicals' classes of flavonoids, terpenoids, amino acid and its derivative, glucose derivatives, phenyl glucoside, fatty acid and its derivative, carbohydrate and its derivatives, and purine. Off the identified compound, 106 were first time reported from this species. Based on activity labelled molecular networking analysis, the fatty acids, [2-acetyloxy-3-(5-dec-9-enyl-2-oxooxolan-3-yl)propyl] acetate (**11**) and 9,10-dihydroxyoctadec-12-enoic acid (**12**) were correlated with NO production activity. These findings suggested that the aerial aqueous extract of *E. indica* with rice infusion possessed higher anti-inflammatory response which may support the traditional practice.

Keywords: *Eleusine*, LCMS, Molecular Networking, fatty acid, ethnomedicine



References

- Zakri, Z.H.M.; Azman, M.F.S.N.; Suleiman, M.; Rasol, N.E.; Husain, K.; Jantan, I.; Afzan, A.; Yusoff, J.; Salim, F. *MJChem* 2024, 26(1), 74-87.
- Sukor, N.S.M.; Zakri, Z.H.M.; Rasol, N.E.; Salim, F. *Molecules* 2023, 28(7), 3111.
- Zakri, Z.H.M.; Suleiman, M.; Ng, S.Y.; Ngaini, Z.; Maili, S.; Salim, F. *J. Agric. Biotech* 2021, 12(2), 68-87

Polarized High-Energy-Resolution Fluorescence Detected-X-ray Absorption Near-Edge Structure of the LSAT Single Crystal

Hiroyuki Asakura*

Kindai University

*Corresponding author: asakura@apch.kindai.ac.jp

Abstract

XANES measurements using High Energy Resolution Fluorescence Detection (HERFD) for X-rays emitted from elements that absorb X-rays can dramatically improve the energy resolution of the XANES spectra. We performed La L_1 -edge HERFD-XANES measurements on LaAlO_3 and found that La L_1 -edge XANES spectra have higher energy resolution when La $L\beta_3$ or La $L\gamma_3$ fluorescence lines is used compared to the usual transmission method, as shown in Figure 1. Two distinct pre-edge peaks were observed with improved energy resolution, and these peaks were attributed to the dipole transition from the 2s orbital to the 6p orbital and the quadrupole transition to the 6p-5d hybrid orbital, but were unclear.

HERFD-XANES spectra of LSAT ((La,Sr)(Al,Ta) O_3) single-crystal with perovskite structure were measured when they were placed at 45 degrees to the incident X-ray and spectroscopic crystal and rotated in the in-plane direction, and a clear horizontal polarization dependence was observed. The trend of the horizontal polarization dependence of the XANES simulation results with FDMNES is almost consistent with the experimental results. After detailed investigation, we found that the peak around 6270 eV is a quadrupole transition to an unoccupied orbital with dz^2 and dx^2-y^2 components, indicating that HERFD-XANES is a powerful local structure analysis method.

Keywords: X-ray absorption spectroscopy, high energy resolution, local structure, synchrotron

References

- Asakura H.; Konno M.; Kawamura N.; Hosokawa S.; Teramura K.; Tanaka T., *J. Phys. Chem. C*, 2023, 127, 50, 24192-24199.

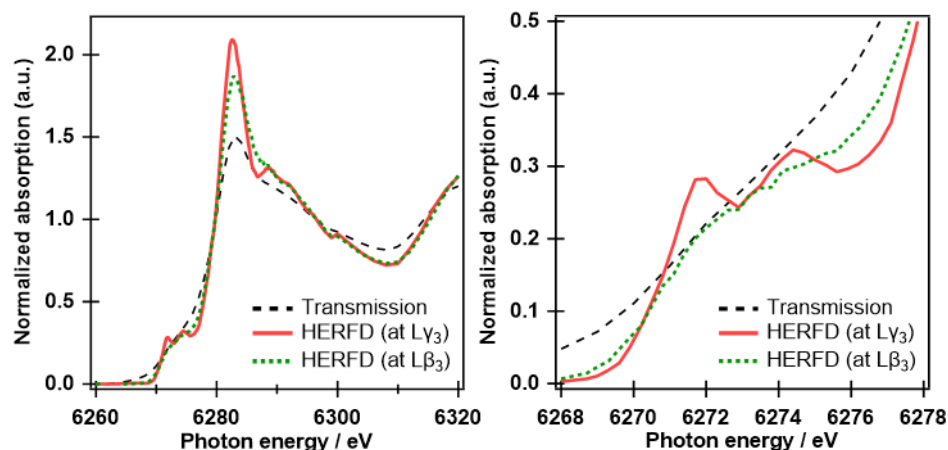


Figure 2 La L_1 -edge (HERFD-)XANES spectra of LaAlO_3

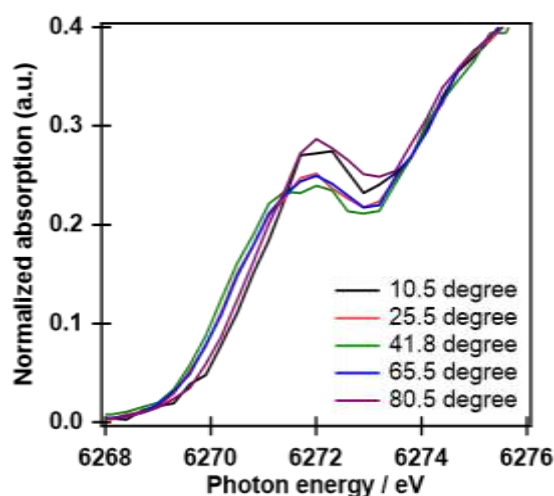


Figure 3 La L_1 -edge polarized HERFD-XANES spectra of LSAT.

Control of Dimensionality and Electron Transfers Based on Cyanide-bridged Metal Complex

Yoshihiro Sekine,^{*ac} Riku Fukushima,^b Shinya Hayami^{ac}

^a Graduate School of Science and Technology, Kumamoto University, Japan

^b Priority Organization for Innovation and Excellence, Kumamoto University, Japan

^c Institute of Industrial Nanomaterials (IINa), Kumamoto University, Japan

*Corresponding author: sekine@kumamoto-u.ac.jp

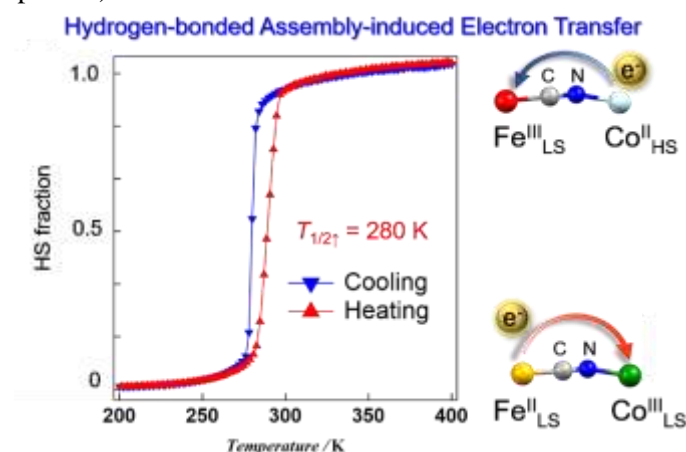
Abstract

The development of switchable metal complexes, such as spin crossover, valence tautomerism, and metal-to metal electron transfers, is an attractive theme in the field of materials science. Numerous metal complexes showing various switching behavior in their electronic, magnetic, optical properties has been reported. Of these, we have recently demonstrated novel tetraoxolene-bridged Fe-based 2-D honeycomb layered systems exhibiting electron transfers between metal ions and bridging ligands.[1,2] The electron transfer behavior in this system is influenced through temperature variation, solvation/desolvation treatment, chemical doping of ligands and pressure application. However, such multi-stable systems are still rare.

We report new stimuli-responsive metal complexes based on cyanide-bridged compounds. Cyano-bridged polynuclear metal complexes, in which multiple metal ions are bridged by cyanide ions (CN⁻), exhibit unique electronic and magnetic properties due to their metal ions. Some cyanide complexes consisting of Co and Fe ions exhibit intramolecular electron transfer coupled spin transition (ETCST), in which the electronic and spin states are significantly changed by external stimuli such as temperatures and light irradiation. In this presentation, we have demonstrated the synthesis of new Co/Fe complex for exploring the external-stimuli-responsive metal complex.

Keywords: Coordination metal complex, stimuli-responsive material, electron transfer, magnetism

Graphical abstract (Optional)



References

1. J. Chen, Y. Sekine, Y. Komatsumaru, S. Hayami, H. Miyasaka, *Angew. Chem. Int. Ed.* 2018, 57, 12043-12047.
2. J. Chen, Y. Sekine, A. Okazawa, H. Sato, W. Kosaka, H. Miyasaka, *Chem. Sci.*, 2020, 11, 3610-3618.

Graphene oxide as a super material

Shinya HAYAMI

Department of Chemistry, Faculty of Advanced science and technology, Kumamoto University

Abstract

Graphene oxide (GO) nanosheets have applications not only in energy devices, but also in environmental and medical applications. This talk will focus on GO nanosheets, which are inexpensive, biocompatible, non-cytotoxic, and have excellent processability and oxidative (degradation) properties and will discuss the development of antiviral materials and their commercialization. In addition, due to the water retention property and cation adsorption of GO, plant growth can be promoted in soil containing GO as a countermeasure for problems such as arid soil and salt damage in barren areas. Furthermore, it can help reduce CO₂ gas emissions based on carbon neutrality.

Keywords: Graphene oxide, Proton conduction, Semi-conductor, Energy devise, Agribio application

References

1. L. I. Ardhayanti, Md. S. Islam, M. Fukuda, Y. Sekine, S. Hayami Thermally stable proton conductivity from nanodiamond oxide, *Chem. Commun.*, 59, 8306-8309 (2023).
2. S. Wakamatsu, Md. S. Islam, Y. Shudo, M. Fukuda, R. Tagawa, N. Goto, M. Koinuma, Y. Sekine, S. Hayami, Efficient oxygen evolution reaction catalyst using Ni-Co layered double hydroxide anchored on reduced graphene oxide, *Energy Adv.*, advance article (2023).
3. Md. S. Islam, M. Fukuda, Md. J. Hossain, N. N. Rabin, R. Tagawa, M. Nagashima, K. Sadamasu, K. Yoshimura, Y. Sekine, T. Ikeda S. Hayami, SARS-CoV-2 suppression depending on the pH of graphene oxide nanosheets, *Nanoscale Adv.*, 5, 2413-2417 (2023).
4. M. A. Rahman, J. Yagy, Md. S. Islam, M. Fukuda, S. Wakamatsu, R. Tagawa, Z. Feng, Y. Sekine, J. Ohyama, S. Hayami, Three-Dimensional Sulfonated Graphene Oxide Proton Exchange Membranes for Fuel Cells, *ACS Appl. Nano Mater.*, 6, 3, 1707-1713 (2023).
5. N. N. Rabin, Md. S. Islam, M. A. Rahman, R. Tagawa, Y. Shudo, Y. Sekine, S. Hayami, Free-standing graphene oxide/oxidized carbon nanotube films with mixed proton and electron conductor properties, *Energy Adv.*, 2, 293-297 (2023).
6. M. A. Rahman, N. N. Rabin, Md. S. Islam, M. Fukuda, J. Yagy, Z. Feng, Y. Sekine, L. F. Lindoy, J. Ohyama, S. Hayami, Synergistic Strengthening in Graphene Oxide and Oxidized Single-walled Carbon Nanotube Hybrid Material for use as Electrolytes in Proton Exchange Membrane Fuel Cells, *Chem. Asian J.*, e202200376 (2022).
7. M. A. Rahman, Md.S. Islam, M.Fukuda, J. Yagy, Z. Feng, Y. Sekine, L. F. Lindoy, J. Ohyama, S. Hayami, High Proton Conductivity of 3D Graphene Oxide Intercalated with Aromatic Sulfonic Acids, *ChemPlusChem*, 87(4), e202200003 (2022).
8. Md.S. Islam, J. Yagy, Y. Sekine, S. Sawa, S. Hayami High water adsorption features of graphene oxide: Potential of graphene oxide-based desert plantation, *Mater. Adv.*, 3(8), 3418-3422 (2022).
9. N. N. Rabin, Md. S. Islam, M. Fukuda, J. Yagy, R. Tagawa, Y. Sekine, S. Hayami, Enhanced mixed proton and electron conductor at room temperature from chemically modified single-wall carbon nanotubes, *RSC. Adv.*, 12(14), 8632-8636 (2022).
10. Y. Shudo, Md. S. Islam, H. Zenno, M. Fukuda, M. Nakaya, N. N. Rabin, Y. Sekine, L. F. Lindoy, S. Hayami, Engineering ferromagnetism in Ni(OH)₂ nanosheets using tunable uniaxial pressure in graphene oxide/reduced graphene oxide, *Phys. Chem. Chem. Phys.*, 23(42), 24233-24238 (2021).

Synthesis and characterization of Pd(II) complex with bis(1-(2-pyridyl)imidazole-2-thione) ligand bridged by diether

Kenji Matsumoto*, Yuya Fujita, Mao Hamada, Takatoshi Kondo, Kei Sato

Faculty of Science and Technology, Kochi University.

*Corresponding author: matsuken@kochi-u.ac.jp

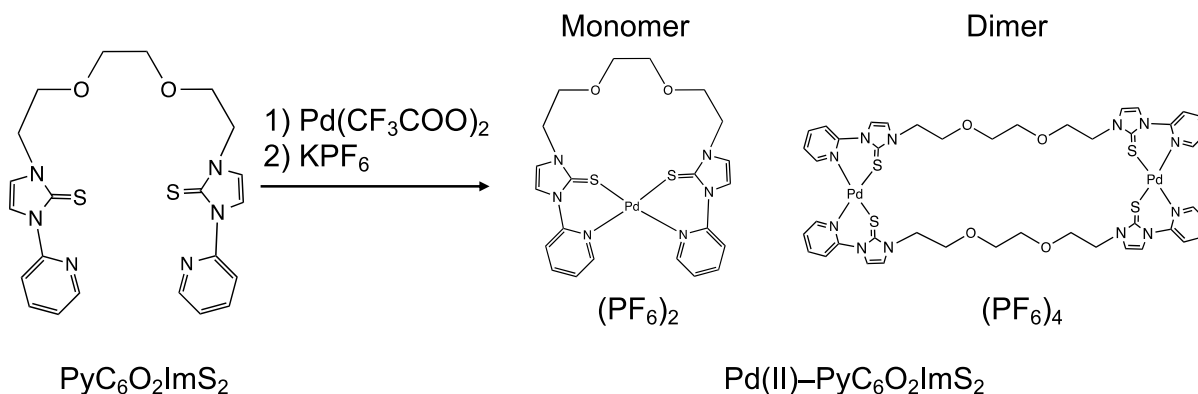
Abstract

Sulfur ligands including sulfide, thiolate, thioether and thioketone act as enzymes and play some important roles in various area involving in vivo. They also belong to soft base in the HSAB rule and have good affinity for soft cations like Cu(I) and Au(I). Among sulfur ligands, imidazole-2-thiones (ITs) have received attention in recent years because of their unique features and functionalities.¹⁻³ We have demonstrated that Cu(I) complexes with diether-bridged bis(1-(2-pyridyl)imidazole-2-thione) ligand (PyC₆O₂ImS₂) and its derivatives have photoluminescence.^{4,5} In this study, we have synthesized and characterized palladium(II) complex with PyC₆O₂ImS₂.

The palladium(II) complex was synthesised by the reaction of the PyC₆O₂ImS₂ ligand with palladium(II) trifluoroacetate and isolated by addition of excess KPF₆ as an orange powder. The ¹H NMR measurement of the palladium(II) complex suggests that the S, N-donors of the ligand coordinate to palladium(II) ion. The ESI mass spectrum showed a parent peak at m/z = 287 and it was suggested that the palladium(II) complex formed monomer and dimer from the isotope simulation.

Keywords: imidazolethione, palladium, complex, sulfur ligand

Graphical abstract



References

1. R. Karri, M. Banerjee, A. Chalana, K. K. Jha, G. Roy, *Inorg. Chem.*, **2017**, *56*, 12102–12115.
2. A. Beheshti, K. Nozarian, N. Ghamari, P. Mayer, H. Motamedi, *J. Sol. St. Chem.*, **2018**, *258*, 618–627.
3. M. M. Kimani, D. Watts, L. A. Graham, D. Rabinovich, G. P. A. Yap, J. L. Brumaghim, *Dalton Trans.*, **2015**, *44*, 16313–16324.
4. K. Matsumoto, T. Kondo, K. Kawano, Y. Nozaki, K. Sato, *International Congress on Pure and Applied Chemistry (ICPAC) Yangon 2019*, **2019**, ICC16.
5. K. Matsumoto, Y. Nozaki, T. Kondo, K. Kawano, K. Sato, *7th Asian Conference Coordination Chemistry (ACCC7)*, **2019**, PCC30.

Trinuclear Co(III)-Co(II)-Co(III) Complexes Having the Doubly Alkoxido-Bridged Core Bridged by Acetato Ligand

Tomoyo Misawa-Suzuki^{a,*}, Ryosei Ito^a, Hiroataka Nagao^a

^a Faculty of Science and Technology, Sophia University, Tokyo, Japan.

*Corresponding author: t_misawa@sophia.ac.jp

Abstract

Multinuclear metal complexes are highly potent for multi-electron and multi-proton transfer reactions regarding with molecular conversion reactions in homogeneous systems. We have been studying cobalt complexes bearing the tridentate alkylbis(2-pyridylmethyl)amine (**Rbpma**; **R** = ethyl, benzyl)^{1,2} or bis(2-pyridylmethyl)ether (bpme) ligand.¹ Previously, mononuclear cobalt(II) complexes bearing **Rbpma** or bpme were reported.^{1,3}

In this study, trinuclear Co(III)-Co(II)-Co(III) complexes having the doubly alkoxido-bridged core {Co₂(μ-OR')₂} bridged by bidentate acetato ligand, [Co^{II}{(μ-OR')₂(κ²:μ-O₂CCH₃)Co^{III}(**Rbpma**)₂}X₂ (X = PF₆, ClO₄, **R'** = CH₃; **1e**, **1b**, C₂H₅; **2e**, **2b**), were synthesized through 3:2 reactions of cobalt(II) acetate tetrahydrate and **Rbpma** in methanol or ethanol at room temperature. The magnetic moments (μ_{eff} / μ_B) were 4.12 for **1e** and 4.07 for **1b** (S = 3/2),² suggesting that the two terminal Co(III) centres are in the low spin (LS) state of 3d⁶ configuration and the central Co(II) centre is in the high spin (HS) state of 3d⁷ configuration in the octahedral crystal field. XRD analyses of both **1e** (**Fig.**) and **1b** revealed that they formed distorted octahedral geometry of linear edge-sharing type structures, in which the {Co₂(μ-OCH₃)₂} core was asymmetric with obviously shorter Co(III)-O(methoxido) bonds (1.883 - 1.897 Å) and longer Co(II)-O(methoxido) bonds (2.047 - 2.119 Å).² Each cobalt center would behave almost independently without little intermetallic interactions.

The electron transition spectra were rather vague except for the π-π* transitions of pyridine, however, weak bands observed in the visible region (around 460 nm for **1e** and 630 nm for **1b**) could be attributed to the d-d transitions of the Co(II) center. In cyclic voltammetry, irreversible reduction and oxidation waves were observed for **1e**, **1b**, **2e**, and **2b** in CH₃CN, indicating that upon redox reactions some structural changes would be involved. We will discuss the detailed properties of those trinuclear complexes and synthetic and electrochemical attempts toward reduction and oxidation reactions.

Keywords: Trinuclear complex, Cobalt, Mixed-valent, Mixed spin state

Graphical abstract

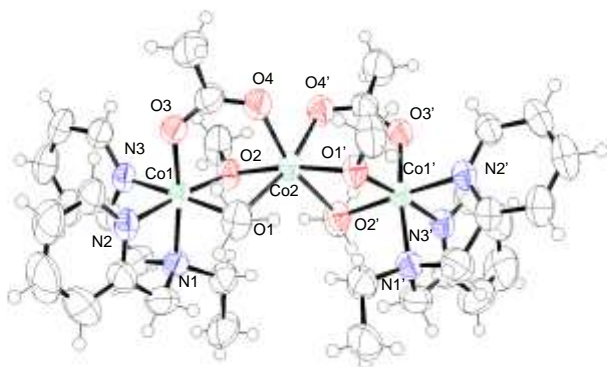


Fig. Crystal structure of **1e**²⁺.

References

1. Misawa-Suzuki, Nagao, H. *et al. Polyhedron* 2022, 218, 115735.
2. Misawa-Suzuki, T.; Ito, R., Nagao, H. *in preparation*.
3. Misawa-Suzuki, T.; Toriba, R., Nagao, H. *ICPAC Bali 2023*, ICC-04, Sept. 15th.

Double Asymmetric Hydrogenation in Total Synthesis of Lycoperdic Acid and Stereoisomers

Masato Oikawa*

Yokohama City University, Japan

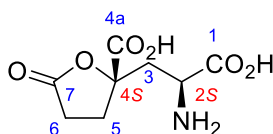
*Corresponding author: moikawa@yokohama-cu.ac.jp

Abstract

Four stereoisomers of lycoperdic acid, a mushroom-derived glutamate natural product, were stereodivergently synthesized in 1.2–7.1% overall yield for total 11 steps starting from 2,2-dimethyl-1,3-dioxan-5-one. In this synthetic study, double asymmetric hydrogenation of racemic enamide was employed as the key step. The hydrogenation outcome, yield and ee, was used to determine matched and mismatched products. By identification of matched and mismatched pairs, the reaction mechanism should be clarified.

The relationships between the structure and the neuronal activity of lycoperdic acid will be also presented.

Keywords: asymmetric hydrogenation, double asymmetric induction, enamide, glutamate, natural product



lycoperdic acid (LPA, 1)
weakly hyperactive in vivo (this work)

References

1. Morokuma, K.; Irie, R.; Oikawa, M. *Tetrahedron Lett.* 2019, 60, 2067-2069.
2. Morokuma, K.; Tanaka, K.; Irie, R.; Oikawa, M. *Tetrahedron* 2023, 145, 133622.
3. Morokuma, K.; Watari, H.; Mori, M.; Sakai, R.; Irie, R.; Oikawa, M. *Tetrahedron* 2023, 145, 133623.

Structural Characteristics Driving High Dielectric Permittivity of Bismuth Silicate Glass

J. R. Stellhorn^{a,*}, A. Masuno^b, T. Ohkubo^c, Y. Onodera^d, S. Kohara^d, H. Taniguchi^e

^aInstitute for Advanced Materials Research and Development, Shimane University, Japan

^bKyoto University, Japan, ^cChiba University, Japan

^dNational Institute for Materials Science, Japan, ^eNagoya University, Japan

*Corresponding author: jrstellhorn@mat.shimane-u.ac.jp

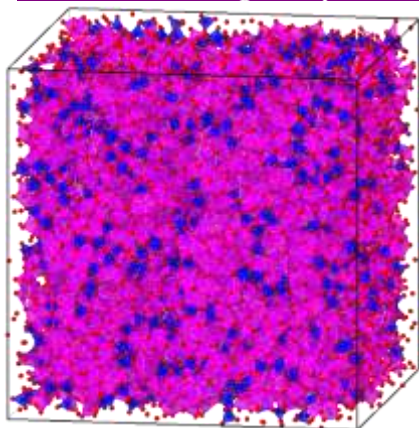
Abstract

Bismuth silicate (Bi_2SiO_5) glasses exhibit exceptional dielectric properties, including a notably high dielectric constant, surpassing that of any other pure amorphous material. While the dielectric properties of crystalline materials have been extensively studied in relation to their atomic structures, amorphous compounds pose a unique challenge due to their inherent structural disorder. To address this challenge and understand the remarkable dielectric behavior of Bi_2SiO_5 glass, we employed a comprehensive structural analysis using high-energy X-ray and neutron scattering (HEXRD, ND), X-ray absorption spectroscopy (XAFS), and Si MAS NMR, coupled with Reverse Monte Carlo (RMC) modeling. The results are substantiated by first principles calculations.

The derived atomic configuration reveals significant short- and intermediate-range structural features. Our analysis indicates that the structure comprises Bi_2O_3 -rich inclusions separated by SiO_4 chains. Notably, the Bi-O_x polyhedra exhibit a coordination similar to that found in the corresponding crystalline phase: bismuth atoms form either BiO_5 or BiO_6 polyhedra, with oxygen atoms constrained to one hemisphere of the coordination shell, while the opposite side is occupied by an electron lone pair. This unique arrangement leads to substantial atomic-level polarizability, contributing to the high dielectric constant observed in the crystalline phase. It is also the cause for the material's particular crystallization characteristics, which include a 2-step process from the glass to Bi_2O_3 and finally to the Bi_2SiO_5 phase [1,2]. This c- Bi_2SiO_5 represents a non-equilibrium state and is only obtained from the glass by a melt-quench container-less aerodynamic levitation process [3].

Keywords: amorphous structure, dielectric permittivity, structure-property relations

Structure of the glass by RMC



References

1. H. Taniguchi et al., *Angew. Chem. Int. Ed.* 52, 8088 (2013).
2. H. Taniguchi et al., *Phys. Rev. Mater.* 2, 04560 (2018).
3. A. Masuno, *J. Phys. Soc. Jpn.* 91, 091003 (2022).

Formation process of halogen-rich argyrodite

Hiroshi Yamaguchi^{a,b,*}, Atsushi Yao^b, Satoshi Hiroi^c, Futoshi Utsuno^b, and Koji Ohara^{a,c},

^aGraduate School of Natural Science and Technology, Shimane University, Japan

^bIdemitsu Kosan Co. Ltd., Japan

^cFaculty of Materials for Energy, Shimane University, Japan

*Corresponding author: hiroshi.yamaguchi.7420@idemitsu.com

Abstract

Conventional Li-ion batteries, while widely used, pose safety risks such as electrolyte leakage and ignition due to the flammable organic solvents employed. All-solid-state batteries, in contrast, significantly mitigate these risks as they contain no liquid components, even in the electrolyte. Numerous materials research studies have focused on argyrodites to develop rare metal-free solid electrolytes with high ionic conductivity^{1,2,3}. Halogen-rich argyrodites, featuring hybrid doping with chlorine and bromine, demonstrate that the Li-ion conductivity is influenced by the degree of elemental disorder among chlorine, bromine, and sulfur at the anion sites (4a, 4d)².

This study employed in situ XRD/PDF during the annealing process of sample synthesis to investigate the formation of disorder at these anion sites. Initially, a sulfur-rich argyrodite phase formed at lower annealing temperatures (200°C–320°C). Subsequently, in the higher temperature range (320°C–460°C), lithium halide amorphization and thermal diffusion led to the formation of a halogen-rich argyrodite phase. This phase is characterized by the substitution of sulfur with halogen at the 4a and 4d sites in argyrodites.

Keywords: electrolytes, argyrodite, thermal diffusion, in situ XRD, in situ PDF

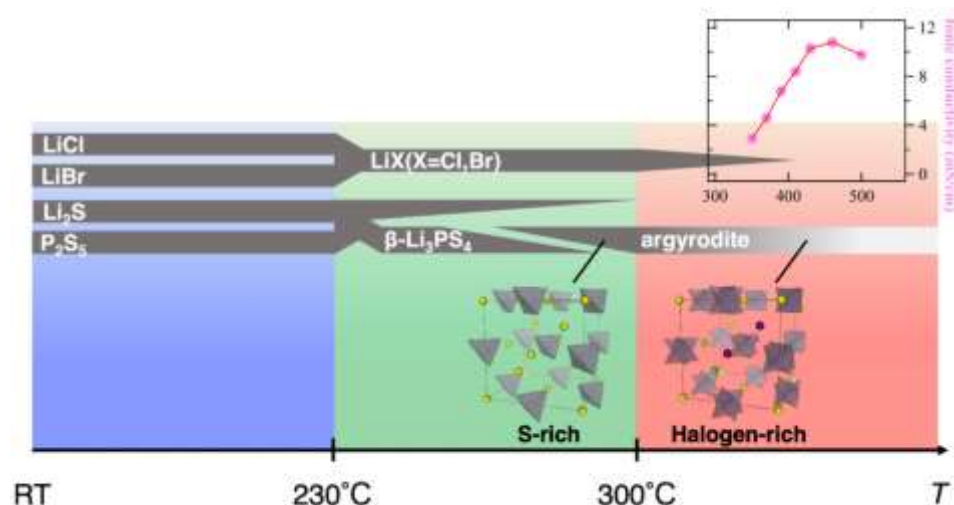


Fig. Schematic diagram depicting the change in each component and the structural transformation of argyrodite during the temperature process⁴, Reproduced with permission from H. Yamaguchi et al, *J Solid State Electrochem.*, (2024). Copyright 2024 Springer⁴.

References

1. Rao, R. P.; Seshasayee, M. *J. Non-Crystal. Solids.* 2006, 352, 3310-3314.
2. Masuda, N.; Kobayashi, K.; Utsuno, F.; Uchikoshi, T.; Kuwata, N. *J. Phys. Chem. C.* 2022, 126, 14067-14074.
3. Patel, S. V.; Banerjee, S.; Liu, H.; Wang, P.; Chien P. H.; Feng, X.; Liu, J.; Ong, S. P.; Hu, Y. *Chem. Mater.* 2021, 33, 1435-1443.
4. Yamaguchi, H.; Yao, A.; Hiroi, S.; Yamada, H.; Tseng, J.; Shimono, S.; Utsuno, F.; Ohara, K. *J Solid State Electrochem.* 2024, DOI: 10.1007/s10008-024-05881-y

Formation and Evolution of Asteroid Ryugu based on Analysis of Spacecraft Return Samples

Tomoki Nakamura^a

^a *Department of Earth Science, Graduate School of Science, Tohoku University
Aoba, Sendai, Miyagi 980-8578, Japan
tomoki.nakamura.a8@tohoku.ac.jp*

Abstract

Asteroids are the first small bodies formed in the solar system and preserve the record of formation of the solar system about 4.6 billion years ago. We analyzed samples from the C-type asteroid Ryugu recovered by the asteroid Explorer Hayabusa2 in order to understand the early chemical evolution occurred in the asteroids in the early solar system. The results presented in the talk are those obtained by the analysis team “Stone [1]”, one of the six initial analysis teams organized in Japan, together with recent results obtained in this year.

Eighteen particles ranging in size from millimeters to 1 cm were analyzed using synchrotron radiation and electron microscopes. The results showed that the Ryugu samples are composed mainly of hydrous silicates and carbonates formed during water-rock reactions in the asteroid. They also contain a variety of organic matter. Liquid water confined trapped FeS crystals as fluid inclusions contained CO₂ and organic matter. Based on these results, the asteroid Ryugu was formed at outer region of the solar nebula at temperatures below -200 °C, beyond the water and CO₂ snow lines, by accretion of rocks, organics, and ices of water and CO₂. The bulk composition of the samples is close to the elemental abundances of the Sun, except for volatile elements. About 3-5 million years after the formation of the solar system, the interior of the asteroid was heated by short-lived nuclear decay heat, melting ice and forming liquid water, and water rock reactions progressed. During the reaction, Ryugu contains water with a water/rock weight ratio <1, at high pH (> 9) and temperature <50°C. The water contains CO₂ and organic matter. The study confirms the possibility that the small bodies rich in water and organic matter, such as asteroid Ryugu, may have been impacted to Earth and provided the raw material for the origin of life and oceans on the Earth.

Keywords: Solar system, Asteroid, Hayabusa2 mission

References

1. Nakamura T, et al., *Science* 379, 2022, eabn8671.

Structure-Property Relationships in Novel Perovskite-Type Iron Oxides Synthesized Using Strong Oxidation Conditions

Masato Goto^{a,*}, Makoto Iihoshi^a, Yuichi Shimakawa^a,

^aInstitute for Chemical Research, Kyoto University, Japan

*Corresponding author: goto.masato.8s@kyoto-u.ac.jp

Abstract

Transition-metal ions in oxides often adopt various valence states. In magneli-phase compounds such as $\text{Mo}_n\text{O}_{3n-1}$ and $\text{V}_n\text{O}_{2n-1}$, for example, the valence state of the transition metal ion varies depending on the oxygen content, which causes a rich variety of chemically and physically interesting phenomena. Thus, exploring materials containing transition-metal ions with unusual valence states could lead to finding novel exotic properties and functionalities.

Fe in oxides typically has valence states between +2 and +3, as seen in the Fe^{2+} of Wustite FeO , the $\text{Fe}^{2.67+}$ of magnetite Fe_3O_4 , and in the Fe^{3+} of α -hematite $\alpha\text{-Fe}_2\text{O}_3$. Higher valence states of Fe like $\text{Fe}^{3.5+}$ and Fe^{4+} are rarely reported and can be stabilized by using appropriate strong oxidation conditions. The electronic instabilities due to such unusually high valence Fe ions often induce nontrivial phase transitions. For example, $\text{LaCu}_3\text{Fe}_4\text{O}_{12}$ with unusually high valence $\text{Fe}^{3.75+}$ ions shows first-order inter-site charge transfer between Cu and Fe ions to relieve the instability of $\text{Fe}^{3.75+}$. Here, we report newly discovered novel two systems, *A*-site-layer ordered double perovskites $\text{LnBaFe}^{3.5+}_2\text{O}_6$ [1] and *B*-site-rock-salt ordered double perovskites $\text{Ln}_2\text{LiFe}^{5+}\text{O}_6$ (*Ln*: Lanthanoids) [2], which were synthesized using different methods.

$\text{LnBaFe}^{3.5+}_2\text{O}_6$ were obtained by topochemically oxidizing *A*-site layer-ordered $\text{LnBaFe}^{2.5+}_2\text{O}_5$ in ozone at a low temperature (Fig. 1). In $\text{LnBaFe}_2\text{O}_6$, the electronic instability of $\text{Fe}^{3.5+}$ was found to induce novel cascade charge transitions, described as $\text{LnBaFe}^{3.5+}_2\text{O}_6 \rightarrow \text{LnBa}(\text{Fe}^{3+}\text{Fe}^{4+})\text{O}_6 \rightarrow \text{LnBa}(\text{Fe}^{3+}_{1.5}\text{Fe}^{5+}_{0.5})\text{O}_6$. These charge transitions accompany drastic structural and magnetic changes. In contrast, $\text{Ln}_2\text{LiFe}^{5+}\text{O}_6$ were synthesized by solid-state reactions under high-temperature and high-pressure conditions. Surprisingly, the unusually high valence Fe^{5+} states were confirmed to be maintained down to 2 K by using the ^{57}Fe Mössbauer spectra (Fig. 2). Detailed syntheses and physical properties of the obtained compounds will be presented and the effects of lanthanoid ions at the *A* site will be discussed.

Keywords: unusually high valence, perovskite-type oxides, high pressure synthesis, ozone oxidation, charge transition,

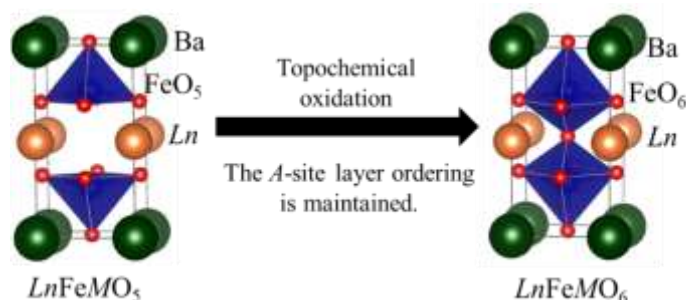


Figure 1. Topochemical reaction of $\text{LnBaFe}_2\text{O}_5$.

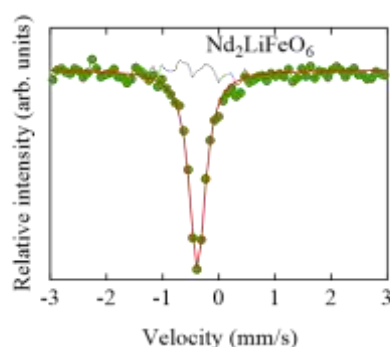


Figure 2. ^{57}Fe Mossbauer spectra of $\text{Ln}_2\text{LiFeO}_6$ (*Ln* = Nd) at room

References

1. Iihoshi, M.; Goto, M.; Kosugi, Y.; Shimakawa, Y. *J. Am. Chem. Soc.* 2023, *145*, 10756-10762.
2. Goto, M.; Oguchi, T.; Shimakawa, Y. *J. Am. Chem. Soc.* 2021, *143*, 19207-19213.

Cation dimerization in ilmenite-type vanadium oxides

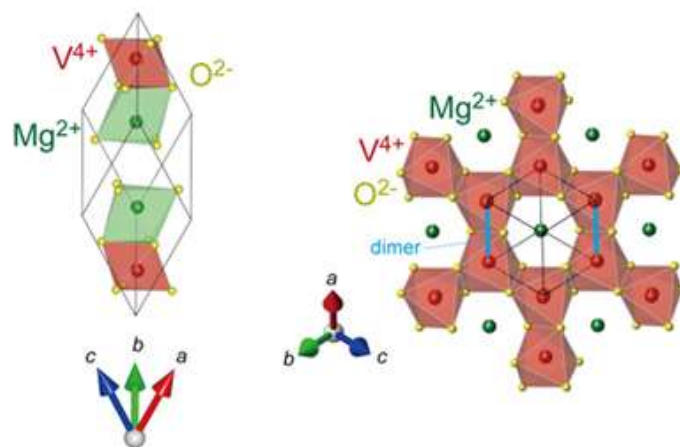
Hajime Yamamoto^{a,*}^aInstitute of Multidisciplinary Research for Advanced Materials, Tohoku University, Japan.

*Corresponding author: hajime.yamamoto.a2@tohoku.ac.jp

Abstract

Cation dimerization refers to the formation of direct chemical bonds between neighboring cations in crystalline compounds. Such a phenomenon is known as the Peierls transition in VO_2 and has been a topic of interest in the field of solid-state physics and chemistry. Recently, we found that a cation dimerization (V-V dimerization) was observed in the ilmenite-type vanadium oxides, such as MgVO_3 , CoVO_3 , MnVO_3 , and NiVO_3 .¹⁻⁵ These compounds are synthesized using a high-pressure synthesis method. Synchrotron X-ray powder diffraction experiments reveal that the V-V dimerization occurs around 500 K, which induces a structure phase transition from a rhombohedral to a triclinic phase. The V-V dimers are arranged in a ladder-like order in the vanadium's honeycomb lattice. The V-V dimerization is accompanied by a magnetic (metal) to nonmagnetic (insulator) phase transition, which is ascribed to the formation of molecular orbital between adjacent vanadium ions. Considering that the V-V dimerization leads to changes in crystal symmetry and electronic structure, the magnetic properties of MVO_3 (in the case that M is a magnetic ion) can be switched by the dimerization.^{3,6} In this presentation, we will discuss the details of the V-V dimerization and characteristic properties in some ilmenite-type vanadium oxides.

Keywords: High-pressure synthesis, vanadium ion, 3d orbital, insulator-to-metal transition, magnetism

**References**

1. Yamamoto, H.; Kamiyama, S.; Yamada, I.; Kimura, H. *J. Am. Chem. Soc.* 2022, *144*, 1082-1086.
2. Yamamoto, H. et al. *Appl. Phys. Lett.* 2022, *120*, 201901.
3. Kamiyama, S.; Yamamoto, H. et al. *Inorg. Chem.* 2022, *61*, 7841-7864.
4. Kamiyama, S.; Yamamoto, H. et al. *Cryst. Growth Design* 2023, *23*, 2296-2300.
5. Yamamoto, H. et al. *Submitted*.
6. Yamamoto, H. et al. *Appl. Phys. Lett.* 2023, *123*, 132404.

Synthesis and Characterization of Silver Nanoclusters with Different Central Anions

**Aoi Akiyama^a, Yoshiki Niihori^a, Sakiat Hossain^a,
Tokuhisa Kawawaki^a, Yuichi Negishi^{a, b, *},**

^a Graduate School of Science, Tokyo University of Science, Japan.

^b Institute of Multidisciplinary Research for Advanced Materials, Tohoku University, Japan.

*Corresponding author: yuichi.negishi.a8@tohoku.ac.jp

Abstract

Metal nanoclusters (NCs) are assemblies of several to several dozen metal atoms. NCs have been studied as novel functional materials because their structure can be controlled with atomic precision, and they exhibit specific properties dependent on the constituent elements. Recently, there have been numerous reports of NCs composed of silver (Ag) and sulfur (S), capable of encapsulating anions inside.¹ Encapsulation of different anions is novel method to control the physical properties of NCs.² Therefore, it is crucial to clarify the influence of encapsulated anions on the physical properties of NCs.

In this study, we synthesized $[X@Ag_{54}S_{20}(tBuS)_{20}(tBuSO_3)_{12}]$ (**X@Ag54**) (X = S or I (iodine), $tBuS = tert$ -butanethiolate, $tBuSO_3 = tert$ -butanesulfonate), encapsulating sulfide or iodide ions which greatly differ in size. Single crystal X-ray diffraction results show that both clusters have very similar geometrical structure except for the central anion. X@Ag54 have an Ag₁₂ icosahedral core, and the flexibility of this core structure allows the clusters to encapsulate anions of different sizes. By comparing the geometrical structures and physical properties of X@Ag54, we aimed to elucidate the influence of encapsulated anions on the physical properties of NCs.

The photoluminescence quantum yield (Φ) of I@Ag54 in toluene solution was more than 100-times higher than that of S@Ag54. This improvement in photoluminescence properties by changing the encapsulated element from S to I is expected to be due to the enhancement of intersystem crossing (ISC) caused by the heavy atom effect.

Keywords: metal nanocluster, atomic level tailoring, single crystal X-ray diffraction measurement, photoluminescence enhancement



References

- Zhang, S.-S.; Alkan, F.; Su, H.-F.; Aikens, C. M.; Tung, C.-H.; Sun, S. *J. Am. Chem. Soc.* **2019**, *141*, 4460–4467
- Horita, Y.; Hossain, S.; Ishimi, M.; Zhao, P.; Kawawaki, T.; Takano, S.; Niihori, Y.; Nakamura, T.; Tsukuda, T.; Ehara, M.; Negishi, Y. *J. Am. Chem. Soc.* **2023**, *145*, 23533–23540

Luminescence of N⁺C⁺N⁺-Coordinated Platinum(II) Complexes in Human Cell

Shingo Hattori*,

School of Science, Yokohama City University.

**Corresponding author: s_hat@yokohama-cu.ac.jp*

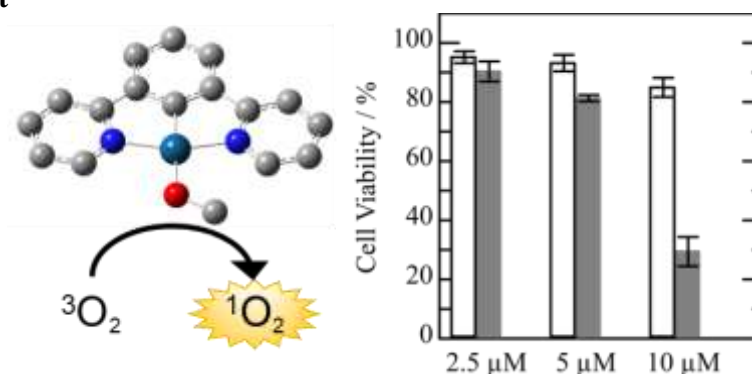
Abstract

Photodynamic therapy (PDT) is a one of the non-invasive cancer treatments which can treat only tumor tissues by light irradiation. Pt(II) complexes are useful for the photosensitizer of PDT because those can produce the excited triplet state followed by production of singlet oxygen. In order to employ the Pt(II) complex photosensitizer to the clinical application, it is important to obtain the amphiphilicity so as to improve cell uptake. Many researchers reported Pt(II) complexes introducing water-soluble substituents to obtain amphiphilicity. However, multiple chemical synthetic procedures are needed to introduce water-soluble substituents. Ionization of hydrophobic Pt(II) complexes is one of the plausible approaches for obtaining amphiphilicity because cationic metal complexes are generally water-soluble. It motivates us to develop the cationic N⁺C⁺N⁺-coordinated Pt(II) complex for PDT.

Here we report PDT photosensitizer of a N⁺C⁺N⁺-coordinated Pt(II) complex: [Pt(L)(MeOH)]⁺ (HL = 1,3-(2-dipyridyl)benzene). Quantum yield of singlet oxygen production for [Pt(L)(MeOH)]⁺ is more than 50 %. Photo-images of human umbilical vein endothelial cell (HUVEC) treated with the Pt(II) complex suggest that [Pt(L)(MeOH)]⁺ is delocalized in entire cell after the fast uptake by diffusion. Photocytotoxicity of [Pt(L)(MeOH)]⁺ is investigated by using HUVEC, a mammary glandular epithelial cell line (MCF10A) for a normal cell model, and a high malignant triple negative human breast cancer cell line (MDA-MB-231). We find that [Pt(L)(MeOH)]⁺ shows photocytotoxicity for HUVEC but for MCF10A and MDA-MB-231. The selective photocytotoxicity of [Pt(L)(MeOH)]⁺ for HUVEC has potential to reconstruct tumor vessels to normal ones only in endothelial cells without damages to the normal tissues. Therefore, the photodynamic effect of [Pt(L)(MeOH)]⁺ may be useful for normalization of abnormal vessel in a tumor.

Keywords: luminescence, Pt(II) complex, photocytotoxicity

Graphical abstract



References

- Hattori, S. et al. *Inorg. Chem.* **2023**, 62, 9491-9500.
- Hattori, S. et al. *Under revision*

Local structure analysis of negative-electrode oxides for large lithium-ion batteries using quantum beams

Naoto Kitamura*

Department of Pure and Applied Chemistry, Faculty of Science and Technology, Tokyo University of Science

*Corresponding author: naotok@rs.tus.ac.jp

Abstract

Effective use of energy is essential to achieve carbon neutrality, and demand for large lithium-ion batteries is expected to increase. One of the key issues for the widespread use of large batteries is to improve the safety, and for this purpose, the use of oxides for the negative electrodes is being promoted. Although oxide-based negative electrode materials are superior to carbon in terms of safety, they have the problem of low discharge capacity. To solve this problem, new oxides are being explored, and A-site deficient perovskites, such as (Li, La)NbO₃¹⁾, and Wadsley-Roth phase TiNb₂O₇²⁾ are considered promising candidates. In general, charge/discharge properties (insertion and deinsertion of Li⁺) are closely related to atomic configuration, but the local structure (distribution and surrounding environment around atoms) of these materials remains unknown. Therefore, no guidelines have been established for making better oxides. In this study, synchrotron X-ray and neutron total scattering measurements were performed on the oxide-based negative electrode materials, and the local structures were investigated by analyzing the obtained structure factors, $S(Q)$, and real-space functions.

The oxide-based negative electrode materials were synthesized by a solid-state reaction method. The electrode properties were evaluated by charge/discharge cycle tests. Synchrotron X-ray total scattering data were measured at BL04B2 (SPring-8), and neutron total scattering data were measured at NOVA (J-PARC). The obtained data were transformed into $S(Q)$ and real-space functions, such as total correlation functions, $T(r)$, using atomic densities calculated from the lattice parameters and compositions. Reverse Monte Carlo modeling was performed using these data simultaneously to visualize the local structures.

Fig. 1 shows the crystal structure (average structure) of the Wadsley-Roth phase TiNb₂O₇, which was refined by the Rietveld method. In this material, TiO₆ and NbO₆ octahedra form a network structure, and Li⁺ ions conduct via the free space of the structure. It is revealed from $T(r)$ of TiNb₂O₇ synthesized by different methods that the distortion of the network depends on the synthetic process. It is also found that the distortion deteriorates the negative electrode properties.

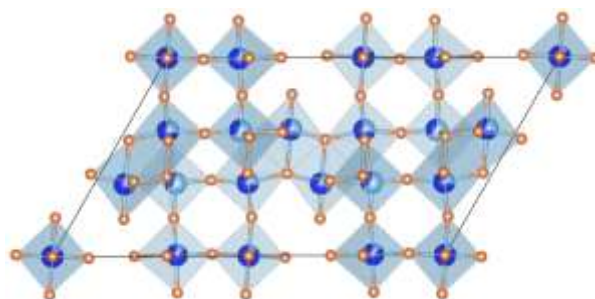


Fig. 1 Average structure of TiNb₂O₇.

Keywords: Lithium ion battery, Negative electrode, Local structure, Total scattering

References

1. Xiong, X.; Yang, L.; Liang, G.; Wang, C.; Chen, G.; Yang, Z.; Che, R. *Adv. Funct. Mater.* 2022, 32, 2106911–1–12.
2. Takami, N.; Ise, K.; Harada, Y.; Iwasaki, T.; Kishi, T.; Hoshina, K. *J. Power Sources* 2018, 396, 429–436.

Optical Properties for Red and Infrared Emitting Scintillators Containing a Novel Emission Center III

Shunsuke Kurosawa^{a,b,c,*}, Shohei Kodama^d, Chihaya Fujiwara^{b,e}, Yusuke Urano^{b,e},
Akihiro Yamaji^{a,b}

^a *New Industry Creation Hatchery Center, Tohoku University, Japan*

^b *Institute for Materials Research, Tohoku University, Japan*

^c *Institute of Laser Engineering, Osaka University,*

^d *Graduate School of Science and Engineering, Saitama University, Japan*

^e *School of Engineering, Tohoku University, Japan*

**Corresponding author: kurosawa@imr.tohoku.ac.jp*

Abstract

The first decommissioning step for the Fukushima Daiichi Nuclear Power Plant (1F) is to evaluate the distribution of the dose-rate before removing the debris, and real-time dose-rate monitors in high dose-rate conditions are required. These monitors are realized when we use a scintillator, which converts gamma rays into detectable photons with photo-detectors, with red or infrared emission. Although commercial-use scintillators doped with Ce³⁺ or Eu²⁺ (5d-4f transition) as emission centres have maximum light outputs of 60,000 photons/MeV, typical emission wavelengths are 400-550 nm.

We found that Cs₂HfI₆ grown by the vertical Bridgman-Stockbarger method had a peak emission wavelength of around 700 nm and high light output of over 60,000 photons/MeV. In addition, Rb₂HfI₆ and other novel scintillators including [HfI₆]²⁻ site were found to have long emission wavelengths of more than 650 nm and relatively high light output of over 30,000 photons/MeV. These scintillation decay times were less than 5 μs, while conventional red/infrared emission centres (i.e. Cr³⁺ d-d transition) have these times of over 100 μs.

On the other hand, such materials have hygroscopic natures, and in some cases, the use of these materials are hard. Thus, we also have developed novel red and infrared scintillation materials with no hygroscopic nature, though the light output was smaller than Cs₂HfI₆.

In this paper, we show the results of scintillation properties for such novel scintillation materials including anion-complex materials, and emission mechanism and bandgap structure including crystal fields were discussed with a relationship between the optical properties and the crystal and bandgap structure.

Keywords: Scintillator, Red and Infrared Emission, halide materials, oxide materials

EFFICIENT COPPER EXTRACTION FROM ASGAT POLYMETALLIC ORE

Nyamdelger Shirchinnamjil^{a,*}, Narangarav Tumen-Ulzii^a, Khulan Byambasuren^a, Sarantsetseg Purevsuren^a, Ulziibadrakh Erdenebat^a, Enkhtuul Surenjav^a, Narandalai Byamba-Ochir^a, Azzaya Tumendelger^a, Alen Silam^a, Ariunaa Garnaad^a

^a*Institute of Chemistry and Chemical Technology, Mongolian Academy of Sciences, Mongolia*

*Corresponding author: nyamdelger_sh@mas.ac.mn

Abstract

This study presents a comprehensive technological process for recovering pure copper from a polymetallic concentrate using a selective and efficient method. The sulfide concentrate, derived from the Asgat silver-polymetallic ore via flotation comprises Ag 0.91%, Cu 19.20%, Sb 18.40%, As 2.03%, and Bi 1.60% as determined by ICP-OES analysis. XRD and SEM-EDX analyses reveal the presence of tetrahedrite as the primary mineral, along with chalcopyrite, bismuthinite, arsenopyrite, and pyrite, and minor amounts of quartz, muscovite, and siderite.

Leaching the tetrahedrite concentrate with an alkaline-sulfide mixture (Na₂S+NaOH) selectively extract toxic compounds such as bismuth and arsenic, resulting in a solid residue enriched in copper sulfide (Cu 33.45%, Fe 14.14%, Ag 0.73%, and S 23.87%). Under optimal leaching conditions, the solution extracts 99.25% Sb, 89.00% As and 44.50% Bi. The leaching residue referred to as technogen concentrate, contains covellite, chalcocite and argentite from the leaching process, alongside chalcopyrite and pyrite which remain insoluble.

Roasting the technogen concentrate at 400°C in an oxygen flow produces soluble copper sulfate and insoluble iron oxides such as hematite (Fe₂O₃) magnetite (Fe₃O₄) and goethite (FeO(OH)). The ICP-OES analysis of the roasted sample shows composition of 28.34% Cu, 14.37% S, 11.28% Fe, 0.35% Zn, 0.58% Sb, 0.20% As, 5.94% SiO₂, and 0.65% Ag. Subsequent water leaching achieves a copper sulfate dissolution rate of 98.48% with iron content in the leaching residue at 48.13% Fe, confirming the presence of hematite, goethite, maghemite (γ-Fe₂O₃) and albite (NaAlSi₃O₈).

Finally, the copper sulfate (II) aqueous solution is processed via SX-EW technology and yielding cathode copper with 98% purity.

Keywords: tetrahedrite, copper sulfide, leaching

References

1. Nyamdelger S., Burmaa G., Narangarav T., Ariunaa G. (2013) Dissolution behaviour of freibergite-tetrahedrite concentrate in acidic dichromate solution. *Mong. J. Chem.*, 14(40), 36-40. <https://doi.org/10.5564/mjc.v14i0.196>
2. Mitovski A., Strbac N., Mihajlovic I., Sokic M., Stojanovic J. (2014) Thermodynamic and kinetic analysis of the polymetallic copper concentrate oxidation process. *J. Therm. Anal. Calorim.*, 118, 1277-1285. <https://doi.org/10.1007/s10973-014-3838-8>
3. Dimitrijevic M. D., Urosevic D.M., Jankovic Z.D., Milic S. M. (2016) Recovery of copper from smelting slag by sulphation roasting and water leaching. *Physicoche. Probl. Miner. Process.*, 52(1), 409-421. <https://doi.org/10.5277/ppmp160134>
4. Ariunaa G., Burmaa G., Nyamdelger S., Altansukh B., Nazgul M., Narangarav T-U. (2021) Some results of studies on leaching of toxic elements in Asgat polymetallic concentrate. *Bulletin of the Institute of Chemistry and Chemical Technology*, 4(9), 17-25. <https://doi.org/10.5564/bicct.v4i9.1814>

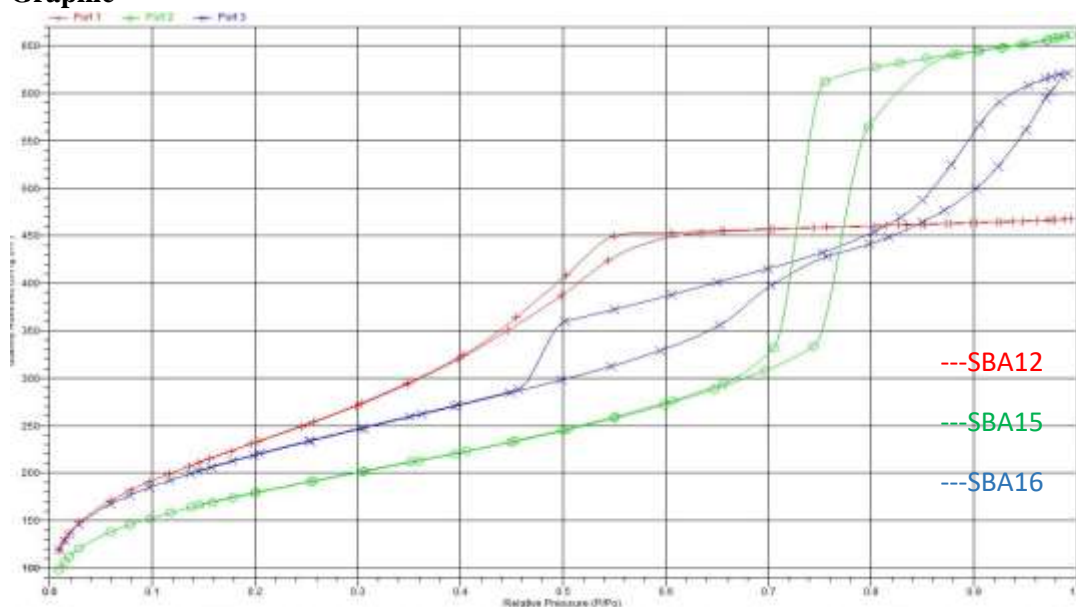
SYNTHESIS OF MESOPOROUS SILICATES

Ulziidelger Byambasuren^{a,*}, Dorjgotov Altansukh^a, Ilchgerel Dash^a^aDepartment of Chemical Engineering, School of Applied Sciences, Mongolian University of Science and Technology, Mongolia.

*Corresponding author: bulziidelger@must.edu.mn

Abstract

In this study, mesoporous SBA12, SBA15, and SBA16 silicates were synthesized. The synthesized SBA 12, SBA 15, and SBA 16 materials, as seen from the XRD graph results, that the synthesized materials consist only of silicon oxide. The results of BET analysis show that SBA12 has a pore size of 3.38 nm and a surface area of 855.12 m²/g, SBA15 has a pore size of 6.75 nm and a surface area of 606.62 m²/g, and SBA16 has a pore size of 5.16 nm, the surface area is 745.10 m²/g.

Keywords: mesoporous, silicates,**Graphic****References**

1. Gang Liu, Xuguang Li, Prabhu Ganesan, Branko N. Popov “Development of non-precious metal oxygen-reduction catalysts for PEM fuel cells based on N-doped ordered porous carbon” SC 29208, USA
2. M. Mesa a, L. Sierra a, J.-L. Guth b,” Contribution to the study of the formation mechanism of mesoporous SBA-15 and SBA-16 type silica particles in aqueous acid solutions” 89093 Mulhouse Cedex, France

Synthesis and Characterization of $\text{Ca}_2(\text{Mn,Ti})\text{O}_4$ Colored Films

Ryohei Oka*, Tomokatsu Hayakawa

Field of Advanced Ceramics, Department of Life Science and Applied Chemistry, Nagoya Institute of Technology, Japan

*Corresponding author: oka.ryohei@nitech.ac.jp

Abstract

Color materials are used for giving color to an object and are indispensable to attain a variety of signs, images, indications, and warnings in daily life. In particular, inorganic pigments have been applied in a wide range of fields, such as ceramics, glasses, plastics, and paints, because of their excellent thermal stabilities and hiding power. In recent years, functional inorganic pigments have attracted much attention, which have not only coloring abilities but also other properties. For example, Ti^{4+} -doped Ca_2MnO_4 black pigments have good black coloration and high near-infrared (NIR) reflectivity.¹⁻² Application of them to road surfaces, building walls and roofs is expected as an effective way to mitigate the urban heat island effect. Coatings with photocatalytic pigments, a typical example of which is TiO_2 , are utilized as an approach leading to decomposition of organic pollutants on surfaces, giving self-cleaning abilities to products.^{3,4} Other functionalities of inorganic pigments are to be explored for their further developments. In our previous research, it was found that Ca-Mn-O films were formed as potential materials not only with coloring abilities but also with photocatalytic abilities.⁵

In this study, $\text{Ca}_2(\text{Mn,Ti})\text{O}_4$ colored films were synthesized by a sol-gel method using acetylacetone as a chelating agent, and their crystal structures, optical properties, and color were characterized. In all samples, the target Ca_2MnO_4 phase was obtained as a main phase, although a CaO phase was detected. The diffraction peaks were shifted to the lower angle side by the substitution of Mn^{4+} (0.53 \AA)⁶ with larger Ti^{4+} (0.605 \AA)⁶. From the results of Raman spectra measurements, the vibration peaks indexed to a Ca_2MnO_4 structure were observed for all samples, whereas an additional peak at approximately 780 cm^{-1} was observed for the Ti^{4+} -doped samples. It has been reported that the additional peak was observed when Ti^{4+} ions were doped into the host lattice.² Therefore, the $\text{Ca}_2(\text{Mn,Ti})\text{O}_4$ films formed solid solutions. The films strongly absorbed all visible light due to the interband transition between O 2p and Mn 3d orbitals,^{2,5} resulting in blackish coloration.

Keywords: color, films, sol-gel methods, calcium manganate

References

1. Oka, R.; Masui, T. *RSC Adv.* 2016, 6, 90952–90957; *ibid.* 2019, 9, 38822–38827.
2. Oka, R.; Hayakawa, T. *Inorg. Chem.* 2022, 61, 6500–6507; *ibid.* 2023, 62, 14647–14658.
3. Kim, J.-H.; Hossain, S.M.; Kang, H.-J.; Park, H.; Tijing, L.; Park, G.W.; Suzuki, N.; Fujishima, A.; Jun, Y.-S.; Shon, H.K.; Kim, G.-J. *Catalysts* 2021, 11, 193.
4. Aranzabe, E.; Blanco, M.; Goitandia, A.M.; Vidal, K.; Casado, M.; Cubillo, J. *J. Sol-Gel Sci. Technol.* 2020, 93, 714–721.
5. Oka, R.; Hayakawa, T. *Phys. Status Solidi-Rapid Res. Lett.* 2023, 2300237
6. Shannon, R.D. *Acta Cryst.* 1976, A32, 751–767.

Isolation of novel high growth *Euglena* strain from Malaysia

Koji Iwamoto^{a,*}, Sabrina Aghazada^a,
Kohei Atsuji^b, Koji Yamada^b, Suzuki Kengo^b, Yu Inaba^b

^a Universiti Teknologi Malaysia.

^b Euglena Co.

*Corresponding author: k.iwamoto@utm.my

Abstract

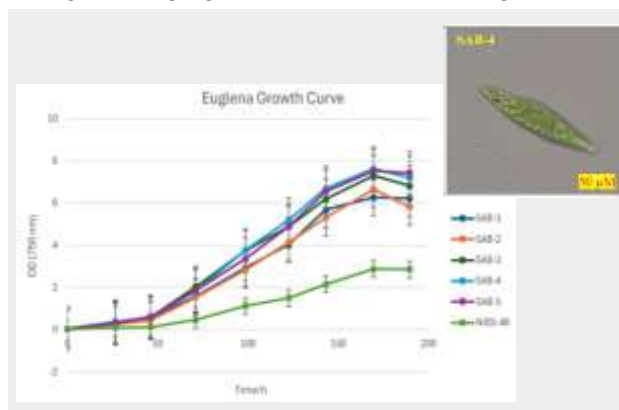
【Background and Objectives】 Malaysia tropical climate, abundant sunlight and water resources make it a desirable location for microalgae cultivation and research. To utilize it effectively, this research aims to isolate and identify new high growth/productive species/strains of *Euglena* from the Malaysia for biomass production, which is one of the target species of bio-fuel production¹.

【Methodology】 The water samples were collected from different environments of Raja Musa Forest Reserve including peatland, paddy field and river. The samples were isolated using single-cell pickup and dilution techniques². The species/strains were screened based on their growth speed assayed by optical density at 750 nm. The identification was carried out using both light microscopy and molecular phylogenetic. *Euglena* species/strains were analyzed based on their specific growth rate per day and productivity.

【Results and Discussion】 In total, 33 *Euglena* species/strains were successfully purified, 24 samples through single-cell pickup and 9 samples through dilution techniques. The top five isolated species/strains, ie. SAB-1 to SAB-5, were selected based on their growth speed. Those strains showed high growth. Particularly, SAB-4 showed to have highest growth properties such as a specific growth rate and a biomass production which were 4.2 and 2.7 times higher than those of the control strain, NIES-48 (*Euglena gracilis*), respectively. The identification by microscopy suggested that the all algal strains were *Euglena*, and SAB-4 was identified as *E. gracilis* by the sequence analysis using ITS2 region. In conclusion, the authors

【Conclusion】 The authors successfully isolated high productive *Euglena* strains including SAB-4, *G. gracilis* from Malaysia. Since those adapt to the Malaysia environment, high biomass production such as bio-fuel is expected by these strains.

Keywords: Euglena, high growth, bio-fuel, microalgae, new strain,



References

1. Chen., et al. (2022). Evaluation of *Euglena gracilis* 815 as a New Candidate for Biodiesel Production. *Front Bioeng Biotechnol.* Retrieved from <https://doi.org/10.3389/fbioe.2022.827513>.
2. Eri., et al. (2022). Isolation and Characterization of acid-tolerant *Stichococcus*-like Microalga (*Tetartostichococcus* sp. P1) from a tropical peatland in Malaysia. *Journal of Applied Phycology.* 34. 10.1007/s10811-022-02762-7.

Towards ultra-sensitive molecular spectroscopy: A temporal-mode selective parametric frequency conversion approach

Tokuei Sako,

*College of Science and Technology, Nihon University.
sako.tokuei@nihon-u.ac.jp*

Abstract

Advances in ultrashort pulsed laser light technology in the last decade have opened a new era of light-matter interaction, namely, manipulating and controlling matter using customized laser pulses. It has been indeed demonstrated both theoretically and experimentally that optical responses of matter depend not only on the central frequencies and intensities of the incident light pulses but also on their temporal profiles or shapes. Recently, a highly selective optical process called temporal-mode selective parametric frequency conversion, where only a specific input pulse's temporal mode is efficiently converted to a distinct output light, is explored. This approach offers significant potential for molecular spectroscopy by isolating a weak signal pulse carrying molecular information from background noise.

In the present study we developed a novel computational method to identify the optimal temporal mode for the highest conversion selectivity, paving the way for ultra-sensitive molecular spectroscopy using tailored light pulses¹. Relying on the symplectic integrator method we have successfully calculated the reliable and accurate Green function of the optical process, whose Schmidt decomposition yields the optimal temporal wave form, i.e., the temporal mode. We further delve into the physics behind this selectivity and propose a possible experimental setup to fully utilize this promising technique.

Keywords: temporal-mode, optical parametric frequency conversion, symplectic integrator, light-matter interaction, laser spectroscopy

References

1. Nomura, K.; Sako, T. *J. Phys. B* 2023, *56*, 095401-18.

High-Sensitivity Hydrogen sensor and Biosensor Based on Silicon Microring Resonators

Taro Arakawa^{a,*}, Shinji Okazaki^a, Yoshiaki Nishijima^a, and Yuhei Ishizaka^b,

^aGraduate School of Engineering, Yokohama National University, Japan

^bCollege of Science and Engineering, Kanto Gakuin University, Japan

*Corresponding author: arakawa-taro-vj@ynu.ac.jp

Abstract

A silicon microring resonator (Si MRR) is an ultra-compact optical device with less than a millimeter dimension. It is fabricated using the Si CMOS-compatible processes and is useful for high-speed photonic networks and ultra-compact optical sensors. The Si MRR is able to sense environmental refractive index and temperature changes with high sensitivity by observing a resonant wavelength shift in the MRR. We have developed high-sensitivity sensors based on Si MRRs, such as hydrogen sensors [1,2] and biosensors [3,4] thus far. In this paper, we discuss the Si MRR hydrogen sensors and biosensors.

Hydrogen has been attracting much attention as a new energy carrier and source. However, hydrogen is a combustible gas with a wide range of explosions; therefore, high-sensitivity hydrogen sensors are crucial for their safe use. In particular, optical hydrogen sensors are attractive for their high reliability, and high-performance sensors using optical fibers have been developed. Figure 1 shows the hydrogen sensing characteristics of the fabricated Si MRR sensor with a Pt-SiO₂ hydrogen-sensitive layer [3]. Hydrogen gas at low concentrations of less than 0.5% was successfully detected.

Next, a high-sensitivity Si MRR optical biosensor for detecting nucleocapsid protein (N protein) of SARS-CoV-2 is proposed and demonstrated, as shown in Fig. 2. The surface of the Si MRR waveguide is modified with antibodies, and the target protein is detected by measuring a resonant wavelength shift of the MRR caused by selective adsorption of the protein to the surface of the waveguide. The sensing characteristics are examined using a polydimethylsiloxane flow channel after the surface of the Si MRR waveguide is modified with IgG antibodies through Si-tagged protein. Various concentrations of N protein solutions are measured. The experimental results show that the proposed sensor has the sensitivity for nucleocapsid on the order of 10 pg/mL, which is comparable to the sensitivity of current antigen tests.

Keywords: biosensor, hydrogen, silicon, microring resonator, nucleocapsid protein

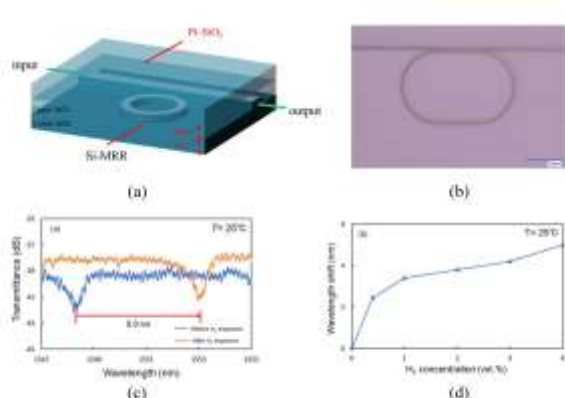


Fig. 1. (a) Schematic Si microring resonator (MRR) hydrogen sensor. (b) Photograph of fabricated Si MRR. (c) Measured optical transmission spectra for 4% hydrogen gas. (d) Measured resonant wavelength shift for various hydrogen concentrations.

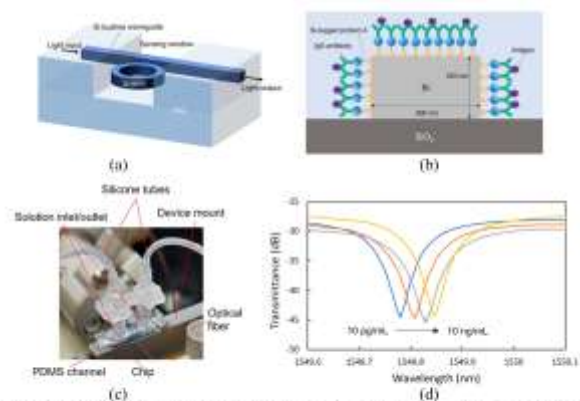


Fig. 2. Si MRR nucleocapsid protein sensor. (a) Schematic overall view of Si-MRR biosensor. (b) Cross-sectional view of Si waveguide with Si-tagged protein G and IgG antibodies. (c) Photograph of Si MRR sensor chip on device mount for measurement. (d) Transmittance spectra of Si MRR during nucleocapsid detection.

References

1. S. Matsuura, N. Yamasaku, Y. Nishijima, S. Okazaki, and T. Arakawa, *Sensors* 2020, 20, 96.
2. S. Yoshida, S. Ishihara, T. Arakawa, and Y. Kokubun, *Jpn. J. Appl. Phys.* 2017, 56, 04CH08.
3. J. Igarashi, S. Okazaki, Y. Nishijima, A. Higo, and T. Arakawa, *Jpn. J. Appl. Phys.* 2024, 63, 05SP17.
4. Y. Uchida, T. Arakawa, A. Higo, and Y. Ishizaka, *Sensors* 2024, 24, 10, 3250.

Design of multiblock copolymers by chain shuttling copolymerization

Philippe ZINCK^{a*}

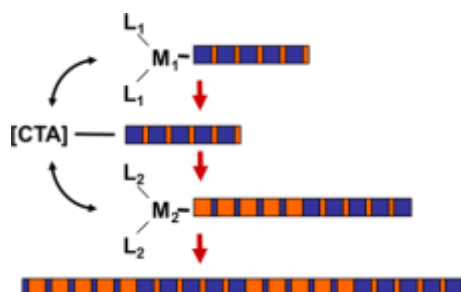
^a *Unity of Catalysis and Solid State Chemistry, Université de Lille, France*

*Corresponding author: Philippe.zinck@univ-lille.fr

Abstract

Chain shuttling copolymerization is a powerful tool allowing the access to multiblock / segmented copolymers with original microstructures in a one-pot one-step route. The process based on Coordinative Chain Transfer Polymerization (CCTP),¹ was initially developed for the production of OBC - olefinic block copolymers - using ethylene and alkenes as comonomers.² The principle of chain shuttling copolymerization is represented in the graphical abstract below. The growing macromolecular chain is allowed to “shuttle” by transmetalation via an organometallic chain transfer agent (CTA) between two catalysts presenting a difference in comonomers reactivity ratios. This result in a multiblock microstructure involving statistical copolymeric blocks of different composition. In this example, the blocks rich in ethylene were able to crystallize, while those rich in 1-octene were fully amorphous, giving rise to thermoplastic elastomers like properties.

Since this seminal work, the synthesis of original multiblock microstructures by chain shuttling copolymerization was successfully extended to styrene / conjugated diene systems using rare earth hemi-metallocene based catalysts,³ and more recently to the ring opening copolymerization of cyclic esters mediated by amino(*bis*)phenolate supported aluminum alkoxides initiators, affording access to new biosourced multiblock copolymers based on polylactide.⁴ We will present in this contribution an overview of the field, from the catalysts design and intricate polymerization catalysis involved to the materials microstructure and properties.



Graphical abstract

Chain shuttling copolymerization leading to various multiblock copolymers including polyolefins, poly(styrene-*co*-isoprene) copolymers and polyesters.

M are metals, L ligands and CTA the Chain Transfer Agent.

Keywords: Catalysis, polymerization, specialty polymers

References

1. Valente, A.; Mortreux, A.; Visseaux, M.; Zinck, P. *Chem. Rev.* 2013, 113, 3836–3857; Mundil, R.; Bravo, C.; Merle, N.; Zinck, P. *Chem. Rev.* 2024, 124, 210–244.
2. Arriola, D. J.; Carnahan, E.; Hustad, P. D.; Kuhlman, R. L.; Wenzel, T. T. *Science* 2006, 312
3. Pan, L.; Zhang, K.; Nishiura, M.; Hou, Z. *Angew. Chem.* 2011, 50, 12012–12015; Valente, A.; Stoclet, G.; Bonnet, F.; Mortreux, A.; Visseaux, M.; Zinck, P. *Angew. Chem.* 2014, 53, 4638–4641.
4. Meimoun, J.; Sutapin, C.; Stoclet, G.; Favrelle, A.; Roussel, P.; Bria, M.; Chirachanchai, S.; Bonnet, F.; Zinck, P. *J. Am. Chem. Soc.* 2021, 143, 21206–21210.

Unique Thermoelectric Power Generating Device without Need for Heat Sources Utilizing Thermoelectric Power Generating Ability, Capillary Action, and Vaporization Heat of Carbon-Nanotube Composite Papers

Takahide OYA

Graduate School of Engineering Science, Yokohama National University, Japan
oya-takahide-vx@ynu.ac.jp

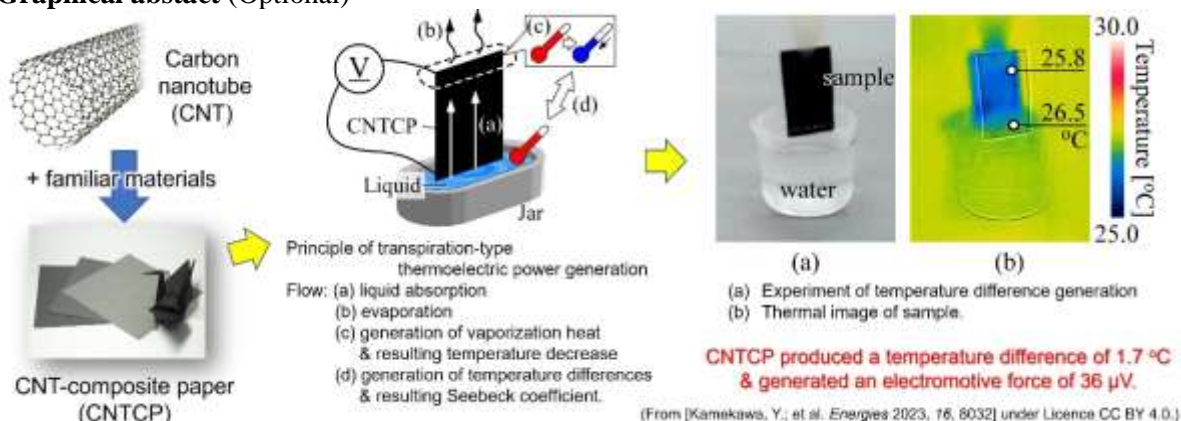
Abstract

It is known that carbon nanotubes (CNTs)¹ have useful properties such as high electrical and thermal conductivity, thermoelectric power generating ability, are great strength. Its unique cylindrical structure (diameter: sub-1 nm~) is based on a graphene sheet and it is also known that CNT has both conductive (metallic) and semiconductive properties depending on its structure². However, CNTs are generally provided as powders and are difficult to handle. Therefore, many CNT composites have been developed for easy to use.

My collaborators and I have developed unique carbon-nanotube composites by compounding CNT and familiar materials such as papers. We call them “CNT-composite papers”³. We can develop many applications based on these CNT-composite papers⁴, such as a thermoelectric power generating cell, a dye-sensitized solar cell, a soft actuator, and a transistor. In our recent research, we discovered that our CNT-composite paper has the ability to absorb liquids and, by utilizing the heat of vaporization when the liquid evaporates, can spontaneously generate a temperature difference similar to what plants do in transpiration. By combining this with thermoelectric power generating ability, we have developed a thermoelectric power generation device that does not require a heat source, i.e., “transpiration-type thermoelectric power generating paper”⁵. In my presentation, I will outline our proprietary CNT-composite papers, especially our transpiration-type thermoelectric power generating papers, which can be used in many situations in our daily lives in the near future.

Keywords: carbon nanotube (CNT), CNT-composite paper, thermoelectric power generation, heat of vaporization, capillary action

Graphical abstract (Optional)



References

1. Iijima, S. *Nature* 1991, 354, 56-58.
2. Dresselhaus, M.S.; Dresselhaus, G.; Avouris, Ph. (Eds.) *Carbon nanotubes: synthesis, structure, properties, and applications* 2001 (Springer-Verlag Berlin Heidelberg).
3. Oya, T.; Ogino, T. *Carbon* 2008, 46, 169-171.
4. See Oya Lab. website for details. https://arrow.ynu.ac.jp/publication_e.html
5. Kamekawa, Y.; Arai, K.; Oya, T. *Energies* 2023, 16, 8032.

Wearable biosensor for non-invasive monitoring of biological information in human oral cavity

Takahiro Arakawa^{a,*}, Kohji Mitsubayashi^b,

^aGraduate School of Engineering, Tokyo University of Technology.

^bInstitute of Biomaterials and Bioengineering, Tokyo Medical and Dental University.

*Corresponding author: arakawath@stf.teu.ac.jp

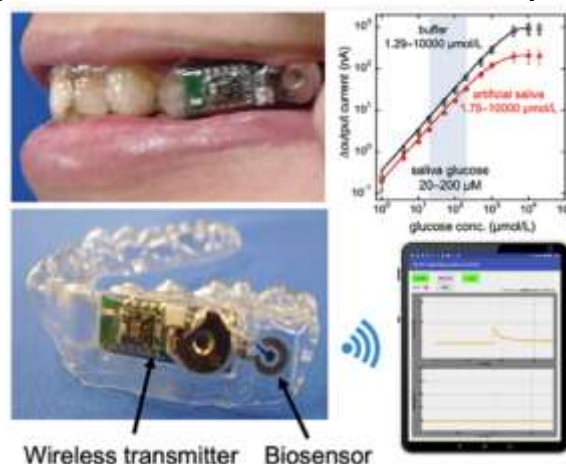
Abstract

The measurement of biophysical quantities of the human body has garnered significant attention in the medical and healthcare fields. Wearable sensors have emerged as promising tools for monitoring relevant parameters in healthcare, sports, and medical applications¹. Leveraging biophysical information with these systems is expected to enable proactive health management, thereby improving public health and reducing medical expenditure.

We developed detachable "cavitas sensors" for the human oral cavity to non-invasively monitor saliva glucose. A salivary biosensor incorporating Pt and Ag/AgCl electrodes on a mouthguard support with an enzyme membrane was developed and tested. It has electrodes that form on the polyethylene terephthalate glycol (PETG) surface of the mouthguard. The Pt working electrode is coated with a glucose oxidase (GOD) membrane. The biosensor is seamlessly integrated with a glucose sensor and a wireless measurement system. The glucose sensor is capable of highly sensitive detection between 5 and 1,000 $\mu\text{mol/L}$ of glucose, encompassing the range of glucose concentrations found in human saliva.

In addition, a cellulose acetate (CA) membrane is formed as an interference rejection membrane on a glucose sensor to measure glucose in saliva. Glucose in saliva is successfully measured in-vivo without any pretreatment of human saliva. Salivary components of ascorbic acid and uric acid inhibit the accurate measurement of the glucose concentration in human saliva. CA-coated electrodes were prepared to investigate the interference rejection membrane. The developed mouthguard sensor could quantify glucose concentrations between 1.75 and 10,000 $\mu\text{mol/L}$. For saliva samples collected from healthy subjects, the measurement output corresponded to the concentration, which suggests that glucose may be measured². This mouthguard glucose sensor can provide a useful method for the unrestricted and noninvasive monitoring of saliva glucose to manage of diabetes patients.

Keywords: mouthguard, glucose sensor, wearable biosensor, oral cavity, enzyme



References

1. T. Arakawa et al., IEEJ Trans. Electr. Electron. Eng, 17, 5, 626–636, 2022.
2. T. Arakawa et al., Anal Chem, 92, 18, 12201–12207, 2020.

Synthesis and properties of stacked boron single-layer materials

Tetsuya Kambe

Osaka University

*Corresponding author: kambe.t.aa@chem.eng.osaka-u.ac.jp

Abstract

Graphene has been the focus of countless research efforts across multiple fields, and various 2D materials have been reported. In my previous work, we investigated finely-controlled inorganic synthesis through bottom-up synthesis of metal complex nanosheets and atomicity-controlled clusters. In this study, we have investigated synthesis of single-layer materials like graphene by using boron elements.¹ The prepared nanosheet demonstrated a liquid crystalline nature, applicable for electronic devices.²

The atomically flat boron network skeleton was synthesized through a simple solution-based method from KBH_4 . X-ray diffraction analysis, electron microscopy, IR spectroscopy, and atomic force microscopy revealed the 2D structure, wherein layers of boron atoms with oxygen atoms to form a hexagonal 2D network were sandwiched between layers of potassium cations. The characteristic conducting properties of stacked borophene-like sheets were also revealed through temperature dependence experiments. Additionally, the liquid crystalline feature was achieved through chemical modification. The obtained liquid crystal exhibited high thermal stability and was applied to a switching device driven by electronic stimuli.

Keywords: Inorganic synthesis, Nanomaterials, Atomic layers

References

1. Kambe, T.; Hosono, R.; Imaoka, S.; Kuzume, A.; Yamamoto, K. *J. Am. Chem. Soc.* 2019, *141*, 12984; Kambe, T.; Nishihara, H.; Yamamoto, K. *Dalton Trans.*, 2023, *52*, 15297.
2. Kambe, T.; Imaoka, S.; Shimizu, M.; Hosono, R.; Yan, D.; Taya, H.; Katakura, M.; Nakamura, H.; Kubo, S.; Shishido, A.; Yamamoto, K. *Nat. Commun.* 2022, *13*, 1037.

Chloride Speciation in Crude Oil & Liquid Hydrocarbon Chain

Norzaimi Azam

Analytical Technology, Group Technical Solutions, PETRONAS

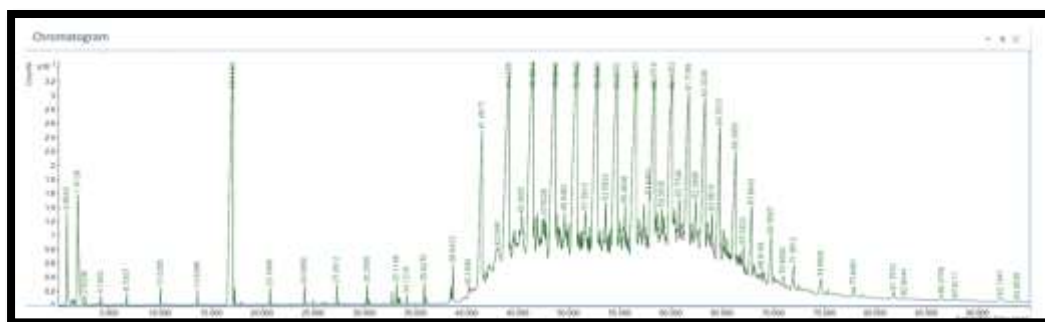
norzaimiazam@petronas.com

Historical data from Refinery Plant reveals significant problems in the Crude Distillation Unit (CDU), Vacuum Distillation Unit (VDU), and downstream atmospheric column due to the carryover of organic and inorganic chlorides, which are not effectively removed during the Desalter stage. Despite treatment, inorganic chloride levels reach up to 1.2 parts per billion, causing serious refinery issues.

Globally, oil and gas industries face similar chloride contamination challenges, worsened by the lack of comprehensive databases to monitor chloride distribution through the supply chain. Additionally, the absence of standardized methods to identify organic chloride species in crude oil complicates refineries' ability to predict and address contamination impacts.

Organic and inorganic chlorides in crude oil come from different sources—organic chlorides are often added at production wells as solvents or additives, while inorganic chlorides stem from crude oil's contact with saline water during extraction. These chlorides cause various types of corrosion in refinery operations due to their distinct chemical behaviours.

Hydrochloride (HCl) corrosion, resulting from the presence of chlorides and free water, significantly affects the overhead system of the atmospheric column and the downstream vacuum column unit, especially in the Light Vacuum Gas Oil (LVGO) fractions. The acidic HCl, formed at high temperatures, rapidly corrodes metal surfaces, compromising refinery equipment integrity and increasing the risk of unexpected shutdowns and safety hazards.



Key words:

1. Chlorides
2. Corrosion
3. Refinery
4. Desalter
5. Contamination

Corrosion and operational downtime have caused significant financial losses for Refinery Plant, with repair and maintenance costs expected to reach RM 20 million between 2018 and 2025. Additionally, the refinery's Loss of Production Opportunity (LPO) is estimated at RM 14 million, impacting efficiency and profitability. This underscores the need for effective chloride management strategies.

Development of Selective PR Antagonists Using Ferrocene as A Three-Dimensional Building Platform

Kotaro Ochiai^{a*}, Hiroyuki Kagechika^a, Shinya Fujii^a

^a Institute of Biomaterials and Bioengineering, Tokyo Medical and Dental University.

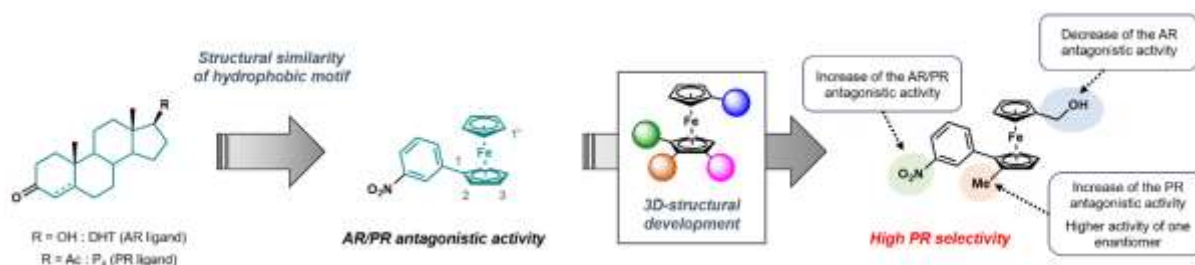
*Corresponding author: ochi.chem@tmd.ac.jp

Abstract

Ferrocene is a chemically stable and intrinsically non-toxic organometallic compounds, and has recently garnered attention in the field of medicinal chemistry.¹ Given the three-dimensional (3D) nature of small molecule-protein interactions, the multi-substituted structure of ferrocene, allowing for the arrangement of multiple pharmacophores in three dimensions, is a fascinating platform for drug design.² In this study, we investigated structural development of nuclear receptor ligands using ferrocene as the 3D building platform.

Progesterone receptor (PR) and androgen receptor (AR), members of steroid hormone nuclear receptors of ligand-dependent transcription factors, are important drug targets of various diseases including cancers. Based on similarities between the phenylferrocene framework and the steroidal skeleton, firstly we designed phenylferrocene derivatives as novel PR and AR ligand candidates, and found that nitrophenylferrocene derivatives and cyanophenylferrocene derivatives acted as potent antagonists toward PR and AR.^{3,4} Since the developed phenylferrocene derivatives were good lead compounds for further structural development, we then investigated the development of multiple substituted ferrocene derivatives to improve the potency and target selectivity. We designed and synthesized a series of disubstituted ferrocene derivatives including regioisomers, and evaluated their PR/AR ligand activities. As a result, the introduction of a hydrophobic substituent at 2-position enhanced PR antagonistic activity compared to the AR antagonistic activity. Separation of planar enantiomers revealed that one of enantiomers of these 1,2-disubstituted derivatives showed more potent activity. On the other hand, introduction of hydrogen bond donor at 1'-position decreased the AR antagonistic activity. Based on these findings, we designed and synthesized 1,1',2-trisubstituted ferrocene derivatives as potent and selective PR antagonist candidates. As expected, the 1,1',2-trisubstituted ferrocene derivatives showed highly selective PR antagonistic activity. The developed compounds are versatile lead compounds for novel PR antagonists, and these results also indicate that ferrocene is a useful 3D building platform for biologically active compounds with improved potency and selectivity.

Keywords: ferrocene, PR antagonist, AR antagonist, 3D building platform, planer chirality



References

1. Patra, M.; Gasser, G. *Nat. Rev. Chem.* **2017**, *1*, 0066.
2. Morrison, C. N.; Prosser, K. E. et. al. *Chem. Sci.* **2020**, *11*, 1216.
3. Ochiai, K.; Yonezawa, R.; Fujii, S. *ChemMedChem* **2024**, *19*, e202400040.
4. Ochiai, K.; Fujii, S. *Bioorg. Med. Chem. Lett.* **2021**, *46*, 128141.

INVESTIGATION ON CHARACTERIZATION OF TEVSHIIN GOVI COAL AND IT'S LIQUID PRODUCTS OBTAINED BY PYROLYSIS AND HYDROGENATION

**Batbileg Sanjaa, Namkhainorov Jargalsaikhan, Shiirav Gandandorj,
Altantuul Amarbayasgalan, Purevsuren Barnasan ***

Institute of Chemistry and Chemical Technology, Mongolian Academy of Sciences, 4th Building of
MAS, Ulaanbaatar, 13330 Mongolia.

*Corresponding author: bpurevsuren.icct@gmail.com

Abstract

Mongolia, one of the top 10 coal-rich countries globally, has 175 billion tons of geological coal resources, predominantly brown coal, which cannot be exported due to its lower quality. To address this, advanced coal processing technologies like pyrolysis and hydrogenation are essential. This research investigates the composition and characteristics of coal from the Tevshiin Govi deposit in Mongolia and examines the outputs of pyrolysis and hydrogenation processes.

Experiments were conducted with coal pyrolysis at 600°C for 80 minutes and hydrogenation at 435°C for 120 minutes under 30 bar hydrogen pressure. The liquid product yield from hydrogenation was 59.97%, significantly higher than the 30.28% yield from pyrolysis. Vacuum distillation of the hydrogenation liquid product revealed light, middle, and heavy fractions at 29.36%, 51.52%, and 19.22%, respectively. The neutral oil in the pyrolysis tar constituted 85.00% and was analyzed using GC/MS after being dissolved in various solvents. Additionally, the middle fraction of petroleum products, containing hydrogenated phenanthrene as a donor solvent, was distilled and analyzed similarly. The technical and elemental analysis of coal from the Tevshiin Govi deposit revealed an ash yield of 21.70%, volatile matter yield of 49.69%, carbon content of 60.89%, hydrogen content of 3.26%, and an H/C atomic ratio of 0.64. The coal ash composition included $\text{AlPO}_4(\text{OH})_3$, along with minerals like SiO_2 , CaSO_4 , and NaAlSiO_8 .

Keywords: brown coal, pyrolysis, hydrogenation, tar, distillate fraction.

References

1. Kuznetsov P.N., Budeebazar A., Fan Xing., Perminov N.V., Kuznetsova L.I., Korolkova I.V. *Journal of Siberian Federal University. Engineering & Technologies*, 2020, 13, 1018–1027
2. Mochida I., Okuma O., Yoon S.H., *Chemical Reviews*, 2014, 114, 1637

Chemical Synthesis of Fe-based Novel Magnets by Topotactic Reaction

Masaki Mizuguchi^{a, b, *}

^a Institute of Materials and Systems for Sustainability, Nagoya University, Japan

^b Materials Process Engineering, Graduate School of Engineering, Nagoya University, Japan

*Corresponding author: mizuguchi.masaki@material.nagoya-u.ac.jp

Abstract

Demand for high-performance magnet materials is increasing in various fields, including the automotive, electronics, and medical industries. However, the current mainstream permanent magnet materials contain rare earths and are faced with the problems of resource depletion and price escalation. Therefore, there is a need for new permanent magnet materials that do not contain rare earths. Particularly, materials with the CuAu crystal lattice structure ($L1_0$) have large uniaxial magnetic anisotropy, thus many studies on $L1_0$ type materials have been reported. However, it is a crucial problem that typical $L1_0$ type materials such as FePt, CoPt, and FePd include noble metals of Pt or Pd. To solve this problem, the development of novel magnetically anisotropic materials without noble metals is now eagerly expected. In this study, we aim to synthesize an $L1_0$ type FeNi alloy with a large magnetic anisotropy¹⁻⁷, which exists only in an iron meteorite as a Widmannstätten structure in nature. Single-phase $L1_0$ type FeNi powders were fabricated through a new chemical method, nitrogen insertion and topotactic extraction (NITE)⁸. In the method, FeNiN, which has the same ordered arrangement as $L1_0$ type FeNi, is formed by nitriding Al-FeNi powder with ammonia gas. Subsequently, FeNiN is denitrided by topotactic reaction to derive single-phase $L1_0$ -FeNi with a chemical order parameter of 0.71. The transformation of disordered phase-FeNi into the $L1_0$ phase increased the coercive force from 14.5 kA/m to 142 kA/m, and an actual motor was fabricated. The proposed method not only significantly accelerates the development of magnets using $L1_0$ -FeNi but also offers a new synthesis route to obtain ordered alloys in non-equilibrium states. In fact, this method was utilized for synthesis of thin films of FeNi and FeCo magnets^{9, 10}. We hope that, in the future, the NITE method will be developed further to facilitate the derivation of completely new ordered alloys that are superior in terms of characteristics such as magnetism, toughness, and catalytic performance.

Keywords: $L1_0$ -FeNi, Widmannstätten structure, nitrogen insertion and topotactic extraction, magnetically anisotropic materials

References

1. Mizuguchi, M.; Sekiya, S.; Takanashi, K. *J. Appl. Phys.* **2010**, *107*, 09A716-1-3.
2. Mizuguchi, M.; Kojima, T.; Kotsugi, M.; Koganezawa, T.; Osaka, K.; Takanashi, K. *J. Magn. Soc. Jpn.* **2011**, *35*, 370-373.
3. Kojima, T.; Ogiwara, M.; Mizuguchi, M.; Kotsugi, M.; Koganezawa, T.; Ohtsuki, T.; Tashiro, T.Y.; Takanashi, K. *J. Phys. Cond. Matt.* **2014**, *26*, 064207-1-10.
4. Takanashi, K.; Mizuguchi, M.; Kojima, T.; Tashiro, T.; *J. Phys. D, Appl. Phys.* **2017**, *50*, 483002-1-9.
5. Tashiro, T.; Mizuguchi, M.; Kojima, T.; Koganezawa, T.; Kotsugi, M.; Ohtsuki, T.; Sato, K.; Konno, T.J.; Takanashi, K. *J. Alloys Compd.* **2018**, *750*, 164-170.
6. Saito, M.; Mizuguchi, M.; *et. al. Appl. Phys. Lett.* **2019**, *114*, 072404-1-5.
7. Thiruvengadam, V.; Mizuguchi, M.; *et. al. Appl. Phys. Lett.* **2019**, *115*, 202402-1-4.
8. Goto, S.; Kura, H.; Watanabe, E.; Hayashi, Y.; Yanagihara, H.; Shimada, Y.; Mizuguchi, M.; Takanashi, K.; Kita, E. *Sci. Rep.* **2017**, *7*, 13216-1-7.
9. Ito, K.; Mizuguchi, M.; *et. al. J. Alloys Compd.* **2023**, *946*, 169450-1-10.
10. Umeda, Y.; Mizuguchi, M.; *et. al. Jpn. J. Appl. Phys.* **2024**, *63*, 04SP80-1-5.

X-ray absorption spectroscopic analysis by ligand field theory in Co ferrites: Understanding of conductivity and magnetic anisotropy

Jun Okabayashi^{a,*}

^aResearch Center for Spectrochemistry, The University of Tokyo

*jun@chem.s.u-tokyo.ac.jp

Abstract

Spinel-compounds CoFe_2O_4 (CFO) is the most famous for Co-based ferrites because they are utilized as device applications using spin filtering, high-frequency performance and magneto-resistive properties. Recent researches focus on the synthesis in the thin film form with perpendicularly magnetic anisotropy and conductive-insulating switching properties. These properties are originated from the control of Fe^{2+} , Fe^{3+} states with O_h and T_d symmetries in the spinel-type unit cell as shown in Fig. 1a. As an issue of solid state chemistry, element-, site-, symmetry-dependent electronic and magnetic states have to be clarified. In this talk, I discuss the microscopic origin of conductive / insulating properties in CFO films from the viewpoints of ligand field theory.

The CFO samples were prepared by pulsed laser deposition method with 20 nm thickness by controlling the oxygen pressure during the deposition. X-ray absorption spectroscopy (XAS) and magnetic circular dichroism (XMCD) were performed at the Photon Factory in KEK, Tsukuba.

XAS and XMCD of CFO are shown in Fig. 1b. Fe L-edge XMCD exhibits the ratio of Fe^{2+} (O_h), Fe^{3+} (O_h) and Fe^{3+} (T_d) sites. These spectra can be fitted by ligand-field theory simulation. The control of conductivity originates from the amounts of Fe^{2+} states. The line shape of Co XMCD indicates large orbital magnetic moments in the Co^{2+} sites of $3d^7$ configuration, which can be interpret as the energy level splitting as shown in Fig. 1c. The down spin electrons in the double degenerated states are essential for the perpendicular magnetic anisotropy. These results suggest that the XMCD can be a powerful technique to probe the conductivity and magnetic anisotropy in the Co ferrites.

This work was performed by the collaboration with Prof. K. Mibu, M.A. Tanaka in Nagoya Institute of Technology.

Keywords: Solid state chemistry, X-ray spectrochemistry, Magnetic properties, ligand-field theory, spinel-type Co ferrites

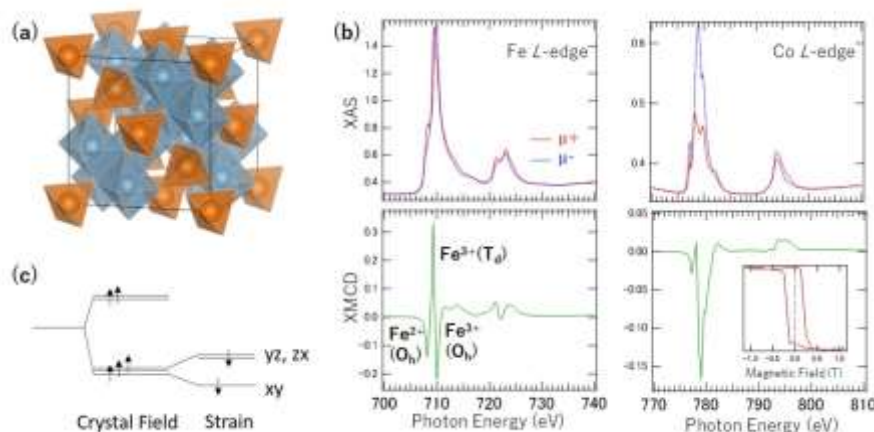


Fig. 1: (a) Schematic illustration of spinel-type unit cell with colored O_h and T_d symmetry sites. (b) XAS and XMCD of Fe and Co L-edges in CoFe_2O_4 . Inset shows the hysteresis curve at Co L_3 -edge. (c) Energy diagram of Co^{2+} ($3d^7$) states. The strain induce the splitting, which enhancing the orbital magnetic moment.

References

1. Okabayashi, J. et al., *Phys. Rev. B* 2021, 105, 134416.
2. Morishita, M., Okabayashi, J. et al., *Phys. Rev. Mater.* 2023, 7, 054402.

Metal-Free Dibenzoxazepinone Synthesis by Hypervalent Iodine-Mediated Iterative Coupling Reactions

Toshifumi Dohi

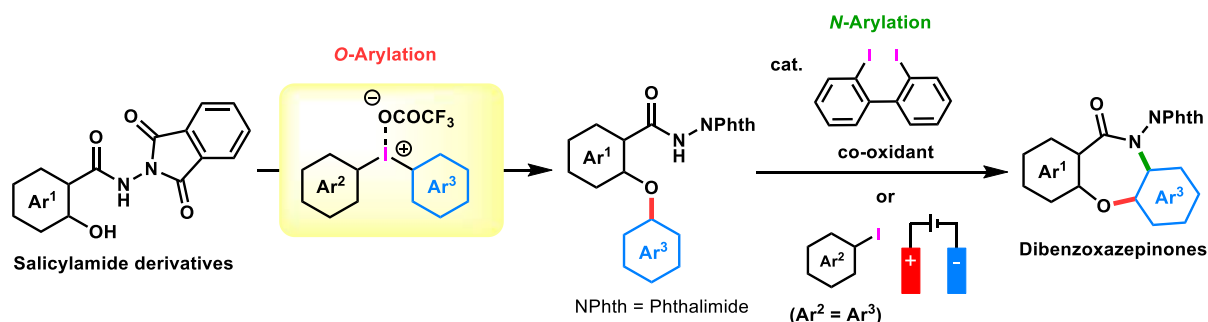
College of Pharmaceutical Sciences, Ritsumeikan University, 1-1-1 Nojihigashi, Kusatsu, Shiga
525-8577, Japan
td1203@ph.ritsumei.ac.jp

Abstract

Hypervalent iodine reagents have several advantages over metal-based oxidants and catalysts, such as the low toxicity, mild reactivity, easy availability, stability, ease of handling, and their recovery and recyclability. These characteristics make them useful alternative reagents for performing metal-free synthesis. Recently, our group developed the metal-free arylation method using aryl(2,4,6-trimethoxyphenyl)iodonium(III) salts (aryl(TMP)iodonium(III) salts) for the reactions of *O*-, *N*-, *C*-nucleophiles¹. We also reported several catalytic C-N coupling reactions using μ -oxo hypervalent iodine reagents². The intermolecular aromatic ring amination by in situ generated μ -oxo hypervalent iodine reagents effectively gave corresponding *N*-aryl amides^{2c}, while the intramolecular amination process afforded useful heterocyclic compounds such as benzolactam and dibenzoxazepinone derivatives^{2d}.

We now extend the strategies to a new metal-free dibenzoxazepinone synthesis through the chemoselective phenol *O*-arylation with diaryliodonium(III) salts and catalytic intramolecular aryl amination sequence. In the reaction between *N*-(1,3-dioxoisindolin-2-yl)-2-hydroxy benzamide and phenyl(TMP)iodonium(III) trifluoroacetate, selective *O*-arylation occurred at the phenol oxygen, and the successive μ -oxo hypervalent iodine-catalyzed intermolecular aryl amination yielded target dibenzoxazepinone. This sequential coupling process was applicable to a wide range of salicylamides and aryl(TMP)iodonium(III) trifluoroacetates³ to give dibenzoxazepinones with electron-donating and withdrawing group as well as halogen functionality. In particular, the iodoarene byproduct produced during the first-stage *O*-arylation could serve as a mediator for the second-stage aryl amination under electrochemical oxidation conditions.

Keywords: iodine, hypervalent compound, coupling, metal-free, dibenzoxazepinone



References

1. Kikushima, K.; Dohi, T. *J. Synth. Org. Chem., Jpn.* **2023**, *81*, 463 and references therein.
2. (a) Dohi, T.; Takenaga, N.; Fukushima, K.; Uchiyama, T.; Kato, D.; Shiro, M.; Fujioka, H.; Kita, Y. *Chem. Commun.* **2010**, *46*, 7697. (b) Kumar, R.; Dohi, T.; Zhdankin, V. V. *Chem. Soc. Rev.* **2024**, *53*, 4786. (c) Sasa, H.; Mori, K.; Kikushima, K.; Kita, Y.; Dohi, T. *Chem. Pharm. Bull.* **2022**, *70*, 106. (d) Sasa, H.; Hamatani, S.; Hirashima, M.; Takenaga, N.; Hanasaki, T.; Dohi, T. *Chemistry* **2023**, *5*, 2155.
3. Miyamoto, N.; Koseki, D.; Sumida, K.; Elboray, E. E.; Takenaga, N.; Kumar, R.; Dohi, T. *Beilstein J. Org. Chem.* **2024**, *20*, 1020.

Subcellular niche segregation of co-obligate symbionts in whiteflies

Akiko Fujiwara^{a,b}, Xian-Ying Meng^c, Yoichi Kamagata^c, Tsutomu Tsuchida^d

^aCenter for Food Science and Wellness, Gunma University, Japan.

^bChemical Genomics Research Group, Center for Sustainable Resource Science, RIKEN, Japan.

^cBioproduction Research Institute, National Institute of AIST, Japan.

^dFaculty of Science, Academic Assembly, University of Toyama, Japan.

*Corresponding author: akiko_fujiwara@gunma-u.ac.jp

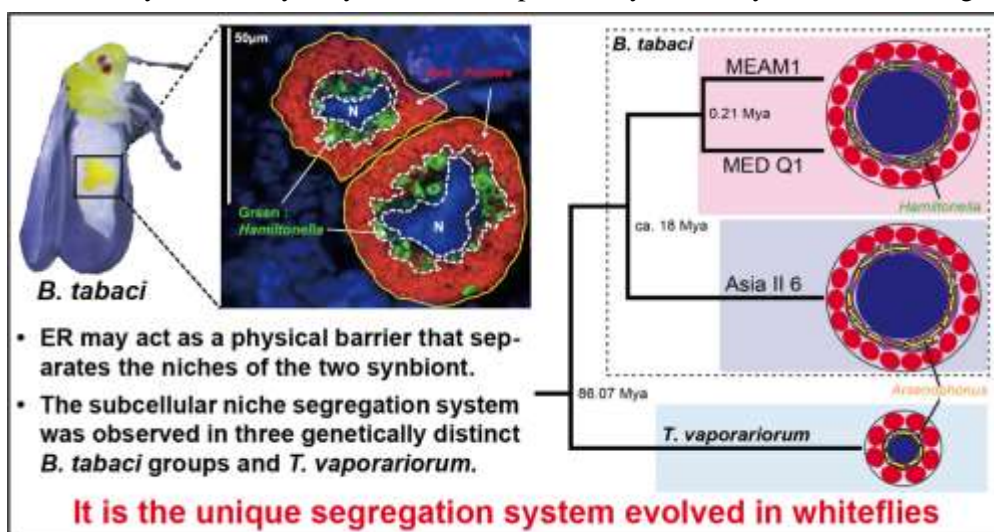
Abstract

The sweet potato whitefly, *Bemisia tabaci* (Hemiptera: Aleyrodidae), is a notorious pest insect on agricultural crops worldwide. *B. tabaci* consists of at least 44 genetic groups based on the mitochondria cytochrome oxidase I sequences. In recent years, two genetic groups of *B. tabaci*, referred to Middle East-Asia Minor 1 (MEAM1) and Mediterranean Subclade Q1 (MED Q1), have been spread globally. Previous studies have reported that the both genotypes possess two phylogenetically distinct endosymbiotic bacteria, *Portiera* and *Hamiltonella*, which form an essential multiple endosymbiotic system in the insect's body¹. Interestingly, these co-obligate symbionts are stably localized within the same bacteriocyte, a specialized cell in the body cavity. This endosymbiotic system is completely different from that of other insects, in which co-obligate symbionts are localized in separate bacteriocytes. We studied to elucidate the mechanisms underlying symbiont coexistence in this unique endosymbiotic system in *B. tabaci*.

Fluorescence *in situ* hybridization, electron microscopy, and immunohistochemical analyses revealed that the two co-obligate endosymbionts in *B. tabaci* occupy distinct subcellular habitats, or niches, within a single bacteriocyte through developmental stages, separated by the cell's endoplasmic reticulum (ER). This subcellular niche segregation was also observed in three genetically distinct *B. tabaci* groups and even in *Trialeurodes vaporariorum*, which belongs to a different genus. This result suggests that the habitat segregation system existed in a common ancestor and has been conserved during evolution in both lineages².

Further research based on our findings is expected not only to reveal details of the evolution of multiple endosymbiotic systems, but also to be applied to novel *B. tabaci* control methods, because this system is essential for host survival and reproduction.

Keywords: whitefly, bacteriocyte, symbiont, multiple endosymbiotic systems, habitat segregation



References

1. Fujiwara, A.; Maekawa, K.; Tsuchida, T. *J. Appl. Entomol.* 2015, 139, 55-66.
2. Fujiwara, A.; Meng, X.Y.; Kamagata, Y.; Tsuchida, T. *Microbiol. Spectr.* 2023, 11, DOI: 10.1128/spectrum.04684-2.

Toxicity Predictor: A Tool to Predict Biochemical Pathways Related to Toxicities from Chemical Structures

Yoshihiro Uesawa^{a*}

^a*Department of Medical Molecular Informatics,
Meiji Pharmaceutical University, Japan*

^{*}*Corresponding author: uesawa@my-pharm.ac.jp*

Abstract

Quantitative structure–activity relationship analysis methods enable the prediction of physiological activities such as enzyme inhibition based on chemical structures. However, toxicity is a complex physiological phenomenon that can develop through different biochemical mechanisms, even for the same phenotypic systems. Therefore, a tool was developed in our laboratory (the Toxicity Predictor) that forecasts activities associated with various nuclear receptors and stress response pathways to predict toxicity.¹⁻⁴⁾

The developed tool predicted 59 biochemical activities associated with toxicity expressions, which were identified in the Tox21 project in the United States. A machine learning model was constructed using the XGBoost algorithm, which utilizes activity values from approximately 10,000 compounds as objective variables and chemical structure descriptors calculated by the mordred software as explanatory variables. The performance of predictive models was rigorously evaluated through external validation, revealing good prediction performance of more than 0.8 as the area under the ROC curve was achieved for many targets.¹⁾ In addition, the models successfully predicted hepatotoxicity and pulmonary toxicity using these biochemical activity predictions. These prediction models are available from the laboratory server.⁵⁾

Keywords: QSAR, machine learning, toxicity, cheminformatics, DILI

References

1. Kurosaki K, Wu R, Uesawa Y. *Int J Mol Sci.* 2020, 23;21(21):7853
2. Kurosaki K, Uesawa Y. *J Toxicol Sci.* 2022;47(3):89-98
3. Okunaka M, Kano D, Uesawa Y. *Int J Mol Sci.* 2022;23(20):12407
4. Hosoya R, Ishii-Nozawa R, Terajima T, Kagaya H, Uesawa Y. *Pharmaceuticals* (Basel). 2024;17(3):379
5. Toxicity Predictor, <http://mmi-03.my-pharm.ac.jp/tox1/>

Spirobipyridine Ligands for Efficient and Selective Synthesis through Noncovalent Interactions

Sobi Asako^{a*}, Yushu Jin^a, Ramadoss Boobalan^a, Laurean Ilies^{a*}

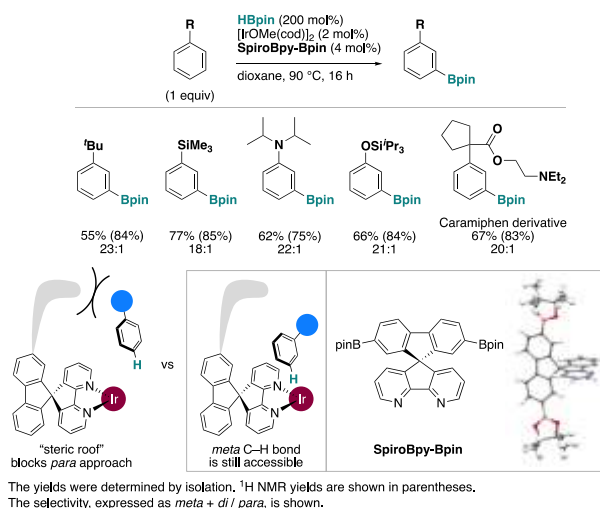
^aRIKEN Center for Sustainable Resource Science

*Corresponding authors: sobi.asako@riken.jp, laurean.ilies@riken.jp

Abstract

Since its discovery 130 years ago, various derivatives of 2,2'-bipyridine have been developed and found numerous applications. The fine-tuning of their structures and properties, achieved by introducing substituents around the periphery of the bipyridine skeleton or through π -extension, has played a crucial role. In contrast, we have recently delved into the function of spirobipyridine (**SpiroBpy**) derivatives, three-dimensionally extended analogues of planar bipyridines. Our first design in this category is the conceptually novel ligand **SpiroBpy-Bpin**. It sterically protects the furthest *para* site in addition to the *ortho* site, enabling *meta*-selective C–H activation in iridium-catalyzed borylation.¹ The rigid Bpin group attached to **SpiroBpy** acts as a “remote steric roof”,² creating a molecular pocket that accommodates substrate approaching the metal center exclusively in the *meta* orientation. This strategy has proven to be general, allowing selective *meta*-borylation of various monosubstituted arenes, including alkylbenzenes, anilines, phenols, and drug molecules. Further investigations revealed that the iridium/**SpiroBpy** catalyst also accelerates C–H borylation reactions. Thus, reluctant electron-rich arenes react more efficiently with **SpiroBpy** than with commonly used flat bipyridine ligands.³ We identified a CH– π interaction between the ligand backbone and the arene substrate as the key factor in this enhanced reactivity. We anticipate that **SpiroBpy** derivatives, capable of recognizing substrates through noncovalent interactions, will find broad applications as ligands in transition metal catalysis, addressing challenges that remain unsolved with conventional planar bipyridines.

Keywords: spirobipyridine, C–H functionalization, remote steric control, noncovalent interaction, iridium



References

- Ramadoss, B.; Jin, Y.; Asako, S.; Ilies, L. *Science* **2022**, *375*, 658.
- Asako, S.; Ilies, L. *Synlett* **2023**, *34*, 2110.
- Jin, Y.; Ramadoss, B.; Asako, S.; Ilies, L. *Nat. Commun.* **2024**, *15*, 2886.

Physicochemical Properties and Application of Phosphine Boranes in Structural Development of Biologically Active Compounds

Shinya Fujii

Institute of Biomaterials and Bioengineering, Tokyo Medical and Dental University

*Corresponding author: fujii.s.chem@tmd.ac.jp

Abstract

Phosphine boranes are complexes of phosphines and boranes bearing P–B bonds. In this study, in order to reveal the potential utility of phosphine boranes in the drug discovery chemistry, we systematically investigated the structure-property relationship of phosphine boranes and their application as structural options in medicinal chemistry.

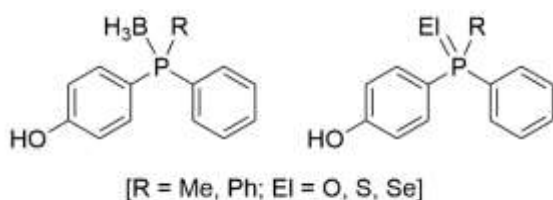
Firstly, using 4-phosphinophenol substructure as the common platform, we designed and synthesized a series of phosphine and related compounds including phosphine boranes, and investigated their physicochemical properties and activity for estrogen receptors (ERs). Several compounds exhibited ER ligand activity, and in interestingly, phosphine borane derivatives bearing P–BH₃ substructure exhibited significant ER antagonistic activity more potent than the corresponding phosphine oxide and other chalcogenide derivatives.[1]

Next, we investigated the substitution on the boron atom. We designed and synthesized phosphine borane derivatives bearing a *B*-hydroxyphenyl group, and then investigated the physicochemical properties such as stability in phosphate buffered saline (PBS), hydrophobicity (Log*P*), membrane affinity (Log*K*_{IAM}), and acidity (p*K*_a). The synthesized phosphineborane derivatives exhibited comparable stability in PBS compared to the corresponding isoelectronic silane and alkane derivatives, with a slight decrease in hydrophobicity and membrane affinity, as well as a decrease in acidity. Biological evaluation revealed that compounds bearing PEt₃, P(*i*-Pr)₃, or P(*c*-Pr)₃ structure showed significant ER α agonistic activity.[2] We also designed and synthesized a series of *B*-(trifluoromethyl)phenyl phosphine borane derivatives, and found the synthesized compounds function as progesterone receptor (PR) ligands.[3]

These results indicated that the phosphine borane substructure is a new option in the structural development study of biologically active compounds, and also the information of physicochemical properties is useful for the rational molecular design of unique bioactive compounds bearing a P–B bond.

Keywords: Phosphine borane, phosphorus, hydrophobicity, estrogen, progesterone

A) 4-Phosphinophenol derivatives



B) *B*-Substituted phosphine borane derivatives



References

- Saito, H.; Matsumoto, Y.; Hashimoto, Y.; Fujii, S. *Bioorg. Med. Chem.* **2020**, *28*, 115310.
- Miyajima, Y.; Noguchi-Yachide, T.; Ochiai, K.; Fujii, S. *RSC Med. Chem.* **2024**, *15*, 119-126.
- Miyajima, Y.; Ochiai, K.; Fujii, S. *Molecules* **2024**, *29*, 1587.

Development of target directing water-soluble cyclooctadiynes and their application to bio-molecules

Masayuki Tera^a

^a*Institute of Engineering, Tokyo University of Agriculture and Technology.*

*Corresponding author: tera@go.tuat.ac.jp

Abstract

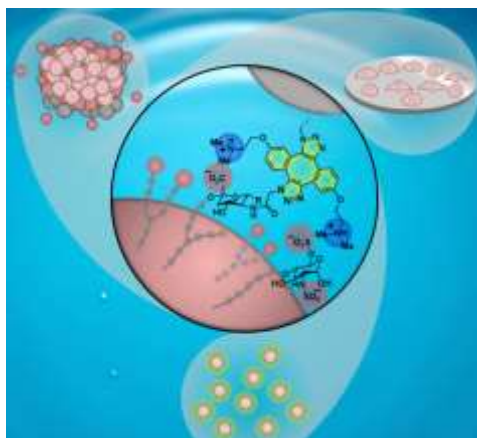
The 2022 Nobel Prize in Chemistry highlighted the utility of click chemistry, a method that enables the efficient linking of two molecules in aqueous conditions at room temperature. This technique is widely used in chemical biology, polymer chemistry, and molecular biology. Among various click reactions, the strain-promoted azide-alkyne cycloaddition (SPAAC) is notable for its broad applications, not requiring metal catalysts. However, increasing the reactivity of strained alkynes often leads to undesired side reactions, creating a trade-off between reactivity and stability.

We developed a water-soluble dibenzo cyclooctadiyne derivative, WS-CODY, with target-directing properties for SPAAC reactions.^{1,2} WS-CODY can link two azide groups, and its ionic side chains enhance reaction rates based on the target molecule's polarity. For instance, DMA-CODY, which has tertiary amine side chains, reacts with negatively charged biomolecules over 1000 times faster than with neutral azide groups. Applied to azide-modified cell surfaces, DMA-CODY facilitated cell-to-cell and cell-to-glass adhesion within 15-30 minutes in culture medium, independent of the cells' intrinsic adhesion properties. Moreover, chemical cell adhesion via DMA-CODY induced the expression of adhesion-related genes.³

In a recent study, we further explored the potential of WS-CODY by linking azide-modified hyaluronic acid (HA-N₃) to azide-modified cell surfaces, achieving rapid and stable cell aggregation. By optimizing HA-N₃ and WS-CODY concentrations, we created cell aggregates within 10 minutes, which remained stable for up to five days with approximately 80% cell viability. Transcriptome analysis revealed significant upregulation of genes associated with cell migration and adhesion, suggesting that HA-N₃-mediated aggregation induces intrinsic cellular responses.⁴ This target directing click chemistry-based approach offers a versatile and efficient method for forming cell aggregates and modulating cell-matrix interactions, with potential applications in tissue engineering and regenerative medicine.

Keywords: click reaction, metabolic labeling, DNA crosslink, 3D culture, spheroid

Graphical abstract



References

1. Tera, M.; Harati Taji, Z.; Luedtke, N. W.* *Angew. Chem. Int. Ed.* **2018**, 57 (47), 15405–15409.
2. Yoshinaga, M.; Tera, M.* *et al.*, *Chem. Commun.* **2023**, 59 (44), 6678–6681.
3. Kitagawa, K.; Tera, M.* *et al.*, *Bioconjug. Chem.* **2023**, 34 (4), 638–644.
4. Sato, F.; Tera, M.* *et al.*, under review.

Chemo-enzymatic transformation of carbohydrates and related substances

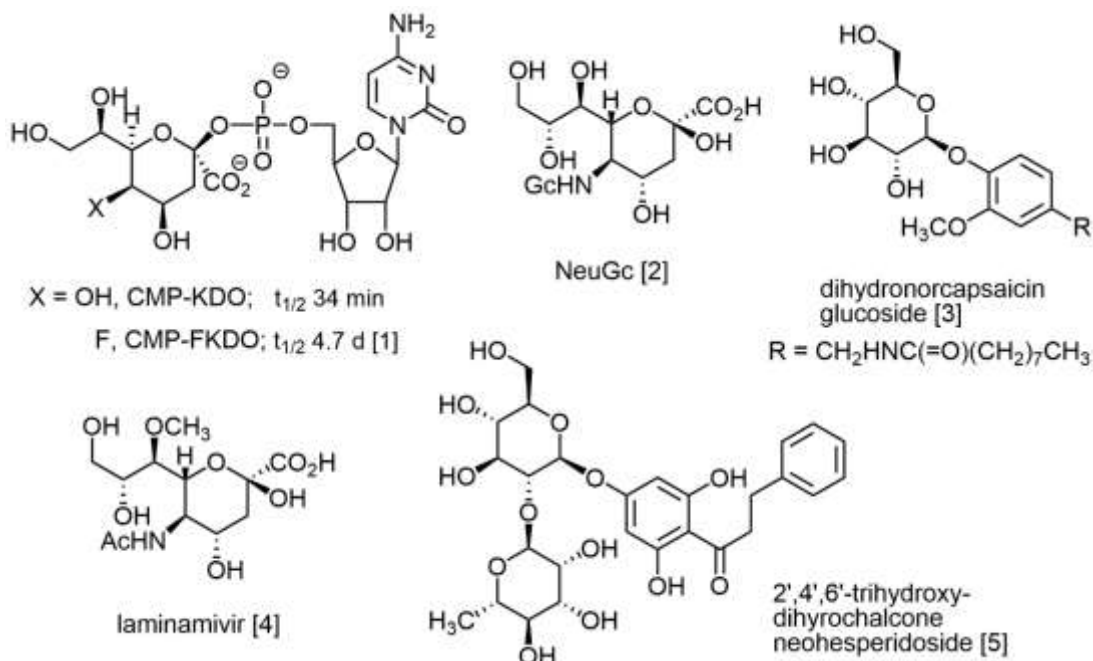
Takeshi Sugai^{a*}, Kengo Hanaya^b, Shuhei Higashibayashi^b^aProfessor Emeritus, Keio University, Japan^bFaculty of Pharmacy, Keio University, Japan

*Corresponding author: sugai@keio.jp

Abstract

In 1991-1992, Prof. C.-H. Wong in Scripps research institute in California accepted T.S. in his group of glycochemistry and glycobiology, and T.S. started his carrier of enzyme-mediated synthesis of carbohydrates. After coming back to Japan, T.S. decided to obey three policies: 1) no use of biosynthetic enzymes; 2) no use of engineering of enzyme protein; 3) reasonable design of substrates and synthetic schemes. In this talk, we present the history of our original chemo-enzymatic transformation of carbohydrates and related substances, towards the syntheses of bioactive substances in both of Faculty of Science and Technology (before 2008) and Faculty of Pharmacy (after 2008), with the examples as shown in graphical abstract.

Keywords: carbohydrate, glycoside, lipase, *N*-acetylglucosamine deacetylase, hydrolysis

**References**

1. Sugai, T.; Lin, C.-H.; Shen, G.-J.; Wong, C.-H. *Bioorg. Med. Chem.* **1995**, *3*, 313-20
2. Kuboki, A.; Okazaki, H.; Sugai, T.; Ohta, H. *Tetrahedron* **1997**, *53*, 2387-2400
3. Sultana, I.; Shimamoto, M.; Obata, R.; Nishiyama, S.; Sugai, T. *Sci. Technol. Adv. Mater.* **2006**, *7*, 197-201
4. Calveras, J.; Nagai, Y.; Sultana, I.; Ueda, Y.; Higashi, T.; Shoji, M.; Sugai, T. *Tetrahedron* **2010**, *66*, 4284-91
5. Tsunekawa, R.; Hanaya, K.; Higashibayashi, S.; Sugai, T. *Biosci. Biotechnol. Biochem.* **2018**, *82*, 1316-22

Visible-Light-Driven Photocatalytic Ammonia Production Using Molybdenum Complexes

Yasuomi Yamazaki^{a,*}, Takahiro Kubo^a, Yoshiki Endo^a, Wang Qiubo^a,
Yoshiaki Nishibayashi^{a,*}

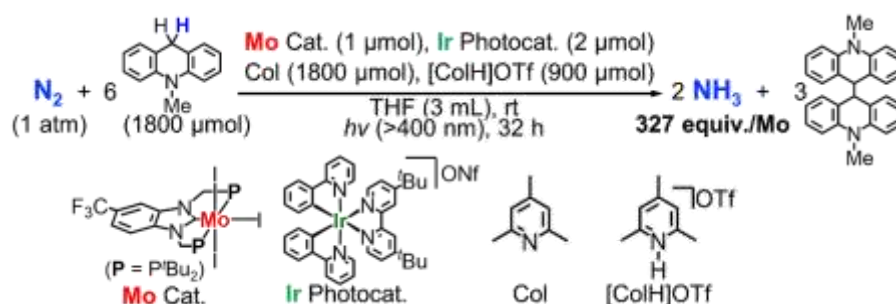
^aSchool of Engineering, The University of Tokyo, Japan.

*Corresponding author: yamazaki-y@g.ecc.u-tokyo.ac.jp, ynishiba@g.ecc.u-tokyo.ac.jp

Abstract

Recently, ammonia has attracted attention as a new energy carrier because it has high energy density and can be easily transported as a liquid. Therefore, it is desirable to develop a synthetic method for green ammonia utilizing renewable energy. One strategy is to use light energy, which can be obtained from sunlight, as a driving force for ammonia synthesis. Quite recently, our group has developed visible-light-driven uphill-type ammonia production.^[1] Ammonia was produced catalytically under visible light irradiation from the reaction with dihydroacridine as an electron donor and a proton source in the presence of molybdenum complexes bearing a PCP-type pincer ligand (Mo cat.) and an iridium complex (Ir photocat.) as catalysts and a photosensitizer, respectively. Under these reaction conditions, 41 equiv. of ammonia were produced based on the Mo atom of the catalyst along with the production of dimerized oxidation products of dihydroacridine. Even though this transformation can potentially convert light energy to chemical energy, the produced amount of ammonia is not so high. These experimental results prompted us to investigate the reaction conditions for details. In this study, we have investigated effective additives to enhance ammonia production. The amount of produced ammonia and reaction rate were largely improved when adding both a pyridine derivative and its conjugate acid. This is probably because the pyridine derivative functioned as a proton mediator to promote both the proton-coupled electron transfer, which is the key process in the ammonia production from dinitrogen, and the deprotonation of dihydroacridine to form a dimer from the dihydroacridine. Furthermore, the amount of produced ammonia reached 327 equivalents when a methyl group was introduced at the nitrogen atom of the dihydroacridine. In the presentation, we will also report on the optimization of reaction conditions and the investigation of the reaction mechanism based on the absorption spectroscopy during the photolysis.

Keywords: Ammonia; Nitrogen Fixation; Photocatalytic Reaction; Molybdenum Complexes



References

1. Y. Ashida, Y. Onozuka, K. Arashiba, A. Konomi, H. Tanaka, S. Kuriyama, Y. Yamazaki, K. Yoshizawa, Y. Nishibayashi, *Nat. Commun.* **2022**, *13*, 7263.

Halogen bonds found in estrogen-related receptor

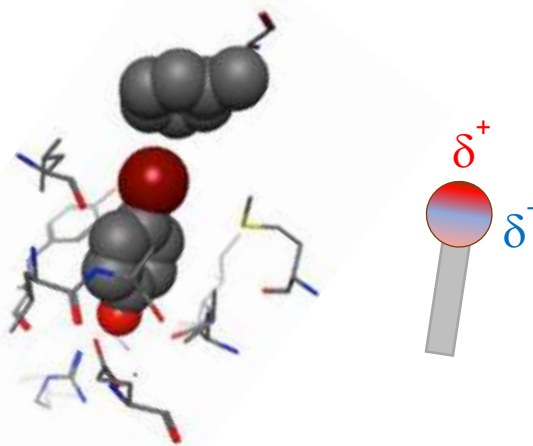
Kotone Ito, Kota Aramaki, Takeru Kajiyama, and Ayami Matsushima*

Laboratory of Structure-Function Biochemistry, Department of Chemistry, Faculty of Science,
Kyushu University, 744, Motoooka, Nishi-ku, Fukuoka 819-0395, Japan

*Corresponding author: ayami@chem.kyushu-univ.jp

Abstract

Interactions between molecules, both within and between them, are vital for protein folding and binding of ligands to receptors. Halogen bonds were introduced in the field of organic chemistry in the 1950s, but it was only in the early 2000s that they were analyzed in biomolecules¹. Halogen atoms are only found in thyroid hormones. Despite being rare in biomolecules, they are essential for the interaction of drugs and toxic environmental chemicals with biomolecules². The strength of halogen bonds is determined by the stabilization energy of the ligand-receptor complex, but calculating the whole structure requires a high cost due to the many atoms in receptor proteins. This necessitates the need for more practical methods to accelerate molecular design and drug discovery. To address this, we propose a coordinate clipping strategy that is suitable for performing the first principal calculation of a protein crystal structure using the DV-X α method. We used estrogen-related receptor γ , a nuclear receptor to which the well-known environmental chemical bisphenols bind, as our model for calculation. We determined the appropriate region for calculation and evaluated the halogen bonds by analyzing the covalent bond located on the opposite side of the halogen bonds. Our findings suggest that clipping nitrogen atoms at the i-1 position in the main chain is beneficial for calculating protein structures. We have also introduced a new index, the HIVE index, to evaluate halogen bonds in biomolecules using DV-X α evaluation³.



Keywords: *ab initio* calculation, estrogen-related receptor, halogen bonds, binding assay

References

1. Auffinger, P.; Hays, F.A.; Westhof, E.; Ho, P.S; *Proc.Nat. Acad. Sci.* 2004, *101*, 16789–16794.
2. Iwamoto, M.; Masuya, T.; Hosose, M.; Tagawa, T.; Ishibashi, T.; Suyama, K.; Nose, T.; Yoshihara, E.; Downes, M.; Evans, R.M.; Matsushima, A.; *J. Biol. Chem.* 2021, *297*, 101173.
3. Masuya, T.; Iwamoto, M.; Liu, X.; Matsushima, A.; *Sci. Rep.* 2019, *9*, 1267.

Photoreaction of *N*-(9*H*-calbazole-1-ylmethylidene)anilines and *N*-(9*H*-calbazole-3-ylmethylidene)anilines

Masatsugu Taneda

Division of Math, Science, and Information Technology in Education, Department of Science Education, Osaka Kyoiku University, Japan

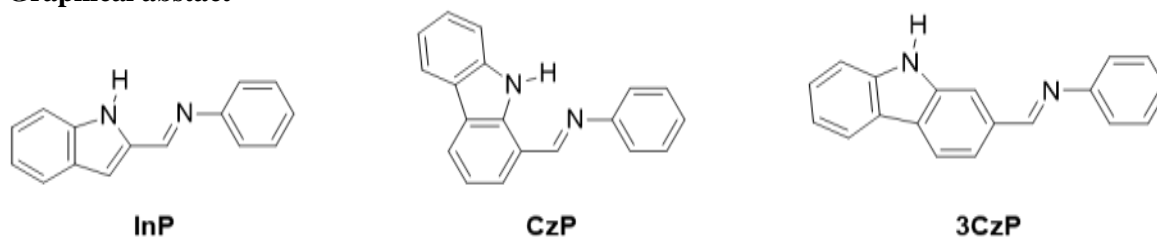
Corresponding author: tane@cc.osaka-kyoiku.ac.jp

Abstract

Carbazole and its derivatives are useful compounds to derive pharmaceutical and biological materials can function as a hydrogen donor of hydrogen bond because of its high acidity of a hydrogen atom at 9 position. *N*-(9*H*-carbazole-1-ylmethylidene)aniline (**CzP**) forms six membered intramolecular hydrogen bond between the hydrogen atom of a carbazole ring and nitrogen atom of an imine moiety. Recently we have reported the photo reactivity of *N*-(1*H*-indole-2-ylmethylidene)aniline (**InP**) and its derivatives in degassed solution. Light irradiation diminish absorbance of a spectrum of solution and the changed spectrum return to its original form in the dark. **CzPs** exhibit resemble behavior with right irradiation. In the crystal, the C=N double bond of **CzPs** and **InPs** adopts an *E* configuration which was caused by intramolecular hydrogen bond formed in solution^{1,2}. Thus the original spectrum is attributed to the *E* configuration. TD-DFT simulation suggests that diminish of absorbance would be caused by *E-Z* isomerization. Although *Z*-isomer of Schiff bases such as *N*-benzilideneanilines would not be observed because of its very short lifetimes, the isomer of **InPs** was stable at room temperature. The intramolecular hydrogen bond of **CzPs** solid state is confirmed by X-ray crystal structural analysis. On the other hand, the formation of intramolecular hydrogen bond of **InPs** is only observed in solution. It suggests that the intramolecular hydrogen bond of **CzPs** is stronger than the intramolecular interaction of **InPs**. In this study, *N*-(9*H*-calbazole-3-ylmethylidene)anilines (**3CzPs**) were synthesized. These compounds can't form intramolecular hydrogen bond. Photo reactivity of **3CzPs** were investigated.

Keywords: *E-Z* isomerization, heterocyclic aromatic compounds, photochromism, Schiff base, intramolecular hydrogen bond

Graphical abstract



References

1. Taneda, M.; Nishi, M.; Kubono, K.; Kashiwagi, Y.; Matsumoto, T. *Acta. Cryst.* 2022, *E78*, 449-452.
2. Kubono, K.; Matsumoto, T.; Taneda, M. *Acta. Cryst.* 2019, *E75*, 1429-1431.

Acknowledgement

This work was performed under the Cooperative Research Program of "Network Joint Research Center for Materials and Devices". This work was supported by JSPS KAKENHI Grant Number 21K0252023.

Chirality Transfer Reaction of Organophosphorus Compounds with a Binaphthyl Group and Their Use

Toshiaki Murai^{a,*}

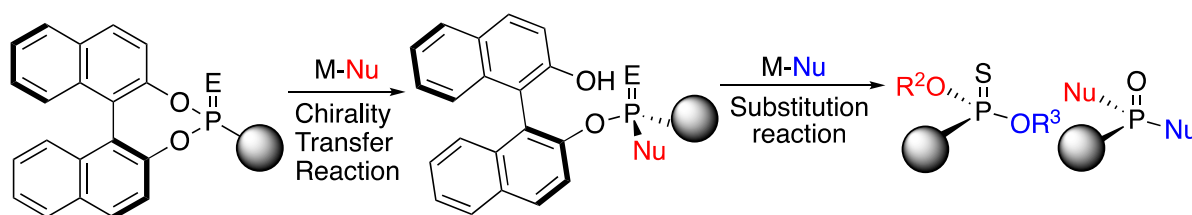
^a Department of Chemistry and Biomolecular Science, Faculty of Engineering, Gifu University, Yanagido, Gifu 501-1193, Japan

*murai.toshiaki.u6@a.gifu-u.ac.jp

Abstract

P-Chirogenic organophosphorus compounds play a crucial role due to their extensive applicability as drugs, prodrugs, optically active ligands, and organocatalysts. Over the past three decades, a range of synthetic methods have been developed, including kinetic resolutions, desymmetrization of prochiral organophosphorus compounds, and the separation of the mixtures of the diastereomers. In this context, we have developed axis-to-central chirality transfer reactions involving pentavalent four-coordinate organophosphorus compounds bearing a binaphthyl group.¹ The key starting materials with a binaphthyl group were prepared from the reaction of phosphoric acid chloride and phosphoselenic acid chloride with carbon and oxygen nucleophiles with high efficiency. We have also explored the conversion of the resulting compounds into enantiomerically enriched P-chirogenic organophosphorus compounds. As an illustrative example, the sequential substitution reaction of phosphonates with a binaphthyl group with aromatic Grignard reagents and methyl Grignard reagents proceeded smoothly, yielding enantiomerically enriched P-chirogenic phosphine oxides in high yields with high enantiomeric ratios.² These two-step reactions entail the transfer of axial chirality from the binaphthyl group to the central chirality of the phosphorus atom, coupled with a stereoselective substitution reaction of the initial products with Grignard reagents. Key substrates employed in these reactions included phosphinates,³ phosphates,⁴ phosphorothioates,⁴ and phosphonothioates⁵ with a binaphthyl group, which reacted with hydroxides and alkoxides as nucleophiles. The transformation described here enabled us to provide P-chirogenic organophosphorus compounds, which are not readily available from other synthetic methods. Further details regarding these reactions will be provided.

Keywords: P-chirogenic; organophosphorus compounds; axial chirality; central chirality; chirality transfer



References

1. Murai, T. *Chem. Lett.* 2023, 52, 703-714.
2. Ono, S.; Sugiyama, A.; Kuwabara, K.; Minoura, M.; Murai, T. *Synlett*, 2023, 34, 1502-1506.
3. Kawajiri, A.; Udagawa, T.; Minoura, M.; Murai, T. *ChemistryOpen*, 2022, 11, e202100294.
4. Endo, C.; Inoue, Y.; Maruyama, T.; Minoura, M.; Murai, T. *Synthesis*, 2023, 55, 934-944.
5. Kuwabara, K.; Maekawa, Y.; Minoura, M.; Maruyama, T.; Murai, T. *J. Org. Chem.*, 2020, 85, 14446-14455.

Simple Amino Alcohol Organocatalysts for Asymmetric Reactions

Hiroto Nakano*

Graduate School of Engineering, Muroran Institute of Technology, Japan

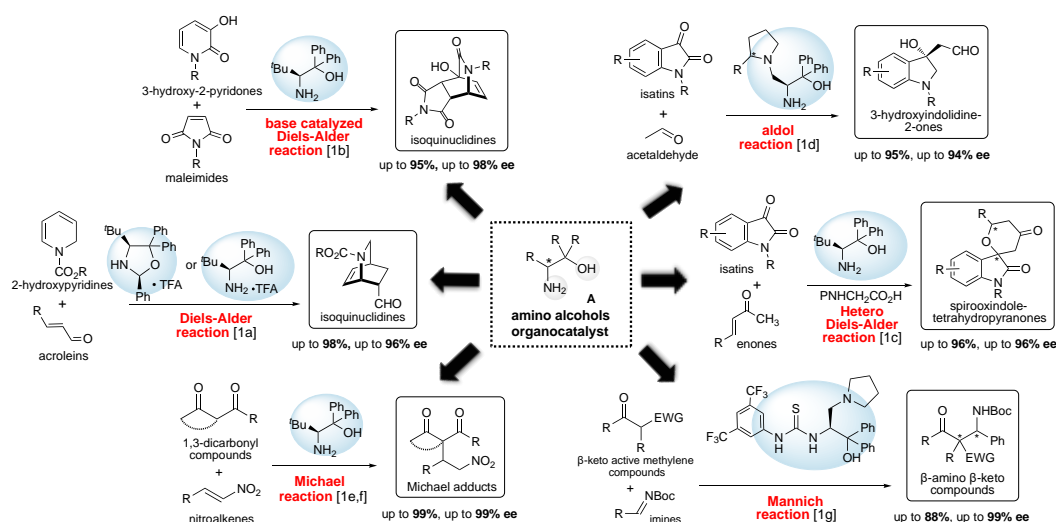
*catanaka@mmm.muroran-it.ac.jp

Abstract

The development of a chiral organocatalyst is very important for producing of a chiral molecule with a high optical purity in an asymmetric reaction. We are currently conducting the research of chiral amino alcohols **A** organocatalyst. This catalyst is easy to prepare and show high level of catalytic activity in a variety of asymmetric reactions despite its small molecular. Namely, it can be derived easily from the corresponding amino acid esters and contains both amino group acting as covalent or basic sites and hydroxyl group acting as hydrogen bonding site in the single molecule. In addition, the steric influences of substituents on the α - and β -positions in **A** also might be effective for control the enantioselective reaction course.

Our recent works for the functionalities of simple primary amino alcohols **A** as chiral organocatalyst in some asymmetric reactions will be introduced.¹

Keywords: amino alcohol, organocatalyst, multipoint recognition catalyst, asymmetric reaction



References

- (a) Kohari, Y.; Okuyama, Y.; Kwon, E.; Furuyama, T.; Kobayashi, N.; Otuki, T.; Kumagai, J.; Seki, C.; Uwai, K.; Dai, G.; Iwasa, T.; Nakano, H. *J. Org. Chem.*, **2014**, *79* (20), 9500-9511. (b) Takahashi, T.; Subba Reddy, U.V.; Kohari, Y.; Seki, C.; Furuyama, T.; Kobayashi, N.; Okuyama, Y.; Kwon, E.; Uwai, K.; Tokiwa, M.; Takeshita, M.; Nakano, H.; *Tetrahedron Lett*, **2016**, *57*, 5771–5776. (c) Parasuraman, P.; Begum, Z.; Chennapuram, M.; Chigusa, S.; Okuyama, Y.; Kwon, E.; Uwai, K.; Tokiwa, M.; Tokiwa, S.; Takeshita, M.; Nakano, H. *RSC Advances.*, **2020** (10), 17486-17491. (d) Subba Reddy, U.V.; Chennapuram, M.; Seki, K.; Chigusa, S.; Anushia, B.; Kwon, E.; Okuyama, Y.; Tokiwa, M.; Takeshita, M.; Nakano, H. *Eur. J. Org. Chem.*, **2017**, 3874-3885. (e) Owolabi, I A.; Chennapuram, M.; Seki, C.; Okuyama, Y.; Kwon, E.; Uwai, K.; Tokiwa, M.; Takeshita, M.; Nakano, H. *Bull. Chem. Soc. Japan*, **2019**, *92*(3), 696-701. (f) Begum, Z.; Sannabe, H.; Chigusa, S.; Okuyama, Y.; Kwon, E.; Kwon, E.; Uwai, K.; Tokiwa, M.; Tokiwa, S.; Takeshita, M.; Nakano, H. *RSC Advances.*, **2021** (1), 203-209. (g) Nomura, M.; Begum, Z.; Chigusa, S.; Okuyama, Y.; Kwon, E.; Uwai, K.; Tokiwa, M.; Tokiwa, S.; Takeshita, M.; Nakano, H. *RSC Advances.*, **2023**, *13*, 3715–3722.

Isolation and Structure Determination of the Colored Products from Cannabinoids and the Fast Blue RR

Kayo Nakamura^{a*}, Hikari Nishiguchi^a, Hideyo Takahashi^{a*}

^aFaculty of Pharmaceutical Sciences, Tokyo University of Science

*Corresponding author: kayo_nakamura@rs.tus.ac.jp, hide-tak@rs.tus.ac.jp

Abstract

Although cannabis is a useful plant that has been used in a wide range of fields such as medicine and pharmacy for a long time, Δ^9 -tetrahydrocannabinol (Δ^9 -THC) in cannabis has a narcotic effect. Therefore, in Japan, Δ^9 -THC is completely prohibited by law. On the other hand, cannabidiol (CBD), which is also contained in cannabis, does not have a narcotic effect and its use is permitted. In addition, CBD has been touted as having relaxing and analgesic effects, and there are many commercially available products containing CBD recently. Because these products use CBD extracted from cannabis, there is a possibility that Δ^9 -THC may be mixed in, and actually, there were some reports of health hazards due to the mixed Δ^9 -THC. Thus, there is a need for an easy method to distinguish between CBD and Δ^9 -THC.

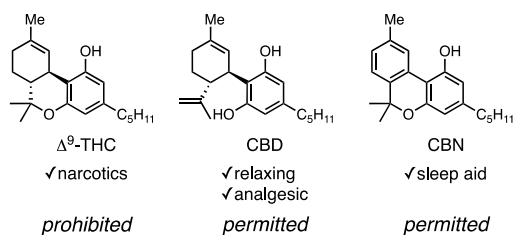
Normally, accurately analyzing cannabis requires expensive and high technical devices, such as TLC, GC, LC/MS, HPLC, and it takes time. In the real crime scene, the color reactions have been used as a method for detecting Δ^9 -THC. This classic method utilizes a coloring reagent that reacts with cannabis to produce color. This is a simple and very easy method, however, many false positives may occur.

We focused on the coloring reaction caused by diazonium salts, such as Fast Blue RR. We attempted to isolate the reaction products of Fast Blue RR and CBD and successfully isolated azo compound **1**. We also isolated products of cannabinol (CBN), and Δ^9 -THC, respectively. It was found that structures of the reaction products were slightly different from that of the reported products.¹ In this presentation, we will discuss these results in detail.

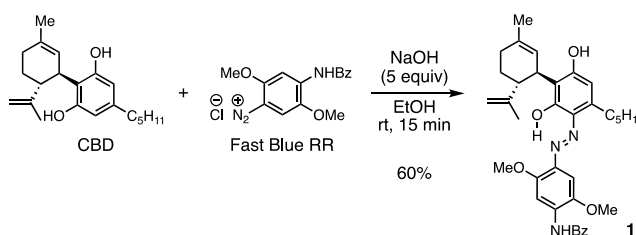
Keywords: color reaction, cannabinoids, Δ^9 -tetrahydrocannabinol, cannabidiol, diazonium salt

Graphical abstract

Cannabinoids



Result



References

1. The isolation of the product from Δ^9 -THC and Fast Blue BB salt: H. S. França, A. Acoara, A. Jamal, W. Romao, J. Mulloor, J. R. Almira, *Forensic Chem.* **2020**, *17*, 100212.

MODELLING OF SCHIFF BASE VANILLIN DERIVATIVES TARGETING *STREPTOCOCCUS PNEUMONIAE* BACTERIAL NEURAMINIDASE

Woon Yi Law^{a*}, Mohd Razip Asaruddin^a, Showkat Ahmad Bhawani^a

^aFaculty of Resource Science and Technology, Universiti Malaysia Sarawak, 94300 Kota Samarahan, Sarawak, Malaysia

*Corresponding author: mendah_wylaw@hotmail.com

Abstract

Streptococcus pneumoniae, or known as pneumococcus, is a pathogenic bacterium with has led to serious pneumococcal infections. Despite the fact that efficient therapeutic agents and vaccinations are available for the treatment of *Streptococcus pneumoniae* infections, more strains of *Streptococcus pneumoniae* have acquired significant resistance towards the available antibiotics. The neuraminidase of *Streptococcus pneumoniae* possess significant contribution in pathogenesis, aiding the release and spread of virus. Simultaneously, Schiff base vanillin derivatives were reported in past literature for their great deal of potential as inhibitors of influenza virus neuraminidase. Hence, the research aims to evaluate the inhibitory activity of Schiff base vanillin derivatives against *Streptococcus pneumoniae* neuraminidase via ligand-based pharmacophore modelling and structure-based molecular docking using LigandScout 4.4 and AutoDock 4.2. Ligand-based pharmacophore modelling was performed to analyse the anti-neuraminidase activity of Schiff base vanillin derivatives based on their pharmacophore fit values and matching pharmacophore features with a pharmacophore model, generated from a list of training sets, which are reported drugs against *Streptococcus pneumoniae* neuraminidase. The derivatives were imported as test sets in the pharmacophore model. In structure-based molecular docking, the Schiff base vanillin derivatives were evaluated based on their docking performances with the active sites of the crystal structure of *Streptococcus pneumoniae* neuraminidase A in complex with its inhibitory ligand, oseltamivir carboxylate (PDB: 2YA8). Evaluations were based on their pharmacophore scores, binding affinity and matching interactions with the inhibitory ligand in the active site of 2YA8. 20 out of 21 Schiff base vanillin derivatives successfully show good fit values and matching features with model in ligand-based pharmacophore modelling, as well as satisfying docking performances in structure-based molecular docking. Furthermore, they also fulfill the Lipinski's Rule of 5, thus displaying appreciable potential as inhibitors of *Streptococcus pneumoniae* neuraminidase and being promising drug candidates and bringing futuristic *in vitro* and *in vivo* tests.

Keywords: *Streptococcus pneumoniae*, neuraminidase, Schiff base vanillin derivatives, pharmacophore modelling, molecular docking

References

1. Lv, Q.; Zhang, P.; Quan, P.; Cui, M.; Liu, T.; Yin, Y.; Chi, G. *Microb. Pathogenesis*. 2020, *140*, 103934
2. Nguyen, T. L. A.; Bhattacharya, D. *Molecules*. 2022, *27*, 2494
3. Bogaert, D.; de Groot, R.; Hermans, P. W. M. *Lancet Infect. Dis*. 2004, *4*, 144–154
4. Li, N.; Wang, F.; Niu, S.; Cao, J.; Wu, K.; Li, Y.; Yin, N.; Zhang, X.; Zhu, W.; Yin, Y. *BMC Microbiol*. 2009, *9*, 129
5. Najafi, M.; Tavakol, S.; Zarrabi, A.; Ashrafizadeh, M. *Arch. Physiol. Biochem*. 2022, *128*, 1438–1452
6. Maragakis, L. L.; Perencevich, E. N.; Cosgrove, S. E. *Expert Rev. Anti-Infe*. 2008, *6*, 751-763
7. Benton, D. J.; Wharton, S. A.; Martin, S. R.; McCauley, J. W. *J. Virol*. 2017, *91*, 2293
8. Kaserer, T.; Beck, K. R.; Akram, M.; Odermatt, A.; Schuster, D.; Willett, P. *Molecules*. 2015, *20*, 22799-22832
9. Kitchen, D. B.; Decornez, H.; Furr, J. R.; Bajorath, J. *Nat. Rev. Drug Discov*. 2004, *3*, 935-949
10. Lengauer, T.; Rarey, M. *Curr. Opin. Struc. Biol*. 1996, *6*, 402-406
11. Gut, H.; Xu, G.; Taylor, G. L.; Walsh, M. A. *J. Mol. Biol*. 2011, *409*, 496-503

Synthesis of *meso*-1,4-dialdehyde and its application to asymmetric Tishchenko reaction

Takeyuki Suzuki

SANKEN, Osaka University, Japan

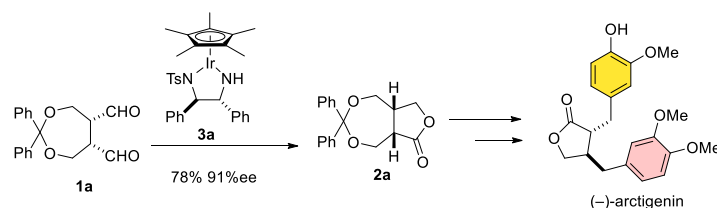
*Corresponding author: suzuki-t@sanken.osaka-u.ac.jp

Abstract

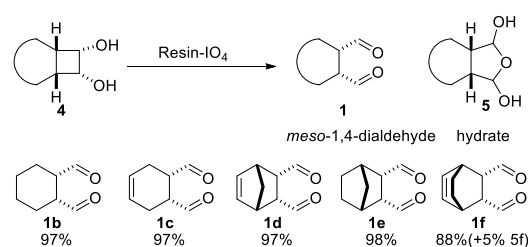
Recently, we developed asymmetric Tishchenko reaction using Ir complex catalyst. The reaction converted *meso*-1,4-dialdehyde **1a** to chiral lactone **2a** with 78% yield and 91% ee.^{1a} Using this reaction, the synthesis of cedarmycin A, B,^{1a} enterolactone^{1b} has been accomplished (Scheme 1).¹

In this study we developed the catalytic asymmetric synthesis of (–)-arctigenin from **2a**.^{1c} Moreover, for the generality of the Ir-catalyzed asymmetric Tishchenko reaction, we developed the practical synthesis of *meso*-1,4-dialdehydes. We found the oxidative cleavage of the corresponding cyclobutanediol **4** is effective for the synthesis of *meso*-1,4-dialdehydes and **1b** was obtained in 97% yield in pure form (Scheme 2). The resin supported periodate^{4a} was more effective than silica gel supported periodate^{4b}, for some sensitive bicyclic *meso*-1,4-dialdehyde which easily form the corresponding hydrate **5**. With the desired *meso*-1,4-dialdehydes **1** in hand, we tried asymmetric Tishchenko reaction of the *meso*-1,4-dialdehydes (Scheme 3).^{1d}

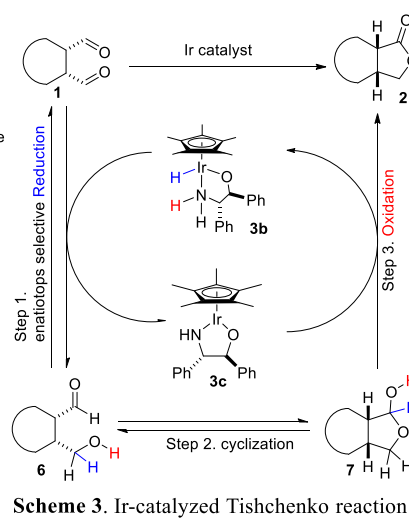
Keywords: arctigenin, *meso*-1,4-dialdehyde, iridium, lactone, Tishchenko reaction



Scheme 1. Ir catalyzed asymmetric Tishchenko reaction



Scheme 2. Synthesis of *meso*-1,4-dialdehydes



Scheme 3. Ir-catalyzed Tishchenko reaction

References

- (a) Ismiyarto; Kishi, N.; Adachi, Y.; Jiang, R.; Doi, T.; Zhou, D.-Y.; Asano, K.; Obora, Y.; Suzuki, T.; Sasai, H.; Suzuki, T., *RSC Adv.* **2021**, *11*, 11606. (b) Jiang, R.; Ismiyarto; Abe, T.; Zhou, D.-Y.; Asano, K.; Suzuki, T.; Sasai, H.; Suzuki, T., *J. Org. Chem.* **2022**, *87*, 5051. (c) Jiang, R.; Zhou, D. Y.; Asano, K.; Suzuki, T.; Suzuki, T., *Tetrahedron* **2023**, *133*, 133287. (d) Zhao, R.; Ismiyarto; Zhou, D. Y.; Asano, K.; Suzuki, T.; Sasai, H.; Suzuki, T., *ACS Omega* **2024**, *9*, 17945.
- Bergens, S. H.; Fairlie, D. P.; Bosnich, B., *Organometallics* **1990**, *9*, 566.
- Jacobi, P. A.; Buddhu, S. C.; Fry, D.; Rajeswari, S., *J. Org. Chem.* **1997**, *62*, 2894.
- (a) Hodge, P., *J. Chem. Soc. Perkin Trans. 1*, **1982**, 509. (b) Zhong, Y.-L.; Shing, T. K. M., *J. Org. Chem.* **1997**, *62*, 2622.

Evaluation of the correlation between porphyrin accumulation in cancer cells and functional positions for application as a drug carrier

Toshifumi Tojo^{a*}, Takeshi Kondo^{b,c}, Shin Aoki^{a,c}, Makoto Yuasa^{b,c}

^aFaculty of Pharmaceutical Sciences, Tokyo University of Science.

^bFaculty of Science and Technology, Tokyo University of Science.

^cResearch Institute for Science and Technology, Tokyo University of Science.

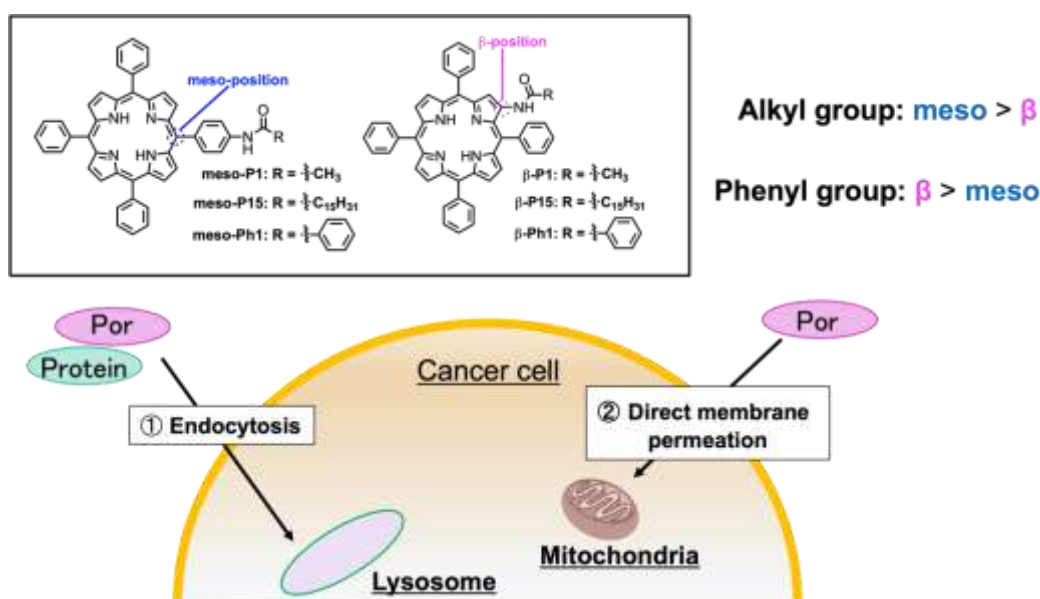
*Corresponding author: (email: tojo-t@rs.tus.ac.jp)

Abstract

Currently, cancer chemotherapy is one of the effective methods used in cancer treatment. But alternatively, the side effect caused by toxicity in normal cells can be problematic, and the construction of drug delivery systems (DDS) that transport drugs selectively to cancer cells are particularly important. To apply for DDS construction, porphyrin has attracted attention as a carrier molecule. Porphyrin is composed of four pyrrole subunits with 18 π -electrons that form a planer, and it can form conjugates with metals (Fe, Ni, and Co) which define its electrochemical and oxidation-reduction characteristics. Additionally, porphyrin's ability to selectively accumulate in cancer cells has been reported. Recently, creating a synergistic effect was tried by combining the potential of porphyrin and the pharmacological effect of anti-cancer drugs, and the discovery of new anti-cancer conjugates constructed by linking porphyrin and anti-cancer drugs have been reported. Alternatively, porphyrin has two functional sites, termed the β - and *meso*-positions. When porphyrin is used as a carrier molecule, the anti-cancer drug is modified using either functional positions of porphyrin. However, little is known about the influence of those functional positions on porphyrin accumulation in cancer cells. Here, we focused on β - and *meso*-positions to elucidate the correlation between functional porphyrin positions and accumulation in cancer cells. Understanding this can lead to the discovery of new molecules with high accumulation in cancer cells.

In this presentation, we will introduce the effect of the functional position of alkyl group or phenyl group on porphyrin accumulation in cancer cells from the viewpoint of cell membrane permeation mechanism (endocytosis/direct membrane permeation).

Keywords: Porphyrin; accumulation in cancer cells; endocytosis; direct membrane permeation



Use of intermolecular FRET for evaluations of lectin— carbohydrate interactions

Koji Matsuoka^{a,b,c,*}, Kota Miyairi^a, Tetsuo Koyama^a, Thakahiko Matsushita^{a,b,c}, Ken Hatano^{a,b,c}

^aDivision of Material Science, Graduate School of Science & Engineering, ^bAdvanced Institute of Innovative Technology (AIIT), and ^cHealth Sciences and Technology Research Area, Strategic Research Center, Saitama University, Sakura, Saitama 338-8570, Japan.

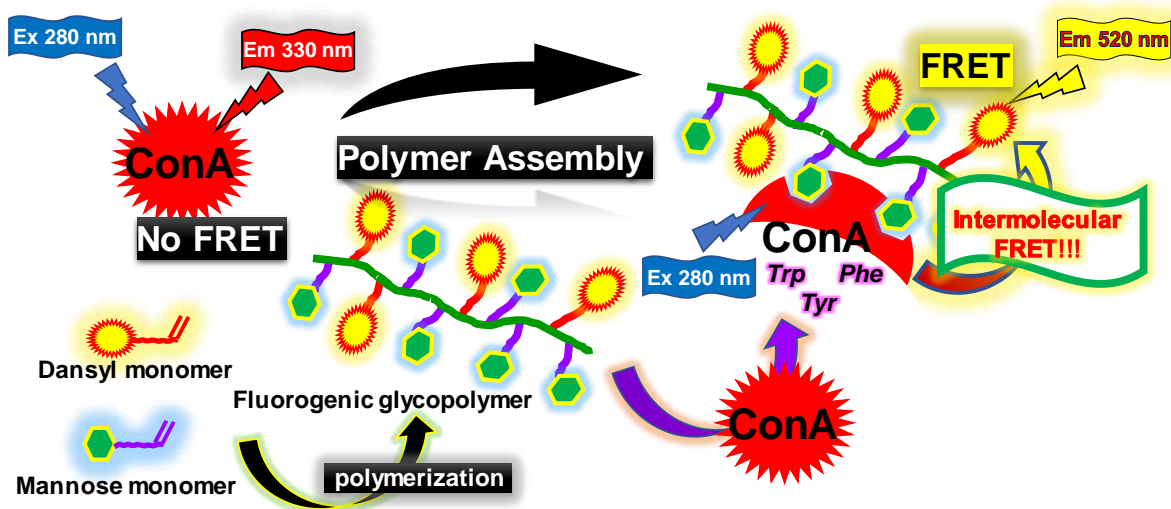
*Corresponding author: koji@fms.saitama-u.ac.jp

Abstract

Carbohydrate-binding proteins and lectins are well-known to interact for carbohydrate chains of glycoconjugates with weak binding affinities (~mM range).¹⁾ In order to enhance the binding affinities, various cluster-type carbohydrate derivatives have been prepared.²⁾ In addition to the preparation of the various substrates, quantitative evaluations of the binding affinities between glycopolymers and lectins in order to investigate the functionality of glycopolymers are of great importance. Recently, we developed fluorogenic glycopolymers that induce Förster resonance energy transfer (FRET) upon binding to lectins and we attempted directly to monitor the interaction followed by evaluation of the binding affinity on the basis of intermolecular FRET.³⁾ In this paper, design and syntheses of fluorogenic glycoclusters having mannose residues were performed. In addition, binding affinities of these glycopolymers for concanavalin A (Con A) were evaluated⁴⁾ and the results will be presented.

Keywords: Carbohydrates, Glycopolymers, Polymerizations, Lectins, Concanavalin A, FRET

Graphical abstract (Optional)



References

1. Y.C. Lee and R.T. Lee, *Acc. Chem. Res.* **28**, 321-327, **1995**.
2. T. Matsushita, M. Nozaki, M. Sunaga, T. Koyama, K. Hatano, and K. Matsuoka, *ACS Omega* **8**, 37451-37460, **2024**.
3. K. Matsuoka, Y. Suzuki, T. Koyama, T. Matsushita, and K. Hatano, *Bioorg. Med. Chem. Lett.* **30**, #127024, **2020**.
4. K. Miyairi, T. Matsushita, T. Koyama, K. Hatano, and K. Matsuoka, *J. Mol. Struct.* **1306**, #137896, **2024**.

Synthesis of Fluoroalkylated Oxazoles Using Carboxylic Acid Anhydrides as the Fluoroalkyl Sources

Tsuyuka Sugiishi^a, Ryohei Motegi^a, Hideki Amii^{a,*}

^aDivision of Molecular Science, Graduate School of Science and Technology, Gunma University.

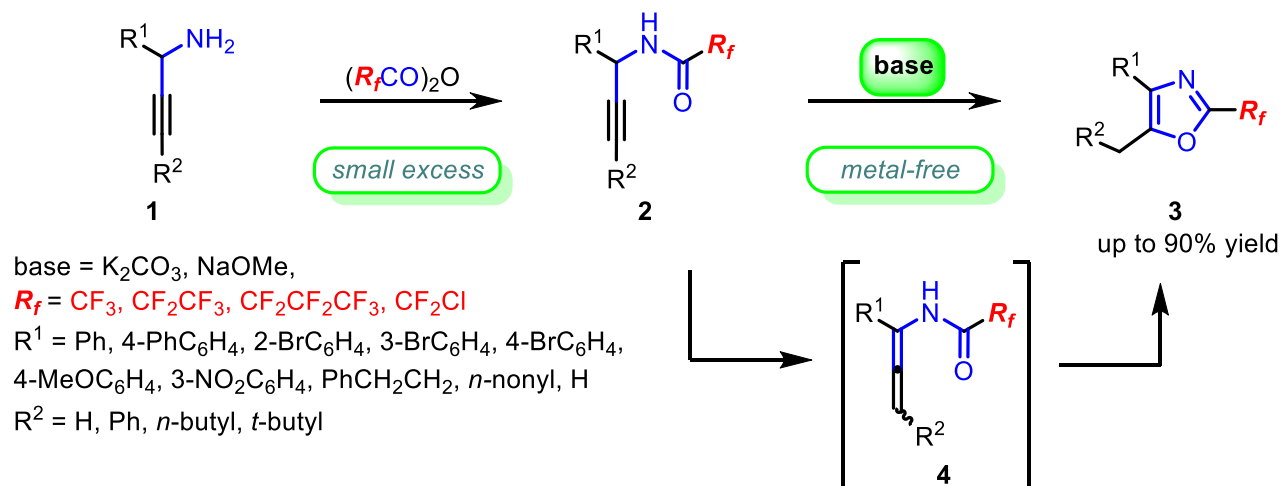
*Corresponding author: amii@gunma-u.ac.jp

Abstract

Methodology for preparation of fluorine-containing heterocyclic compounds, which can be applied to various medicines, might contribute to drug discovery. We focused on fluorocarboxylic acid anhydrides ((R_f CO) $_2$ O), or trifluoroacetic anhydride (TFAA) derivatives, as the commercially available and inexpensive fluoroalkyl sources. Herein, we report the atom-economical synthesis of fluoroalkylated oxazoles by intramolecular cyclization of *N*-propargylic amides, which are synthesized from *N*-propargylic amines with fluorocarboxylic acid anhydrides, without transition-metal catalysis.¹

Propargylic amines **1** reacted with 1.2 equivalents of fluoroalkylated carboxylic acid anhydrides to afford *N*-propargylic amides **2**. Fluoroalkylated oxazoles **3** were synthesized from corresponding propargylic amides **2** under the optimized basic conditions in moderate to high yields. The substrate scope and limitation are consistent with the proposed reaction mechanism including the allenamide intermediates **4**.

Keywords: fluoroalkyl, oxazole, carboxylic acid anhydrides, *N*-propargylic amides, intramolecular cyclization



References

- Sugiishi, T.; Motegi, R.; Amii, H. *Synthesis* 2023, 55, 1984-1995.

Liquid-Liquid Phase Separation of Nucleic Acids

Mitsuki Tsuruta^a, Ryosuke Suzuki^a, Keiko Kawauchi^a, **Daisuke Miyoshi^{a,*}**,

^a Faculty of Frontiers of Innovative Research in Science and Technology (FIRST)
Konan University, 7-1-20 Minatojima-minamimachi, Chuo-ku, Kobe, Hyogo 650-0047, Japan

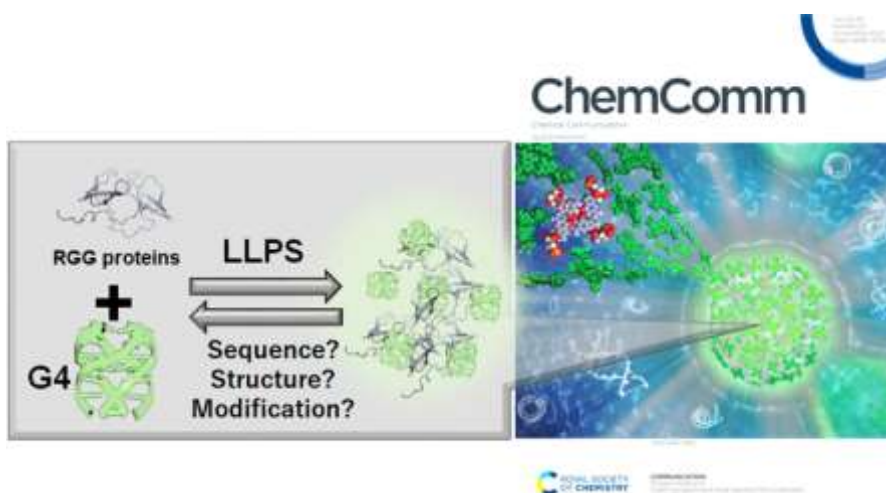
*Corresponding author: miyoshi@konan-u.ac.jp

Abstract

Liquid-liquid phase separation (LLPS) of biomacromolecules, such as protein and nucleic acid, is a recently re-discovered phenomenon, which shed a light on a new phase in living cells and biotechnologies¹. Especially, LLPS involving nucleic acids participates in the regulation of gene expression at various levels such as the replication, transcription, processing, localization of coding and non-coding RNA, and translation². LLPS couples with the well-known molecular machineries for regulating the central dogma. Notably, LLPS is linked to the onset of neurodegenerative and other diseases. Although LLPS is induced by different molecular compositions, RNAs and RNA binding proteins (RBPs) are essential components. Furthermore, it has been considered that LLPS even with different molecular compositions has common assembly and disassembly mechanisms. However, critical factors which make LLPS different from aggregation, gelation, and interaction in solution are unknown yet.

We have developed small molecules targeting DNA and RNA G-quadruplexes (G4s) which are thermodynamically stabilized in molecular crowding conditions³. We and other groups reported recently that RNA and DNA oligonucleotides forming G4 underwent LLPS with proteins and peptides. For example, RNA G4s and a model peptide derived from RGG domain, which is frequently observed in proteins such as FMRP undergoing LLPS with RNAs (Figure)⁴. To our knowledge, this is the smallest model system of biomolecular LLPS, which could be useful to investigate molecular mechanism of LLPS and to develop a new method to control LLPS. Based on this model system, factors affecting the G4 LLPS have been identified. In my talk, how sequence, structure, and chemical (epigenetic) modifications on nucleic acids affect degree of LLPS.

Keywords: liquid-liquid phase separation, condensate, nucleic acid, G-quadruplex, peptide



References

1. Shil S. *et al.*, *BioTech* 2023, 12, 26.
2. Kohata K.; Miyoshi, D. *Biophys. Rev.* 2020, 12, 669.
3. Nakano, S.; Miyoshi, D.; Sugimoto, N. *Chem. Rev.* 2014, 114, 2733.
4. Tsuruta, M. *et al.*, *Chem. Commun.* 2022, 58, 12931.

Iridium-Catalyzed *ortho*-C–H Silylation of 2-Arylpyridine Derivatives by Using Phosphine–Borane Ligand

Gen Onodera*

Graduate School of Integrated Science and Technology, Nagasaki University, Japan

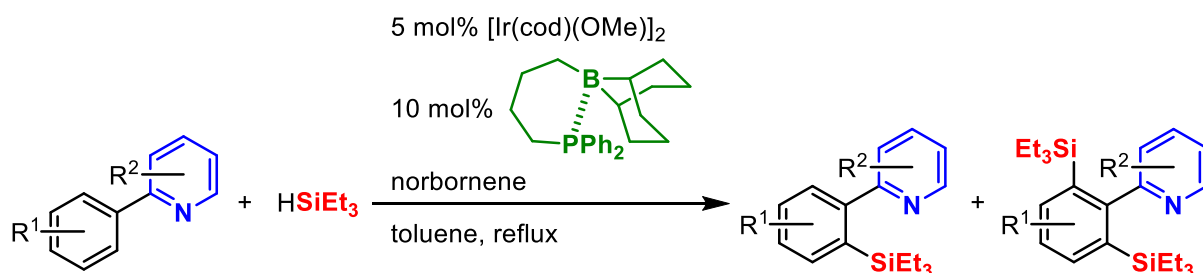
*Corresponding author: onodera@nagasaki-u.ac.jp

Abstract

Transition metal-catalyzed C–H functionalization is one of the most reliable methods for organic synthesis. In the pioneering work of Murai and his co-workers, the directing group in the substrate coordinates to the transition metal center to bring it to the *ortho*-C–H bond, and then this C–H bond is cleaved via an oxidative addition to the central metal.¹ This strategy has been widely used in a variety of catalytic C–H functionalizations. On the other hand, Kuninobu and his co-workers developed the *ortho*-C–H borylation of thioanisole using the iridium catalyst with the bipyridine ligand bearing a Lewis acidic boryl group.² In this reaction, the Lewis basic sulfur of a substrate does not coordinate to the iridium center, but to the Lewis acidic boron in the ligand. This Lewis acid-base interaction between the substrate and ligand is the key factor leading the iridium to an *ortho*-C–H bond. Meanwhile, we have been interested in the catalysis of transition metal complexes with phosphine–borane ligand.³ Inspired by Kuninobu's work, we investigated C–H functionalization using Lewis acid-base interaction between a substrate and a phosphine–borane ligand. We found that the iridium/phosphine–borane system catalyzed the *ortho*-C–H silylation of 2-arylpyridine derivatives.⁴ After the screening of ligands, the butylene-linked phosphine–borane ligand enabled the *ortho*-C–H silylation of 2-(*o*-tolyl)pyridine with triethylsilane to give the corresponding silylated product in 93% yield. When ethyldiphenylphosphine and 9-(*n*-hexyl)-9-BBN were used instead of the phosphine–borane ligand, the yield decreased to 47%. This result indicated that the link between phosphorus and boron is important for this reaction. We investigated this reaction using other 2-arylpyridine derivatives as substrates. In the case of 2-phenylpyridine, the disilylated product was obtained along with the monosilylated product. Other 2-arylpyridine derivatives could also be used in this catalytic reaction.

Keywords: phosphine–borane, iridium, C–H activation, silylation, 2-arylpyridine

Graphical abstract



References

1. a) Murai, S.; Kakiuchi, F.; Sekine, S.; Tanaka, Y.; Kamatani, A.; Sonoda, M.; Chatani, N. *Nature* **1993**, *366*, 529-531. b) Kakiuchi, F.; Murai, S. *Acc. Chem. Res.* **2002**, *35*, 826-834.
2. Li, H.-L.; Kuninobu, Y.; Kanai, M. *Angew. Chem. Int. Ed.* **2017**, *56*, 1495-1499.
3. a) Hirata, G.; Satomura, H.; Kumagae, H.; Shimizu, A.; Onodera, G.; Kimura, M. *Org. Lett.* **2017**, *19*, 6148-6151. b) Shimizu, A.; Hirata, G.; Onodera, G.; Kimura, M. *Adv. Synth. Catal.* **2018**, *360*, 1954-1960. c) Onodera, G.; Kumagae, H.; Nakamura, D.; Hayasaki, T.; Fukuda, T.; Kimura, M. *Tetrahedron Lett.* **2020**, *61*, 152537-152540.
4. Anoyama, K.; Onodera, G.; Fukuda, T.; Kimura, M. *Adv. Synth. Catal.* **2022**, *364*, 1223-1227.

Computer simulations for atomic-scale to cellular-scale phenomena

Takefumi Yamashita^{a,b,*}

^aDepartment of Physical Chemistry, School of Pharmacy and Pharmaceutical Sciences, Hoshi University, 2-4-41 Ebara, Shinagawa-ku, Tokyo 142-8501, Japan.

^bResearch Center for Advanced Science and Technology, The University of Tokyo, 4-6-1 Komaba, Meguro-ku, Tokyo 153-8904, Japan.

*Corresponding author: yamashita@lsbm.org

Abstract

Advancements in computational technology have revolutionized our ability to simulate complex systems across various scales, from the atomic to the cellular level. Understanding biological phenomena requires insights across these scales, and thus this presentation explores cutting-edge techniques and applications of computer simulations.

We begin with atomic-scale simulations, focusing on all-atom (AA) molecular dynamics (MD) methods [1-6]. Recent studies using AA-MD simulations have provided new insights into rational antibody drug design. For example, research on the antibody B5209B targeting ROBO1 in liver cancer revealed the critical role of salt bridge stabilization [2]. Additionally, studies on egg white lysozyme (HEL) and its antibody HyHEL-10 highlighted the importance of nearby hydrophobic amino acids [3]. These findings suggest potential strategies for antibody modification.

Next, we transition to cellular-scale simulations. A study applying the cellular automaton method to cardiac remodeling after myocardial infarction revealed clear effects of cellular interactions on domain formation [7]. As mechano-sensing genes like *Csrp3* contribute to these interactions, multiscale simulations incorporating molecular-level information will be essential to deeply understand such cellular-scale changes.

This presentation highlights the importance of understanding biological phenomena across multiple scales. By integrating atomic and cellular-scale simulations, we gain comprehensive insights into complex biological systems.

Keywords: simulation; molecular dynamics; cellular automaton

References

1. Yamashita, T. Toward Rational Antibody Design: Recent Advancements in Molecular Dynamics Simulations. *Int. Immunol.* **2018**, *30* (3), 133–140.
2. Yamashita, T. et al. Affinity Improvement of a Cancer-Targeted Antibody through Alanine-Induced Adjustment of Antigen-Antibody Interface. *Structure* **2019**, *27* (4), 519–527.
3. Okajima, R.; Hiraoka, S.; Yamashita, T. Environmental Effects on Salt Bridge Stability in the Protein–Protein Interface: The Case of Hen Egg-White Lysozyme and Its Antibody, HyHEL-10. *J. Phys. Chem. B* **2021**, *125* (7), 1542–1549.
4. Yamashita, T.; Miyamura, N.; Kawai, S. Classification of the HCN Isomerization Reaction Dynamics in Ar Buffer Gas via Machine Learning. *J. Chem. Phys.* **2023**, *159* (12), 124116.
5. Miyabe, K.; Yamashita, T.; Tsumoto, K. Thermodynamic and Molecular Dynamic Insights into How Fusion Influences Peptide-Tag Recognition of an Antibody. *Sci. Rep.* **2024**, *14* (1), 8685.
6. Nasrin, S. R.; Yamashita, T.; Ikeguchi, M.; Torisawa, T.; Oiwa, K.; Sada, K.; Kakugo, A. Tensile Stress on Microtubules Facilitates Dynein-Driven Cargo Transport. *Nano Lett.* **2024**. DOI: 10.1021/acs.nanolett.4c00209.
7. Yamashita, T. (in preparation).

Diversity-oriented synthesis of hydrophobic building blocks of biofunctional molecules using hydroboration of vinylsilanes

Nao Namba^{*a}, Hiroyuki Kagechika^a, Shinya Fujii^a

Institute of Biomaterial and Bioengineering, Tokyo Medical and Dental University, Japan

**Corresponding author: namban.chem@tmd.ac.jp*

Abstract

Hydroboration of vinylsilanes with BH_3 , unlike that of simple alkene compounds, affords two regioisomers (α - and β -isomers) in approximately equal proportion. Since these isomers were readily separable by silica-gel column chromatography, it is considered that various silyl alcohols could be accessible by this reaction. Further, silyl functionalities are used not only in organic synthesis, but also as structural options in medicinal chemistry. Our previous studies showed that a series of commercially available silyl reagents were versatile options in structural development^{1,2}. In this study, we investigated diversity-oriented synthesis of silylethanols from vinylsilanes to demonstrate the usefulness of these silylethanols in the structural development of biofunctional molecules³.

At first, we investigated the regioselectivity of hydroboration of vinylsilanes **1** by focusing on the substituents on the silicon atom (Fig 1a). As a result, both α -isomer **2** and β -isomer **3** were obtained as the products from all investigated vinylsilanes. Interestingly, as the number of phenyl ring on the silicon atom increased, the ratio of the sterically more hindered 1-silylethanols increased. The results of DFT calculation agreed well with the observed regioisometric ratios of products. Increase of electrophilicity of β -carbon by phenyl ring on the silicon atom was considered one possible factor for the regioselectivity.

Next, we investigated the application of the obtained silylethanols as unique building blocks for hydrophobic structure. Specifically, we designed novel silylethoxy-contained molecules as nuclear progesterone receptor (PR) ligand candidates (Fig 1b). The designed compounds **4** and **5** showed significant PR agonistic or antagonistic activity, and the most potent compounds showed antagonistic activity with IC_{50} values of around 30 nM. Notably, some regioisomers such as **4a** and **5a** exhibited opposite activities, namely, **4a** exhibited PR agonistic activity whereas **5a** acted as a potent PR antagonist. Docking simulation suggested that **4a** and **5a** form hydrophobic interactions with PR in a different manner.

The details of regioselectivity in hydroboration and structure development study will be discussed.

Keywords: Organosilicon compound, Hydroboration, Biofunctional molecule

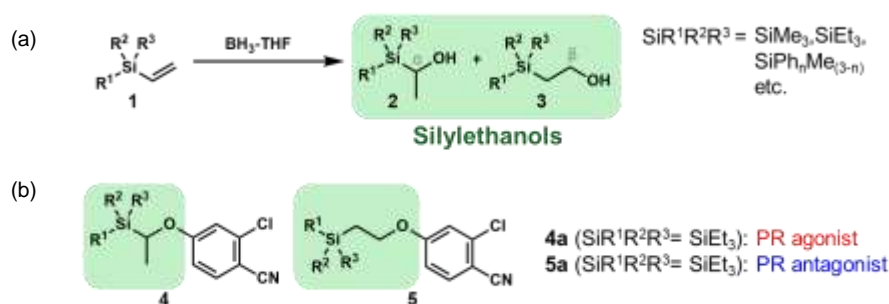


Fig.1 (a) investigation of the regioselectivity on hydroboration of vinylsilanes **1**. (b) Application of the silylethanols to the development of PR ligands.

References

- Oikawa, T.; Fujii, S.; Mori, S.; et al. *ChemMedChem*, 2022, 17, e202200176.
- Namba, N.; Nogichi-Yachide, N.; Matsumoto, Y.; et al. *Bioorg. Med. Chem*, 2022, 66, 116792.
- Namba, N.; Fujii, S. *Org. Biomol. Chem.*, in press. DOI: 10.1039/D4OB00632A.

Synthesis of Phosphine Chalcogenides using Chalcogenocyanate Ions

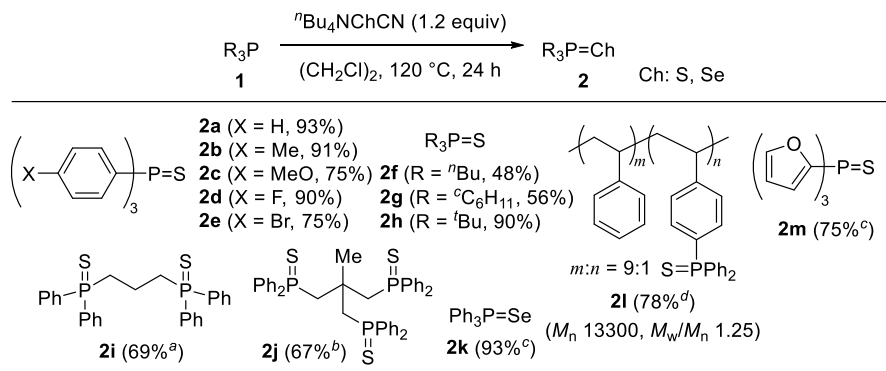
Shunsuke Sueki^{a,b*}, Azumi Watanabe^a, Minori Nakamura^a, Naoyuki Machida^a,
Asuka Shuto^a, Kosho Makino^{a,b}, Masahiro Anada^{a,b*}^a Faculty of Pharmacy, Musashino University.^b Research Institute of Pharmaceutical Sciences, Musashino University.

*Corresponding author: s_sueki@musashino-u.ac.jp, m_anada@musashino-u.ac.jp

Abstract

Phosphine chalcogenides¹ have a wide range of important applications such as ligands for transition metal catalysts,² organocatalysis,³ sulfurization agent for transition metal phosphides⁴ and molecular junction units for electronic devices.⁵ Although treatment of phosphines with elemental sulfur or selenium is one of the general methods for the preparation of phosphine chalcogenides,⁶ there are major drawbacks in that it often requires excess amount of reagents, high reaction temperature, long reaction times and tedious purification task. We now addressed the chalcogenylation of phosphines using chalcogenocyanate ions as chalcogen atom source. We found the reaction of triphenylphosphine (**1a**) with tetrabutylammonium thiocyanate in 1,2-dichloroethane at 120 °C proceeded smoothly to provide triphenylphosphine sulfide (**2a**) in 93% yield. This protocol was applicable to the synthesis of various phosphine sulfides **2b-2j**, phosphine selenide **2k** and poly(styrene-co-4-styryldiphenylphosphine) (**2l**). In the case of the sulfurization of electron deficient phosphine **1m**, the use of 0.5 equiv of CuI as an additive was found to be effective.

Keywords: phosphine chalcogenide, thiocyanate ion, selenocyanate ion, polymer reaction



^a ⁿBu₄NSCN (2.4 equiv) was used. ^b ⁿBu₄NSCN (3.6 equiv) was used. ^c The reaction was carried out at 65 °C. ^d 0.12 equiv of ⁿBu₄NSCN (1.2 equiv per phosphorus atom) was used. ^e The reaction was conducted in the presence of CuI (0.5 equiv).

References

- Hayashi, M. *Chem. Lett.* **2021**, 50, 1.
- (a) Hayashi, M.; Takezaki, H.; Hashimoto, Y.; Takaoki, K.; Saigo, K. *Tetrahedron Lett.*, **1998**, 39, 7529. (b) Hayashi, M.; Hashimoto, Y.; Yamamoto, Y.; Usuki, J.; Saigo, K. *Angew. Chem., Int. Ed.*, **2000**, 39, 631.
- Ruan, Z.; Wang, M.; Yang, C.; Zhu, L.; Su, Z.; Hong, R. *JACS Au* **2022**, 2, 793.
- Arnosti, N. A.; Wyss, V.; Delley, M. F. *J. Am. Chem. Soc.* **2023**, 145, 23556.
- Fukazawa, A.; Kiguchi, M.; Tange, S.; Ichihashi, Y.; Zhao, Q.; Takahashi, T.; Konishi, T.; Murakoshi, K.; Tsuji, Y.; Staykov, A.; Yoshizawa, K.; Yamaguchi, S. *Chem. Lett.* **2011**, 40, 174.
- Maddox, S. M.; Nalbandian, C. J.; Smith, D. E.; Gustafson, J. L. *Org. Lett.* **2015**, 17, 1042.

Synthesis and functions of bacterial lipid A for safe vaccine adjuvant development

Atsushi Shimoyama^{a,*}

^a Graduate School of Science, Osaka University, Japan.

*Corresponding author: ashimo@chem.sci.osaka-u.ac.jp

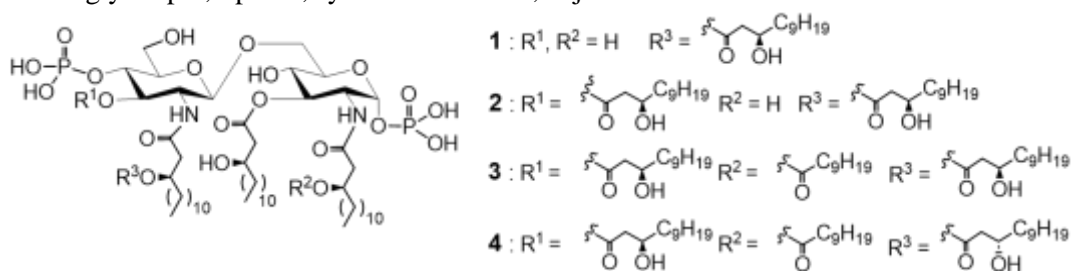
Abstract

Lipopolysaccharide (LPS) is a major glycoconjugate in outer membrane of Gram-negative bacteria and canonical *Escherichia coli* LPS activate innate immunity to induce lethal strong inflammation. The terminal glycolipid lipid A is the active principle of LPS. Low inflammatory lipid A have been expected as adjuvants.

We hypothesized that co-evolved parasitic and symbiotic bacterial components should modulate host immunity moderately with low toxicity. We synthesized parasitic¹, symbiotic² and fermentation³ bacterial lipid A and elucidated the molecular basis of immunoregulation, and developed safe and useful adjuvants. In this lecture, we introduce the structure determination, chemical synthesis, and structure-activity relationship studies of lipid A from *Alcaligenes faecalis* inhabiting gut-associated lymphoid-tissue (GALT) that is responsible for the mucosal immunity regulation.

We synthesized *A. faecalis* lipids A **1-3** with diverse acyl group patterns and identified the active center as hexa-acylated **3**². Lipid A **3** was confirmed to exhibit non-toxic but useful adjuvant function (enhancing antigen-specific IgA and IgG production)⁴⁻⁷, and that vaccine model using **3** was found to be significantly protective against bacterial infection⁵. Since IgA is responsible for mucosal immune homeostasis, by focusing on GALT symbiotic bacteria, we found promising adjuvant that can safely regulate mucosal immunity. Furthermore, lipid A **4**, which reversed the stereochemistry of the acyl side chain hydroxy group, was found to be more active than **3**, and the molecular basis of the adjuvant function is also becoming clear.

Keywords: glycolipid, lipid A, symbiotic bacteria, adjuvant



Synthesized symbiotic bacterial lipid A **1-3** and derivative **4**

References

1. Shimoyama, A.; Fujimoto, Y.; Fukase, K. et al, *Chem. Eur. J.* 2011, 17, 14464-74.
2. Shimoyama, A.; Molinaro, A.; Fukase, K. et al, *Angew. Chem. Int. Ed.* 2021, 60, 10023-31.
3. Shimoyama, A.; Yamaura, Y.; Fukase, K. *Angew. Chem. Int. Ed.* 2024, e202402922.
4. Wang, Y.; Hosomi, K.; Shimoyama, A.; Kunisawa, J. et al, *Vaccines* 2020, 8, E395.
5. Yoshii, K.; Hosomi, K.; Shimoyama, A.; Kunisawa, J. et al, *Microorganisms* 2020, 8, 1102.
6. Liu, Z.; Hosomi, K.; Shimoyama, A.; Fukase, K.; Kunisawa, J. et al, *Frontiers in Pharmacology* 2021, 12, 763657.
7. Sun, X.; Hosomi, K.; Shimoyama, A.; Fukase, K.; Kunisawa, J. et al, *Int. Immunopharmacol.* 2023, 117, 109852.
8. Sun, X.; Hosomi, K.; Shimoyama, A.; Fukase, K.; Kunisawa, J. et al, *Int. Immunol.* 2024, 36, 33-43.

Efficient Synthetic Approach Based on Cu-Catalyzed Coupling Reaction of Alkynylborate with Aldehyde

Masanari Kimura^{a,*}, Sena Toyofuku^b, Gen Onodera^a, Tsutomu Fukuda^a

^aGraduate School of Integrated Science and Technology, Nagasaki University, Japan

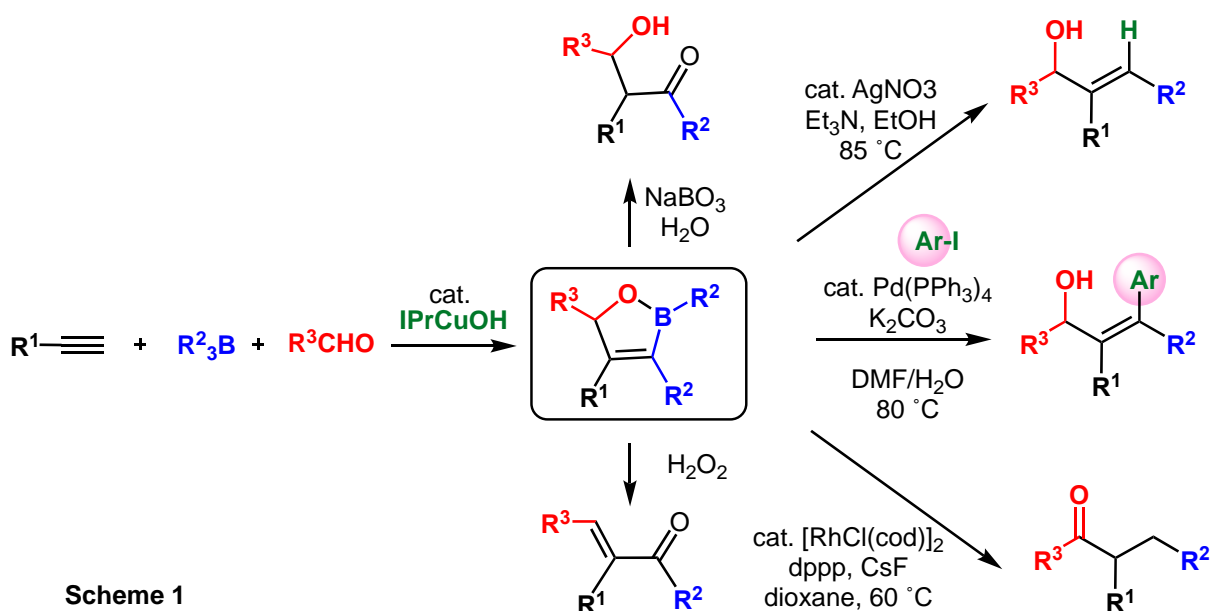
^bGraduate School of Engineering, Nagasaki University, Japan

*Corresponding author: masanari@nagasaki-u.ac.jp

Abstract

Alkynylborate is an efficient key intermediate for constructing the stereodefined substituted alkenylboranes. We have developed the Cu-catalyzed highly regio- and stereoselective formation of α,β -dialkylated acrylic acids from terminal alkynes with trialkylboranes under CO₂ atmospheric pressure.¹ Alkynylborates were produced in the presence of Cu-catalyst, trialkylborane, and terminal alkyne in situ, and then underwent the protonation at β -position. Thus, the formed alkenylboranes reacted with CO₂ smoothly promoted by Cu(I) catalyst to provide (*E*)- α,β -substituted acrylic acids with high regio- and stereoselectivities. Based on these results for the coupling reactions with alkynylborates, we could achieve the coupling reactions with an aldehyde as an electrophile. In the presence of IPrCuOH catalyst, three-component coupling reactions of terminal alkyne, organoborane, and aldehyde combined with high regio- and stereoselectivities to form 2,5-dihydro-1,2-oxaboroles under nitrogen atmosphere. These transformations are convenient and straightforward synthetic methods for the stereodefined construction of 2,5-dihydro-1,2-oxaboroles in a single operation. We disclose the scope and limitations of the three-component coupling reactions with a wide variety of terminal alkynes, organoboranes, and aldehydes, and the applicable synthetic utilities involving oxaborole analogues as important key intermediates (Scheme 1).

Keywords: Cu-catalyst, trialkylborane, alkynes, aldehyde, carbon dioxide



References

1. Kuge, K.; Luo, Y.; Fujita, Y.; Mori, Y.; Onodera, G.; Kimura, M. *Org. Lett.*, 2017, 19, 854-857.

Switching of Circularly Polarized Luminescence via Dynamic Axial Chirality Control of Chiral Boron Difluoride Complexes

Masahiro Ikeshita^{a,*}, Ayumu Kuroda^a, Seika Suzuki^b, Yoshitane Imai^b, Takashi Tsuno^a,

^a College of Industrial Technology, Nihon University

^b Graduate School of Science and Engineering, Kindai University

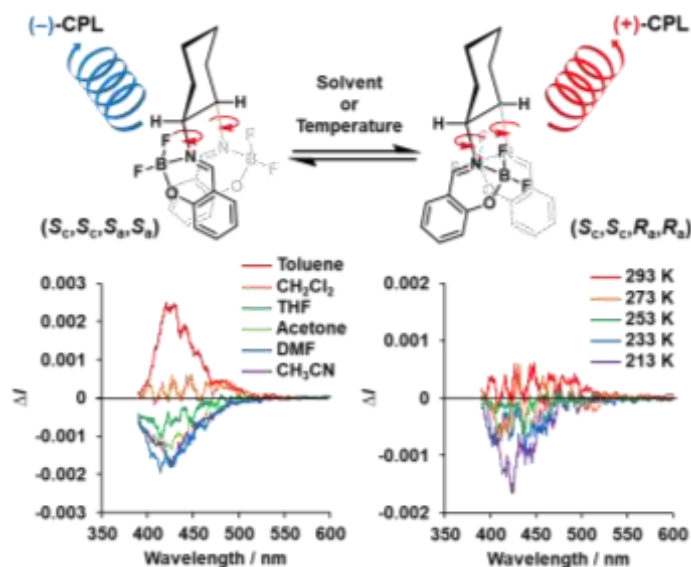
*Corresponding author: ikeshita.masahiro@nihon-u.ac.jp

Abstract

Circularly polarized luminescent materials have received increasing attention owing to their potential applications in various forward-looking optical devices. In particular, the development of methodologies for switching circularly polarized luminescence (CPL) properties has recently become an important topic for the creation of molecular sensors and biological probes.¹ Our research group has been developing efficient and controllable CPL emitters based on chiral Schiff-base complexes. In the course of these studies, we have achieved control of their CPL signs and intensities by tuning the coordination geometry² or aggregation state³ of the complexes.

In this work, we demonstrate CPL switching based on dynamic molecular rotation using bis(boron difluoride) complexes with chiral salen ligands.⁴ In these complexes, the two boron coordination platforms are in a face-to-face structure bridged by the 1,2-cyclohexyl linkage. The rotation of the C-N bond axis of the (*S,S*) enantiomer produces atropisomers assigned to the (*S_C,S_C,R_a,R_a*) and (*S_C,S_C,S_a,S_a*) forms with different face-to-face conformations of the boron coordination platform. The equilibrium between these atropisomers was found to change with the external environment such as solvent polarity and temperature, allowing precise control of their CPL signs without luminescence color shifts. Density functional theory (DFT) calculations revealed the mechanism of the dynamic rotational behavior and CPL properties.

Keywords: circularly polarized luminescence, chirality, molecular rotation, atropisomer



References

1. J.-L. Ma, Q. Peng, C.H. Zhao, *Chem. Eur. J.* **2019**, *25*, 15441–15454.
2. M. Ikeshita, Y. Imai, T. Tsuno *et al.* *Chem. Commun.* **2022**, *58*, 7503–7506.
3. M. Ikeshita, Y. Imai, T. Tsuno *et al.* *Chem. Asian J.* **2024**, *19*, e202301024.
4. M. Ikeshita, Y. Imai, T. Tsuno *et al.* *ChemPhotoChem* **2024**, *in press* (DOI: 10.1002/cptc.202400110).

Obtaining of chemicals and pitch products by solvolysis of Russian and Mongolian coals using coal- and petroleum-derived heavy residues as solvents

Avid Budeebazar^a, Navchtsetseg Nergui^a, Peter Kuznetsov^b, Ludmila Kuznetsova^b, Namkhainorov Jargalsaikhan^a, Azzaya Tumendelger^a, Eugeny Kamensky^b, Purevsuren Barnasan^a

^a*Institute of Chemistry and Chemical Technology, Mongolian Academy of Sciences, Mongolia,*

^b*Institute of Chemistry and Chemical Technology SB RAS, Russia*

**Corresponding author: Navchtsetseg Nergui e-mail: navchtsetseg@mas.ac.mn*

Abstract

Developing clean coal utilization has become a strategic choice around the world for tackling climate change, ensuring energy security and producing chemicals and carbon materials. It is a common vision to jointly promote the coal utilization technologies to a cleaner, low-carbon and sustainable direction. The world innovate experience in the development of the coal industry has already proved wide possibilities and prospects for using coal not only as a raw material for electricity and heat generation, but also for the chemical industry.

Russia and Mongolia have large reserves of coals of various grades; the development of effective processing technologies will make it possible to produce both clean fuels and products of high added value, including in-demand carbon materials for various purposes - electrodes, high-quality cokes, carbon fibers, graphite materials and other products.

This paper is devoted to study low-temperature process of the thermosolvolysis conversion of coals into solubles, establishing the chemical, group and molecular composition of the resulting products. The set of samples of bituminous coals from the Mongolia and Russia deposits were used in the dissolution experiments at temperatures of 350 and 380 °C at 2-3 MPa. High-boiling hydrocarbon residue fractions of coal and petroleum origin were used as solvents.

The products obtained from the joint conversion of coal and solvent were solid pitch-like matter, soluble in quinoline up to 90-95%, the yield of gaseous products did not exceed 0.5%. The distillation of pitch-like products yielded 14.7–18.7% of liquid oil with boiling point below 350 °C and 81.3–85.3% of pitch residues. According to GC-MS, the light distillates and hexane solubles consisted of mainly aromatic compounds. The pitch products were studied by chemical, group and thermal analysis, the plastometric properties were characterized by softening point. FTIR and CP/MAS ¹³C NMR techniques showed the pitches to consist of mainly polycondensed aromatics, the aromaticity factor ranged of 0.87 to 0.91 depending on coal and solvent used. According to the analytical data obtained, the products of co-conversion of coal and heavy hydrocarbon residues can be considered as promising raw materials for the production of chemicals, fuels and various carbon materials.

Keywords: coal, solvents, coal dissolution, aromatics, pitch, carbon materials.

Funding: The work was funded by the Russian Science Foundation (grant 24-43-03001) and the Science and Technology Foundation of Mongolia using the equipment of the Krasnoyarsk Regional Center for Collective Use of the Federal Research Center KSC SB RAS and the Center for Collective Use of the Institute of Coal Chemistry and Material Science SB RAS FRC, Kemerovo.

Au-Catalyzed Diverse Regiospecific α -Methylene C–H functionalization of Tertiary Amines via Concerted Electron Transfer to O₂

Takafumi Yatabe^{a,b*}

^a School of Engineering, The University of Tokyo, Japan

^b JST, PRESTO, Japan

*Corresponding author: yatabe@appchem.t.u-tokyo.ac.jp

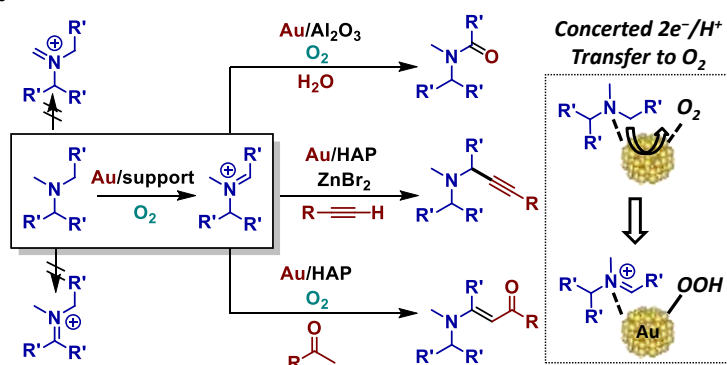
Abstract

Oxidative α -C–H functionalization of tertiary amines, which are ubiquitously present in medicines and natural products, is an extremely beneficial transformation to enable molecular modification to new medicinal candidates without changing their original skeletons. So far, there are many reports on α -methyl selective oxidative functionalization of tertiary amines via stepwise single electron transfer (SET)/deprotonation/SET; however, α -methylene selective oxidative functionalization applicable to a wide range of tertiary amines has been hardly reported without using specific substrates such as *N*-substituted tetrahydroisoquinolines (THIQs), *N*-protected amines, and symmetric amines, in spite of the frequent appearance of α -methylene-substituted amines in pharmaceutical fields.

In this presentation, I report supported Au nanoparticles-catalyzed α -methylene regiospecific aerobic oxidation of tertiary amines and its diverse utilization. Based on our previous work on aerobic α -oxygenation of secondary and tertiary amines¹, after various investigation, we have developed the first α -methylene specific alkylation of various tertiary amines to produce propargylic amines in the presence of hydroxyapatite-supported Au nanoparticle (Au/HAP) and ZnBr₂ catalysts using O₂ as the sole oxidant.² From various control experiments by utilizing α -alkynylation of tertiary amines, we revealed that the unique regioselectivity is derived from a concerted one-proton/two-electron transfer from tertiary amines to O₂ on Au nanoparticles. In addition, by combining other Au catalysis for oxidative dehydrogenation^{3,4,5}, we have successfully developed an unprecedented enaminone synthesis from tertiary amines and ketones via tandem oxidation: amine oxidation/ketone addition/oxidative dehydrogenation.

Keywords: Au nanoparticles, C–H bond functionalization, tertiary amines, regioselectivity, aerobic oxidation

Graphical abstract



References

- Jin, X.; Kataoka, K.; Yatabe, T.; Yamaguchi, K.; Mizuno, N. *Angew. Chem. Int. Ed.* 2016, 55, 7212-7217.
- Yatabe, T.; Yamaguchi, K. *Nat. Commun.* 2022, 13, 6505.
- Yatabe, T.; Jin, X.; Yamaguchi, K.; Mizuno, N. *Angew. Chem. Int. Ed.* 2015, 54, 13302-13306.
- Yoshii, D.; Jin, X.; Yatabe, T.; Hasegawa, J.; Yamaguchi, K.; Mizuno, N. *Chem. Commun.* 2016, 52, 14314-14317.
- Xia, K.; Yatabe, T.; Yonesato, K.; Yabe, T.; Kikkawa, S.; Yamazoe, S.; Nakata, A.; Yamaguchi, K.; Suzuki, K. *Angew. Chem. Int. Ed.* 2022, 61, e202205873.

Hierarchically self-assembled liquid crystal built from short DNA

Makiko Tanaka*

Department of Engineering Science, Graduate School of Informatics and Engineering, The University of Electro-Communications, 1-5-1 Chofugaoka, Chofu, Tokyo 182-8585, Japan

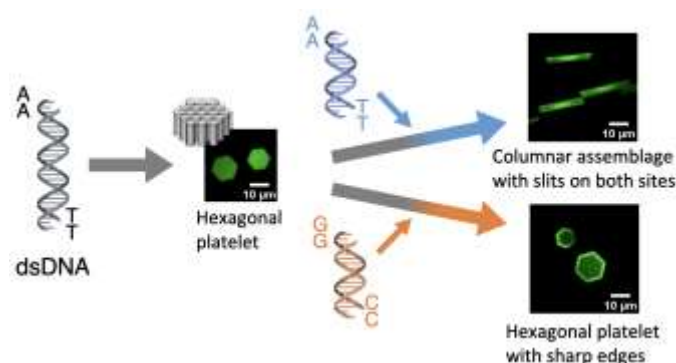
*Corresponding author: makiko.tanaka@uec.ac.jp

Abstract

The formation of self-assemblies with various hierarchical structures by chemically synthesized supramolecular building blocks have been studied in the field of materials science. DNA has also been attracting attention as a biological building block. It has been known that double-stranded DNA (dsDNA) can be packed into a liquid crystalline phase under high-concentration conditions.^{1,2} Furthermore, adding high-concentrated nonadsorbing crowder to dsDNA homogeneous solutions results in the formation of liquid crystalline assemblages. However, far too little attention has been paid to controlling the morphology of liquid crystalline DNA assemblage. In recent years, we demonstrated that in the presence of poly(ethylene glycol) (PEG), a short dsDNA in an aqueous-salt solution assembled into hexagonal platelets.³ The self-assembly in the presence of nonadsorbing polymer can be explained by depletion force.

We show herein controlling morphology of hexagonal liquid crystals built from short dsDNA. A short dsDNA containing 23 complementary bases and two base overhangs in an aqueous-salt PEG solution assembled into hexagonal platelets. The addition of shorter dsDNA containing 16 complementary bases and sticky AA/TT overhangs dramatically changed the morphology of the DNA assemblage. We observed columnar assemblages with slits on both sites after heating and subsequent slow cooling of the mixed solution. On the other hand, the addition of shorter dsDNA containing 16 complementary bases and GG/CC overhangs to the solution caused the transition into hexagonal platelets with sharp edges. Polarization microscopy strongly indicated parallel alignment of dsDNA in a hexagonal platelet. X-ray scattering measurements revealed that both columnar assemblages and hexagonal plates with sharp edges were composed of hexagonal columnar liquid crystalline phase as well as uniform thickness hexagonal platelet composed of one pair of dsDNA. I will also discuss hierarchical organization processes of these assemblies.

Keywords: DNA, liquid crystalline phase, self-assembly



References

1. Livolant, F.; Levelut, A. M.; Doucet, J.; Benoit, J. P., *Nature*, 1989, 339, 724.
2. Nakata, M.; Zanchetta, G.; Chapman, B. D.; Jones, C. D.; Cross, J. O.; Pindak, R.; Bellini, T.; Clark, N. A., *Science*, 2007, 318, 1276.
3. Makino, T.; Nakane, D.; Tanaka, M., *ChemBioChem*, 2022, 23, e202200360.

Development of Recoverable and Reusable Reagents for Aromatic Trifluoromethylation

Akari Matsuoka, Mizuki Kita, Tsuyuka Sugiishi, Hideki Amii*

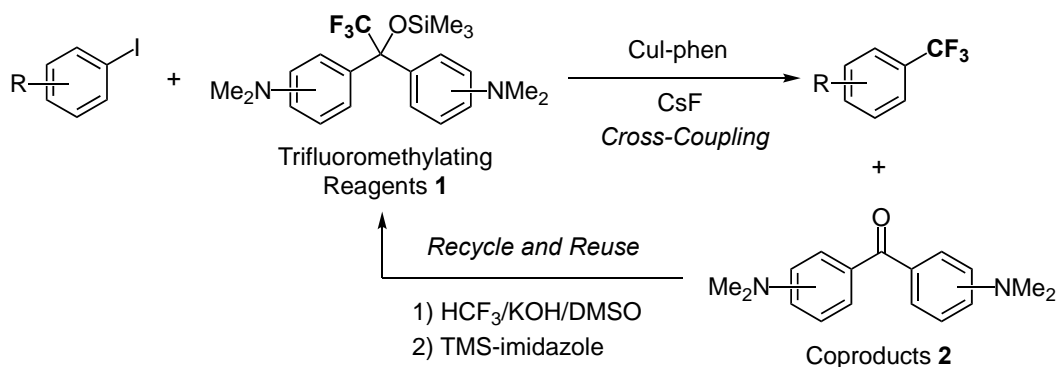
^aGraduate School of Science and Technology, Gunma University, Japan

**Corresponding author: amii@gunma-u.ac.jp*

Abstract

Trifluoromethylated aromatic compounds (Ar-CF₃) are substances of considerable interest for wide fields of sciences. With respect to the high regiochemical fidelity in aromatic substitution, the cross-coupling of aryl halides with CF₃-sources is one of the most versatile methods to construct Ar-CF₃.^{1,2} For catalytic aromatic trifluoromethylation using silylated trifluoromethyl carbinol,³ it is difficult to remove benzophenone, a co-product with close polarity to the target products. Therefore, we have developed trifluoromethylation agents in which the coproducts are easily removed and recovered by introducing dimethylamino groups on the benzene rings. Silylated trifluoromethyl carbinols **1** with dimethylamino groups at the benzene rings were synthesized as aromatic trifluoromethylating agents. *O*-silyl carbinols **1** were found to be quite effective for the Cu-catalyzed cross-coupling with iodoarenes (Ar-I) to give the corresponding Ar-CF₃ in good yields. We also attempted to regenerate the CF₃-carbinols **1** by reacting the recovered coproducts **2** with trifluoromethane (HCF₃). The coproducts, aminobenzophenones **2**, obtained by the catalytic aromatic trifluoromethylation can be easily removed and recovered by an acidic workup. Nucleophilic trifluoromethylation of the recovered coproducts **2** using trifluoromethane and the subsequent *O*-silylation resulted in regeneration of trifluoromethylating reagents **1**.

Keywords: fluorine, trifluoromethylation, cross-coupling, copper, reuse



Reference

1. Shimizu, N.; Kondo, H.; Oishi, M.; Fujikawa, K.; Komoda, K.; Amii, H. *Org. Synth.* **2016**, 93, 147-162 and references therein.
2. Amii, H. *Chem. Rec.* **2023**, e202300154 and references therein.
3. Amii, H.; Kawauchi, D.; Komoda, K.; Shimizu, N.; Kobayashi, M. Japan Patent 6830599 (2021/01/29).

Investigating the Solid-State [2+2] Photodimerization of Trifluoromethyl Substituted *trans*-Cinnamic Acid Derivatives within KBr Pellet

Bayasgalan Ulambayar^{a,*}, Khongorzul Batchuluun^a, Tobias E. Schrader^b

^a*Institute of Chemistry and Chemical Technology*

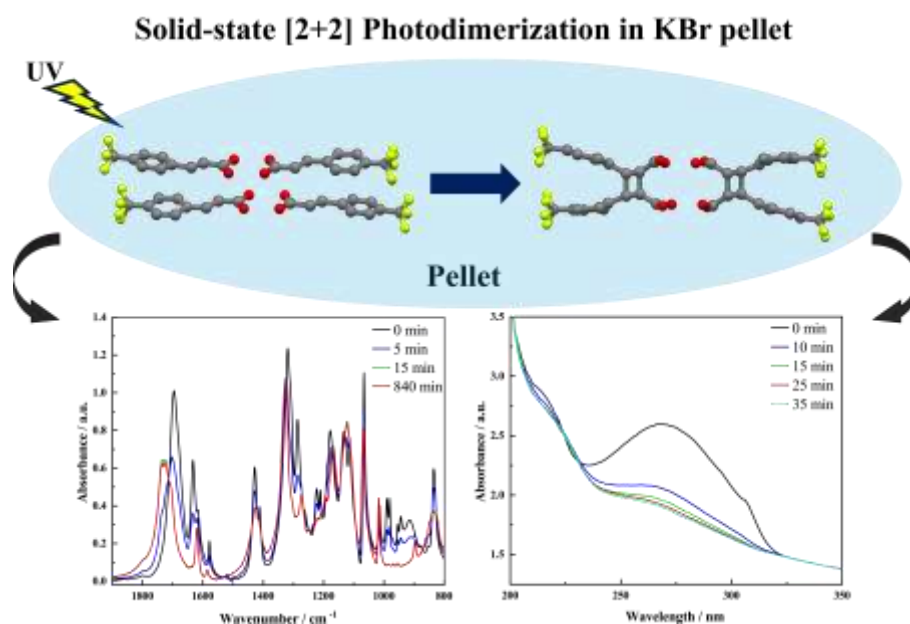
^b*Forschungszentrum Jülich, Jülich Centre for Neutron Science at Heinz Maier-Leibnitz Zentrum (MLZ)*

*Corresponding author: bayasgalan_u@mas.ac.mn

Abstract

Solid-state photoreactions are particularly interesting from the stereochemistry and crystal-engineering perspective¹. For such reactions molecular configuration of the resulting product is dictated by the geometric arrangement of the reacting molecules in the crystal structure and as such they afford stereospecific products that are difficult to acquire from the solution phase. A classic example of one such reaction is the [2+2] photodimerization of *trans*-cinnamic acid and its derivatives, which are frequently used as a model system in photoreaction studies since they are simple molecules with predictable photoreactivity². Yet, certain aspects of the reaction still lack complete understanding compared to its solution phase counterpart. Thus, in this work, we have studied the potential [2+2] photodimerization of *trans*-cinnamic acid derivatives, *trans*-4-(trifluoromethyl) cinnamic acid (4-tfmca) and *trans*-3-(trifluoromethyl) cinnamic acid (3-tfmca) via optical spectroscopy and X-ray diffraction. Instead of taking the sample in its neat powder or single crystal state herein we used powder samples embedded in a potassium bromide (KBr) pellet and were able to assess the spectroscopical changes accommodated by the photoreaction. The obtained results showed that 4-tfmca had undergone photodimerization in the pellet to yield the photoproduct in roughly 100% conversion, while 3-tfmca in the pellet showed signs of photoreactivity that may not be apparent in its neat powder or single crystal form. We hope that our new convenient model system and the suggested method of using KBr pellets as shown here will help to provide further insights into photochemical reactions.

Keywords: cinnamic acid, photodimerization, KBr pellet



References

1. Biradha, K.; Santra, R. *Chem. Soc. Rev.* **2013**, *42*, 950-967.
2. Schmidt, G. M. J. *J. Chem. Soc.* **1964**, 2014-2021.

CONTROLLING THE SUBSTITUTION PATTERN IN MULTIFUNCTIONALIZED CYCLOPENTADIENES

Nikola Topolovčan^{a*}, Marko Gobin^a

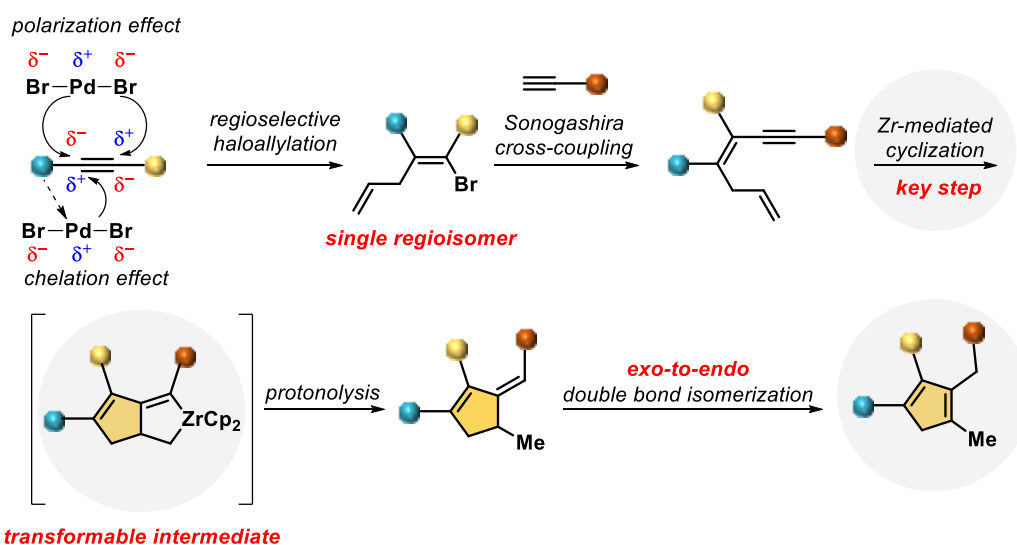
^aRuđer Bošković Institute

*Corresponding author: ntopolov@irb.hr

Abstract

By having control over the positioning of functionalities in multisubstituted cyclopentadienes it is possible to fine-tune their chemical and steric properties reflecting on their performance, especially as ligands in organometallic catalysis.¹ Contemporary synthetic procedures quite often do not result in regio- and chemoselective substitution so it is highly desirable to devise a single method that would allow controllable molecular decoration of the Cp ring. Herein we present our design based on i) *regioselective cis-bromoallylation* of internal alkynes² mediated by polarization or chelation effect,³ ii) *Sonogashira cross-coupling*, iii) *Zr-mediated cyclization of dienynes* as a key step and iv) *acid catalyzed exo-to-endo double bond isomerization*. With this approach it is possible to control the installation of various functionalities already in the early stage of synthetic sequence, while reactivity of zirconocene intermediate expands the possibilities for molecular editing of resulting multisubstituted cyclopentadienes.

Keywords: controlled substitution, haloallylation, ligands, multisubstituted cyclopentadienes, Zr-mediated cyclization



References

1. Topolovčan, N.; Kotora, M. *Topics in Organometallic Chemistry*, **2023**, 1-28.
2. Topolovčan, N.; Panov, I.; Kotora, M. *Org. Lett.* **2016**, *18*, 3634-3637.
3. Topolovčan, N.; Hara, S.; Čisářova, I.; Tošner, Z.; Kotora, M. *Eur. J. Org. Chem.* **2020**, 234-240.

Flexible Implementation of Web Applications for the Statistical Analysis of the Structure-Function Relationship among Metalloproteins.

Yusuke Kanematsu^{a*}

^aGraduate School of Advanced Science and Engineering, Hiroshima University, Japan

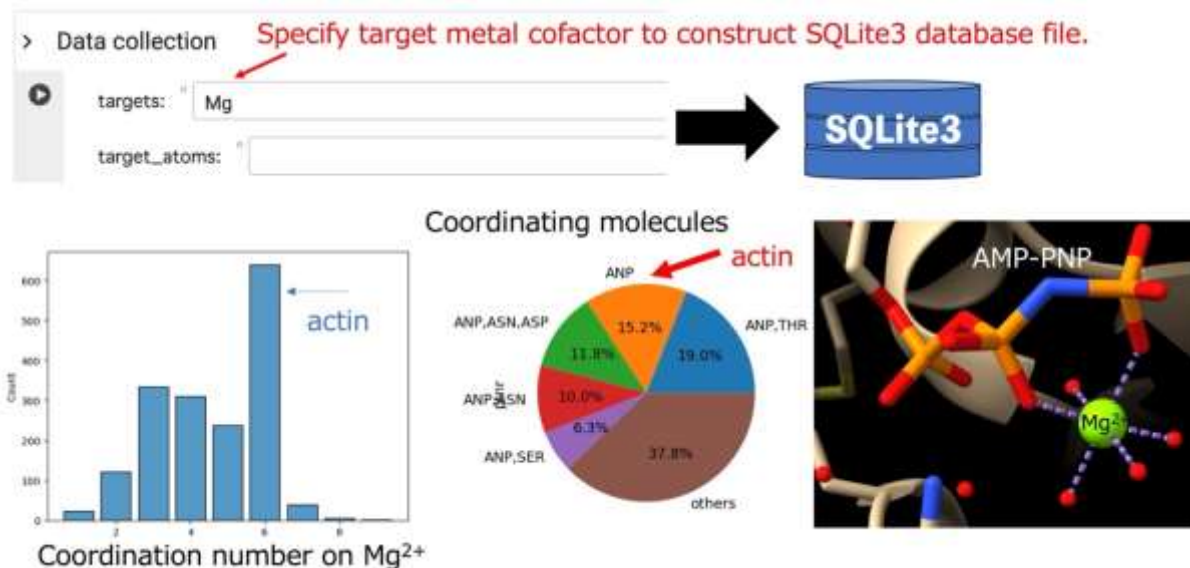
*Corresponding author: yanem@hiroshima-u.ac.jp

Abstract

Recent significant growth of protein structural data in the Protein Data Bank (PDB) has enabled statistical analysis of the structure-function relationship of proteins. Moreover, rapid advancements in AI technology have yielded highly functional and user-friendly data analysis tools, opening doors to a deeper understanding of protein design.

This presentation will introduce the web application for the characterization of metalloproteins implemented in Google Colab. Users can create metalloprotein databases for specific metal cofactors, visualize entries, and perform statistical analyses, all within a web browser. The application's utility will be demonstrated using actin ATPase, an enzyme with unique reactivity and reaction mechanisms.¹ Additionally, the compatibility of our PyDISH^{2,3} hemeprotein database with AlphaFold3⁴ for predicting novel protein activity will be discussed.

Keywords: metalloprotein, hemeprotein, actin, bioinformatics, de novo design



References

1. Kanematsu, Y.; Narita, A.; Oda, T.; Koike, R.; Ota, M.; Takano, Y.; Moritsugu, K.; Fujiwara, I.; Tanaka, K.; Komatsu, H.; Nagae, T.; Watanabe, N.; Iwasa, M.; Maéda, Y.; Takeda, S.; *Proc. Natl. Acad. Sci. USA* 2022, *119*, e2122641119.
2. Kondo, H. X.; Kanematsu, Y.; Masumoto, G.; Takano, Y. *Database* 2020, 2023, baaa066.
3. <https://pydish.bio.info.hiroshima-cu.ac.jp>.
4. Abramson, J.; Adler, J.; Dunger, J.; Evans, R.; Green, T.; Pritzel, A.; Ronneberger, O.; Willmore, L.; Ballard, A.J.; Bambrick, J.; *et al. Nature* 2024, 1-3.

Functionalization of single walled carbon nanotubes for controlling their near infrared photoluminescent properties

Yutaka Maeda*

^aDepartment of Chemistry, Tokyo Gakugei University, Japan

*Corresponding author: ymaeda@u-gakugei.ac.jp

Abstract

Single-walled carbon nanotubes (SWCNT) with a tubular graphene structure have attracted significant attention owing to their outstanding mechanical strength and distinct electronic and optical properties. The electronic structure of SWCNT depends on the geometrical structure of SWCNT, which is distinguished by the chiral index (n,m). Semiconducting SWCNT has been attracted attention due to their near-infrared (NIR) photoluminescent properties.¹ For example, NIR light can be used for deep bioimaging because it has highly penetration through biological tissue.² In addition, SWCNT have been found to generate single photon at room temperature in the optical communications band.³

Recent studies have revealed that photoluminescence (PL) wavelength has been manipulated by chemical functionalization depending on the functionalization methods and molecular structures.⁴ Chemical functionalization can change the PL wavelength by locally reducing the band gap energy, which not only expands the choice of the wavelengths, but also improves the PL efficiency and reduces internal quenching. In this presentation, recent research results on controlling NIR PL characteristics of SWCNT by chemical functionalization.⁵⁻⁸

Keywords: carbon nanotubes, near infrared, functionalization, photoluminescence

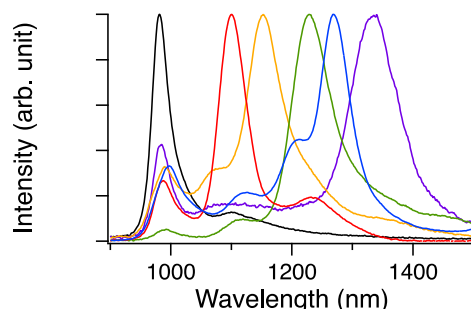


Fig. PL spectra of (6,5) SWCNT, ⁿBu-(6,5) SWCNT-H, (6,5) SWCNT-C₄F₉, (6,5) SWCNT-C₄H₈, (6,5) SWCNT-C₃H₄Me₂ (Δ), and (6,5) SWCNT-C₄F₈.

References

1. Bachilo, S. M.; Strano, M. S.; Kittrell, C.; Hauge, R. H.; Smalley, R. E.; Weisman, R. B. *Science* 2002, 298, 2361-2366.
2. Boghossian, A. A.; Zhang, J.; Barone, P. W.; Reuel, K. R.; Kim, J. H.; Heller, D. A.; Ahn, J. H.; Hilmer, A. J.; Rwei, A.; Arkalgud, J. R.; Zhang, C. T.; Strano, M. S. *ChemSusChem*. 2011, 4, 848-863.
3. Endo, T.; Ishi-Hayase, J.; Maki, H. *Appl. Phys. Lett.* 2015, 106, 113106.
4. Brozena, A. H.; Kim, H.; Powell, L. R.; Wang, Y. *Nat. Rev. Chem.* 2019, 3, 375-392.
5. Maeda, Y.; Suzuki, Y.; Konno, Y.; Zhao, P.; Kikuchi, N.; Yamada, M.; Mitsuishi, M.; Dao, A. T. N.; Kasai, H.; Ehara, M. *Commun. Chem.* 2023, 6, 159.
6. Maeda, Y.; Morooka, R.; Zhao, P.; Uchida, D.; Konno, Y.; Yamada, M.; Ehara, M. *J. Phys. Chem. C* 2023, 127, 2360-2370.
7. Maeda, Y.; Morooka, R.; Zhao, P.; Yamada, M.; Ehara, M. *Chem. Commun.*, 2023, 59, 11648-11651.
8. Maeda, Y.; Zhao, P.; Ehara, M. *Chem. Commun.*, 2023, 59, 14497-14508.

Catalytic Enantioselective Nitron Cycloadditions Enabling Collective Syntheses of Indole Alkaloids

Xiaochen Tian^a, Yang Wang^{a,b,*}

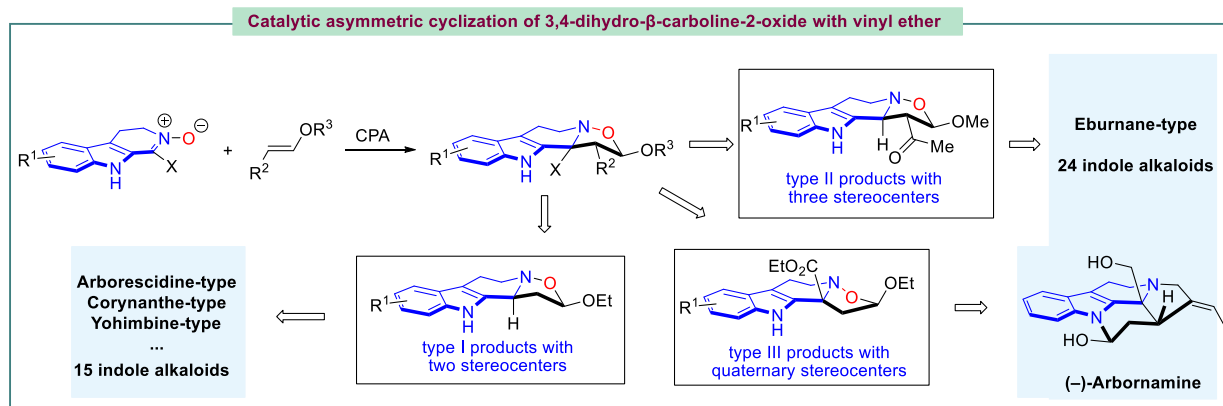
^a Molecular Synthesis Center & Key Laboratory of Marine Drugs, Chinese Ministry of Education, School of Medicine and Pharmacy, Ocean University of China, 5 Yushan Road, Qingdao 266003, China

^b Laboratory for Marine Drugs and Bioproducts, Qingdao Marine Science and Technology Center, Qingdao 266237, China

*Corresponding author: wangyang@ouc.edu.cn

Tetrahydro- β -carboline skeletons are prominent and ubiquitous in an extraordinary range of indole alkaloid natural products and pharmaceutical compounds. Novel and powerful synthetic approaches for stereoselective synthesis of tetrahydro- β -carboline skeletons have immense impacts and have attracted enormous attention. Here, we outlined a general chiral phosphoric acid catalyzed asymmetric 1,3-dipolar cycloaddition of 3,4-dihydro- β -carboline-2-oxide type nitron that enabled access to three types of chiral tetrahydro- β -carbolines bearing continuous multi-chiral centers and quaternary chiral centers. The method displayed different endo/exo selectivity from traditional nitron chemistry. The distinct power of this new strategy has been illustrated by application to collective and enantiodivergent total syntheses of 40 TH β C-type indole alkaloid natural products including first total syntheses of 7 natural products with divergent stereochemistry and varied architectures.

Keywords: Tetrahydro- β -carbolines; 3,4-Tetrahydro- β -carboline-2-oxide; Asymmetric catalysis; Total synthesis of indole alkaloid natural products



References

1. Tian, X.; Xuan, T.; Gao, J.; Zhang, X.; Liu, T.; Luo, F.; Pang, R.; Shao, P.; Yang, Y.; Wang, Y. *Nat. Commun.* **2024**, in revision.

Synthesis of multisubstituted fluoroalkenes using halothane as a fluorine-containing building block

**Yukiko Karuo^a, Keita Hirata^a, Yukari Akamatsu^a, Atsushi Tarui^a, Kazuyuki Sato^a,
Kentaro Kawai^a, Masaaki Omote^{a,*}**

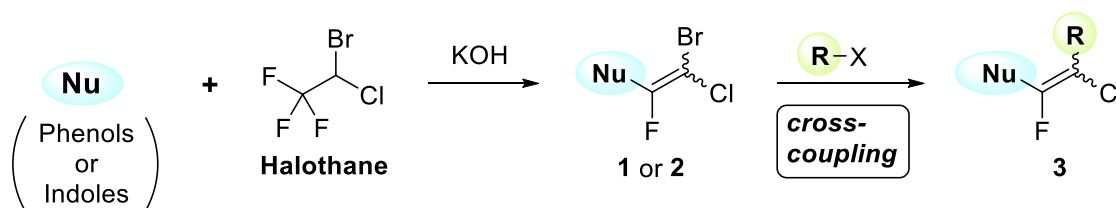
^a Faculty of Pharmaceutical Sciences, Setsunan University.

*Corresponding author: omote@pharm.setsunan.ac.jp

Abstract

Fluoroalkene skeleton is utilized in the industrial fields such as medicines, agrochemicals, polymers and liquid crystals, and the numerous synthesis methods of fluoroalkene skeleton have been reported. For example, one of the methods is using fluoroalkanes as fluorine-containing building blocks under basic conditions.^{1,2} Recently, we have developed the methods to synthesize fluoroalkenes (**1** or **2**) from 2-bromo-2-chloro-1,1,1-trifluoroethane (halothane) and nucleophiles (phenols or indoles).³ **1** or **2** possesses some halogens, especially reactive bromine atom, is useful for further transformation of **1** or **2** to new fluorocompounds. Thus, we try to afford various multisubstituted fluoroalkenes (**3**) by Suzuki–Miyaura or Sonogashira cross-coupling reactions.⁴

Keywords: fluorine-containing building blocks, 2-bromo-2-chloro-1,1,1-trifluoroethane, fluoroalkenes, fluoroenynes



References

1. Wu, K.; Chen, Q.-Y.; *Tetrahedron*, **2002**, *58*, 4077-4084.
2. Tang, X.-J.; Chen, Q.-Y.; *Synlett*, **2020**, *31*, 2046-2048.
3. Karuo, Y.; Tarui, A.; Sato, K.; Kawai, K.; Omote, M. *Beilstein J. Org. Chem.*, **2022**, *18*, 1567–1574.
4. *Submitted*.

Development of Anti Amoeba Active Fumagillin Derivatives Based on the Incorporation of Fluorine Atom Strategy

Yuji Sumii^{a,*}

^aGraduate School of Engineering, Nagoya Institute of Technology.

*sumii.yuji@nitech.ac.jp

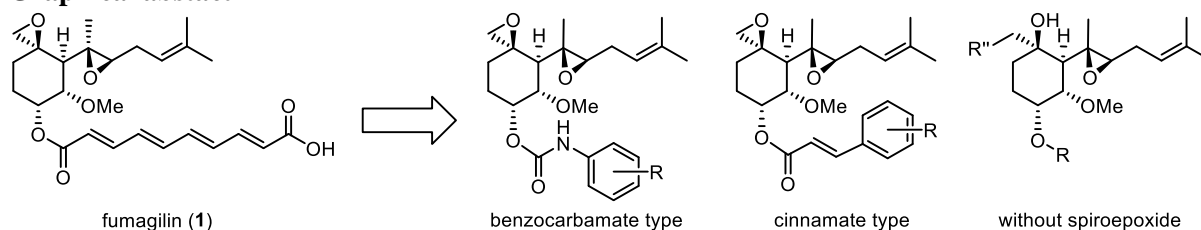
Abstract

Dysentery amebiasis is an infection caused by the parasitic protozoan *Entamoeba histolytica*. The annual number of infected people in the world is estimated to be 50 million, and the annual number of deaths worldwide is reported to be 40,000 to 70,000, especially it has become a serious social problem in developing countries. Therefore, development of new novel anti-amoebic agents is demanded. Mori, Nozaki et al. carried out a research to discover anti-amoebic compounds, and found that fumagillin showed good anti-amoebic activity. Fumagillin has been reported to have bioactive activities such as antibacterial activity and angiogenesis inhibitory activity, and TNP-470 (anticancer, Takeda Pharmaceutical Company Limited), Beloranib (anti-obesity, Zafgen), and ZGN-1061 (diabetes drug, Zafgen) have been developed so far, but the development of these drugs was dropout at the clinical trial stage because of their cytotoxic effects. Therefore, development of fumagillin derivatives having high anti-amoebic activity and no cytotoxicity.

Fluorofunctionalization of compounds alter the physicochemical and biological properties of organic compounds, and has become a useful strategy in drug discovery development. We designed a variety of fumagillin derivatives based on the introduction of fluorine atoms, and synthesized the derivatives from fumagillin, such as benzocarbamate type, cinnamate type. As the results of evaluation of the cytotoxicity and anti-amoeba activity of the fumagillin derivatives, introduction of fluorine affected the biological properties. Furthermore, we synthesized fumagillin derivatives without spiroepoxide moiety to increase the chemical stability, and found that the spiroepoxide moiety plays an important role in the anti-amoeba activity.

Keywords: Fumagillin, Anti amoebic activity, Fluorine, Cytotoxicity

Graphical abstract



References

1. Mori, M. et al., 3C15a08, JSBBA 2017 annual meeting

Highly Efficient Selective Monohydrolysis of Symmetric Diesters

Satomi Niwayama^{a,*}

^aGraduate School of Engineering

Muroran Institute of Technology

27-1, Mizumoto-cho, Muroran, Hokkaido

*Corresponding author: niwayama@muroran-it.ac.jp

Abstract

Developing environmentally benign and cost-effective organic reactions has been paramount in the production of various significant classes of organic compounds. Water is the least expensive and the most environmentally friendly solvents. Water-mediated organic reactions thus represent a typical “green chemistry.” Among various synthetic conversions, desymmetrization of symmetric compounds is one of the most cost-effective reactions, because the starting symmetric compounds are typically obtained easily on a large scale from inexpensive sources, or commercially available at low cost. Therefore, water-mediated desymmetrization of symmetric organic compounds would be of considerable value for the synthesis of a wide range of organic compounds, although distinguishing identical functional groups existing in the starting compounds is challenging.

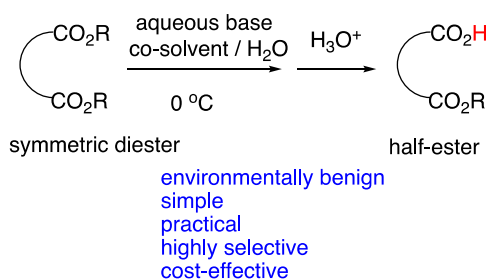
In this regard we have developed highly efficient and practical monohydrolysis reactions of symmetric diesters in aqueous media without requiring special reagents or device, enabling anyone to utilize. Our reactions are among the first water-mediated reactions applied to desymmetrization without relying on enzymes. Half-esters, produced by such monohydrolysis of symmetric diesters, are versatile building blocks in organic synthesis, which are applied to the synthesis of various significant compounds such as polymers, natural products, and pharmaceuticals.

We have been applying these reactions to the synthesis of pharmaceuticals and libraries of polymers including amphiphilic polymers in a well-controlled manner, and finding their unique anti-cancer activities. Based on the mechanisms of the selectivity we elucidated, we have also been developing other water-mediated desymmetrization reactions.

This presentation will describe the current progress and the scope of this selective monohydrolysis reactions.

Keywords: green chemistry, water-mediated reaction, desymmetrization, practical reaction, half-esters

Graphical abstract



References

- Niwayama, S. *J. Org. Chem.* **2000**, *65*, 5834-5836
- Niwayama, S.; Cho, H.; Zabet-Moghaddam, M.; Whittlesey, B. R. *J. Org. Chem.* **2010**, *75*, 3775-3780
- Shi, J.; Hayashishita, Y.; Takata, T.; Nishihara, Y.; Niwayama, S. *Org. Biomol. Chem.* **2020**, *18*, 6634-6642.
- Barsukova, T.; Sato, T.; Takumi, H.; Niwayama, S. *RSC Adv.* **2022**, *12*, 25669-25674
- Lin, X.; Shi, J.; Niwayama, S. *RSC Adv.* **2023**, *13*, 3494-3504.
- Niwayama, S.; Hiraga, Y. *ACS Omega* **2023**, *8*, 33819-33824, and references cited therein.

The Photochemistry of Xanthophyll Carotenoid-binding Rhodopsins

Keiichi Inoue*

The Institute for Solid State Physics, The University of Tokyo, Japan

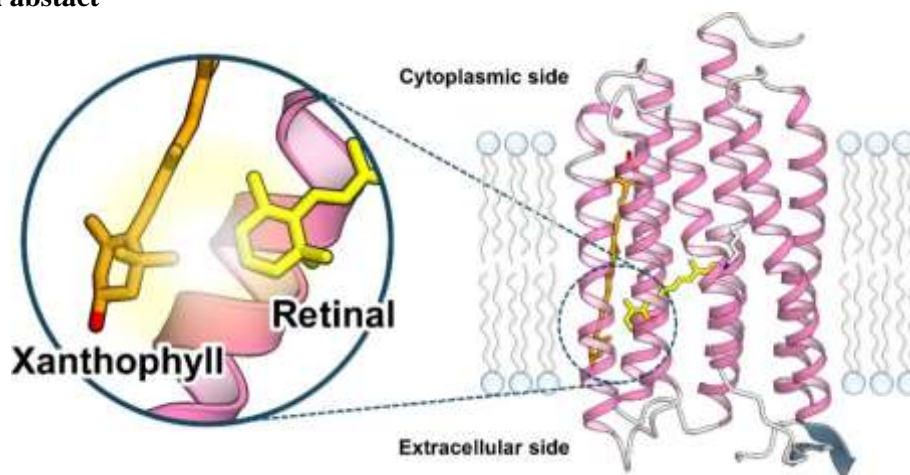
**Corresponding author: inoue@issp.u-tokyo.ac.jp*

Abstract

Microbial rhodopsins are photoreceptive membrane proteins that use all-*trans*-retinal chromophore. While they exhibit various biological functions driven by light, the most abundant microbial rhodopsins are outward light-driven proton pumps. These pumps transport protons from the cytoplasmic side to the extracellular side, generating a proton motive force to drive ATP synthesis and proton-coupled transport. Whereas microbial rhodopsins typically have only the retinal chromophore, xanthorhodopsin (XR) from *Salinibacter ruber* binds an antenna carotenoid molecule, salinixanthin, on the protein surface¹. However, only 2–3 microbial rhodopsins are known to bind the antenna carotenoid. In this study, we discovered new types of outward proton-pumping microbial rhodopsins that bind xanthophyll carotenoids such as lutein and zeaxanthin². Surprisingly, 18–33% of microbial rhodopsins in the marine environment are thought to bind xanthophyll as an antenna. We further investigated the efficiency of energy transfer from the xanthophyll to the retinal chromophore using transient absorption spectroscopy. As a result, the quantum efficiency of the excitation energy transfer between lutein, a member of xanthophyll, and the retinal chromophore was estimated to be 0–17%, which varied depending on the peak of xanthophyll excited, and higher values were observed when the higher vibronic bands were excited compared to the lowest band. This vibronic band-dependent excitation energy transfer differs from XR using salinixanthin, where no difference in quantum yield was observed between the vibronic bands, indicating a new mechanism of excitation energy transfer in xanthophyll-binding rhodopsins different from that in typical salinixanthin-binding XR.

Keywords: Microbial rhodopsin, retinal, carotenoids, photocycle, optogenetics

Graphical abstract



References

1. Balashov, S. P.; Imasheva, E. S.; Boichenko, V. A.; Anton, J.; Wang, J. M.; Lanyi, J. K., *Science*, 2005, 309, 2061-2064
2. Chazan, A.; Das, I.; Fujiwara, T.; Murakoshi, S.; Rozenberg, A.; Molina-Márquez, A.; Sano, F. K.; Tanaka, T.; Gómez-Villegas, P.; Larom, S.; Pushkarev, A.; Malakar, P.; Hasegawa, M.; Tsukamoto, Y.; Ishizuka, T.; Konno, M.; Nagata, T.; Mizuno, Y.; Katayama, K.; Abe-Yoshizumi, R.; Ruhman, S.; Inoue, K.; Kandori, H.; León, R.; Shihoya, W.; Yoshizawa, S.; Sheves, M.; Nureki, O.; Béjà, O., *Nature*, 2023, 615, 535-540

PREPARATION AND CHARACTERIZATION OF CHITOSAN CROSS-LINKING WITH GLUTARALDEHYDE

Erdenechimeg N^a, Bayarmaa B^a, Purevdorj E^a, Munkhgerel L^a, Odonchimeg M^{a,*}

^a*Institute of Chemistry and Chemical Technology, Mongolian Academy of Sciences, Ulaanbaatar
13330, Mongolia*

*Corresponding author: odonchimegm@mas.ac.mn

Abstract

Chitosan is a natural cationic biopolymer derived from chitin by deacetylation. Compared with synthetic polymers, chitosan has advantages like biocompatibility, biodegradability, and no toxicity. The reactive amino and hydroxyl groups of chitosan play crucial roles in facilitating the synthesis of the three-dimensional hydrogel. These hydrogels quickly swell in water or biological fluids; therefore, they have become a potential candidate for carriers of bioactive macromolecules. Nowadays, chitosan-based hydrogels are widely used in medicine and the food industry.

Chitosan-glutaraldehyde hydrogels were prepared using the chemical cross-linking method and characterized by UV-Vis, FTIR, X-ray diffraction, thermogravimetric analysis, CHN elemental analysis, and scanning electron microscopy (SEM). The FT-IR spectra of hydrogel showed the presence of an imine bond (C=N) and an ethylenic bond (C=C) at 1635 cm⁻¹ and 1560 cm⁻¹, respectively. These results confirm that the effective cross-linking of chitosan hydrogel with glutaraldehyde has occurred in the amino groups of chitosan. SEM results showed that increasing the percentage of glutaraldehyde leads to a decrease in wrinkles and grooves on the surface of the hydrogel. The chitosan hydrogels exhibit time-dependent swelling in a phosphate buffer solution (pH 7.2) at room temperature. As the degree of cross-linking increases, the swelling ratio decreases. The cross-linked chitosan derivatives showed a more amorphous structure compared to raw chitosan.

Keywords: Hydrogel, chitosan, glutaraldehyde, swellability, cross-linking

References

1. Kildeeva, N.R.; Perminov, P.A.; Vladimirov, L.V.; Novikov, V.V.; Mikhailov, S.N. *Russ. J. Bioorg. Chem.*, **2009**, *35*, 397-407
2. Akakuru, O.U.; Isiuku, B.O. *J. Phys. Chem. Biophys.*, **2017**, *7*.
3. Poon, L.; Wilson L.D.; Headley J.V. *Carbohydr. Polym.*, **2014**, *109*, 92-101
4. Craciun A.M.; Morariu, S.; Marin, L. *J. Polym.*, **2022**, *14*, 2570.
5. Hong, F.; Qiu, P.; Wang, Y.; Ren, P.; Liu, J.; Zhao, J.; Gou, D. *Food Chem.: X*, **2024**, *21*, 101095

Analysis of physicochemical properties of Mongolian lignite

S.Jargalmaa*, A.Altantuul*, B.Munkhtsesteg*, N.Navchtsetseg*, G.Shiirav*, B.Avid*,
Y.Xing**

*Institute of chemistry and chemical technology, Mongolian Academy of Sciences

**Chinese National Engineering Research Center of Coal Preparation and Purification, Xuzhou
221116, China

Abstract

Lignites from Mongolia were characterized by elemental, XRD, XRF, SEM, XPS, and FTIR analyses. Flotation tests were done to reduce impurities, like ash.

Both types of lignite have lower carbon and higher oxygen elements, with lower metamorphism degree. Lignite 1 and Lignite 2 both contain a large amount of mineral impurities, such as quartz and kaolinite. Lignite 1 has a rough surface, while Lignite 2 has a relatively smooth surface, many clay particles are adhered both. Both types of lignite surfaces contain abundant oxygen-containing functional groups and have lower ζ potentials.

Diesel has a very low flotation recovery for both lignites. Plant oils have a higher flotation recovery, however, the selectivity of plant oils was poor.

Keywords: Lignite, elemental analysis, minerals, flotation

Mineral-Cluster Chemistry in Space: Planetary Formation Regions and Planetary Atmospheres

Masashi Arakawa^{a,*}

^a Department of Earth and Planetary Sciences, Faculty of Science, Kyushu University, Japan

*Corresponding author: arakawa@geo.kyushu-u.ac.jp

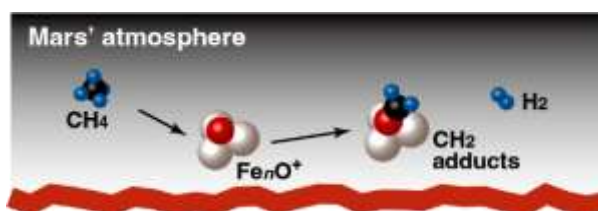
Abstract

Silicate (e.g., (Mg,Fe)SiO₃ and (Mg,Fe)₂SiO₄) and silica (SiO₂) are among the most abundant materials in space. It is prevalent hypothesis that particles of such minerals contribute to molecular evolution in planetary formation regions. It has recently been suggested that small clusters of silica and silicates could be highly abundant in the interstellar medium.^{1,2} In this context, we have reported reactions of gas-phase free silicate, Mg_lSiO_m⁻, and silica, Si_nO_m⁻, cluster anions with CO and H₂O molecules.^{3,4} In addition, coadsorption and subsequent reaction of CO and H₂ molecules on cobalt cluster cations, Co_n⁺, has been examined to discuss formation of organic molecules on the cluster.⁵

Another chemical process among recent topics in space is rapid methane loss in Mars' atmosphere.⁶ Observation by the Curiosity rover found temporary spikes of methane and its rapid loss, but the mechanism of the loss has not been elucidated yet. Mars' soil is rich in iron oxide, and storms of iron-oxide particles (dust devils) occur very frequently. Hypervelocity impacts of small bodies on Mars would have also evaporated or made molten the surface materials.⁷ Because the iron-oxide cluster, Fe₂O₂, is known as an active center of enzyme, methane monooxygenase, we hypothesized that iron-oxide particles/clusters were responsible for the rapid loss. Numerous theoretical studies on the interaction of Fe₂O₂ with methane have been reported.⁸ As for an experimental study, FeO⁺ was reported to mediate activation of methane.⁹ In the present study, we report gas-phase reaction of size-selected iron-oxide cluster cations, Fe_nO_m⁺, with methane molecules to verify our hypothesis, where methane activation was observed to produce Fe_nO_mCH₂⁺ and Fe_nO_mC⁺. The reactivity exhibited size dependence. For example, the rate coefficients of the methane activation for Fe₃O⁺ was estimated to be 1 × 10⁻¹³ cm³ s⁻¹. Based on this value, the presence of iron-oxide clusters/particles of 10⁷ cm⁻³ (10⁻⁷ Pa at -50°C) in Mars' atmosphere would explain the loss of methane.¹⁰

Keywords: iron-oxide cluster, methane, Mars' atmosphere, molecular evolution, silicate

Graphical abstract



References

1. Reber, A. C.; Paranthaman, S.; Clayborne, P. A.; Khanna, S. N.; Castleman, A. W., Jr. *ACS Nano* 2008, 2, 1729–1737.
2. Guiu, M.; Ghejan, B.-A.; Bernhardt, T. M.; Bakker, J. M.; Lang, S. M.; Bromley, S. T. *ACS Earth Space Chem.* 2022, 6, 2465–.
3. Arakawa, M.; Yamane, R.; Terasaki, A. *J. Phys. Chem. A* 2016, 120, 139–144.
4. Arakawa, M.; Omoda, T.; Terasaki, A. *J. Phys. Chem. C* 2017, 121, 10790–10795.
5. Arakawa, M.; Okada, D.; Kono, S.; Terasaki, A. *J. Phys. Chem. A* 2020, 124, 9751–9756.
6. Webster, R. et al. *Science* 2018, 360, 1093–1096.
7. Ganino, C.; Libourel, G.; Nakamura, A. M.; Jacomet, S.; Tottereau, O.; Michel, P. *Meteorit. Planet. Sci.* 2018, 53, 2306–2326.
8. Yoshizawa, K.; Yumura, T. *Chem. Eur. J.* 2003, 9, 2347–2358.
9. Schröder, D.; Schwarz, H. *Angew. Chem. Int. Ed.* 1990, 29, 1433–1434.
10. Arakawa, M.; Kono, S.; Sekine, Y.; Terasaki, A. *Phys. Chem. Chem. Phys.* 2024, 26, 14684–14690.

Crystal Structure and Physical Properties of Basket-Shaped Polyoxometalates

Masaru Fujibayahsi^{a,*}

^aNational Institute of Technology, Ube College

*fujiba@ube-k.ac.jp

Abstract

Clathrate materials have attracted much attention due to their wide range of application such as dielectrics, drug delivery, and superconductors. In recent years, we have reported basket-shaped polyoxometalates (POMs) grafted with organic functional groups, $[\text{Na}^+\text{C}(\text{SO}_3)_2(\text{R-PO}_3)_4\text{Mo}^{\text{V}}_4\text{Mo}^{\text{VI}}_{14}\text{O}_{49}]^{5-}$ ($\text{R} = \text{phenyl, propyl, } t\text{-butyl, and } n\text{-butyl}$), as a sodium ion encapsulated metal-oxide molecule¹⁻³. The single-crystal X-ray analysis has divided the molecular structure into symmetric and asymmetric forms. The symmetric form has C_2 symmetry, and the encapsulated sodium ion was located on the symmetry center. On the other hand, the asymmetric form has a distorted Mo-O molecular framework accompanied by a positional shift of sodium ion, which generates molecular polarization. These symmetry differences are expected to develop in dielectric materials such as ferroelectrics. Especially, basket-shaped POM grafted with n -butyl groups showed a phase transition between symmetric and asymmetric forms with temperature control. Below the phase transition temperature, asymmetric molecular frameworks were fully disordered whole in single-crystal, thus crystal structure was assigned as centrosymmetric space groups of $C2/c$. However, rapid or slow cooling process of single-crystal showed another feature of the X-ray diffraction pattern and the formation of the superlattice during slow cooling process was observed. In addition, when applying the external electric fields to the single-crystal, the phase temperature shifted to the higher temperature with increasing the strength of the electric fields like ferroelectrics were observed. These results suggested that n -butyl derivatives formed crystal domains during the order-disorder type phase transition and these domains can be controlled by external electric fields.

for dielectrics and control of the symmetry and molecular orientation is necessary to develop the ferroelectricity.

Keywords: polyoxometalate, dielectrics, ferroelectricity, phase transition

References

1. I. Nakamura, H. N. Miras, A. Fujiwara, M. Fujibayashi, Y.-F. Song, L. Cronin, and R. Tsunashima, *J. Am. Chem. Soc.*, **2015**, *137*, 6524-6530.
2. M. Fujibayashi, M. Shiga, R. Tsunashima, and T. Nakamura, *Bull. Chem. Soc. Jpn.*, **2019**, *92*, 918-922.
3. M. Fujibayashi, Y. Watari, R. Tsunashima, S. Nishihara, S. Noro, C.-G. Lin, Y.-F. Song, K. Takahashi, T. Nakamura, and T. Akutagawa, *Angew. Chem. Int. Ed.*, **2020**, *59*, 22446-22450.

Evaluation of Intramolecular Interactions with Negative Fragmentation Approach including Basis-Set Superposition Error Correction

Yu Takano^{a,*}, Hiroko X. Kondo^b, Haruki Nakamura^c

^aGraduate School of Information Sciences, Hiroshima City University, Japan.

^bFaculty of Engineering, Kitami Institute of Technology.

^cInstitute for Protein Research, Osaka University, Japan.

*Corresponding author: ytakano@hiroshima-cu.ac.jp

Abstract

Inter- and intramolecular interactions such as hydrogen bonds (H-bonds), C–H···O, C–H··· π , and π ··· π stacking play an important role in many chemical and biological phenomena. These phenomena include protein folding, crystal engineering, supramolecular architectures, and host–guest chemistry. Precise and quantitative estimations of these interactions are required to understand the principles underlying the formation of three-dimensional structures.

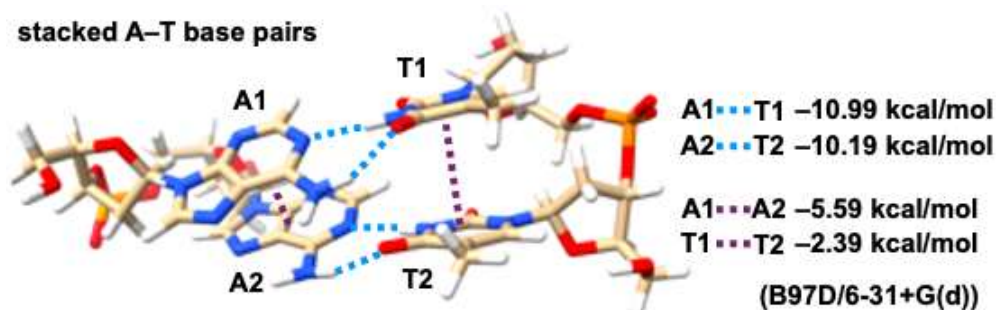
There are few general methods available for estimating such individual inter- and intramolecular interaction energies. For example, the estimation of individual H-bonding interaction energies in an α -helix is not straightforward because the H-bond donor and acceptor are linked through covalent bonds. Recently, we have proposed a negative fragmentation approach (NFA) to calculate intramolecular H-bonding interactions and applied it to helical secondary structures of proteins such as α -helix, 3_{10} -helix, and π -helix.^{1–3} NFA, in its formulation, can also evaluate intermolecular energies in molecular complexes. One advantage of NFA is that it does not require modification of the program code, although multiple calculations are needed. This indicates that we can utilize the NFA with any quantum chemical calculation programs.

However, it is well-known that the basis set superposition error (BSSE) can seriously affect the quantitative accuracy of interaction analysis, especially when small- or medium-size basis sets are used. The origin of this error lies in the possibility that the unused basis functions of the second unit in the associated complex may augment the basis set of the first unit, thereby lowering its energy compared to a calculation of this unit alone. Correction with the counterpoise (CP) procedure is commonly utilized for accurate estimation of intermolecular interaction energy.⁴

In the present work, we propose a CP correction of BSSE in the NFA framework to precisely evaluate individual inter- and intramolecular interaction energies and show its application to various molecular systems such as formamide dimer, stacked A–T base pairs, and α -helices.

Keywords: intermolecular interaction, intramolecular interaction, negative fragmentation approach (NFA), basis set superposition error (BSSE), counterpoise (CP) procedure

Graphical abstract



References

1. Takano, Y; Kondo, H. X.; Nakamura, H. *Biophys. Rev.* 2022, 14, 1369–1378.
2. Kondo H. X.; Nakamura, H.; Takano, Y. *Int. J. Mol. Sci.* 2022, 23, 9032.
3. Kondo H. X.; Nakamura, H.; Takano, Y. *Chem. Phys. Lett.* 2023, 815, 140361.
4. Boys, S. F.; Bernardi, F. *Mol. Phys.* 1970, 533–566.

Electric field assisted low-temperature CO₂ reduction over supported metal catalysts

Shuhei Ogo^{a,b,*}, Masaki Yamaoka^a, Keidai Tomozawa^a, Tadaharu Ueda^{a,b,c}

^a Department of Marine Resources Science, Kochi University

^b Marine Core Research Institute, Kochi University

^c MEDi Center, Kochi University

*Corresponding author: ogo@kochi-u.ac.jp

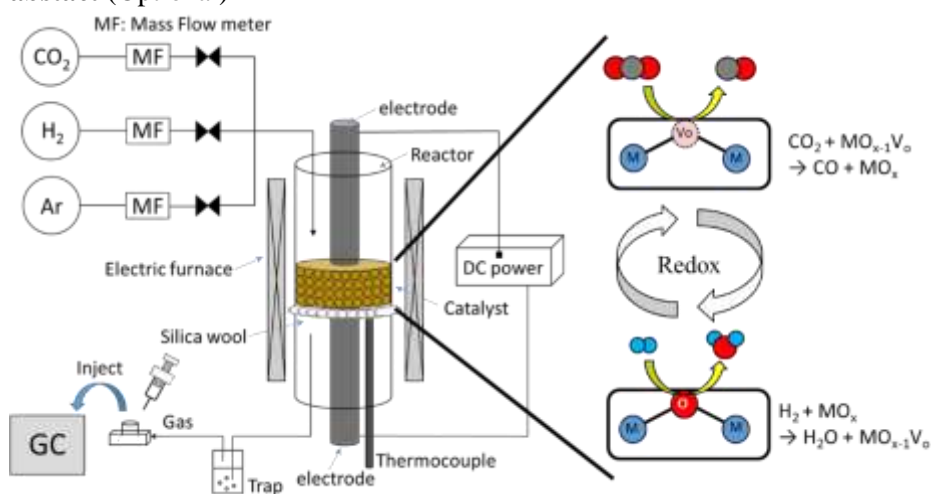
Abstract

Extensive attention has been given to solving the important issue that anthropogenic emissions of greenhouse gases such as CO₂ could accelerate global warming. Recently, a variety of CO₂ capture and utilization (CCU) technologies have been developed because they are regarded as effective ways to reduce artificial CO₂ emissions. CO production from CO₂ through the reverse water-gas shift (RWGS) reaction is quite important because CO can be further converted into high-value chemicals and fuels, which is mainstream for C1 chemistry. However, high-temperature heating is theoretically required to obtain high CO₂ conversion due to the thermodynamic equilibrium constraints for the RWGS reaction, leading to many problems in terms of energy and catalyst durability. Therefore, CO₂ conversion at low temperatures requires unconventional catalytic reaction techniques. The application of an external direct current electric field to metal-supported metal oxide semiconductor catalysts has enabled CO₂ reduction to proceed even at low temperature.¹

We report developments of high-performance supported metal catalysts without precious metals for low-temperature RWGS reaction under an external direct current electric field. For Fe-based catalysts, controlling the interaction between support oxide and supported Fe was effective to improve the catalytic activity under an electric field. 10 wt% Fe supported on Ce_{0.4}Al_{0.1}Zr_{0.5}O₂ (Fe/CAZO) showed high catalytic activity, CO selectivity (≈100%), and durability even at the low temperature of 423 K.² The apparent activation energy was estimated to be 5.9 kJ mol⁻¹ under an electric field, which was much lower than that without an electric field (61.4 kJ mol⁻¹). Mechanistic studies implied that the RWGS reaction over Fe/CAZO catalyst proceeded through a redox mechanism using lattice oxygen/lattice oxygen vacancies.

Keywords: electric field, reverse water gas shift, low-temperature, supported metal catalysts

Graphical abstract (Optional)



References

- Oshima, K.; Shinagawa, T.; Nogami, Y.; Manabe, R.; Ogo, S.; Sekine, Y. *Catal. Today*, 2014, 232, 27-32.
- Yamaoka, M.; Tomozawa, K.; Sumiyoshi, K.; Ueda, T.; Ogo, S. *Sci. Rep.* 2024, 14, 10216.

Precise Synthesis of Ligand-Protected Metal Nanoparticles and Nanoclusters for Photoelectrochemical Applications

Tokuhisa Kawawaki^a, Yuichi Negishi^{a,b,*}

^a Graduate School of Science, Tokyo University of Science, Japan

^b Institute of Multidisciplinary Research for Advanced Materials, Tohoku University, Japan

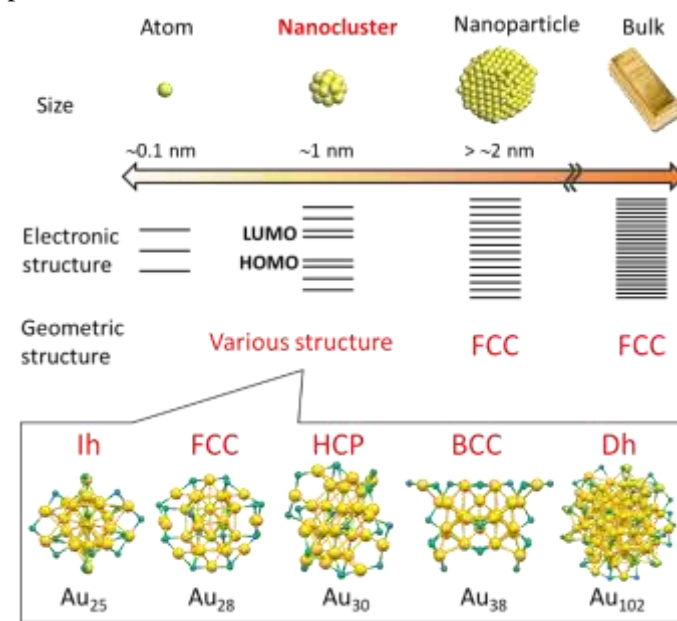
*Corresponding author: yuichi.negishi.a8@tohoku.ac.jp

Abstract

Nanosized metal particles have two major singularities as their size decreases. Metal nanoparticles with a size of about 100 nm generate a confinement effect beyond the diffraction limit of light due to localized surface plasmon resonance. I have clarified that the near-field light of metal nanoparticles can be used to improve the efficiency of photochemical reactions and the influence of their structural factors (size, shape, distance, etc.) on the activity enhancement. Furthermore, metal clusters with a size of approximately 1 nm will have an electronic structure like a molecule based on quantum size effects and will have a crystal structure that cannot be obtained with bulk metals. I have created novel metal clusters, clarified their physicochemical properties, and established a method to apply them as highly active photo- and electrocatalysts.¹⁻⁴ I will present that the understanding of the science of metal nanomaterials and its applied research of both metal nanoparticles and clusters.

Keywords: metal nanocluster, cluster, nanoparticle, electrocatalysts, photocatalysts

Graphical abstract (Optional)



References

1. Kawawaki, T.; Mori, Y.; Wakamatsu, K.; Ozaki, S.; Kawachi, M.; Hossain, S.; Negishi, Y. J. Mater. Chem. A 2020, 8, 16081-16113.
2. Yazaki, D.; Kawawaki, T.; Hirayama, D.; Kawachi, M.; Kosaku, K.; Oguchi, S.; Yamaguchi, Y.; Kikkawa, S.; Ueki, Y.; Hossain, S.; Osborn, D. J.; Ozaki, F.; Tanaka, S.; Yoshinobu, J.; Metha, Gregory. F.; Yamazoe, S.; Kudo, A.; Yamakata, A.; Negishi, Y. Small 2023, 19, 2208287.
3. Akinaga, Y.; Kawawaki, T.; Kameko, H.; Yamazaki, Y.; Yamazaki, K.; Nakayasu, Y.; Kato, K.; Tanaka, Y.; Hanindriyo, A. T.; Takagi, M.; Shimazaki, T.; Tachikawa, M.; Yamakata, A.; Negishi, Y. Adv. Funct. Mater. 2023, 33, 2303321.
4. Yamazaki, Y.; Tomoyasu, Y.; Kawawaki, T.; Negishi, Y. in preparation.

Photoredox Catalysis of Vitamin B₁₂ Derivative for Green Molecular Transformation

Hisashi Shimakoshi*

Department of Chemistry and Biochemistry, Graduate School of Engineering,
Kyushu University, Japan

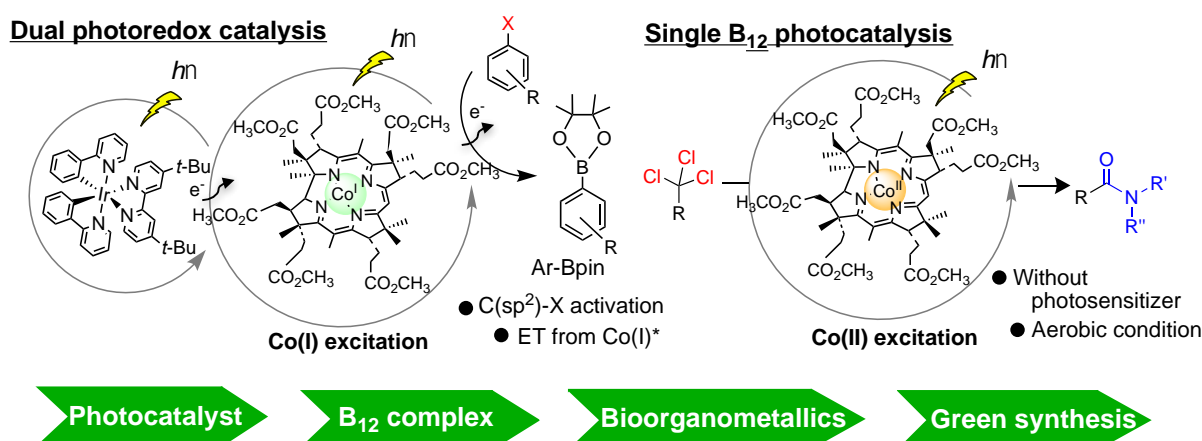
*Corresponding author: shimakoshi@mail.cstm.kyushu-u.ac.jp

Abstract

The combined use of bio-related metal complex such as cobalamin derivative with photochemical technique has been developed in green organic synthesis due to its efficient and non-toxic reaction system.^{1,2} We report a reductive dehalogenation of aryl halides by the photo-excited B₁₂ complex, heptamethyl cobyrinate, with the labile Co(I) oxidation state.³ This reaction pathway could overcome the substrate limitations during conventional catalysis of the B₁₂ cobalt complex which could not be applied to Ar-X with the C(sp²)-X bond. Based on this finding, we developed the new catalytic reaction of the B₁₂ derivative for the borylation of Ar-X with the combined use of photosensitizer based on a dual photoredox strategy by visible light irradiation.⁴ The excited Co(I) species (¹Co^I) species of heptamethyl cobyrinate acted as a reductant for the Ar-X reduction and an arylboronate was formed in the presence of bis(pinacolato)diboron (B₂pin₂) as the radical trapping reagent. The reaction proceeded with a very low amount of catalyst loading of 0.025 mol% towards the substrate and the highest 3,880 TON was achieved at room temperature. The dual photoredox system provides advantages for the reaction under mild conditions, a low amount of catalyst loading, and simple procedure.

In addition, we discovered the single photocatalytic system of B₁₂ derivative without additional photosensitizer.⁵ As an advance to this reaction, one-pot synthesis of amide from trichloromethylated organic compounds under aerobic condition is developed.

Keywords: vitamin B₁₂, photoredox catalyst, organic halide, oxygenation



References

1. K. Shichijo, H. Shimakoshi, *ChemPlusChem*. **2024**, e20240004 (Concept).
2. H. Shimakoshi *Chem. Rec.* **2021**, *21*, 2080 (Outside front cover).
3. H. Shimakoshi *et al*, *Chem. Lett.*, **2020**, *49*, 820.
4. K. Sasaki, K. Shichijo, M. Fujitsuka, H. Shimakoshi, *J. Por. Phthalocyanines*, **2023**, *27*, 1270.
5. H. Shimakoshi *et al*, *Chem. Commun.*, **2011**, *47*, 10921.
6. K. Sasaki, K. Shichijo, M. Fujitsuka, H. Shimakoshi, *Submitted*.

Computational Chemistry for Data-driven Material Development and Its Application to Multi-element Materials

Michihisa KOYAMA^{a,*}

^aResearch Initiative for Supra-Materials, Shinshu University, Japan

*Corresponding author: koyama_michihisa@shinshu-u.ac.jp

Abstract

The challenges in applying materials informatics to functional materials are to predict not only functionality but also stability, and to realize activity prediction that incorporates the heterogeneity of the active site structure of the real system.¹ The author has clarified the origin of the properties that differ from those of the bulk by first-principles calculations of real systems that incorporate the real system structure without simplification by using a supercomputer.²⁻¹³ In addition, about 10,000 data points have been accumulated using nano-alloy structural models.

In order not only to discover active new materials but also to create materials useful to society, it is important to construct a digital twin corresponding to physical space (physical space) in virtual space (cyberspace) to explore and evaluate materials at a throughput that surpasses that of experimental science. The author will present the details of ongoing efforts and future prospects, based on concrete examples in the multi-element materials.

Keywords: Computational Chemistry; Multi-element material; Real-system; Digital Screening

Acknowledgements

Part of the research is supported by KAKENHI (20H05623), Demonstration Project of Innovative Catalyst Technology for Decarbonization through Regional Resource Recycling by the Ministry of Environment, Japan, and JST-CREST (JPMJCR21B3), Strategic Innovation Promotion Program by Cabinet Office, Government of Japan. Part of first-principles calculations are conducted using MASAMUNE-IMR, Institute for Materials Research, Tohoku University.

References

1. J. Dean, M. G. Taylor, G. Mpourmpakis, *Sci. Adv.* 2019, 5, eaax5101.
 2. Y. Nanba, M. Koyama, *Phys. Chem. Chem. Phys.* 2022, 24, 15452-15461.
 3. D. Wu, K. Kusada, Y. Nanba, M. Koyama, T. Yamamoto, T. Toriyama, S. Matsumura, O. Seo, I. Gueye, J. Kim, L. S. R. Kumara, O. Sakata, S. Kawaguchi, Y. Kubota, H. Kitagawa, *J. Am. Chem. Soc.* 2022, 144, 3365–3369.
 4. Y. Nanba, M. Koyama, *Bull. Chem. Soc. Jpn.* 2021, 94, 2484-2492.
 5. D. S. Rivera Rocabado, Y. Nanba, M. Koyama, *ACS Omega* 2021, 6, 17424–17432.
 6. K. Kusada, D. Wu, Y. Nanba, M. Koyama, T. Yamamoto, X. Quy Tran, T. Toriyama, S. Matsumura, A. Ito, K. Sato, K. Nagaoka, O. Seo, C. Song, Y. Chen, N. Palina, L. S. R. Kumara, S. Hiroi, O. Sakata, S. Kawaguchi, Y. Kubota, H. Kitagawa, *Adv. Mater.* 2021, 2005206.
 7. Y. Nanba, M. Koyama, *ACS Omega* 2021, 6 (2021) 3218–3226
 8. D. S. R. Rocabado, Y. Nanba, M. Koyama, *Comput. Mater. Sci.* 2020, 184, 109874.
 9. Y. Nanba, M. Koyama, *J. Phys. Chem. C* 2019, 123, 28114–28122.
 10. D. S. R. Rocabado, T. Ishimoto, M. Koyama. *SN Appl. Sci.* 2019, 1, 1485.
 11. T. Ishimoto, M. Koyama, *J. Chem. Phys.* 2018, 148, 034705.
 12. Y. Nanba, T. Ishimoto, M. Koyama, *J. Phys. Chem. C* 2017, 121, 27445–27445.
 13. T. Ishimoto, M. Koyama, *J. Phys. Chem. Lett.* 2016, 7, 736–740.
- Seki, Y.; Ishiyama, T.; Sasaki, D.; Abe, J.; Sohma, Y.; Oisaki, K.; Kanai, M. *J. Am. Chem. Soc.* 2016, 138, 10798-10
14. Sonobe, T.; Oisaki, K.; Kanai, M. *Chem. Sci.* 2012, 3, 3249-3258.

***In situ* formation of isolated metal species in zeolites from bulk metals/metal oxides and their unique catalytic and adsorption property**

Zen Maeno*

^a School of Advanced Engineering, Kogakuin University, Japan

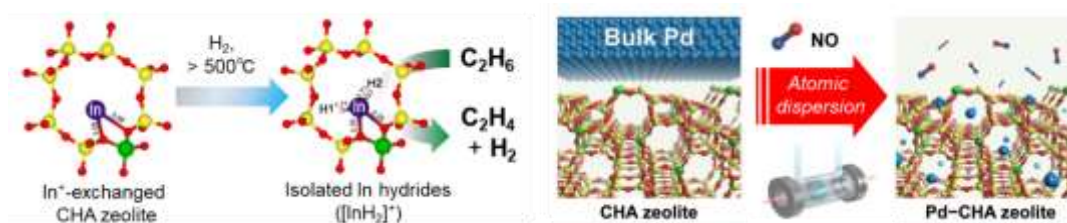
*Corresponding author: zmaeno@cc.kogakuin.ac.jp

Abstract

Metal species on solid catalysts change their oxidation state and local structure depending on temperature and atmosphere. The study on structural analysis under reaction conditions is essential to elucidate the active species and reaction mechanism. In this presentation, *in situ* generation of unique metal species in zeolites under high temperature reaction conditions is described. Their local structures were determined by a combination of *in situ*/operando spectroscopic measurements and theoretical investigations. Their catalytic and adsorption properties were also successfully developed.

Zeolites modified with 13-group metals, such as In and Ga, have attracted attention as promising catalysts to activate CH₄ and light alkanes [1]. We found isolated In hydrides were formed in CHA zeolites from In₂O₃ under H₂ flow at high temperature. *In situ* FTIR spectroscopic study and vibration analysis using density functional theory (DFT) calculations revealed that isolated [InH₂]⁺ ions coordinated to Al sites are formed. In the ethane dehydrogenation, In-CHA exhibited 97% selectivity for ethylene and maintained its activity for at least 90 h. The mechanistic investigation demonstrated that [InH₂]⁺ ions are plausible catalytically active sites [2]. The controlled formation of [GaH₂]⁺ in GAFI was investigated to improve the selectivity and durability in ethane dehydrogenation [3].

We also found the atomic dispersion of bulk Pd into Pd²⁺ cations into CHA zeolites under NO flow at high temperature, as revealed by microscopic and spectroscopic characterizations. By using this method, the high-loading Pd-CHA was successfully synthesized [4]. The obtained Pd-CHA was applied for passive NO_x adsorption where the increase in the Pd loading resulted in a shift in the NO desorption temperature toward a higher regime. The DFT calculation revealed that the local structure of Al sites stabilizing Pd cations influences their NO adsorption property [5].



Keywords: Zeolites, Atomic dispersion, Isolated metal hydrides, Ethane dehydrogenation, Passive NO_x adsorber (PNA)

References

1. M. Huang, S. Yasumura, T. Toyao, K. Shimizu, **Z. Maeno**, *Phys. Chem. Chem. Phys.*, **2023**, *25*, 10211.
2. **Z. Maeno**, S. Yasumura, X. Wu, M. Huang, C. T. Toyao, K. Shimizu, *J. Am. Chem. Soc.*, **2020**, *142*, 4820.
3. M. Huang, S. Yasumura, L. Li, T. Toyao, **Z. Maeno**, K. Shimizu, *Catal. Sci. Technol.*, **2022**, *12*, 986.
4. S. Yasumura, H. Ide, T. Ueda, Y. Jing, C. Liu, K. Kon, T. Toyao, **Z. Maeno**, K. Shimizu, *JACS Au*, **2021**, *1*, 201.
5. S. Yasumura, T. Ueda, H. Ide, K. Otsubo, C. Liu, N. Tsunoji, T. Toyao, **Z. Maeno**, K. Shimizu, *Phys. Chem. Chem. Phys.*, **2021**, *23*, 22273-22282.

BIS-CARBENE RUTHENIUM OLEFIN METATHESIS CATALYSTS

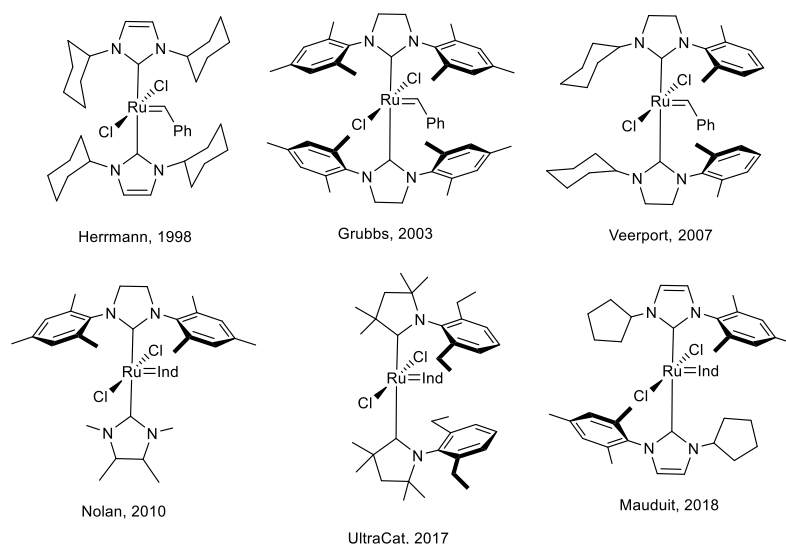
Bartosz Trzaskowski^{a,*}^aCentre of New Technologies, University of Warsaw, Poland

*Corresponding author: b.trzaskowski@cent.uw.edu.pl

Abstract

The olefin metathesis reaction of forming new C-C bonds is one of the most important reactions in organic synthesis. Today, most commonly used olefin metathesis bear only one N-heterocyclic carbene moiety, due to the fact that the Ru-carbene carbon bond is usually relatively strong and the ruthenium-based precatalyst requires a second ligand, which is able to readily dissociate upon catalyst activation. However, as soon as in 1998 Herrmann synthesized a series of stable bis-NHC ruthenium complexes.¹ Only later it was realized that such slowly-activating, latent catalysts, often requiring a thermal stimulus to reach satisfactory activities, can be very useful in a) reactions requiring a perfect control of the catalyst initiation, such as polymerization and b) sterically challenging metathesis reactions leading to tetrasubstituted olefins. Interestingly, in most cases such bis-carbene complexes are synthesized from specific azolium salts (NHC precursors), and e.g., the commercially available (PCy₃)₂Cl₂Ru-indenylidene complex **M1** or a corresponding benzylidene complex, and during such synthesis both carbenes replace two phosphines of the ruthenium complex precursor. On the other hand, identical methods and conditions are used to prepare standard benzylidene and indenylidene complexes bearing only one NHC moiety and one phosphine moiety.² This implies, that the proclivity to form either mono-NHC or bis-NHC complexes is dependent on the structure of the NHC in question and the final Ru complex. Our computational DFT studies aim to obtain a better understanding of the chemistry behind this phenomenon and answer the question whether either steric, electronic, or a combination of both properties are driving the formation of either mono-carbene or bis-carbene species.

Keywords: olefin metathesis, ruthenium, complexes, DFT, computational chemistry

**References**

1. Weskamp, T.; Schattenmann, W.C.; Spegler, N.; Herrmann, W.A.. *Angew. Chem. Int. Ed.* 1998, 37, 2490.-2493
2. Trnka, T.; Morgan, J.P.; Sanford, T.E.; Wilhelm, M.; Scholl, M.; Choi, T.-L.; Ding, S.; Day, M.W.; Grubbs, R.H. *J. Am. Chem. Soc.* 2003, 125, 2546-2558.

Minimizing Voltage Loss of Organic Photovoltaics by Local Dipole Moment Change of Non-Fullerene Acceptors

Akira Yamakata,^{1*} Kosaku Kato,¹ Takumi Urakami,² Masahiro Higashi,³ Hirofumi Sato,² Tomokazu Umeyama,⁴ and Hiroshi Imahori^{2,5,6}

¹Graduate School of Natural Science and Technology, Okayama University, Okayama 700-8530, Japan

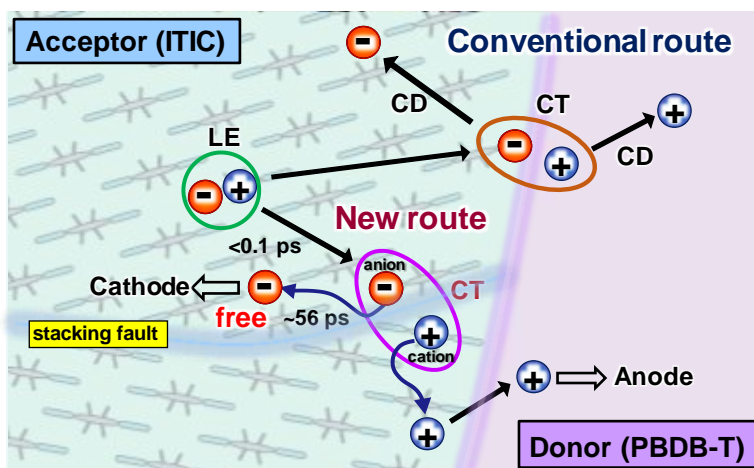
²Graduate School of Engineering, Kyoto University, Kyoto 615-8510, Japan

³Graduate School of Informatics, Nagoya University, Furo-cho, Chikusa-ku, Nagoya 464-8601, Japan

⁴Graduate School of Engineering, University of Hyogo, 2167 Shosha, Himeji, Hyogo 671-2201, Japan

*yamakata@okayama-u.ac.jp

Recently, the power conversion efficiency (PCE) of organic photovoltaics (OPVs) has reached more than 19% due to the rapid development of non-fullerene acceptors (NFAs). To compete with the PCEs (26%) of commercialized silicon-based inorganic photovoltaics, the drawback of OPVs should be minimized. This drawback is the intrinsic large loss of open-circuit voltage; However, a general approach to this issue remains elusive. Here, we report a discovery regarding highly efficient NFAs, specifically ITIC [1,2]. We found that charge-transfer (CT) and charge dissociation (CD) can occur even in a neat ITIC film without the donor layer. This is surprising, as these processes were previously believed to take place exclusively at donor/acceptor heterojunctions. Femtosecond time-resolved visible to mid-infrared measurements revealed that in the neat ITIC layers, the intermolecular CT immediately proceeds after photoirradiation (<0.1 ps) to form weakly-bound excitons with a binding energy of 0.3 eV, which they are further dissociated into free electrons and holes with a time-constant of 56 ps. Theoretical calculations indicate that stacking faults in ITIC (i.e., V-type molecular stacking) induce instantaneous intermolecular CT and CD in the neat ITIC layer. In contrast, J-type stacking does not support such CT and CD. This previously unknown pathway is triggered by the larger dipole moment change on the excited state generated at the lower symmetric V-type molecular stacking of ITIC. This is in sharp contrast with the need of sufficient energy offset for CT and CD at the donor-acceptor heterojunction, leading to the significant voltage loss in conventional OPVs. These results demonstrate that the rational molecular design of NFAs can increase the local dipole moment change on the excited state within the NFA layer. This finding paves the way for a groundbreaking route toward the commercialization of OPVs.



Keywords: Organic solar cells, Charge separation, Recombination, Time-resolved spectroscopy,

References

1. A. Yamakata, K. Kato, T. Urakami, M. Higashi, H. Sato, T. Umeyama, and H. Imahori, submitted for publication.
2. S. Jinnai, K. Murayama, K. Nagai, M. Mineshita, K. Kato, A. Muraoka, A. Yamakata, A. Saeki, Y. Kobori, Y. Ie *J. Mater. Chem. A*, **2022**, *10*, 20035.

Data-driven Approach To Materials Exploration

Kenta Hongo^{a,*},

^a *Reserach Center for Advanced Computing Infrastructure, JAIST, Japan*

^{*} *Corresponding author: hongo@jaist.ac.jp*

Abstract

Materials Informatics (MI)¹—an incorporation of information and data science into materials science—has emerged in the past decade as a new approach to computational materials design, pursuing the ultimate goal of discovering novel or unknown materials with desirable properties *in silico*. Not only high-throughput virtual screening based on machine learning (ML)², but also more sophisticated approaches based on Bayesian inference³⁻⁵ have been proven to successfully explore new materials with improved properties. Since ML or regression models can predict physical properties much faster than typical *ab initio* simulations, the former expand the search space into much wider subspaces (10^4 - 10^6 compounds) than the latter. Furthermore, Bayesian inference can efficiently propose candidate compounds with desired properties, significantly accelerating materials exploration. These technologies have played an important role in data-driven materials exploration.

Combined with *ab initio* simulations, the evolutionary algorithm has been found useful for exploring novel structures for given material compositions. Examples include a new high-pressure phase of hydrogen solid⁶, new high-pressure phases of metal hydrides exhibiting high superconducting transition temperatures⁷, a high-pressure polymerized phase of metal carbodiimide⁸, and mixed anion compounds⁹. In practice, these structure searches require a huge amount of computations, including evolutionary-algorithm-based search for candidate structures, convex hull analysis for relative enthalpies, and *ab initio* phonon simulations for validating their dynamic stabilities. This is achieved with the help of recent advanced massively parallel computers.

The success in these "ab initio materials informatics (AIMI)" studies can be attributed to the fact that density functional theory (DFT) simulations are appropriate for these systems. As is well known, DFT works well in most cases, but it sometimes fails to properly describe electronic structures even qualitatively¹⁰. In such cases, more sophisticated *ab initio* methods are crucial for generating materials property data. One of the most promising *ab initio* simulations is quantum Monte Carlo (QMC), which is suitable for next-generation exascale parallel computers. Although QMC requires much larger computational costs than DFT, it provides more accurate and reliable property data. Thus, QMC can be used as a "data generation engine" in the next-generation AIMI.

In this talk, I will briefly refer to MI/AIMI and then demonstrate our recent achievements in the above-mentioned materials exploration.

Keywords: Materials Informatics, Machine Learning, Ab Initio Simulations

References

1. Gómez-Bombarelli, R.; *et al. Nat. Mater.* 2016, 15, 1120-1127.
2. Yoshida, T.; *et al. J. Phys. Chem. C* 2019, 123, 14126-14132; *ACS Appl. Nano Mater.* 2021, 4, 1932-1940.
3. Ikebata, H.; *et al. J. Comput. Aided Mol. Des.* 2017, 31, 379-391.
4. Wu, S.; *et al. npj Comput. Mater.* 2019, 5, 66-74.
5. Yoshida, T.; *et al. ACS Omega* 2020, 5, 13403-13411.
6. Ichibha, T.; *et al. Phys. Rev. B* 2021, 104, 214111-214118.
7. Song, P.; *et al. Mater. Chem.* 2021, 33, 9501-9510; *J. Phys. Chem. C* 2022, 126, 2747-2756; *Adv. Theory Simul.* 2022, 5, 2100364-2100371; *Mater. Today Phys.* 2023, 28, 100873-100881.
8. Song, P.; *et al. Comput. Mater. Sci.* 2023, 226, 112202-112211.
9. Kato, D.; *et al. Angew. Chem., Int. Ed.* 2023, 62, e202301416.
10. Hongo, K.; *et al. J. Phys. Chem. Lett.* 2010, 1, 1789-1796; *J. Chem. Theory Comput.* 2013, 9, 1081-1089; *ibid* 2015, 11, 907-915; 2017, 13, 5217-5225.

Dielectric properties of wheel-shaped polyoxometalate depending on inner cations

Yuma Takemoto^{a*}, Chisato Kato^a, Jun Manabe^a, Cosquer Goulven^{b,c},
Masaru Fujibayashi^d, Katsuya Inoue^{a,b,c}, Sadafumi Nishihara^{a,c,e*},

^a Graduate School of Advanced Science and Engineering, Hiroshima University

^b The International Institute for Sustainability with Knotted Chiral Meta Matter, Hiroshima University

^c Chirality Research Center (CResCent), Hiroshima University

^d National Institute of Technology, Ube College

^e Precursory Research for Embryonic Science and Technology (PRESTO),
Japan Science and Technology Agency

*Corresponding author: snishi@hiroshima-u.ac.jp

Abstract

Ferroelectric materials are used for non-volatile memory. Recently, the memory density is struggling to grow up because of the limit on minimization. It is an intrinsic limitation which is due to the necessity of long-range order of dipole-dipole interactions to observe ferroelectricity.

We reported single-molecule electret (SME) [1][2] that behaves like ferroelectric materials without long-range order. These behaviors were observed in cage-shaped inorganic molecule (Preyssler-type polyoxometalate (POM)) that incorporates one terbium ion in a central cavity (Fig.1). The cation has two stable sites in the cavity, creating a molecular polarization depending on its position, with an energy barrier between the two stable sites. At high temperature the cation delocalizes between the two sites, and at lower temperature we can control the position of the cation by applying electric fields. Because of these mechanisms, this molecule is considered as a material for ultra-high-density memory. However, this molecule has a weak point: ferroelectric hysteresis is observed only from 285 K to 325 K.

In my work, we focused on $K_{28}Li_5H_7P_8W_{48}O_{184}$ ($K^+@W48$), which incorporates eight potassium cations (K^+) in its cavity (Fig.2). As four of them are delocalized between two stable sites in the cavity, this molecule will behave as SME (Fig.2(b)). As a result, ferroelectric hysteresis was observed from 300 K to 440 K, so this molecule will behave as new high tolerance SME (Fig.2(c)). In addition, if the inner K^+ was exchanged to NH_4^+ , this molecule behaves also as SME. From this result, we can exchange inner cations and this POM remain as SME.

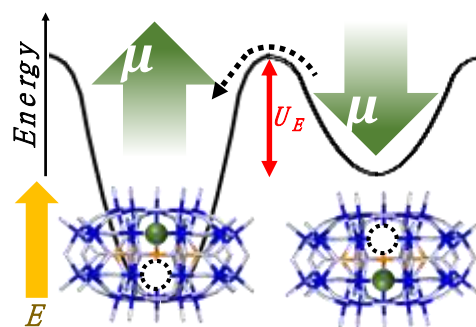


Fig1. Double-well potential of Preyssler-type POM which applied electric field.

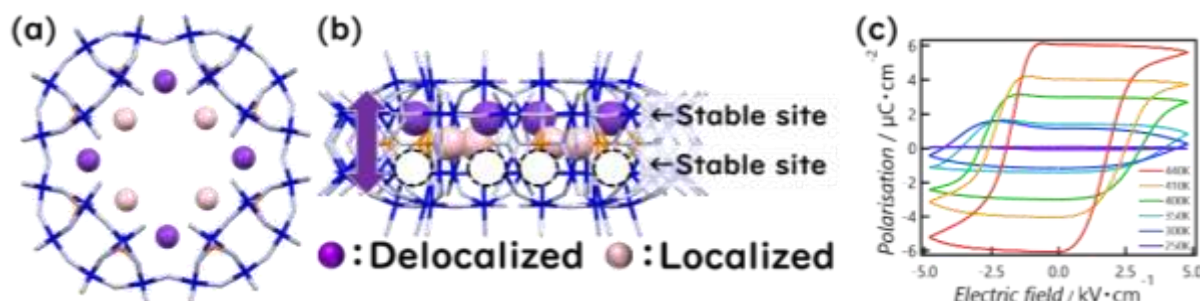


Fig2. (a)Top view, (b)side view, (c)ferroelectric hysteresis of $K^+@W48$.

Keywords: Polyoxometalate, Single-molecule electret, Ferroelectrics, Dielectrics

References

[1] C.Kato, S. Nishihara, *et. al.*, *Angew. Chem. Int. Ed.*, **2018**, 57, 13429-13432. [2] S.Nishihara, *Nat. Nanotech.*, **2020**, 15, 1065. [3] R. Contant, *et. al.*, *Inorg. Chem.*, **1985**, 24, 4610-4614.

Gold Nanocluster Connections by Pyridine Complexes

Taiga Kosaka^a, Yoshiki Niihori^a, Yuichi Negishi^{a,b,*}

^aGraduate School of Science, Tokyo University of Science, Japan.

^bInstitute of Multidisciplinary Research for Advanced Materials, Tohoku University, Japan.

*Corresponding author: yuichi.negishi.a8@tohoku.ac.jp

Abstract

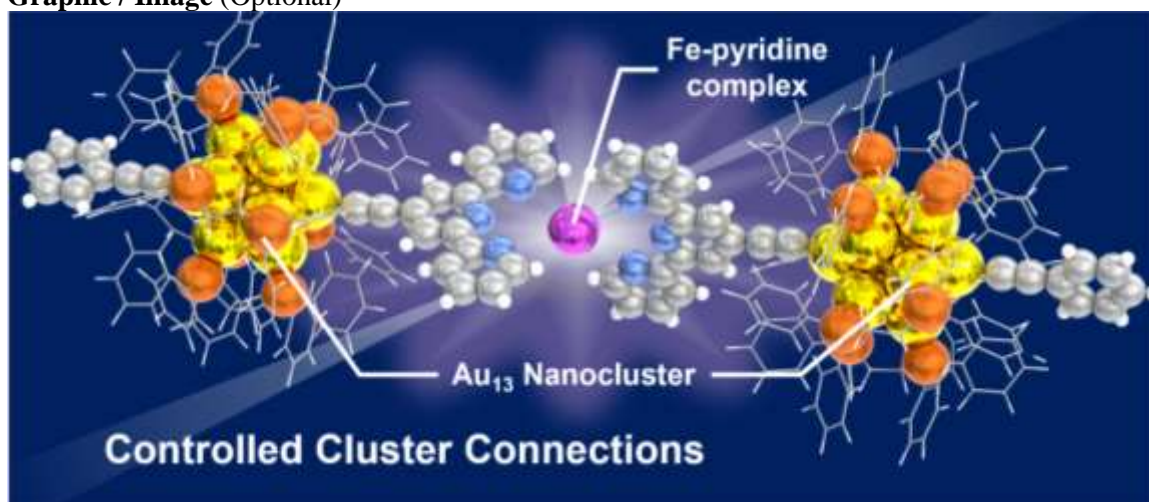
Metal nanoclusters (NCs) are materials composed of approximately 100 or fewer metal atoms, with a size of about 1 nm. Due to their microscopic structure and unique composition, they have great potential as functional materials, including catalysts, and in particular, research on single NC has been widely conducted. In recent years, a new material creation method that induces new physical properties by assembling such NCs as a building unit has been attracting attention. However, it is difficult to control the structure and freely assemble NCs in isotropically coordinated NCs with a single ligand.

In this study, we focused on clusters protected by two or more types of ligands and worked on the synthesis of cluster dimers utilizing ligand exchange¹ at specific coordination sites. The building units of the dimer were $\text{Au}_{13}(\text{dppe})_5\text{Cl}_2$ (dppe = 1,2-bis(diphenylphosphino)ethane) clusters protected by chlorine and phosphine. One of the two chlorines on this cluster was replaced with phenylacetylene, and the other with a terpyridine ligand bearing an ethynyl group. Subsequently, by adding iron, a complex with the pyridine moiety of the cluster was formed, synthesizing the dimer.

In the UV-Vis absorption spectrum of the product, characteristic peaks originating from the ligands were observed, along with a peak around 570 nm derived from the MLCT transition of the terpyridine-iron complex. Additionally, through electrospray ionization mass spectrometry, peaks corresponding to the cluster dimer mediated by iron were identified. The obtained dimer is expected to exhibit properties specific to the dimer, such as a decrease in photoluminescence intensity. To elucidate these properties, density functional theory calculations and similar methods will be employed.

Keywords: metal nanocluster, nanocluster connection, metal complex, precise synthesis

Graphic / Image (Optional)



References

1. Sugiuchi, M.; Shichibu, Y.; Nakanishi, T.; Hasegawa, Y.; Konishi, K. *Chem. Commun.* 2015, 51, 13519-13522.
2. Zhang, J.; Zhou, Y.; Zheng, K.; Abroshan, H.; Kauffman, D. R.; Sun, J.; Li, G. *Nano Res.* 2018, 11, 5787-5798.

Development of In-Silico Material Design Tool Based on the Molecular Theory of Solvation

Norio Yoshida*

Graduate School of Informatics, Nagoya University, Nagoya 464-8601 (Japan)

**noriwo@nagoya-u.jp*

Abstract

Computer assistance has become indispensable in contemporary endeavors aimed at designing medicines and materials beneficial to humanity. Material molecules exhibit specific structures and properties, necessitating a profound understanding of molecular behavior at the atomic level to tailor molecules that fulfill these criteria. Hence, computational methodologies capable of delineating intricate hierarchical molecular chemical processes are imperative. Our research group has pioneered a multiscale theory based on the 3D-RISM theory, a solvation theory for complex molecular systems, integrated with quantum chemical calculation methods and molecular simulations. This innovative approach empowers us to dissect essential chemical processes pivotal for material molecular design.

Molecular recognition, the non-covalent binding of a host molecule to a specific guest molecule, stands as a cornerstone in the design of drug molecules and materials. Leveraging the 3D-RISM method, we can prognosticate the binding site, affinity, and selectivity of molecules.

The formation of higher-order structures in biomolecules and material molecules, such as proteins and DNA, parallels the molecular recognition process. Our proposed hybrid Monte Carlo 3D-RISM method allows meticulous consideration of solvent effects.

Chemical reactions, encompassing the formation and dissociation of covalent bonds between atoms, constitute pivotal aspects of molecular design. Accurate depiction of such reactions necessitates quantum chemical methods. We advocate for the QM/MM/3D-RISM method, a fusion of QM/MM and 3D-RISM approaches, to delineate chemical reactions in intricate molecular systems. This methodology enables prediction and analysis of chemical reactions in large, complex molecules within solution environments.

These methodologies are encapsulated within RISMiCal, a software package developed by our group. This open-source program is accessible for utilization by the scientific community freely.

Keywords: 3D-RISM, QM/MM/3D-RISM, Hybrid MC/3D-RISM, RISMiCal

Graphical abstract



References

1. N. Yoshida, *J. Comput. Info. Model* 57, 2646 (2017).
2. N. Yoshida, S. Phongphanphanee, Y. Maruyama, T. Imai and F. Hirata, *J. Am. Chem. Soc. (Communication)*, 128, 12042-12043, (2006)
3. N. Yoshida, T. Yamaguchi, *J. Mol. Liquids*, 385, 122418 (2023)
4. N. Yoshida, Y. Kiyota, F. Hirata, *J. Mol. Liquids*, 159, 83 (2011)
5. Y. Maruyama, N. Yoshida, *J. Comput. Chem.* 45, 1470 (2024)

Unlocking the Secrets of CO Interaction and Activation on Inhomogeneous Ru Nanoparticles Using the Electronic Structure Decomposition Approach

David S. Rivera Rocabado^{a,*}, Mika Aizawa^a, Takayoshi Ishimoto^c,

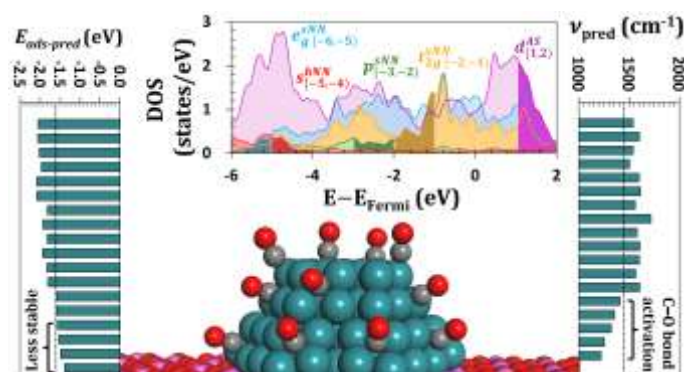
^a Graduate School of Advanced Science and Engineering, Hiroshima University.

*Corresponding author: dauidsrr@hiroshima-u.ac.jp

Abstract

Historically, catalyst discovery relied on trial and error. The advent of systematic rules, increasingly supported by quantum chemical calculations, has significantly accelerated the design of new catalysts. While density functional theory (DFT) method is widely used for its accuracy, modeling heterogeneous systems, especially supported transition metals, poses significant computational challenges. To address these challenges, we introduce the Electronic Structure Decomposition Approach (ESDA), a novel method that identifies specific areas of the catalyst density of states (DOS) as descriptors of catalytic activity. As a case study, we investigate the influence of α -Al₂O₃(0001) as a support material on CO interaction, approximated by the adsorption energy, and activation, approximated by the stretching frequency of the C–O bond, on Ru nanoparticles (NPs). Using multiple linear regression analysis, ESDA models were trained with data from isolated Ru NPs and adjusted using supported NP sample data. The ESDA models accurately predict CO adsorption energies and C–O vibrational frequencies, demonstrating strong linear correlations with DFT-calculated values and low errors across various adsorption sites for both isolated and supported Ru NPs compared to our previous approaches.^{1,2} The ESDA models revealed the localized effect of α -Al₂O₃(0001) on the DOS areas influencing adsorption energies and vibrational frequencies particularly at the NP/support interface. Beyond pinpointing the DOS areas responsible for CO adsorption and C–O bond activation, this study provides insights into manipulating these DOS regions to control CO activation, facilitating CO dissociation. Additionally, ESDA significantly reduces computational time compared to traditional DFT calculations, making it a more efficient tool for exploring catalytic properties. ESDA's reliance on electronic structure as a descriptor suggests its potential for predicting properties beyond catalysis, broadening its applicability across scientific domains.

Keywords: electronic structure decomposition approach, density of states, density functional theory method, machine learning, support effect



Acknowledgements: This work is supported by the New Energy and Industrial Technology Development Organization and JSPS KAKENHI (No. 23K04890)

References

1. Rivera Rocabado, D. S.; Nanba, Y.; Koyama, M. *ACS Omega* **2021**, *6* (27), 17424–17432.
2. Rivera Rocabado, D. S.; Aizawa, M.; Ishimoto, T. *J. Phys. Chem. C* **2023**, *127* (47), 23010–23022.

Structure Tuning of Low-dimensional Titania Nanotubes and their Physicochemical and Photochemical Functions

Tohru Sekino^{a,*}

^aSANKEN, Osaka University, Japan

*Corresponding author: sekino@sanken.osaka-u.ac.jp

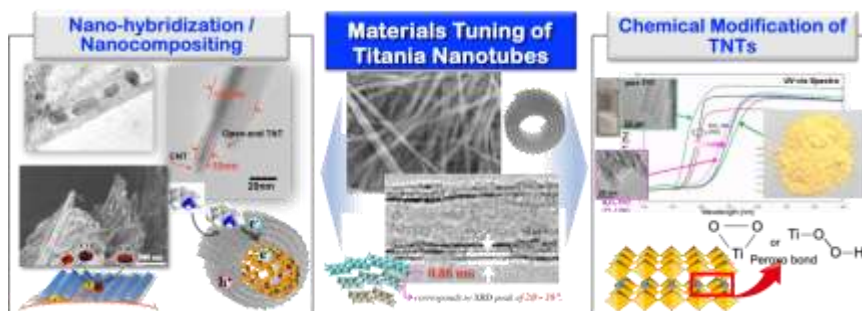
Abstract

Nano-tubular titania or titanates (TNT) with a diameter of 10 – 20 nm have been successfully synthesized from TiO₂ powder by wet-chemical processing using alkaline solution at around 110°C, where spontaneous formation of titanate nano-sheet and followed scrolling to form nanotubes progressed^{1,2}. Synthesized TNT exhibited excellent photocatalytic performances under the ultraviolet (UV) light due to its fundamental properties of TiO₂-based structure. TNT could also be composed with functional materials such as noble metal nanoparticles, nanocarbons and functional polymers. These TNT-based nanocomposites exhibit photocatalytic water splitting and molecular degradation as well as gas-sensing performances.

Since pure TNT was only responsive to UV light, we added visible light responsive property to TNT for the further materials tuning. For this purpose, we have attempted two chemical protocols; one is chemical modification of TNT using hydrogen peroxide solution, and the other is the direct and facile one-step bottom-up synthesis from titanium-peroxide complex solution as a starting material^{3,4}. Both synthesis methods produced yellowish nanotubular powers according to the tuning of electrical band structure of titania by the introduction of peroxy functional groups to the crystal structures (denoted as PTNT). In addition, PTNT exhibited better photocatalytic activity under the visible light irradiation. The photochemical properties were investigated to clarify the role of modification of TNTs and to understand redox characteristics in relation to the energy band structures. These facts imply us that the TNTs and their derivatives are attractive materials that can be applicable to multi-purposes such as energy, environmental and biomedical application. In this paper, design concept, synthesis processes, nanostructures and function of TNT-based nanomaterials will be discussed.

Keywords: titania nanotubes, chemical synthesis, visible-light responsibility, photocatalytic properties

Graphical abstract



References

1. Kasuga, T.; Hiramatsu, M.; Hoson, A.; Sekino, T.; Niihara, K. *Langmuir*, 1998, 14, 3160-3163.
2. Sekino, T. *Bull. Ceram. Soc. Japan*, 2006, 41, 267-271.
3. Park, H.S.; Goto, T.; Cho, S.; Nishida, H.; Sekino, T. *ACS Omega*, 2020, 5, 21753–21761.
4. Park, H.S.; Goto, T.; Han, D.H.; Cho, S.; Nishida, H.; Sekino, T. *ACS Applied Nano Materials*, 2020, 3, 7795–7803.

Metallic molecular conductors based on hyperconjugated electrons

Toshio Naito, Misako Ikeda, Yoshiki Sasaki, Yoshino Fujikawa, Shigeki Mori, Kensuke Konishi, Keishi Ohara, and Masayoshi Takase

Ehime University, 2-5 Bunkyo-cho, Matsuyama, 790-8577 Ehime, Japan

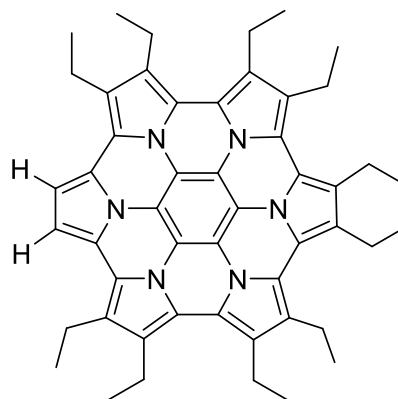
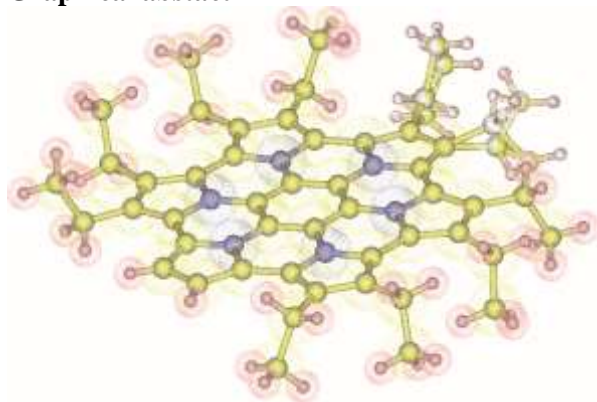
**Corresponding author: tnaito@ehime-u.ac.jp*

Abstract

Aromatic compounds have always garnered attention of a wide spectrum of chemists, as they exhibit non-classical chemical and physical properties based on their unique electronic states of the frontier orbitals. Thus far, most of them are π -conjugated molecules characterized by the delocalized electrons over the planar parts of the molecules. Here we report a newly synthesized metallic conductor $(\text{EtHAC})_2\text{I}_3$. The molecular structure of EtHAC is characterized by the ten ethyl groups almost orthogonally extended from the periphery of the π -conjugated system of a coronene derivative. The ethyl groups play a significant role to delocalize unpaired electrons in the entire crystals of $(\text{EtHAC})_2\text{I}_3$. As a result, all the radical cationic $\text{EtHAC}^{+0.5}$ in $(\text{EtHAC})_2\text{I}_3$ cooperatively form a three-dimensional weak intermolecular interaction network in the solid state, which is a typical feature of metallic bonds. Note that the network is based on “inter-ethyl” atomic contacts instead of π - π interactions often observed in this type of compounds. Such structural features are supported by the tight-binding band calculation, which reveals a three-dimensional complicated band structure: a characteristic of elemental metals unlike “synthetic metals”. In fact, it exhibits metallic properties at 2–300 K including high electrical conductivity increasing with decreasing temperature and nearly temperature-independent paramagnetism. At the same time, the observed physical properties and calculated band structure reveal that $(\text{EtHAC})_2\text{I}_3$ possesses degenerated flat bands accommodating the unpaired electrons as charge carriers. Such a kind of metals have been elusive for a long time despite rich theoretical studies to expect unique conducting and magnetic properties. Both electron spin resonance and electrical conductivity consistently indicate that the charge carriers in $(\text{EtHAC})_2\text{I}_3$ possess ~ 100 times longer relaxation time than existing metals, demonstrating the unique band structure.

Keywords: hyperconjugation, molecular metal, multi-dimensional intermolecular interaction, flat band

Graphical abstract



References

1. Sasaki, Y.; Takase, M.; Mori, S.; Uno, H. *Molecules* 2020, 25, 2486.

Crystalline logic gate through ion and molecule exchange in an aqueous solution

Jun Manabe^a, Mizuki Ito^a, Katsuya Ichihashi^a, Katsuya Inoue^{a,b,c},
Tomoyuki Akutagawa^d, Takayoshi Nakamura^{a,e}, Sadafumi Nishihara^{a,c,f,*}

^a Grad. Sch. Adv. Sci. Eng., Hiroshima Univ., Japan

^b WPI-SKCM², Hiroshima Univ., Japan

^c CResCent, Hiroshima Univ., Japan

^d IMRAM, Tohoku Univ., Japan

^e RIES, Hokkaido Univ., Japan

^f PRESTO, JST, Japan

*Corresponding author: snishi@hiroshima-u.ac.jp

Abstract

Muscle cells function as biological logic gates, exhibiting collective contraction and relaxation in the presence and absence of Ca^{2+} ions, respectively. While reversible transformations in shape and physical properties in response to environmental changes are crucial for mimicking biological systems, most chemical logic gates alter the microscopic properties of molecules and ions in solution. Therefore, developing chemical logic gates that affect macroscopic properties, such as crystal structure and magnetic and electrical properties, is essential for replicating collective in vivo phenomena.

In this study, we focused on $\text{Li}_2([\text{18}]\text{crown-6})_3[\text{Ni}(\text{dmit})_2]_2(\text{H}_2\text{O})_4$ (**Li salt**), where an ion channel structure comprises two Li^+ ions and three [18]crown-6 ethers per unit, allowing for Li^+ ion conduction (Figure 1a). Additionally, solid-state ion exchange occurs when Li^+ ions are replaced by K^+ ions by immersing **Li salt** in a KCl aqueous solution. Herein, we developed single-crystal chemical logic gate systems utilizing the ion exchange of **Li salt**. For Ca^{2+} ion exchange, the ion exchange acts as an INHIBIT Gate inhibited by [18]crown-6 in solution (Figure 1b, **Li**→**Ca salt**). The reverse reaction can function as an AND Gate involving the exchange of Li^+ ions and [18]crown-6. For Na^+ ion exchange, the process does not proceed with Na^+ ions alone in the solution; however, in the presence of both Na^+ ions and [15]crown-5, the exchange proceeds, functioning as an AND Gate (Figure 1c, **Li**→**Na15c5 salt**). These ion exchanges proceed, keeping a single crystal state despite the process involving the exchange of molecules and ions, resulting in significant changes in volume and physical properties. The details of the exchanges and the resulting physical properties will be discussed in the presentation.

Keywords: ion exchange, single crystal, logic gate, crown ether

References

1. K. Ichihashi, S. Nishihara, *et al.*, *Chem. Mater.*, **2018**, *30*, 7130-7137.
2. K. Ichihashi, S. Nishihara, *et al.*, *Angew. Chem. Int. Ed.*, **2019**, *58*, 4169-4172.

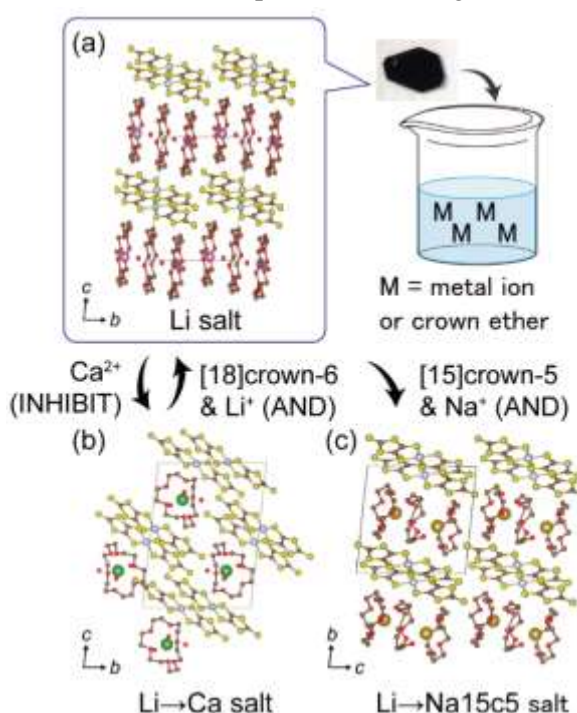


Figure 1. Schematic diagram of solid-state ion and molecule exchange function. The crystal structure of (a) **Li salt**, (b) **Li**→**Ca salt** and (c) **Li**→**Na15c5 salt**. Each transformation acts as a chemical logic gate.

In Silico Composition Optimization of Ammonia Absorption Materials

Manabu Sugimoto^{a,b,c,d*}, Yusuke Tateishi^c

^a*Faculty of Advanced Science and Technology, ^bInstitute of Industrial Nanomaterial*

^c*Graduate School of Science and Technology, Kumamoto University, Japan*

^d*Green Ammonia Research Center, National Institute of Technology, Numazu College, Japan*

^{*}*Corresponding author: sugimoto@kumamoto-u.ac.jp*

Abstract

Green ammonia is considered one of the most important renewable energies for decarbonization. It has been suggested that the ammonia separation process be incorporated into the synthesis process for efficient ammonia production. Thus, searching for promising ammonia separation material is a research target. We are now performing the Bayesian optimization method to find the optimal composition of the ammonia absorption material. In this approach, we apply molecular dynamics (MD) simulation using the machine-learning-based force field to evaluate the amount of absorbed ammonia, and the composition of the ammonia-absorbing material is updated until the amount converges. In the presentation, we will describe our computational method and suggest the so-far predicted optimal composition of ammonia absorption material.

Keywords: ammonia absorption, computer simulation, design of experiments, Bayesian optimization

Li ion transport environment in ion-conducting sulfide glasses

Koji Ohara^{a,b,*}, Kentaro Kobayashi^a, Satoshi Hiroi^a, Atsushi Sakuda^c, and Akitoshi Hayashi^c^aFaculty of Materials for Energy, Shimane University, Japan^bDiffraction and Scattering Division, Japan Synchrotron Radiation Research Institute (JASRI), Japan^cGraduate School of Engineering, Osaka Metropolitan University, Japan

*Corresponding author: ohara@mat.shimane-u.ac.jp

Abstract

Controlling Li ion transport in glasses at atomic and molecular levels is key to realising all-solid-state batteries, a promising technology for electric vehicles. In this context, Li₃PS₄ glass, a promising solid electrolyte candidate, exhibits dynamic coupling between the Li⁺ cation mobility and the PS₄³⁻ anion libration, which is commonly referred to as the paddlewheel effect.¹ In addition, it exhibits a concerted cation diffusion effect (i.e., a cation–cation interaction), which is regarded as the essence of high Li ion transport. However, the correlation between the Li⁺ ions within the glass structure can only be vaguely determined, due to the limited experimental information that can be obtained. We report that the Li ions present in glasses can be classified by evaluating their valence oscillations via Bader analysis to topologically analyse the chemical bonds. We found that three types of Li ions are present in Li₃PS₄ glass, and that the more mobile Li ions (i.e., the Li3-type ions, see Figure (a)) exhibit a characteristic correlation at relatively long distances of 4.0–5.0 Å.² Furthermore, the neutron quasi-elastic scattering (QENS) spectra at $Q_{av} = 1.36 \text{ \AA}^{-1}$ ($Q = 1.25\text{--}1.48 \text{ \AA}^{-1}$) of Li ions is clearly observed as shown in Figure (b). The analysis shows that the jump distance of Li ions is 4.0–5.0 Å, which is consistent with our analysis. Thus, considering the molecular vibrations in the glass during the evaluation of the Li ion valences is expected to lead to the development of new solid electrolytes.

Keywords: sulfide glass, solid electrolyte, valence oscillation, pair distribution function

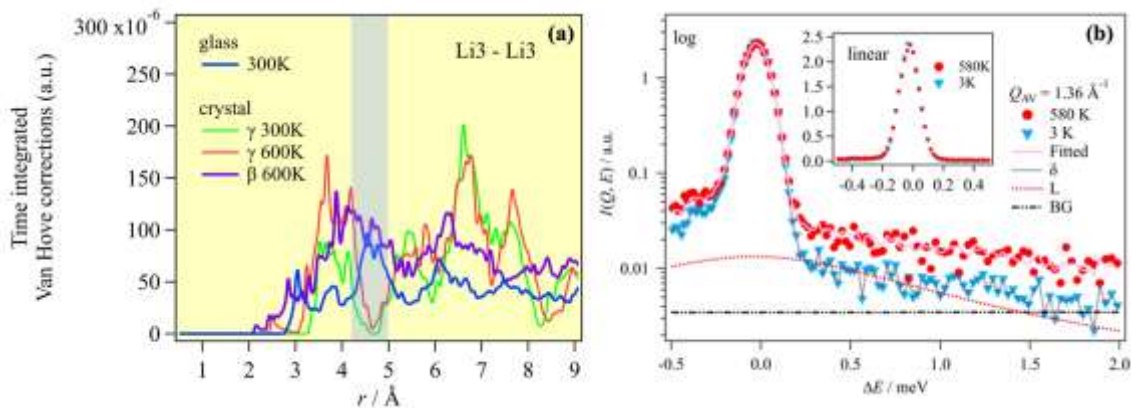


Figure. (a) Comparison of the Li3–Li3 correlations for the glassy, β -, and γ -crystal phases, (b) QENS spectra of the β -phase.

References

1. Smith, J. G.; Siegel, D. J. *Nat. Commun.* 2020, 11(1), 1483.
2. Yamada, H.; Ohara, K.; Hiroi, S.; Sakuda, A.; Ikeda, K.; Ohkubo, T.; Nakada, K.; Tsukasaki, H.; Nakajima, H.; Temleitner, L.; Pusztai, L.; Ariga, S.; Matsuo, A.; Ding, J.; Nakano, T.; Kimura, T.; Kobayashi, R.; Usuki, T.; Tahara, S.; Amezawa, K.; Tateyama, Y.; Mori, S.; Hayashi, A. *Energy Environ. Mater.* 2024, e12612.

Theoretical Approach to Coordination Polymer Photocatalysis

Yuta Tsuji,^{a*} Sayoko Yamamoto,^a Yoshinobu Kamakura,^b Chomponoot Suppasso,^b
Daisuke Tanaka,^c Kazuhiko Maeda^{b,d}

^a Faculty of Engineering Sciences, Kyushu University, Kasuga, Fukuoka 816-8580, Japan.

^b Department of Chemistry, School of Science, Tokyo Institute of Technology, Meguro-ku, Tokyo 152-8550, Japan.

^c Department of Chemistry, School of Science, Kwansei Gakuin University, Sanda, Hyogo 669-1337, Japan.

^d Living Systems Materialogy (LiSM) Research Group, International Research Frontiers Initiative (IRFI), Tokyo Institute of Technology, 4259 Nagatsuta-cho, Midori-ku, Yokohama, Kanagawa 226-8502, Japan.

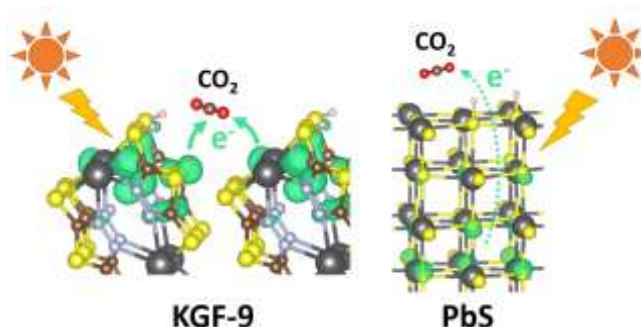
*Corresponding author: tsuji.yuta.955@m.kyushu-u.ac.jp

Abstract

In this study, a comprehensive theoretical analysis was undertaken to elucidate the remarkably efficient conversion of CO₂ into HCOO⁻ employing a coordination polymer featuring Pb–S bonds, namely [Pb(tadt)]_n (where tadt stands for 1,3,4-thiadiazole-2,5-dithiolate), referred to as KGF-9.^{1,2} The catalytic activity of this visible-light responsive solid photocatalyst has been carefully compared with that of PbS, a typical compound that also contains the Pb–S bond. The former shows a very high catalytic activity, while the latter shows almost no activity. The photoreduction process of CO₂ on the KGF-9 surface was analyzed in detail using periodic density functional theory calculations. The reduced catalyst surface was modeled as a hydrogenated surface. The reaction at the active center of a formate dehydrogenase provides an interesting contrast, suggesting that the S–H group plays an important role in the conversion of CO₂ to HCOO⁻. However, the S–H group on the reduced PbS surface does not facilitate the conversion to the same extent as KGF-9. This is because the electrons supplied to CO₂ on the PbS surface come from deep within the solid, whereas on KGF-9, they come from the top surface. This difference is due to differences in the electronic structure of the S–H bond, band gap, and valence band maximum position between the two surfaces, accounting for the marked difference in their catalytic activity. These insights are consistent with experimental and computational results on the thermodynamic and kinetic characteristics of the CO₂ reduction reaction of KGF-9 and PbS, and provide guidance for the design of CO₂ photoreduction catalysts.³

Keywords: photocatalyst, CO₂ reduction, CO₂ adsorption, coordination polymer, DFT calculation

Graphical abstract



References

1. Kamakura, Y.; Sakura, C.; Saeki, A.; Masaoka, S.; Fukui, A.; Kiriya, D.; Ogasawara, K.; Yoshikawa, H.; Tanaka, D. *Inorg. Chem.* **2021**, *60*, 5436–5441.
2. Kamakura, Y.; Yasuda, S.; Hosokawa, N.; Nishioka, S.; Hongo, S.; Yokoi, T.; Tanaka, D.; Maeda, K. *ACS Catal.* **2022**, *12*, 10172–10178.
3. Tsuji, Y.; Yamamoto, S.; Kamakura, Y.; Suppasso, C.; Tanaka, D.; Maeda, K. *ACS Appl. Energy Mater.* **2024**, in press.

Infrared Induced Changes in the Microscopic Hydrogen Bond Structures of Hydrated Phenol Cations

Haruki Ishikawa*, Masatoshi Moto, Yu Sakaue

School of Science, Kitasato University, Japan

*Corresponding author: harukisc@kitasato-u.ac.jp

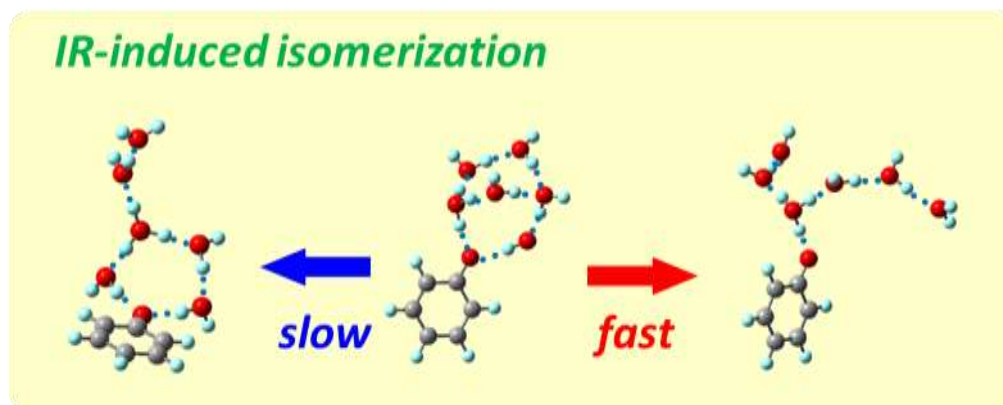
Abstract

To understand the microscopic nature of hydrogen bond networks, we perform ultraviolet photodissociation spectroscopy on hydrated phenol cations, $[\text{PhOH}(\text{H}_2\text{O})_n]^+$, trapped in our variable-temperature ion trap. At low temperatures, only the most stable isomer is present. As the temperature increases, other isomers with different hydrogen bond structures appear. In addition, isomerization between these isomers can occur. In the previous study, we observed a clear change in the dominant isomers of $[\text{PhOH}(\text{H}_2\text{O})_5]^+$ with increasing temperature.¹ Such behavior is the most fundamental temperature effect.

In the present study, to gain insight into the dynamical behavior of the microscopic hydrogen bond networks, we observed the infrared-induced isomerization of $[\text{PhOH}(\text{H}_2\text{O})_6]^+$ followed by the backward isomerization due to the collisions with cold He-buffer gas. We have searched for the isomerization paths both experimentally and theoretically. As a result, the isomerization rates are found to depend on the hydrogen bond structures. In this paper, we report the details of the infrared induced isomerization observed in the present study.

Keywords: Microscopic hydrogen6 bond structure, gas-phase cluster, cold ion trap, ultraviolet spectroscopy

Graphical abstract



References

1. Ishikawa, H.; Kurusu, I.; Yagi, R.; Kato, R.; Kasahara, Y. *J. Chem. Phys. Lett.* 2017, 8, 2541-2546.

Machine-Learning-Assisted Discovery of Molecules with High Charge Mobility in Amorphous Phase

Toshio Asada^{a,b,*}

^aDepartment of Chemistry, Osaka Metropolitan University, Japan

^bRIMED, Osaka Metropolitan University, Japan

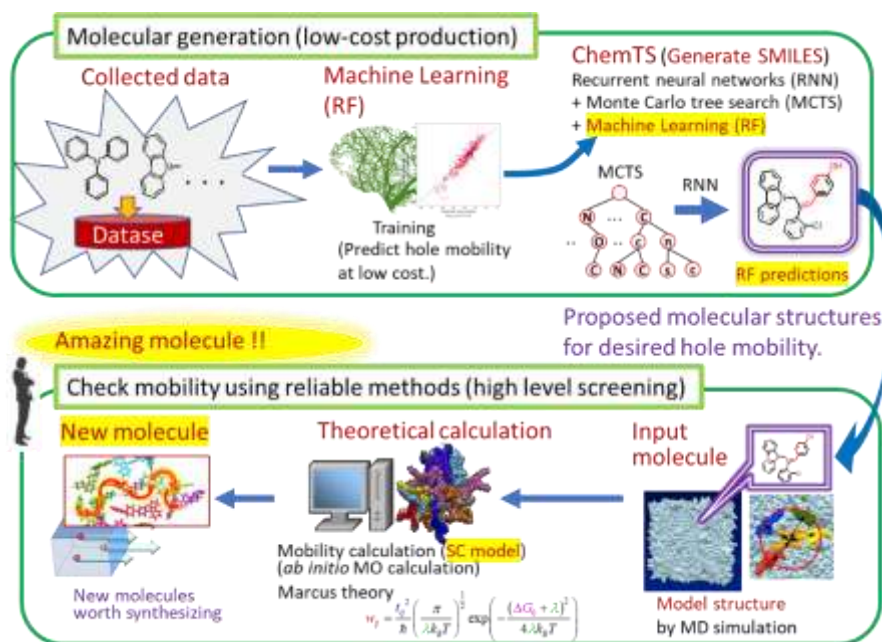
*Corresponding author: t_asada@omu.ac.jp

Abstract

The charge mobility in the amorphous phase is one of an important physical property for designing charge transport layers in electronic devices such as the organic light emitted diode. However, the new molecules have been discovered by trial-and-error approaches. Recently, the theoretical and computational approaches have been developed to evaluate the hole mobility for a given molecule. We have previously proposed the successive conduction (SC) model¹, which is a statistical approach to evaluate hole mobility in the amorphous phase using a limited number of evaluated kinetic rate constants by the molecular orbital calculations and the Marcus theory. While the SC model can evaluate hole mobility when the molecular structure is provided, it is difficult to propose the reliable molecules to realize the desired hole mobility.

In order to realize the automated system for the molecular design with a desired hole mobility, the random forest approach of the machine learning techniques have been applied in this study. We have constructed a data base² with hole mobilities for 321 molecules from the published papers. The new molecules have been designed using the ChemTS python module proposed by Tsuda et al., which is the combined approach of Monte Carlo tree search and recurrent neural networks. The hole mobilities of generated molecules have been evaluated by both the random forest model and the SC model. Since some novel molecules with high hole mobilities could be automatically proposed², we will discuss the techniques in this conference.

Keywords: machine learning, hole transfer, amorphous, molecular simulation, OLED



References

1. K.Nakaguro, Y.Mitsuta, S.Koseki, T.Oshiyama, *T.Asada, *Bull. Chem. Soc. Jpn.* 2023, 96, 1099.
2. *T. Asada and S.Koseki, *Org.Elec.* 2018, 53, 141-150.

Chirality Recognition of Propylene Oxide Dimer Induced by Hydrogen Bond with Achiral Pyrrole

Yoshiteru Matsumoto^{a,*}

^aShizuoka University

*Corresponding author: matsumoto.yoshiteru@shizuoka.ac.jp

Abstract

Propylene oxide (PO) is one of the smallest chiral molecules. It has attracted attention as an important molecule in understanding the intermolecular interactions of chiral molecules, which is referred to as chirality recognition. Xu and coworkers have studied PO dimer (PO₂), the simplest system to elucidate chirality recognition, by MW spectroscopy and *ab initio* computation.¹ They showed there are 6 homo (*RR* or *SS*) and 6 hetero (*RS* or *SR*) dimers, which have almost the same binding energies within 1 kJ/mol. This result indicates PO₂ exhibits no chirality recognition. In this study, we present IR cavity ringdown spectroscopy² of jet-cooled pyrrole (Py) – PO 1-2 clusters (Py₁-PO₂). The concept of this study is based on the hypothesis that chirality recognition of PO₂ is induced by an external hydrogen bond (H-bond) due to an achiral Py. The NH stretching band intensities provide the population ratio of homo-chiral and hetero-chiral Py₁-PO₂, and the computations support the dominant chirality recognition of hetero-chiral Py₁-PO₂. Figure 1 shows the IR spectrum of Py₁-PO₂ clusters, which are produced under the condition of racemic PO vapor. The decomposed two spectra, which are obtained by our technique of the statistic consideration,² are due to homo-chiral and hetero-chiral Py₁-PO₂. A couple of bands in each spectrum are addressed to be isomeric structures, which are derivative of the cyclic structure shown in the inset. Comparison of the integrated band intensities reveals 1.4 times greater populations of hetero-chiral clusters than homo-chiral ones. Thus, we conclude the preference of chirality recognition in hetero PO₂ with the H-bond with an achiral Py. This is confirmed by the computational analysis of interaction energies.

Keywords: Chirality recognition, Hydrogen-bonded clusters, IR cavity ringdown spectroscopy, propylene oxide, Pyrrole

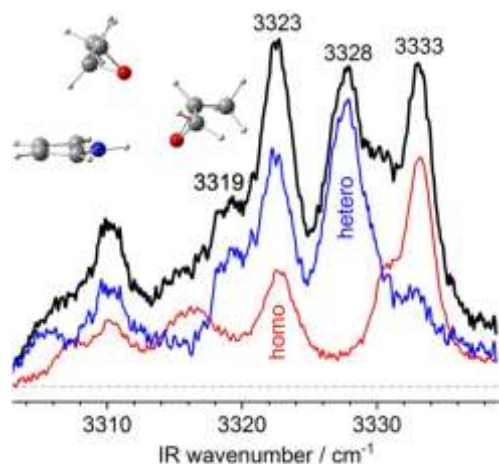


Figure 1. NH stretching vibrations of Py₁-PO₂ observed by IR cavity ringdown spectroscopy. An inserted pic is a typical structure of Py₁-PO₂ obtained by computations.

References

1. Su, Z.; Borho, N.; Xu, Y. *J. Am. Chem. Soc.* 2006, *128*, 17126-17131.
2. Matsumoto, Y.; Honma, K. *J. Chem. Phys.* 2007, *127*, 184310-9.
3. Matsumoto, Y.; Sakurai, K. in preparation.

INTERNAL ENERGY DEPENDENCE OF THE PYRROLE DIMER CATION STRUCTURES FORMED IN A SUPERSONIC PLASMA EXPANSION

Dashjargal Arildii^a, Yoshiteru Matsumoto^b, Otto Dopfer^{a,c*}

^aTechnische Universität Berlin

^bShizuoka University

^cTokyo Institute of Technology

*Corresponding author: dopfer@physik.tu-berlin.de

Abstract

Aside from π H-bonding, cation/anion- π , and π - π stacking interactions, the charge resonance (CR) is a fundamental and very strong force in charged arene dimers.¹ In aromatic dimer cations, the positive charge is shared between the molecules depending on their ionization energy (IE) differences. Even though the CR interactions have been studied extensively over the years, only a rough estimation of the asymmetry in the charge distribution in the dimer is possible because of the peak broadness of the CR transition. To this end, we previously demonstrated a new high-resolution experimental approach (infrared photodissociation spectroscopy (IRPD)) to precisely probe the charge distribution and the CR interaction in aromatic dimer cations for the prototypical case of the pyrrole dimer cation (Py_2^+) in the gas phase. Py ($\text{C}_4\text{H}_5\text{N}$) is a five-membered heterocyclic ring which has a single isolated and uncoupled NH stretch oscillator whose frequency is strongly dependent on its charge state.¹⁻³ However, due to the finite width of the free NH stretch peak in the IRPD spectrum of Py_2^+ , the structural isomers of Py_2^+ are not easily and directly distinguishable (Fig. 1a, b). Therefore, herein we generate the Py_2^+ cluster with different internal temperatures in the supersonic plasma expansion and characterize the cluster structures by IRPD and dispersion-corrected density functional theory calculations. The analysis of IRPD spectra of mass-selected Py_2^+ and its cold Py_2^+Ar and Py_2^+N_2 clusters combined with geometric parameters of intermolecular structures and binding energies reveals an exclusive formation of the CR stabilized π -stacked antiparallel Py_2^+ structure (Fig. 1a) under cold conditions. The IRPD of the bare Py_2^+ dimers produced with higher internal energy suggests a minor population of less stable hydrogen-bonded isomers composed of heterocyclic Py/Py^+ structures formed after intramolecular H atom transfer and ring opening (Fig. 1c) additional to the CR stabilized Py_2^+ structures.⁴

Keywords: Charge resonance, pyrrole dimer, infrared spectroscopy, gas phase, internal energy.

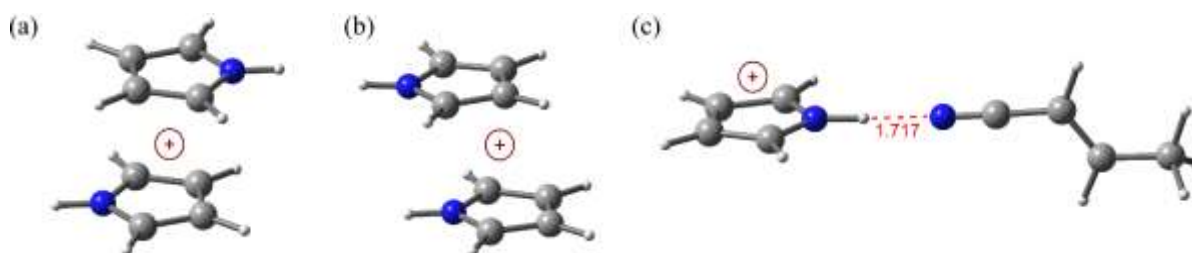


Fig. 1 Optimized isomers of Py_2^+ at the B3LYP-D3/aug-cc-pVTZ level: (a) antiparallel, (b) parallel, and (c) H-bonded isomer.

References

1. Chatterjee, K.; Matsumoto, Y.; Dopfer, O. *Angew. Chem. Int. Ed.* 2019, 58, 3351-3355.
2. Schütz, M.; Matsumoto, Y.; Bouchet, A.; Öztürk, M.; Dopfer, O. *Phys. Chem. Chem. Phys.* 2017, 19, 3970-3986.
3. Arildii, D.; Matsumoto, Y.; Dopfer, O. *J. Phys. Chem. A* 2023, 127, 2523-2535.
4. Arildii, D.; Matsumoto, Y.; Dopfer, O. *J. Phys. Chem. A* 2024, 128, 3993-4006.

Catalyst Discoveries from Scratch

Toshiaki Taniike^aGraduate School of Advanced Science and Technology, Japan Advanced Institute of Science and Technology, Japan

*Corresponding author: taniike@jaist.ac.jp

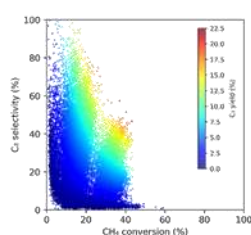
Abstract

Data-driven approaches in catalysis have attracted great attention due to their potential to accelerate catalyst discovery and understanding. However, their application to practical catalyst development has been hindered by the scarcity of appropriate datasets and the empirical nature of descriptor design. Here, we demonstrate that combining high-throughput experimentation with automatic feature engineering can realize catalyst discoveries from scratch.^{1,2} Specifically, we: (i) apply random sampling to a vast combinatorial and compositional catalyst space, (ii) experimentally test the sampled catalysts, (iii) apply automatic feature engineering to the resulting dataset, and (iv) propose the next set of catalysts, which is used either to refine the machine learning model or to identify promising catalysts. We will present a case study illustrating the use of this advanced catalyst discovery methodology.

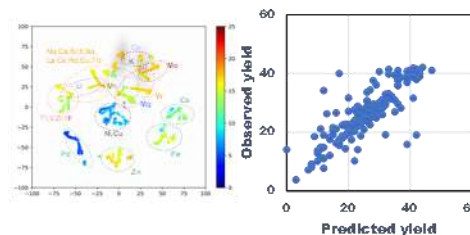
Keywords: Catalysis, high-throughput experimentation, machine learning



1. High-throughput experimentation



2. High-quality catalyst data



3. Data-driven hypothesis extraction

← Experimental/materials design

References

1. Nguyen, T. N.; Nakanowatari, S.; Tran, T. P. N.; Thakur, A.; Takahashi, L.; Takahashi, K.; Taniike, T. *ACS Catal.* 2021, 11, 1797–1809
2. Taniike, T.; Fujiwara, A.; Nakanowatari, S.; García-Escobar, F.; Takahashi, K. *Commun. Chem.* 2024, 7, 11.

Surface & Interface Sciences in Energy Conversion Materials

Taketoshi Minato^{a,*}

^a Institute for Molecular Science, National Institutes of Natural Sciences
Okazaki, Aichi, Japan 444-8585

*Corresponding author: minato@ims.ac.jp

Abstract

Social interest in energy, including the efficient use of renewable energy, is expanding day by day. The performance of rechargeable batteries is expected to further develop by understanding and controlling the physical properties and reaction mechanisms at the electrode/electrolyte interface [1]. In this talk, I will present the results of the analysis of the electrode/electrolyte interface in rechargeable batteries (Fig. 1) using scanning probe microscopy and other surface and interface science techniques. The density of lithium ions changes within the electrode active material of lithium-ion batteries during charging and discharging. While the effect of lithium-ion density on the electronic conductivity of the electrode is understood, the effect of lithium ion ordering within the active material has not yet been elucidated. We have demonstrated that the ordering of lithium ions affects the electronic conductivity of electrodes by measuring local conductivity using scanning tunneling microscopy/spectroscopy [2]. I will also present an analysis of the reaction mechanism of fluoride shuttle batteries, which exceed the theoretical energy density of current rechargeable batteries [3, 4]. Additionally, I will share recent achievements using scanning probe microscopy, including interface analysis of the electric double layer and viscosity [5], the spin selectivity of chiral structures [6] and single protein [7].

Keywords: Surface, Interface, Rechargeable Battery, Scanning Probe Microscopy, Electrode/Electrolyte Interface

Graphic / Image

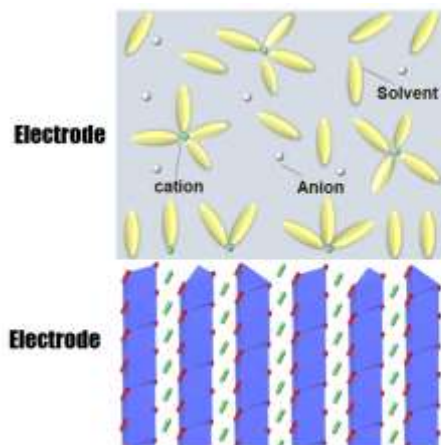


Fig. 1 A schematic illustration of electrode/electrolyte interface in rechargeable batteries.

References

- [1] Taketoshi Minato and Takeshi Abe, *Prog. Surf. Sci.*, **92**, 240–280 (2017). [2] K. Iwaya *et al.*, *Phys. Rev. Lett.*, **111**, 126104 (2013). [3] Hiroaki Konishi *et al.*, *J. Phys. Chem. C*, **16**, 10246–10252 (2019). [4] Hiroyuki Nakano *et al.*, *Chem. Mater.*, **33**, 459–466 (2021). [5] Kenichi Umeda *et al.*, *Phys. Rev. Lett.*, **122**, 116001 (2019). [6] Hiroki Aizawa *et al.*, *Nature Comm.*, **14**, 4530 (2023). [7] Jun Nishida *et al.*, *Nano Lett.*, **24**, 836–843 (2024).

High-Entropy Intermetallics: Serving Isolated Pt Sites For Ultrastable Propane Dehydrogenation Catalysis

Yuki Nakaya^{a,*}, Shinya Furukawa^{a,*}

^aGraduate School of Engineering, Osaka University, 565-0871 Osaka, Japan.

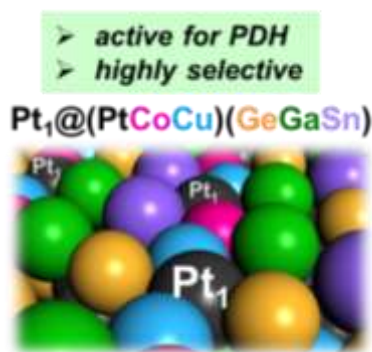
*Corresponding author: nakaya@chem.eng.osaka-u.ac.jp

Abstract

Propane dehydrogenation (PDH: $C_3H_8 \rightarrow C_3H_6 + H_2$) has attracted increasing attention with great industrial promise to meet the growing global demand for propylene, which is one of the most important industrial feedstocks.¹ However, catalyst deactivation in a short time is a major problem. Due to the high endothermicity of PDH, high reaction temperatures ($\geq 600^\circ\text{C}$) are required to obtain sufficient propylene yield. Therefore, even Pt, which is among the most selective metals, shows a rapid deactivation due to coke formation induced by side reactions. Therefore, it is of great importance to develop highly durable catalysts for the future practical applications. Studies on developing efficient catalysts for PDH have suggested that isolating Pt atoms using alloy materials is one of the most promising approaches because Pt–Pt ensembles, which strongly adsorbing propylene, typically trigger undesired side reactions leading to coking.² To date, Pt–Cu single-atom alloys,² Pb-decorated PtGa intermetallic,³ and PtZn intermetallic⁴ have been reported as state-of-the-art materials to serve isolated Pt (Pt_1) sites. However, these catalysts still deactivate due to coke formation and/or nanoparticle sintering. Therefore, to overcome these difficulties, a more sophisticated concept of catalyst design is required that serves Pt_1 sites more selectively catalyzing PDH while having greater thermal stability.

In this context, we focused on the multimetalization of binary intermetallics A_mB_n to form high-entropy intermetallics [HEIs: $(A_{1-x-y}A'_x A''_y)_m(B_{1-p-q}B'_p B''_q)_n$]. Due to the "ordered structures" and "multimetalization," HEIs can easily dilute Pt–Pt ensembles for "site-isolation" and provide "greater thermal stability" due to the increase in mixing entropy.² In addition, the unique electronic property of intermetallics is expected for selective PDH. In this study, we applied HEIs in thermal catalysis for the first time and successfully constructed thermally stable Pt_1 sites for PDH.⁵ Herein, we introduce a unique catalyst material and design concept based on HEIs for highly efficient PDH.

Keywords: propane dehydrogenation, platinum, site-isolation, high-entropy intermetallics



References

1. Y. Nakaya, S. Furukawa, *Chem. Rev.*, 2023, 123, 5859–5947.
2. G. Sun, J. Gong et al., *Nat. Commun.*, 2018, 9, 4454.
3. Y. Nakaya, J. Hirayama, S. Yamazoe, K. Shimizu, S. Furukawa, *Nat. Commun.*, 2020, 11, 2838.
4. S. Chen, J. Gong et al., *Chem*, 2021, 9, 1–19.
5. Y. Nakaya, E. Hayashida, H. Asakura, S. Takakusagi, S. Yasumura, K. Shimizu, S. Furukawa, *J. Am. Chem. Soc.*, 2022, 144, 15944–15953.

Low-temperature Catalytic Methane Combustion using Ozone

Shunsaku Yasumura^{a,*}

^a *Institute of Industrial Science, The University of Tokyo, Meguro, Tokyo 153-8505, Japan.*

^{*} *Corresponding author: yasumura@iis.u-tokyo.ac.jp*

Abstract

In recent decades, natural gas has become a widely used cleaner energy source for vehicles and power plants. A key method to reduce emissions of unburned methane (CH₄), which has a greenhouse gas effect 22 times greater than carbon dioxide (CO₂), is the catalytic combustion of CH₄ to CO₂. Platinum group metal (PGM)-based catalysts have shown exceptional catalytic activity for CH₄ combustion. However, PGM-based catalysts have limitations, including aggregation at high operating temperatures (>500°C) under humid conditions and irreversible deactivation due to sulfation when exposed to steam and SO₂. To address these issues, this study utilizes automated reaction route mapping to design catalysts for low-temperature methane combustion using ozone.¹ Computational screening has identified strong Brønsted acid sites (BASs) as promising candidates for facilitating methane combustion with ozone. These BASs can effectively catalyze the reaction at lower temperatures, thus mitigating the issues faced by PGM-based catalysts. Experimental results support these computational predictions. We tested beta (β) zeolite catalysts, which possess strong Brønsted acid sites, and found that they exhibit superior CH₄ conversion at 250°C. This temperature is significantly lower than the operating temperatures typically required for PGM-based catalysts, demonstrating the potential for more efficient and stable methane combustion under these conditions. The alignment of experimental data with theoretical predictions validates our approach. This study showcases the successful application of automated reaction route mapping in the rational design of heterogeneous catalysts. This methodology not only addresses the environmental concerns associated with methane emissions but also provides a framework for designing advanced catalysts for various industrial applications.

Keywords: Methane combustion, Ozone, Automated reaction route mapping

References

1. S. Yasumura, K. Saita, T. Miyakage, K. Nagai, K. Kon, T. Toyao, Z. Maeno, T. Taketsugu, K. Shimizu, *Nat. Commun.* 2023, 14 3926.

Catalysis of Intermetallic Compounds for Propyne Hydrogenation

Takayuki Kojima

*Faculty of Textile Science and Technology, Shinshu University, Japan
tkojima@shinshu-u.ac.jp*

Abstract

Intermetallic compounds possess unique crystal structures that are totally different from the parent metals, consequently giving unique electronic structures. Thus, they exhibit novel catalytic properties.¹ In particular, excellent selectivity is often obtained for selective reactions because of unique active sites with the ordering of different elements, which add a restriction to elementary steps such as the adsorption of reactants. The activity can also be drastically changed due to forming compounds; for example, Al₁₃Fe₄ shows high activity for acetylene hydrogenation² despite the fact that both pure Al and Fe show low activity.

I aim to find rules on the catalysis of intermetallic compounds, like a classification of pure metal catalysts that the group 10 elements are suited for hydrogenation and the group 8 elements are suited for ammonia synthesis. We have investigated the catalysis of Heusler alloys,^{3–10} which are the group of ternary intermetallic compounds X₂YZ with the L2₁ (bcc-based) structure. Since Heusler alloys have many possible elemental sets of X, Y, and Z, they are suitable for investigating the catalytic characteristics of component elements under the same crystal structure.¹⁰ Propyne hydrogenation is suitable as a model reaction because it never causes the oxidation of non-noble metal components and less significantly causes poisoning due to the formation of oil species than acetylene hydrogenation.

In studies on Heusler catalysts for propyne hydrogenation, the characteristics of each element have been found.^{3,8} For example, Ga gives high activity, Ge gives high selectivity, and only Sn causes the cracking and coupling of carbon chains.³ The activity and selectivity can be controlled by elemental substitution like Co₂Mn_xFe_{1-x}Ga_yGe_{1-y} due to electronic and/or geometric effects.⁸ In a very recent study on binary intermetallic catalysts, we have found a close correlation between the crystal structure and catalytic properties, in addition to the importance of p-block elements.¹¹

Keywords: intermetallic catalyst, propyne hydrogenation, Heusler, alloy catalyst

References

1. Nakaya, Y.; Furukawa, S. *Chem. Rev.* 2023, 123, 5859–5947.
2. Armbrüster, M.; Kovnir, K.; Friedrich, M.; Teschner, D.; Wowsnick, G.; Hahne, M.; Gille, P.; Szentmiklósi, L.; Feuerbacher, M.; Heggen, M.; Girgsdies, F.; Rosenthal, D.; Schlögl, R.; Grin, Y. *Nat. Mater.* 2012, 11, 690–693.
3. Kojima, T.; Wakayama, T.; Oi, Y. *Mater. Trans.* 2024, 5, 530–533.
4. Kojima, T.; Nakaya, Y.; Tate, S.; Kameoka, S.; Furukawa, S. *ChemistryOpen* 2023, 12, e202300131.
5. Iwase, K.; Kojima, T.; Todoroki, N.; Honma, I. *Chem. Commun.* 2022, 58, 4865–4868.
6. Kojima, T.; Koganezaki, T.; Fujii, S.; Kameoka, S.; Tsai, A.-P. *Catal. Sci. Technol.* 2021, 11, 4741–4748.
7. Kojima, T.; Kameoka, S.; Tsai, A.-P. *ACS Omega* 2019, 4, 21666–21674.
8. Kojima, T.; Kameoka, S.; Fujii, S.; Ueda, S.; Tsai, A.-P. *Sci. Adv.* 2018, 4, eaat6063.
9. Kojima, T.; Kameoka, S.; Tsai, A.-P. *ACS Omega* 2017, 2, 147–153.
10. Kojima, T.; Kameoka, S.; Tsai, A.-P. *Sci. Technol. Adv. Mater.* 2019, 20, 445–455.
11. Seo, Y.; Kojima, T. *submitted*.

Impact of acid-base amounts for proton conductivity and molecular dynamics of phosphonic acid-modified mesoporous silica/imidazole composite

Yasuhiro Shigeta, Motohiro Mizuno*

NanoMaterials Research Institute, Kanazawa University

**Corresponding author: mizuno@se.kanazawa-u.ac.jp*

Abstract

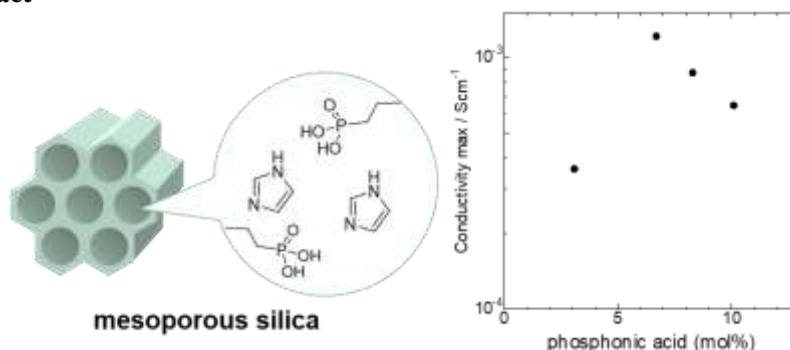
Proton exchange membrane fuel cell (PEFC) have drawn considerable attention because of their potential to generate energy without pollutants. To achieve high-performance, electrolytes are one of the key factors. Most electrolytes are used H₂O as a proton carrier. However, at elevated temperature, conductivity is dropped due to desorption of H₂O. To avoid this, various materials and attempts were reported.

Among them, replacement of proton carrier is one of the possible strategies to aim anhydrous proton conductor. Particularly, imidazole is extensively studied as a proton carrier. Proton conduction mechanism with imidazole-incorporated materials is understood as the Grotthus mechanism. In this mechanism, imidazole molecules transfer their protons to other molecules through hydrogen bonding. Further, imidazole molecules subsequently regenerate hydrogen bonding formation by their rotational motion. Therefore, molecular motion of imidazole is important to understand proton conduction mechanism and to achieve high proton conductivity. However, to the best of our knowledge, it is unclear how to enhance molecular motion of imidazole in the matrices, towards high proton conductivity.

In this study, we have prepared phosphonic acid-modified mesoporous silica (SBA-15)/imidazole composites and their relationship among amount of phosphonic acid and imidazole, proton conductivity and molecular motion were examined. Phosphonic acid-modified mesoporous silica was prepared by published method¹ with slight modification. Incorporation of imidazole was confirmed by solid state ¹³C NMR measurements and thermogravimetric analysis. Proton conductivity measurements revealed that higher amount of imidazole leads higher proton conductivity. However, too much modification of phosphonic acid tended to suppress proton conductivity. Solid state ²H NMR measurements suggested that higher amount of phosphonic acid prevents molecular motion of imidazole and resulting in proton conductivity was decreased. This finding demonstrates that appropriate amount of phosphonic acid would exists to reach higher proton conductivity within same amount of imidazole.

Keywords: proton conductivity, mesoporous silica, solid state NMR

Graphical abstract



References

1. Y.-C. Pan, H.-H. G. Tsai, J.-C. Jiang, C.-C. Kao, T.-L. Sung, P.-J. Chiu, D. Saikia, J.-H. Chang, H.-M. Kao, *J. Phys. Chem. C* **2012**, *116*, 1658-1669.

Development of Photocatalytic or Photoelectrochemical System for CO₂ Reduction Using Water as Electron Donor

Tomoaki TAKAYAMA^{a,*}

^aGraduate School of Science and Technology, Division of Materials Science, Nara Institute of Science and Technology (NAIST), 8916-5 Takayama, Ikoma, Nara 630-0192, Japan.

*Corresponding author: takayama.tomoaki@ms.naist.jp

Abstract

Photocatalytic or photoelectrochemical CO₂ reduction using water as an electron donor have gathered attention in terms of CO₂ fixation utilizing renewable powers such as solar energy.¹ This paper exhibits two examples of the developments about a new photocatalytic or photoelectrochemical system for the CO₂ reduction.

Metal oxides have been widely studied as photocatalysts due to their stability under photocatalytic reaction conditions. However, most metal oxide photocatalysts generally possess wide band gaps, resulting in that they respond to irradiation lights with shorter wavelengths. Therefore, many efforts have been made to narrow their band gaps. For narrowing the band gaps, Ag⁺ substitution is one of the effective strategies. Then, an AgSr₂Ta₅O₁₅ photocatalyst has emerged for water splitting and CO₂ reduction. DFT calculation and diffuse reflection spectra revealed that the Ag *d*-orbital formed a new valence band, leading to a narrow band gap (3.91 eV) compared to that of NaSr₂Ta₅O₁₅ (4.11 eV).²

Pd nanoparticles work as electrocatalysts for CO₂ reduction at relatively low applied potentials. However, the Pd-based electrocatalysts' performances are decreased with an increase in the reaction times due to poisoning by CO formed *via* CO₂ reduction. For solution of this problem, formation of intermetallic compounds (IMCs), some of the binary alloys, are expected to bring durability for the CO poisoning. This is because their surface-atom-arrangements are expected to be regular, which arise from well-ordered atom-arrangements in their crystal structures. Indeed, nanoparticulate IMC PdIn combined both the activity for electrochemical CO₂ reduction and a significant durability to CO poisoning. This was revealed through control experiments and DFT calculations to estimate the CO adsorption energy on the surfaces. Furthermore, the PdIn electrocatalyst was useful as the cathode part of the electrochemical cell combined with a CoO_x/BiVO₄:Mo photoanode, which was active for artificial photosynthetic CO₂ reduction to form CO under simulated solar light.³

Keywords:

Metal-oxide-photocatalysts, Pd-based intermetallic compounds, electrocatalysts, CO₂ reduction, artificial photosynthesis

References

1. Yoshino, S.; Takayama, T.; Yamaguchi, Y.; Iwase, A.; Kudo, A. *Acc. Chem. Res.*, **2022**, *55*, 966–977.
2. Takayama, T.; Iwase, A.; Kudo, A. *Chem. Commun.*, **2023**, *59*, 7911–7914.
3. Takayama, T.; Sakai, M.; Yamazoe, S.; Komatsu, T. *ACS Appl. Energy Mater.*, **2023**, *6*, 2793–2803.

OXIDATION STABILITY of MXene ($Ti_3C_2T_x$) NANOSHEETS

Sarangerel D.^{a*}, Suvdanchimeg S.^a, Selengesuren S.^b, Solongo P.^b, Tumentsereg O.^c, Munkhjargal B.^{b,d}, Purevlkham M.^b, Ashley D.S.^e, Abdulaziz S. R. B.^d, Joseph G. Sh.^d, Dorj O.^c, and Munkhbayar B.^b

^aNational University of Mongolia

^bGriffith University

^cIncheon National University

^dUniversity of Queensland

^eUniversity of Adelaide

*Corresponding author: sarangerel@num.edu.mn

Abstract

Transition metal carbides and nitrides, known as MXenes in the form of nanosheets, represent intriguing two-dimensional materials. However, their susceptibility to oxidation and degradation when exposed to water and oxygen can impact their storage and applications. Despite significant research advances, the precise oxidation kinetics of MXene ($Ti_3C_2T_x$) and the resulting products post-oxidation remain incompletely understood. In our study, we meticulously monitored the oxidation process of few-layer $Ti_3C_2T_x$ nanosheets in an oxygen-rich aqueous solution at room temperature over several weeks. Our findings revealed that the MXene degrades exponentially following first-order kinetics. Detailed experimental analyses, including X-ray photoelectron spectroscopy, Raman spectroscopy, and transmission electron microscopy, illustrated that severe oxidation of $Ti_3C_2T_x$ in an oxygen-rich water solution yields three distinct final components: white titanium (IV) oxide, black titanium (III) oxide, and disordered carbon. Theoretical density functional theory calculations aligned with the experimental findings, indicating rapid oxidation to oxidized species of MXene with higher formation energies compared to the initial Ti_3C_2 product. Further oxidation leads to the desorption of titanium atoms from the $Ti_3C_2O_2$ layers beneath the surface oxygen upon additional oxygen adsorption, resulting in the simultaneous generation of Ti^{3+} and Ti^{4+} compounds as the final products.

Interestingly, the oxidized MXene displayed potential for developing efficient electrocatalysts, showing an overpotential of 400 mV and a Tafel slope of 108 mV dec⁻¹. Importantly, these different products can be harnessed for various applications, showcasing a significant advancement in comprehending the behavior of $Ti_3C_2T_x$ and its potential applications. In summary, our study comprehensively explored the oxidation process of $Ti_3C_2T_x$ nanosheets in an oxygen-rich aqueous solution, shedding light on the catalytic performance of oxidized MXene for electrochemical hydrogen production in acidic environments. The findings underscore the potential of oxidized MXene as a promising candidate for efficient electrocatalysts, opening up possibilities for diverse applications.

Keywords: 2D materials; MXene; chemical degradation; catalysis; black titanium (III) oxide

References

1. Suvdanchimeg S., Selengesuren S., Solongo P., Ochirkhuyag T., Munkhjargal B., Purevlkham M., Ashley D. Slattery, Abdulaziz S.R.Bati, Joseph G.Shapter, Odkhuu D., Sarangerel D. and Munkhbayar B., *J.Energy Chem.*, 2024, 88, 437-445

The Z-scheme type photocatalyst based on interlayer expanded MoS₂ coupled with Bi₂O₂CO₃ under 1 W LED light

Magdeline Tze Leng Lai ^a, Thomas Chung Kuang Yang ^b, Chin Wei Lai ^a, Chia-Yun Chen ^{c,d}, Mohd Rafie Johan ^a, Kian Mun Lee ^a, Joon Ching Juan ^{a,e,*}

^aNanotechnology & Catalysis Research Centre, Institute for Advanced Studies, University of Malaya, 50603 Kuala Lumpur, Malaysia.

^bDepartment of Chemical Engineering and Biotechnology, National Taipei University of Technology, Taipei, Taiwan

^cDepartment of Materials Science and Engineering, National Cheng Kung University, Tainan, 70101, Taiwan

^dHierarchical Green-Energy Materials (Hi-GEM) Research Center, National Cheng Kung University, Tainan, 70101, Taiwan

^e Faculty of Engineering, Technology and Built Environment, UCSI University, Cheras, 56000, Kuala Lumpur, Malaysia

*Corresponding author: jcjuan@um.edu.my (JC Juan)

Abstract

The development of photocatalysts to degrade organic pollutants from wastewater under visible light has attracted a lot of interest. Herein, a series of Bi₂O₂CO₃ (BOC) coupled with interlayer expanded MoS₂ (IEM) photocatalysts were synthesized via a facile two-pot hydrothermal technique. Among all the samples, 5% of BOC with IEM (5% BOC-IEM) nanocomposite exhibited the highest photodegradation with 94% ($4.97 \times 10^{-2} \text{ min}^{-1}$) for Methylene Blue (MB) dye removal under 1 W LED visible light. The performance by 5% BOC-IEM is 1.5 times and 13.4 times higher than the parent IEM and BOC, respectively. Increased photocurrent density, lowest PL intensity, and smallest EIS arc further evidenced the lowered charge carrier's recombination rate in the optimized 5% BOC-IEM heterostructure. Moreover, the outstanding photocatalytic performance of 5% BOC-IEM was due to the presence of oxygen vacancies, enhanced light absorption, and improved migration and separation of charge carriers. An Ohmic contact formed on the interfaces of BOC and IEM boosts the Z-scheme charge transfer mechanism, which greatly improved the photocatalytic activity of 5% BOC-IEM.

Keywords: Methylene blue, interlayer expanded MoS₂, photocatalytic Z-scheme, oxygen vacancies, LED light

BIOLEACHING OF RARE EARTH ELEMENTS FROM ALKALINE ROCK-CARBONATITE RELATED DEPOSIT IN MONGOLIA

Bayarbayasgalan B.^{a,b}, **Altangerel A.**^{a*}, **Purevjargal D.**^{a,c}, **Sarangerel D.**^a,

^a*National University of Mongolia, Ulaanbaatar*

^b*New Mongol Institute of Technology*

^c*Khanlab LLC*

**Corresponding author: a_aitaid@num.edu.mn*

Abstract

In Mongolia, rare earth elements (REE) are primarily found in minerals like monazite, bastnaesite, and synchysite, situated in deposits associated with alkaline rocks and carbonatites. For instance, the ore sourced from the Lugiin Gol deposit, containing synchysite and bastnaesite minerals, necessitates activation under tough conditions and leaching with highly concentrated sulfuric acid. This process is demanding in terms of energy, harmful to the environment, and results in a significant amount of toxic waste. Consequently, researchers are concentrating on bioleaching studies as they present more suitable and cost-effective approaches to leaching and concentrating low-grade ores. To explore the potential of bioleaching REE, numerous microorganisms were isolated from the carbonatite ore housing synchysite minerals. Bioleaching experiments were carried out with seven different bacterial cultures for 42 days at 30°C with particle size smaller than 0.074 mm. The highest metal recovery was observed on the 7th day, with the total REE in the leachate ranging from 20.4 mg/kg to 376.25 mg/kg. Following the 7th day, the REE' content decreased as the pH rose above 4, causing a certain form precipitation of elements. Among the tested bacteria, the thiobacteria proved to be the most effective bacterial system. When investigating the impact of particle size on leaching using thiobacteria, the TRE₂O₃ recovery was 9.13% for larger particle sizes of 5-10 mm highlighting particle size as a vital parameter affecting bioleaching efficiency. Mineralogical analysis of the solid residue after bioleaching revealed new peaks for synchysite and bastnaesite, indicating that bacterial activity weakened the interaction between these minerals and the host rock. While the REE' recovery through bacterial leaching was not remarkably high, the results suggest that combining bioleaching with subsequent chemical treatment or roasting under severe conditions could improve the processing of alkaline carbonatite rocks.

Keywords: Bacterial culture, Synchysite, Bastnaesite, Metal recovery, Biohydrometallurgy

References

1. Purevjargal, D., Bayarbayasgalan, B., et al., Bulletin of Institute of Chemistry and Chemical Technology, 2023, 11, 1-8
2. Purevjargal, D., Altangerel, et al., The 2nd International Conference on resources and Technology, 19-20 June 2023, Ulaanbaatar, Mongolia
3. Bayarbayasgalan, B., Nomin-Erdene, D., et al., The 2nd International Conference on Resources and Technology, 19-20 June 2023, Ulaanbaatar, Mongolia

Atomic/molecular-scale structural analysis on ionic-liquid electrolyte/electrode interfaces by atomic force microscopy

Takashi Ichii*

Department of Materials Science and Engineering, Kyoto University, Japan

*Corresponding author: ichii.takashi.2m@kyoto-u.ac.jp

Abstract

Since electrochemical reactions proceed at the electrode/electrolyte interfaces, high-resolution structural analysis of these interfaces is of crucial importance. Atomic force microscopy (AFM) can be used not only in vacuum or in air but also in liquid, and can investigate the anisotropic density distribution of liquid molecules near the solid-liquid interface, so-called solvation structure, as well as the solid surface structures on the atomic or molecular scales. Therefore, high-resolution AFM analysis of the electrode/electrolyte interfaces is expected to provide important insights into electrochemistry. Here, we report AFM investigations on ionic-liquid (IL) electrolyte/electrode interfaces. A key feature of our AFM is the use of a quartz tuning fork (QTF)-based force sensor, which shows a high-quality factor even in viscous liquids, including ILs [1].

Figure 1(a) shows electrochemical AFM topographic images of lithium titanate (LTO) electrodes in an IL electrolyte before and after Li-ion insertion. Atomic-scale surface structural change was successfully detected [2]. Analysis of the interfacial solvation structure also provides important information. When Li salts are added to an ionic liquid, the formation of a layered solvation structure is disrupted (Fig. 2)[3-5]. This means that the Li-ion insertion/extraction at the interface can be visualized on a molecular scale via solvation structure analysis.

Keywords: Atomic force microscopy, solid/liquid interface

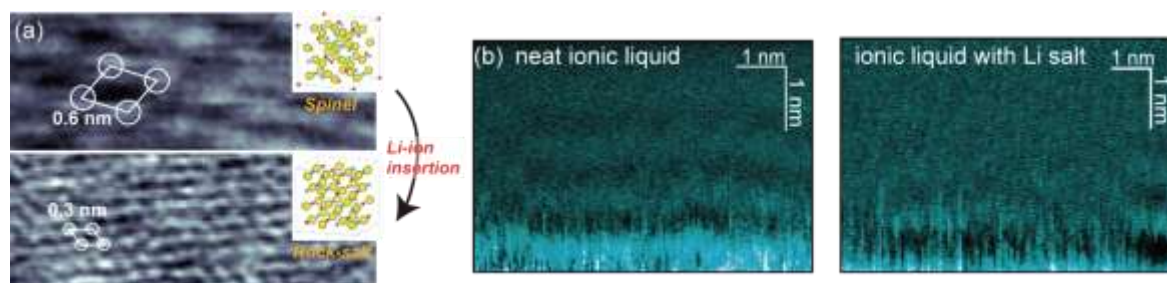


Fig. 1(a) Electrochemical AFM topographic image of LTO electrode before and after Li-ion insertion in IL electrolyte, (b) Interfacial solvation structure of IL/LTO interfaces with and without Li salt.

References

1. T. Ichii, M. Negami, H. Sugimura, *J. Phys. Chem. C.*, **118**(46), 26803-26807 (2014).
2. T. Ichii, Y. Takara, T. Uchida, M. Kitta, T. Utsunomiya, H. Sugimura, *J. Phys. Chem. C.*, **127** 14468-14475 (2023)
3. Y. Bao, M. Kitta, T. Ichii, T. Utsunomiya, H. Sugimura, *Jpn. J. Appl. Phys.*, **60**, SE1004 (2021)
4. Y. Bao, M. Kitta, T. Ichii, T. Utsunomiya, H. Sugimura, *Jpn. J. Appl. Phys.*, **61**, SL1007 (2022)
5. T. Ichii, K. Itakura, Y. Bao, T. Utsunomiya, H. Sugimura, *Jpn. J. Appl. Phys.*, *in press*.

THE ROLE OF CARBON BLACK IN THE GALVANIC LEACHING OF CHALCOPYRITE IN THE PRESENCE OF MANGANESE DIOXIDE

Altangerel A., Nomin-Erdene D., Bayarmaa N., Sukhbaatar B., Sarangerel D.*

National University of Mongolia

**Corresponding author: Sarangerel@num.edu.mn*

Abstract

Chalcopyrite is one of the most widespread and refractory copper-containing minerals globally, contributing to around seventy percent of global copper resources. Researchers are focusing more on chalcopyrite leaching using hydrometallurgical methods with various leaching agents. Sulfuric acid is most commonly used agent for the chalcopyrite leaching among the leaching agents. Initially, leaching by sulfuric acid is intense, but it slows down after a certain period of leaching due to the formation of an inactive sulphur layer on the mineral's surface. To reduce this layer and accelerate leaching, oxidation agents like MnO_2 , pyrite and H_2O_2 are used, aided by the galvanic effect and charge carriers including carbon black. Therefore, we aimed to investigate the role of carbon black during chalcopyrite leaching with manganese dioxide, leading to increased copper recovery through additional oxidation. In our study, we conducted chalcopyrite leaching using a 1.0 M sulfuric acid in four different systems under ambient conditions. The copper recovery in $\text{CuFeS}_2+\text{FeS}_2+\text{MnO}_2+\text{C}$ system reached to 91.6%, significantly higher than the $\text{CuFeS}_2+\text{FeS}_2$ system at 1.0% after sulfuric acid leaching, thanks to the galvanic effect. Introducing MnO_2 during leaching increased oxidation-reduction potential to 1062 mV, facilitating leaching by producing Fe^{3+} , Cu^{2+} and SO_4^{2-} ions. While some researchers view carbon black solely as a charge carrier, we propose that it acts as the active center of the reaction. To support this claim, we obtained a cyclic voltammogram by measuring current at the working electrode. During chalcopyrite leaching in sulfuric acid with MnO_2 , carbon black activates passive layers, as indicated by peak at 313 mV and 224 mV in the cyclic voltammogram representing chalcocite and elemental sulphur oxidation half reactions. This demonstrates that carbon black enhances the charge carrier during chalcopyrite leaching and becomes the active centre of the reaction.

Keywords: copper recovery, mechanism, sulfuric acid leaching, cyclic voltammetry, charge carrier

References

1. Altangerel.A, Nomin-Erdene.D, Bayarmaa.N, Sukhbaatar.B, Sarangerel.D.; *Min. Metall. & Explor.* 2024.

ACQUISITION OF CATALYST DESIGN RULES THROUGH FEATURE ENGINEERING

Aya Fujiwara^a, Sunao Nakanowatari^a, Toshiaki Taniike^{a*}

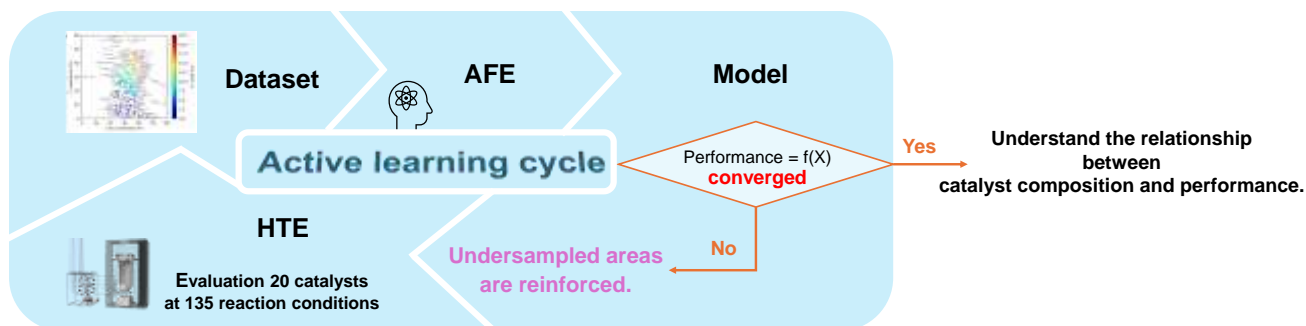
^aJapan Advanced Institute of Science and Technology

*Corresponding author: taniike@jaist.ac.jp

Abstract

Materials informatics (MI) aims to accelerate the discovery and understanding of materials through data science, particularly when complexity exceeds human perception. However, there are two challenges to the practical application of MI. One is the lack of data that meets the quality, scale, and consistency required for effective machine learning (ML). The other is the need of sophisticated domain knowledge in tailoring descriptors (numerical representation of catalysts). To address the data issue, we developed a high-throughput screening (HTS) system that automates the evaluation of 20 catalysts under programmed reaction conditions.¹ Meanwhile, the descriptor issue was successfully addressed by an automatic feature engineering (AFE) method that we have recently developed for allowing descriptor design without domain knowledge.² This method generates a numerous number of features from a multitude of physicochemical characteristics of catalyst components, then extracts features relevant to describing the catalyst performance.

In this study, we practiced a combination of HTS and AFE in the active learning loop, as shown in Figure. HTS generates consistent, unbiased, and reasonably sized data, based on which AFE proposes a ML model with designed descriptors, corresponding to a proposal of a hypothesis for a catalyst design-performance relationship. The data and hypothesis are subsequently sophisticated by augmenting under-sampled features, and it eventually leads to a robust and accurate ML model being useful for extracting catalyst design heuristics on oxidative coupling of methane (OCM), catalysis of practical interests of directly converting methane into C₂ products in the presence of molecular oxygen.



Keywords: catalyst informatics, heterogeneous catalysis, oxidative coupling of methane

Acknowledgements: this work was supported by JST Mirai Program (Grant Number JPMJMI22G4). The research of A. F. was supported by JST SPRING (JPMJSP2102).

References

1. Nguyen, T. N.; Tran, T. P. N.; Takimoto, K.; Thakur, A.; Nishimura, S.; Ohyama, J.; Miyazato, I.; Takahashi, L.; Fujima, J.; Takahashi, K.; Taniike, T. *ACS Catal.* **2020**, *10*, 2, 921–932.
2. Taniike, T.; Fujiwara, A.; Nakanowatari, S.; García-Escobar, F.; Takahashi, K. *Commun. Chem.*, **2024**, *7*, 11.

Identification of a Single Molecule in Nanoelectrodes using Surface-Enhanced Raman Scattering and Electric Current

Satoshi Kaneko*

Department of Materials Science and Engineering, Tokyo Institute of Technology

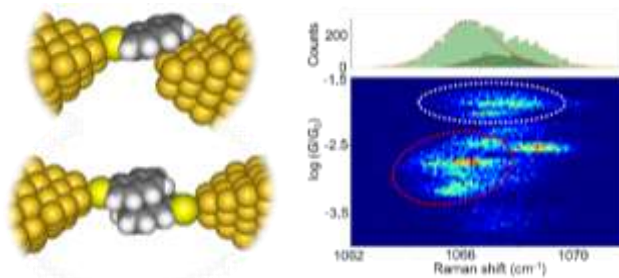
*Corresponding author: kaneko.s.aa@m.titech.ac.jp

Abstract

Developments in the field of nanotechnology enable the realization of various efficient nanometer-scale devices. The metal-molecule interface needs to be studied in detail because it has a huge impact on the charge injection in the organic semiconductor, solar cells, etc. The electron transport in a single-molecule junction (SMJ), which can be regarded as the ultimate metal-molecule-metal interface structure, has attracted significant attention in the areas of interface science, nanoscience, and fundamental physics. Although the junction structure is important for the electron transport of an SMJ, the experimental technique for the detection of the structural information of an SMJ under operation is limited.

Surface-enhanced Raman scattering (SERS) is a highly suitable option for detecting the vibrational mode from a single-molecule; however, detecting the single-molecule under operation, which is trapped in the metal nanogap, and obtaining its vibrational mode remains a challenge. Our research group has investigated SERS in an SMJ by collaboration with the electric measurement. We found the relationship between SERS signal and the electric current of SMJ and succeeded in the detection of the SERS signal from an SMJ [1-5]. The vibrational shift and change in the SERS intensity revealed the structural change concomitant with the electron transport modulations [1-3]. The electric states, which are revealed by the current measurements, in turn, revealed the effect of the charge transfer on the signal enhancement and vibrational mode observation in SERS enhancement [4,5]. Recently, the correlation of the vibrational energy and conductance recognized the π stacked dimer of naphthalene derivative in metal nanogap [6].

Keywords: Single-molecule junction, metal-molecule interface, Surface-enhanced Raman scattering, current voltage response.



References

1. Kaneko, S.; Murai, D.; Marqués-González, S.; Nakamura, H.; Komoto, Y.; Fujii, S.; Nishino, T.; Ikeda, K.; Tsukatashi, K.; Kiguchi, M. *J. Am. Chem. Soc.*, 2016, 138, 1294–1300.
2. Kaneko, S.; Montes, E.; Suzuki, S.; Fujii, S.; Nishino, T.; Ikeda, K.; Kano, H.; Nakamura, H.; Vázquez, H.; Kiguchi, M. *Chem. Sci.* 2019, 10, 6261–6269.
3. Kobayashi, S.; Kaneko, S.; Kiguchi, M.; Tsukagoshi, K.; Nishino, T. *J. Phys. Chem. Lett.* 2020, 11, 16, 6712–6717.
4. Kaneko, S.; Yasuraoka, K.; Kiguchi, M. *J. Phys. Chem. C* 2019, 123, 11, 6502–6507.
5. Yasuraoka, K.; Kaneko, S.; Kobayashi, S.; Tsukagoshi, K.; Nishino, T. *ACS Appl. Mater. Interfaces* 2021, 13, 51602–51607.
6. Homma, K.; Kaneko, S.; Tsukagoshi, K.; Nishino, T. *J. Am. Chem. Soc.* 2023, 145, 29, 15788–15795.

Pt₁₇ Nanocluster Electrocatalysts: Preparation and Origin of High Oxygen Reduction Reaction Activity

Yuichi Negishi

Institute of Multidisciplinary Research for Advanced Materials, Tohoku University, Japan.

E-mail: yuichi.negishi.a8@tohoku.ac.jp

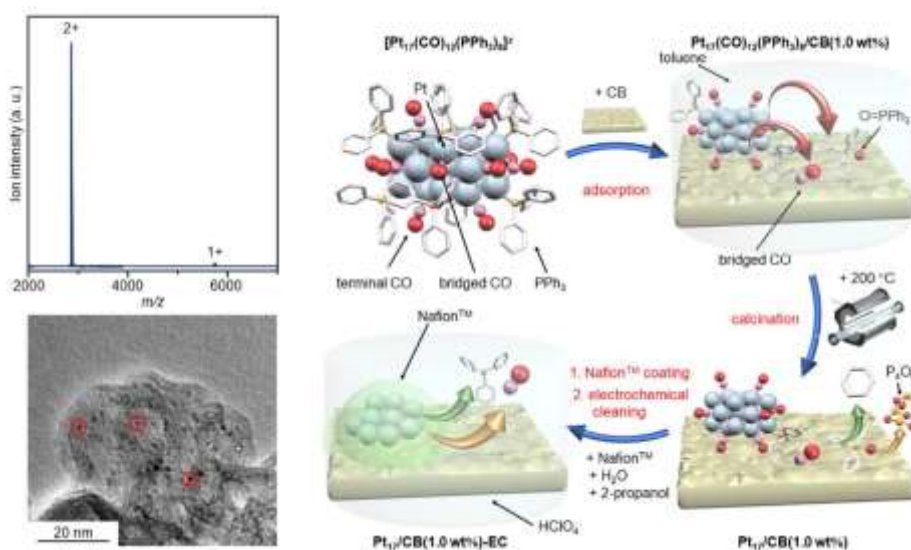
Abstract

In polymer electrolyte fuel cells (PEFCs), the oxygen reduction reaction (ORR) at the cathode is the rate-determining reaction, and catalysts with Pt nanoparticles (Pt NPs) of 2–3 nm in diameter supported on carbon black (Pt NPs/CB) are widely used for such cathode catalysts. However, previous studies have shown that Pt nanoclusters (NCs) of ~1 nm in size exhibit higher ORR activity than Pt NPs of 2–3 nm in size. It is thus expected that the use of precisely synthesized Pt NCs of ~1 nm in size as ORR electrocatalysts would afford reduced amounts of Pt to be used in PEFCs.

Pt nanoclusters (NCs) and their alloy NCs of ~1 nm in size can be synthesized with atomic precision when carbon monoxide (CO) and phosphine (PR₃) are used as ligands (Pt_n(CO)_m(PR₃)_l; *n*, *m*, *l* = the number of Pt atom, CO ligand, and PR₃ ligand, respectively). However, most of the Pt_n(CO)_m(PR₃)_l NCs reported to date face stability issues under atmospheric conditions, and consequently few studies have been conducted on their application as ORR electrocatalysts.

We recently found that [Pt₁₇(CO)₁₂(PPh₃)₈]^z (PPh₃ = triphenylphosphine; *z* = 1+ or 2+) is a Pt NC that can be synthesized with atomic precision in air. The present study demonstrates that it is possible to prepare a Pt₁₇-supported carbon black (CB) catalyst (Pt₁₇/CB) with 2.1 times higher ORR activity than commercial Pt nanoparticles/CB by the adsorption of [Pt₁₇(CO)₁₂(PPh₃)₈]^z onto CB and subsequent calcination of the catalyst. Density functional theory calculation strongly suggests that the high ORR activity of Pt₁₇/CB originates from the surface Pt atoms that have an electronic structure appropriate for the progress of ORR. These results are expected to provide design guidelines for the fabrication of highly active ORR catalysts using Pt NCs with a diameter of about 1 nm and thereby enabling the use of reduced amounts of Pt in polymer electrolyte fuel cells [1].

Keywords: platinum nanoclusters, polymer electrolyte fuel cells, oxygen reduction reaction, Density functional theory calculation



References

1. T. Kawawaki, K. Iida, Y. Negishi, et al, *Nanoscale*, 2023, 15, 7272.

THE EFFECTS OF MELANIN ON PROPERTIES YAK HAIR**Batchimeg Ganbaatar^{a, b*}**, **Nansalma Shirnen^b**, **Nadmid Gongor^b**,^a *School of Applied Science of Mongolian University of Science and Technology*^b *Research and Development Institute of Light Industry belong to Mongolian University of Science and Technology***Corresponding author: batchimeg.gan@must.edu.mn, ORCID: 0009-0001-5798-3939***Abstract**

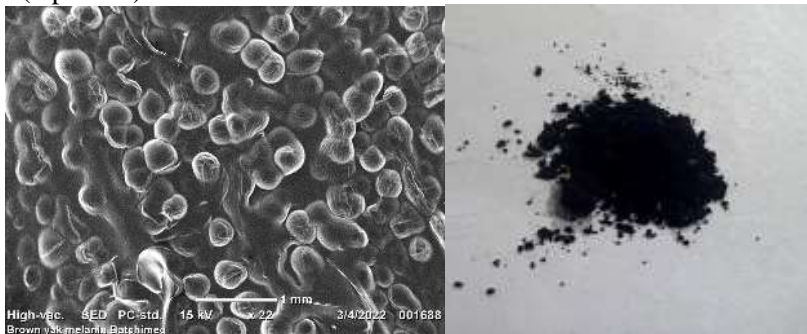
Yak hair is Mongolian wool industry a strategic raw material¹. The beneficial properties such as warmth, strength of yak hair products have been studied in relation to the melanin in the internal microstructure of the fibers. Melanin is mainly located in the paracortex. The cortex layer of the yak fine fiber included 70-80% paracortex and 20-30% ortho-cortex. Melanin extracted from yak hair is contains C 45.57%, N 20.78%, O 26.46%, S 1.01%, and CI 6.18% by EDS. Depending on the diameter of the fiber, melanin is distributed along the length of oval-shaped granules².

Melanin was extracted by acid hydrolysis from yak dark brown wool, goat brown cashmere, camel brown wool, sheep dark brown wool. The yield of extraction melanin is determined in 20% yak hair, 2.5% goat cashmere, 2.6% camel wool and 8% sheep wool. In order to determine the bundle tenacity is yak fine fiber 9.3 cN/tex, goat cashmere 6.9 cN/tex, camel wool 8.1cN/tex, sheep wool 7.6 cN/tex³.

When the melanin content of yak hair was reduced 70% by depigmentation technology, the solubility in alkali increased by 19%, and the breaking load decreased by 20-28%. Also, when determining the changes in the consumption characteristics of the knitted samples, the air permeability increases by 22.8 mm/sec, the combustion state increases by 12 m/sec and the heat index decreases by 33.7%³.

Compared to other animal fibers, yak hair is stronger, more durable, and warmer, and it is an innovative research work that has been studied in connection with melanin in its internal microstructure.

Keywords: cortex, thermal properties, Insert maximum of 5 keywords

Graphic / Image (Optional)

The melanin granule by SEM and powder melanin from yak hair

References

1. Batchimeg G.; Nadmid G.; Yak wool book., 2021, 77
2. Batchimeg G.; Oyunchuluun L.; Dagvasuren E.; Batsuren Ch.; Nadmid G.; ICASE, 2023, 61-67
3. Batchimeg G., Nansalma Sh, unpublished data.
4. Batchimeg G.; Nadmid G.; 2022,

Electron Spin Resonance Spectroscopy for Clear Observation of Reactions during Radical Polymerizations

Atsushi Kajiwara

Nara University of Education, Takabatake-cho, Nara 6308528, Japan

*Corresponding author: kajiwara@cc.nara-edu.ac.jp

Abstract

In radical polymerization reactions, various radical species are generated as reaction-active species. Electron Spin Resonance (ESR) spectroscopy can observe electrons directly under microwave irradiation. Electrons dominate the chemical world. In the same actual radical polymerization system, the spectrum of propagating radicals can be observed by measuring steady-state ESR (SS ESR), while only the initiation process can be extracted and observed by time-resolved ESR (TR ESR), which observes a phenomenon known as CIDEP. These observations permit the detailed structural analysis of the radicals, their molecular dynamics, concentration, as well as the observation of chain transfer reactions and penultimate unit effects and so on.

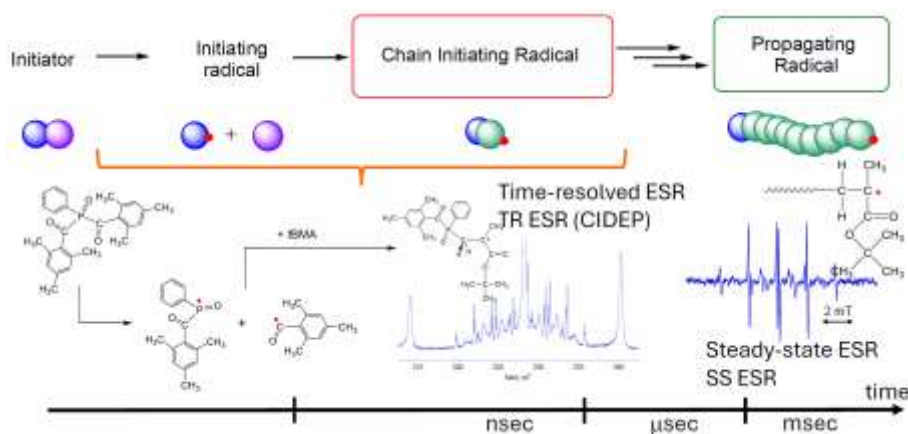


Figure 1 Radical polymerizations in various time scales.

In recent years, it has become possible to observe time-resolved ESR spectra of various photoinitiators. Figure 2 provides an illustrative example, showing the spectra of a system with 1-Benzoylcyclohexanol as initiator, initiator alone, and *tert*-butyl acrylate (*t*BA) added. The CIDEP spectra in the middle of Figure 1 appear upward (absorptive), whereas in Figure 2 they appear downward (emissive). This discrepancy can be attributed to the spin state of the radicals. This result allows for a discussion of the spin state and reactivity of the radicals, which can contribute to the fundamentals of radical polymerization reactions.

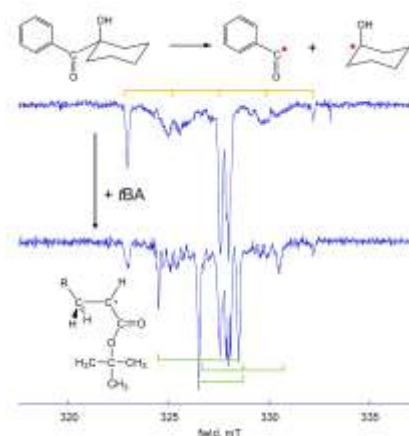


Figure 2 Time-resolved ESR spectra of 1-Benzoylcyclohexanol in the absence (top) and presence (bottom) of *t*BA

Keywords: Radical Polymerization, ESR/EPR Time-resolved ESR, CIDEP

References

1. Kajiwara, A., *Pure & Appl. Chem.*, **2018**, *90*, 1237-1254

SYNTHESIS AND CHARACTERISATION OF CARRAGEENAN/POLYANILINE FILM AND ITS ANTIBACTERIAL PROPERTIES

Sook-Wai PHANG*, Wen-Qing YANG, Ying-Chiang LOW

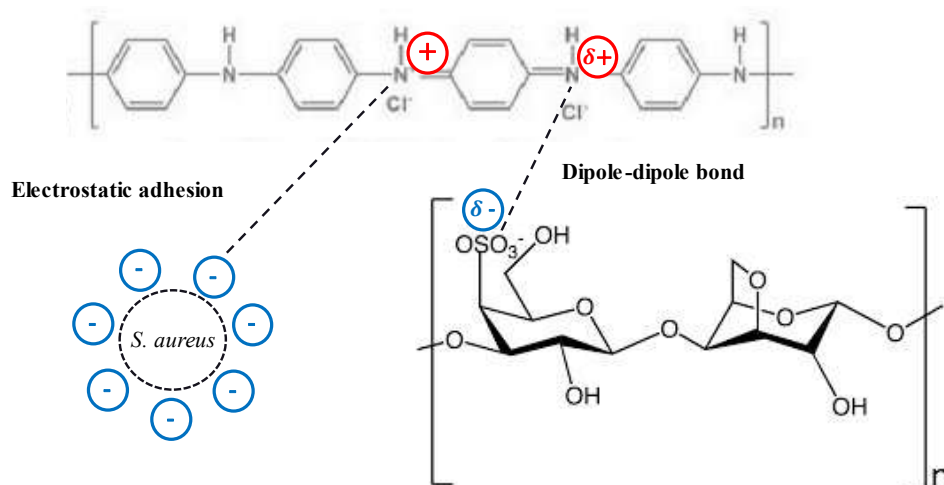
Faculty of Applied Science, Tunku Abdul Rahman University of Management and Technology (TAR UMT), Jalan Genting Klang, Setapak, 53300 Kuala Lumpur, Malaysia.

*Corresponding author e-mail: phangsw@tarc.edu.my; pinkyphang@gmail.com

Abstract

Researchers had developed wound dressings made up of biodegradable polymers to reduce the abundant use of synthetic and non-biodegradable dressings. However, being antibacterial for improved wound healing is one of the features of an ideal modern wound dressing and these polymers do not acquire it. In this research study, polyaniline (PANI) was developed as a potential antibacterial agent and incorporated a biopolymer matrix of κ -carrageenan (κ -CGN). PANI were polymerised through chemical oxidative method using HCl dopant and ammonium persulfate as oxidising agent. Ex-situ polymerisation was applied by adding PANI into κ -CGN with glycerol as plasticiser to produce κ -CGN/PANI films and further characterised by FTIR, electrical conductivity, tensile test and TGA analyses. κ -CGN had its conductivity ($1.89 \times 10^{-3} \text{ Scm}^{-1}$), mechanical properties (tensile strength: 2.47 MPa; modulus: 17 MPa; elongation at break: 16.17MPa) and thermal stability (T_{deg} : 390.28°C) improved with optimum amount of PANI 0°C (5 wt%). The antibacterial activity test was conducted on the films against both bacteria which were Gram-positive, *S. aureus* and Gram-negative, *P. aeruginosa* by agar disc diffusion method. Among κ -CGN/PANI films, only κ -CGN/PANI 0°C 10% films demonstrated good antibacterial activity against *S. aureus* (Gram- positive) with the best inhibition percentage of 37.26% for 24 hours but showed negative result with Gram-negative, *P. aeruginosa*. The mechanism between PANI and *S. aureus* were confirmed and shown in Figure 1.

Keywords: polyaniline; biopolymer; carrageenan; antibacterial films.



1. Es Neamtu, B.; Barbu, A.; Negrea, M. O., Berghea-Neamtu, C. Ş.; Popescu, D.; Zăhan, M.; Mireşan, V. *International Journal of Molecular Sciences*. 2022, 23(16), 9117.
 2. Shojaee-Aliabadi, S.; Hosseini, H.; Mohammadifar, M. A.; Mohammadi, A.; Ghasemlou, M.; Hosseini S. M.; Khaksar, R. *Carbohydrate Polymers*, 2014, 101, 582–591.
- El-Fawal, G. *Journal of Food Science and Technology*, 51(9), 2014, 2234–2239.

MICROSTRUCTURE AND RHEOLOGICAL INVESTIGATION OF BIO-BASED PICKERING EMULSIFIERS DERIVED FROM MODIFIED SPHERICAL CELLULOSE NANOCRYSTALS

Hwei Voon Lee¹, Mazlita Yahya^{1,4}, Mochamad Zakki Fahmi², Cheng Hock Chuah³

¹Nanotechnology and Catalysis Research Centre (NANOCAT), University of Malaya, 50603 Kuala Lumpur, Malaysia.

²Department of Chemistry, Faculty of Science and Technology, Universitas Airlangga, Campus C, Mulyorejo, Surabaya 60115, Indonesia.

³Department of Chemistry, Faculty of Science, University of Malaya, Kuala Lumpur 50603, Malaysia.

⁴Pre University department, INTI International College Subang, No. 3, Jalan SS15/8, Ss 15, 47500 Subang Jaya, Selangor, Malaysia.

*Corresponding author: leehweivoon@um.edu.my

Abstract

An environmentally friendly acid hydrolysis agent, ascorbic acid, was utilized in the production of mangosteen rind-derived nanocellulose (NC-L), which was subsequently modified with milk protein (sodium caseinate) to serve as a sustainable Pickering emulsifier (NC-S). The effectiveness of NC-S in stabilizing emulsions containing different concentrations of caseinate (milk protein) ranging from 1.5% to 4.0% (w/v) was evaluated in a water-in-oil (W/O) emulsion system. Among the prepared NC-S Pickering emulsifiers, the emulsion (3.0LN-E) with a W/O ratio of 40:60 stabilized by 3.0NC-S demonstrated optimum emulsion stability for over 3 months. The 3.0LN-E displayed a minimal creaming index and exhibited a well-distributed network between the water-Pickering emulsifier-oil, and it also showed an improved rheology profile under stress. Moreover, the optimal 3.0LN-E emulsion exhibited a rheological profile comparable to that of commercial oil-based formulation, thereby offering a promising alternative with reduced caloric intake and dietary fiber content to address health concerns. Microstructure properties of optimal 3.0NC-S was further investigated. XRD revealed that the nanocellulose from mangosteen rind was cellulose nanocrystals, which exhibited type I beta crystalline structure with a crystallinity index of 65.14%. The morphology profile showed that the mangosteen-derived NC-S was present as spherical particles without any surface structure changes after the surface modification process. The NC-S indicated the presence of nanosized particles, with diameters ranging from 14.26 ± 4.60 nm and lengths of 14.96 ± 4.94 nm.

Keywords: Biopolymer, biomaterial, biomass, cellulose, colloids and interfaces

Graphic / Image (Optional)



References

1. Yahya, M., Sakti, S. C. W., Fahmi, M. Z., Chuah, C. H., & Lee, H. V. International Journal of Biological Macromolecules, 2024, 257, 128696.
2. Teo, S. H., Chee, C. Y., Fahmi, M. Z., Wibawa Sakti, S. C., & Lee, H. V. Molecules, 2022, 7(21), 7170.

Supramolecular Approach to Multiferroics

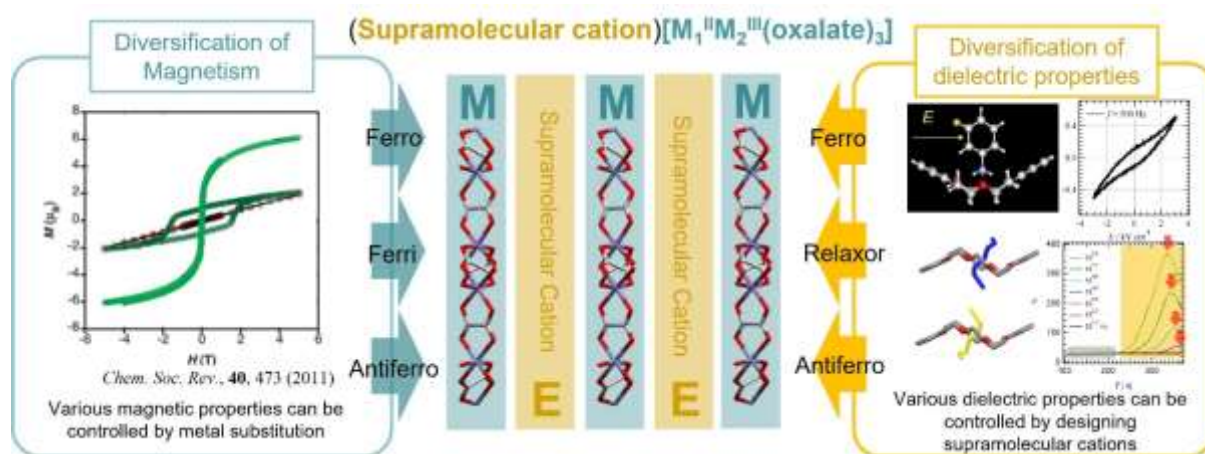
T. Nakamura^{a,b*}^a Research Institute for Electronic Science, Hokkaido University, Sapporo, Japan^b Graduate School of Advanced Science and Engineering, Hiroshima University, Higashi-hiroshima, Japan.

*Corresponding author: Author: tnaka@es.hokudai.ac.jp

Abstract

Molecular machines have undergone comprehensive investigation, leading to the reporting of various artificial molecular machines encompassing molecular motors, propellers, switches, and shuttles. Our focus lies in the development of supramolecular systems demonstrating molecular motion within crystals. Within a crystal lattice, molecules assume fixed positions, forming a directional and high-density array. The coordinated motion of individual molecules, facilitated by intermolecular interactions, induces diverse functionalities in crystals, such as polarity conversion and mass transport, resulting from the periodic nature of these crystals [1, 2]. This paper presents type-I multiferroic developed by introducing supramolecular cations into ferromagnetic 2D honeycomb layers of $[\text{Mn}^{\text{II}}\text{Cr}^{\text{III}}(\text{oxalate})_3]$.

Keywords: Supramolecule, ferroelectric, ferromagnet, multiferroic

**References**

1. T. Nakamura *et al.*, *Nature*, **394**, 159-161 (1998).
2. Wu *et al.*, *Dalton Trans.*, **51**, 10595-10600 (2022).

Thin Film Synthesis of Cu-based Metal–Organic Frameworks by Physical Vapor Deposition and Solvent Vapor Annealing

Ryo Nakayama^{a,*}, Chon Seoungmin^b, Shunta Iwamoto^b,

Shigeru Kobayashi^a, Ryota Shimizu^a, Taro Hitosugi^a

^aDepartment of Chemistry, The University of Tokyo

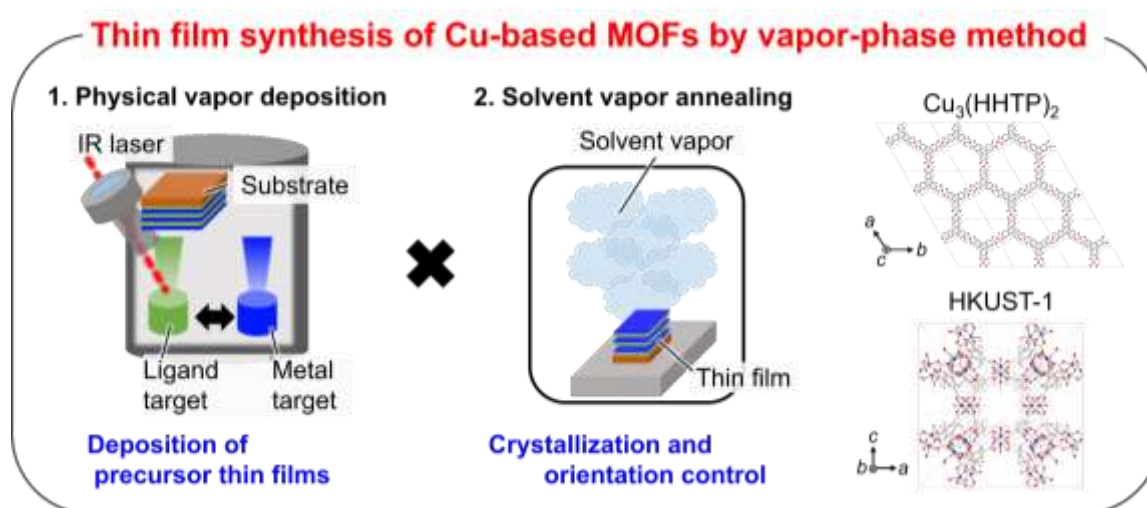
^bSchool of Materials and Chemical Technology, Tokyo Institute of Technology

*Corresponding author: ryo-nakayama@g.ecc.u-tokyo.ac.jp

Abstract

Metal-organic frameworks (MOFs) are crystalline porous materials formed by the coordination bonds between metal ions or metal atom clusters and organic ligands. Among MOFs, Cu-based MOFs exhibit high specific surface areas, tunable porous structures, structural diversity, and unsaturated coordination metal centers.¹ Additionally, recent reports have shown that some Cu-based MOFs exhibit electrical conductivity.² Due to these attractive properties, thin film synthesis of copper-based MOFs is highly desired for electronic device applications. Vapor deposition of MOF thin films is preferred for their implementation in micro- and nanofabrication research and industries.³ However, thin film synthesis of MOFs is typically achieved using liquid-phase methods, where metal salts and ligands react in a polar organic solution, following efficient procedures for MOF powder synthesis. Consequently, the vapor-phase synthesis of MOF thin films is still in development. For instance, there have been no reports of thin film synthesis of the representative Cu-based MOF, HKUST-1 ($\text{Cu}_3(\text{BTC})_2$, BTC: 1,3,5-benzenetricarboxylate) or the electrically conductive MOF, $\text{Cu}_3(\text{HHTP})_2$ (HHTP: hexahydroxytriphenylene) on insulating substrates using physical vapor deposition methods. In this study, we synthesized HKUST-1 and $\text{Cu}_3(\text{HHTP})_2$ thin films on insulating substrates using a two-step dry process that combines physical vapor deposition and solvent vapor annealing.⁴

Keywords: Metal–Organic Frameworks, Thin film, Vapor deposition, Electrical conductivity



References

1. Chen, Y.; Zhang, Y.; Huang, Q.; Lin, X.; Zeb, A.; Wu, Y.; Xu, Z.; Xu, X. *ACS Appl. Energy Mater.* 2022, 5, 7842-7873.
2. Xie, L. S.; Skorupskii, G.; Dincă, M. *Chem. Rev.* 2020, 120, 8536-8580.
3. Stassen, I.; De Vos, D.; Ameloot, R. *Chem. Eur. J.* 2016, 22, 14452-14460.
4. Chon, S.; **Nakayama R.***; Iwamoto, S.; Kobayashi, S.; Shimizu, S.; Hitosugi, T., *ACS Appl. Mater. Interfaces*, 2023, 15, 56057-56053.

APPLICATION OF LITHIUM PERCHLORATE BASED POLYMER ELECTROLYTE IN MEETING REQUIREMENTS OF ELECTRIC DOUBLE LAYER CAPACITOR

Koh Sing Ngai^{a,*}, S. Ramesh^a, K. Ramesh^a, Joon Ching Juan^b

^aCentre for Ionics University of Malaya, Department of Physics, Faculty of Science, Universiti Malaya, 50603 Kuala Lumpur, Malaysia

^bNanotechnology & Catalysis Research Centre (NANOCAT), Institute of Postgraduate Studies (IPS), Universiti Malaya 50603 Kuala Lumpur, Malaysia

*Corresponding author: ngai.ks@physics.org, rameshtsubra@gmail.com

Abstract

An electric double-layer capacitor (EDLC) is an energy storage device that stores electrical energy through the electrostatic separation of charges by forming a double layer of positive and negative charges between the interface of an electrode and an electrolyte. EDLCs are important due to their unique combination of high power density and long life cycle. The property to provide rapid charge and discharge capability making EDLCs essential in modern electrical and electronic applications. Polymer electrolyte is a crucial component in EDLC by enhancing their performance, safety, and versatility. Characterization of a polymer electrolyte in relation to the properties of the EDLC involves the evaluation of several key parameters such as ionic conductivity, electrochemical stability window, thermal stability and structural analysis. A lithium perchlorate (LiClO₄) based polymer electrolyte offers a highest ionic conductivity of 10⁻⁶ S cm⁻¹ was examined using an electrochemical impedance spectroscopy. The high ionic conductivity enables fast ion transport between the electrodes, allowing the rapid charge and discharge processes of the capacitor. A wider electrochemical stability window which allows the material to operate over a wide range of voltage. This characteristic also allows the capacitor achieving higher energy density and to operate at higher voltages. LiClO₄ based polymer electrolyte demonstrates a stable thermal profile via thermogravimetric analysis in which a total weight loss of 77.5% is measured. XRD analysis reveals that orderly arrangement of the polymer chain is disrupted by the addition of LiClO₄. The increase in amorphous nature of the polymer electrolyte can trigger the ionic hopping mechanism which further enhance the ionic conductivity. Evidently, the LiClO₄ based polymer electrolyte meeting the requirements of EDLC and potential to be used in development of advanced energy storage devices.

Keywords: Ionic conductivity, polymer electrolyte, lithium perchlorate, electric double layer capacitor

References

1. Sangwan, B.; Mathela, S.; Dhapola, P. S.; Singh, P. K.; Tomar, R. *Mater. Today Proc.* 2022, 49, 3306-3309.
2. Gairola, Y.; Rajput, K.; Tomar, R.; Kumar, S.; Konwar, S.; Aldbea, F. W.; Yadav, T.; Yahya, M. Z. A.; Singh, P. K. *Energy Storage*, 2024, 6, e614.
3. Mohammed, M. I.; Bouzidi, A.; Zahran, H. Y.; Jalalah, M.; Harraz, F. A.; Yahia, I. S. *J. Mater. Sci: Mater. Electron.* 2021, 32, 4416-4436.

Evaluation of an Electrochromic Device consisting of a Molten Viologen Polymer and Ferrocene Ionic Liquid

Hiroto Murakami*, Hironobu Tahara,

Institute of Integrated Science and Technology, Nagasaki University, Japan

*Corresponding author: hiroto@nagasaki-u.ac.jp

Abstract

Poly(ionic liquid) (PIL) is an ionic polymer synthesized from monomers with ionic liquid moieties. Unlike conventional ionic polymers, it exhibits solubility or compatibility with various substances like an ionic liquid, and has mechanical and thermal properties like a polymer. Recently, we have synthesized a viologen-based PIL (VPIL(TFSI), Figure 1) that possesses redox activity and shows electrochromism. In this presentation, we will describe the fabrication of an electrochromic (EC) device using a VPIL and its coloring behavior.

VPIL(TFSI) was synthesized by radical polymerization of alkyl viologen bearing styrene at one end. After removing unreacted monomers by dialysis, ion exchange was performed to obtain VPIL(TFSI), which is viscous at room temperature. A ferrocene-based ionic liquid ([FcC₆ImC₁][TFSI]) [1] was employed as the anode material to drive the EC device. An EC device was fabricated by mixing the viologen unit of VPIL(TFSI) and [FcC₆ImC₁][TFSI] at a molar ratio of 1:1, and sandwiching this mixture between two ITO substrates.

Figure 2 shows the differential absorption spectra when a voltage of 1.2 V was applied to the fabricated EC device. As voltage was applied, absorption bands at 530 nm and 890 nm attributed to the reduced form (dimer) of viologen appeared, and their absorbance increased with time. The time required for the absorbance of the band to become constant was approximately 1000 s, which was much longer than the time of 80 s we previously reported [1]. This is because the viscosity of VPIL(TFSI) is very high. The 90% bleaching time of the 530 nm absorption band during short circuit was 1500 s. Although the response speed was slower by using VPIL(TFSI), it was found that the coloring time was longer. Analysis of the coloring speed and efficiency of this EC device will also be presented.

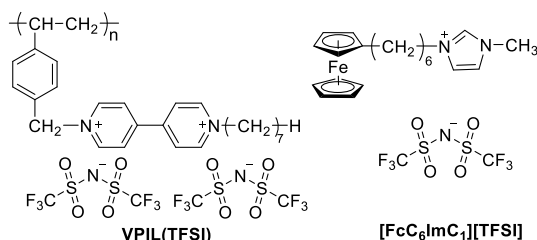


Figure 1. Chemical structures of VPIL(TFSI) and [FcC₆ImC₁][TFSI].

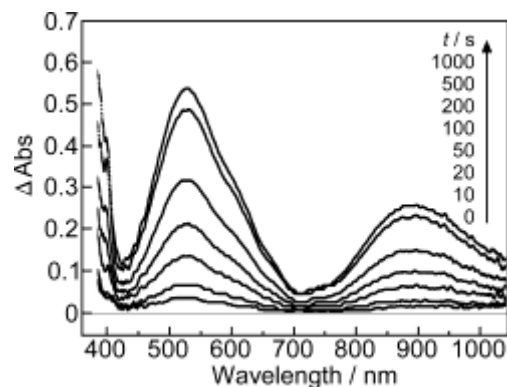


Figure 2. Differential absorption spectra of the EC device consisting of VPIL(TFSI) and [FcC₆ImC₁][TFSI]. Applied voltage: 1.2 V.

Keywords: Electrochromism, Ionic Liquid, Viologen-based Polymer, Ferrocene-based Ionic Liquid

References

1. Tahara, H.; Uranaka, K.; Hirano, M.; Ikeda, T.; Sagara, T.; Murakami, H. *ACS Appl. Mater. Interfaces*, 2019, 11, 1-6

Preparation of Polysilsesquioxane-based CO₂ Separation Membranes with Thermally Degradable Units

Joji Ohshita^{a,b}

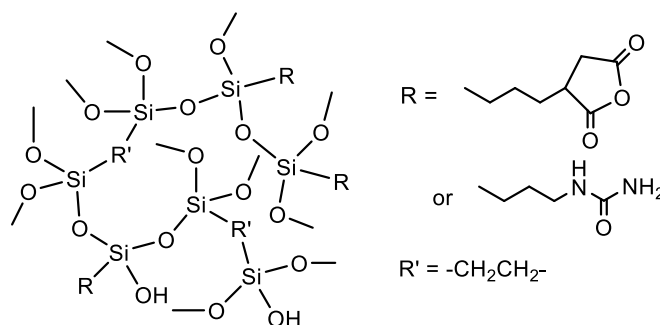
^aSmart Innovation Program, Graduate School of Advanced Science and Engineering, Hiroshima University, Higashi-Hiroshima 739-8527, Japan.

^bDivision of Materials Model-Based Research, Digital Monozukuri (Manufacturing) Education and Research Center, Hiroshima University, Higashi-Hiroshima 739-0046, Japan.
jo@hiroshima-u.ac.jp

Abstract

CO₂ separation by membranes have attracted recent attention as a simple CO₂ recovery process and many types of CO₂ separation membranes have been developed. Of those, polysilsesquioxane (PSQ)-based membranes have been extensively studied as typical organic–inorganic hybrid membranes, which possess such characteristics as high processability and durability arising from those of organic and inorganic materials. Recently, we prepared PSQ membranes containing amine, urea, and isocyanurate groups as CO₂-philic units and found that an isocyanurate-containing membrane showed high performance (CO₂ permeance = 3.2×10^{-7} mol m⁻²s⁻¹Pa⁻¹, CO₂/N₂ = 18). However, there is a trade-off relationship between CO₂ permeance and selectivity, two important parameters of CO₂ separation performance and simultaneous improvement of both the parameters is essentially difficult.¹

To develop a new methodology to improve the performance of PSQ-based CO₂ separation membranes, we prepared PSQ precursors that possessed thermally degradable succinic anhydride and monoalkylurea units, expecting that the degradation of the organic units would permit the fine tuning of PSQ network structures to improve CO₂ permeance by the controlled formation of void spaces. In fact, the succinic anhydride and monoalkylurea units were thermally converted into ester and dialkyl urea units by heating the membranes, respectively, with the liberation of CO₂ molecules to improve the CO₂ permeance.²



Keywords: CO₂ separation, polysilsesquioxane, membrane

Reference

1. Kajimura, K.; Horata, K.; Adachi, Y.; Kanezashi, M.; Tsuru, T.; Ohshita, J. *J. Sol-Gel Sci. Technol.* **2023**, *106*, 149-157
2. Horata, K.; Yoshio, T.; Miyazaki, R.; Adachi, Y.; Kanezashi, M.; Tsuru, T.; Ohshita, J. *Separations* **2024**, *11*, 110.

Control of marine biodegradation of poly(ethylene succinate) using endospores

Miwa Suzuki ^{a*}, Yuya Tachibana ^{a b}, Phouvilay Soulethone ^b, Tomoya Suzuki ^b,
Hiroyuki Takeno ^{a b}, Ken-ichi Kasuya ^{a b}

^a Gunma University Center for Food Science and Wellness.

^b Division of Molecular Science, Graduate School of Science and Technology, Gunma University.

*Corresponding author: miwasuzuki@gunma-u.ac.jp

Abstract

Chemosynthetically biodegradable plastics are not well controlled in terms of the rate and timing of biodegradation. To overcome these challenges, we propose a new system that encapsulates endospores of degrading bacteria into plastics with typically slow biodegradation rates. Endospores of bacterial strain YKCMOAS1 germinated and initiated biodegradation when triggered by surface wear of an aliphatic biodegradable polyester, poly(ethylene succinate) (PESu). The weight loss rate of endospore-containing PESu film immersed in seawater was approximately 7-fold faster than that of PESu film without endospores. The YKCMOAS1 strain used in this study grew in seawater and showed PESu film-degrading activity in a marine mineral medium. Based on the weight loss rate of the endospore-containing PESu films, they were estimated to have completely degraded into water-soluble compounds within approximately 400 d. Furthermore, the biochemical oxygen demand degradation test revealed that the water-soluble products from PESu, produced by the vegetative cells, were completely biodegraded within 10 d. Taken together, these results indicate that material hydrolysis by bacterial strain YKCMOAS1 was triggered by material wear, followed by rapid biodegradation. This is the first report of the application of bioaugmentation to the stable expression of environmental degradation of biodegradable plastics. These results might provide insight into the design concept of novel biodegradable plastics that not only exhibit environmentally independent biodegradation, but also allow control of the onset time.

Keywords: Marine biodegradation, Endospore, *Bacillus*, Poly(ethylene succinate) (PESu), Biodegradable polymer



References

1. Suzuki, M.; Tachibana, Y.; Soulethone, P.; Suzuki, T.; Takeno, H.; Kasuya, K. *Polym. Degrad. Stab.* 2023, 215, 110466

Ferroelectric Semiconductor: Alkylamide-substituted BTBT

Tomoyuki Akutagawa* and Kohei Sambe

Institute of Multidisciplinary Research for Advanced Materials,
Tohoku University, Katahira 2-1-1, Aoba-ku, Sendai 980-8577, Japan.

*Corresponding author: akutagawa@tohoku.ac.jp

Abstract

BTBT derivatives are organic semiconductors known to exhibit high hole mobility due to the formation of two-dimensional electronic structures. In this presentation, we report on the phase transition behavior, molecular assembly structures, semiconductor properties, and ferroelectric properties of alkylamide-substituted organic ferroelectrics, R-BTBT-NHCOC₁₄H₂₉ (**1**: R = H, **2**: R = C₈H₁₇) (Fig. 1a).^{1, 2} The temperature- and frequency-dependent dielectric constants of **1** and **2** show the transition to SmE and SmC phases at 412 and 431 K, respectively, and melting at 468 and 479 K. The real part of the dielectric constant of **2** decreases monotonically with increasing temperature and shows a sharp frequency-dependent increase in dielectric constant from around 390 K. The dielectric constant of **1** is also affected by the temperature and frequency. This behavior is due to the activation of thermal motion of polar amide groups; both *P*-*E* curves of **1** and **2** show the hysteresis behavior of ferroelectrics near the solid-liquid crystal phase transition point, and the remanent polarization values and coercive electric field at 418 K and 0.1 Hz in **2** are 11.7 μC cm⁻² and *E*_c = 3.36 V μm⁻¹, respectively (Fig. 1b). Top-contact OFET devices were fabricated using the high-temperature deposited thin films **1** and **2**, and both showed p-type semiconducting output characteristics (Fig. 1c). The mobility of the deposited film **2** was 1.01 × 10⁻³ cm² V⁻¹ s⁻¹.

Keywords: ferroelectrics, organic semiconductor, hydrogen bond, switching, BTBT

References

1. Sambe, K.; Akutagawa, T., et al, *ACS. Appl. Mater. Inter.*, 2023, 15, 58711.
2. Sambe, K.; Akutagawa, T. et al, *J. Am. Chem. Soc.* 2024, 146, 8557.

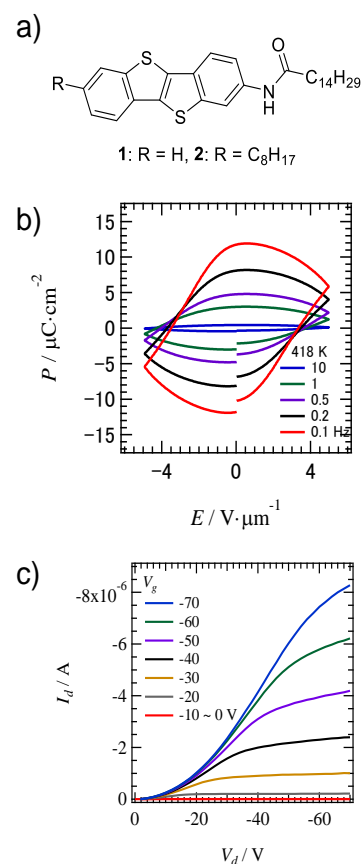


Fig. 1. Alkylamide-substituted BTBT derivatives **1** and **2**. a) Molecular structure, b) ferroelectric properties, and c) semiconductor properties.

Anhydrous Proton Conduction in Crystalline Molecular Assemblies Based on Molecular Internal Degrees of Freedom

Shun Dekura^{a,b,c,*}

^aThe Institute for Solid State Physics, The University of Tokyo, Japan

^bGraduate School of Engineering, Tohoku University, Japan

^cInstitute of Multidisciplinary Research for Advanced Materials (IMRAM), Tohoku University, Japan

*Corresponding author: s.dekura@tohoku.ac.jp

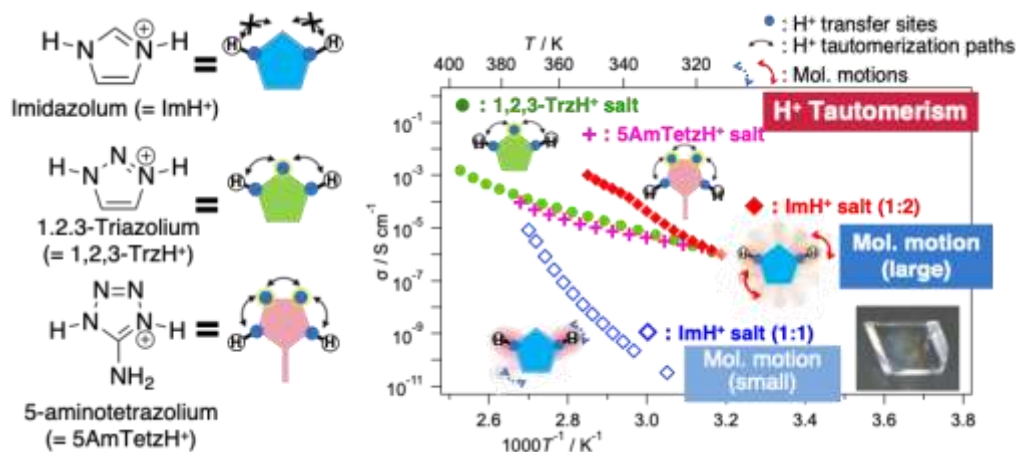
Abstract

Anhydrous organic proton (H^+) conductors have attracted much attention as candidates for next-generation solid electrolytes in fuel cells operating in the medium temperatures above 100 °C without humidification. However, mechanism of anhydrous H^+ conduction has not been fully revealed yet because most of the previously reported anhydrous super- H^+ conductors ($\sigma > 10^{-4}$ S/cm) were acid- or base-doped polymers or microporous materials. To approach this problem, we have focused on single-crystalline molecular materials, which are suitable to investigate conduction mechanisms to establish the materials design guideline. For the first step, based on the comprehensive study on a series of imidazolium hydrogen dicarboxylates, we disclosed that the anhydrous H^+ conduction mechanism can be discussed based on Grotthuss-type picture; high anhydrous H^+ conductivity can be achieved by (1) construction of the extended H-bond network (for H^+ conduction pathway), (2) the small intermolecular pK_a differences, i.e. ΔpK_a (for inter-molecular H^+ transfer), and (3) the molecular rotational motions in crystals (for intra-molecular H^+ transfer).¹⁻³

In this study, we focused on (3) the molecular rotational motions, and realized anhydrous super- H^+ conductors utilizing molecular motions in crystals.⁴ In addition, we successfully developed new H^+ conduction mechanism, H^+ tautomerism, which is advantageous for systematically realizing low-barrier H^+ conduction. In summary, utilization of such molecular internal degrees of freedom is good strategy for the development of anhydrous super- H^+ conducting molecular crystals.

Keywords: molecular solids, anhydrous proton conduction, molecular dynamics, proton tautomerism

Graphical abstract



References

1. Sunairi, Y.; Ueda, A.; Yoshida, J.; Suzuki, K.; Mori, H. *J. Phys. Chem. C* **2018**, *122*, 11623–11632.
2. Sunairi, Y.; Dekura, S.; Ueda, A.; Ida, T.; Mizuno, M.; Mori, H. *J. Phys. Soc. Jpn.* **2020**, *89*, 051008.
3. Hori, Y.; Dekura, S.; Sunairi, Y.; Ida, T.; Mizuno, M.; Mori, H.; Shigeta, Y. *J. Phys. Chem. Lett.* **2021**, *12*, 5390–5394.
4. Dekura, S.; Mizuno, M.; Mori, H. *Angew. Chem. Int. Ed.* **2022**, *61*, e202212872.

Development of metal-like lustrous films using oligo(3 alkoxysephenone)

Satoru Tsukada

Department of Materials Science, Graduate School of Engineering, Chiba University,
Japantsukada@chiba-u.jp

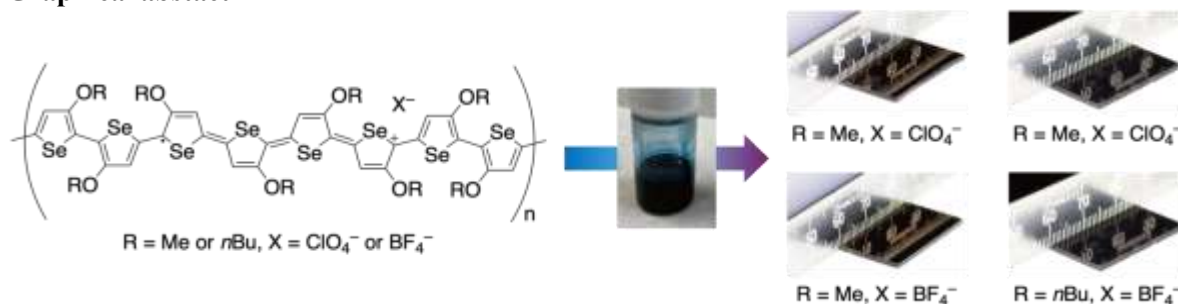
Abstract

Metallic luster or metallic colors, deeply rooted in society, culture, and religion, often symbolize luxury and nobility. Conventional metal-like luster paints comprise metal effect pigments, namely fine powders of flaky aluminum or zinc dispersed in a binder resin solution containing colorant. However, using metal flakes has certain limitations, including susceptibility to corrosion, color migration, increased paint weight, and electromagnetic shielding. Additionally, metal flakes often pollute the environment. Under this background, metal-free organic solids that exhibit metal-like lusters have been discovered. These organic materials have attracted considerable attention because they have the potential to solve various issues associated with paints that contain metal flake pigments.

We have developed a gold-like luster film based on oligo(3-methoxythiophene) obtained *via* chemical polymerization of 3-methoxythiophene.¹⁻⁹⁾ We also synthesized oligo(3-alkoxythiophene) with linear or branched chains and investigated the effect of substituent structure on film properties. Depending on the slight difference in the substituents, we obtained metallic glossy films with different color tones.¹⁰⁾ So far, we have studied only thiophene derivatives. We thought that heterocyclic compounds containing other elements could be used to fabricate metallic glossy films with properties different from those of thiophene derivatives. In this study, we focused on selenophene, a high-period analog of thiophene. Selenophene has a smaller HOMO-LUMO gap than thiophene, and polymers containing selenophene have been studied as electronic materials. Compared to polythiophene, polyselenophene has a rigid main chain backbone because of its stronger quinoid properties. In addition, selenium atom has an electronegativity comparable to carbon atom, a larger atomic radius, and higher polarizability than sulfur atoms, resulting in a larger atomic refractive index. These properties of (poly)selenophene resulted in a glossy film different from that of polythiophene.¹¹⁾

Keywords: Metal-like luster, Alkoxysephenone, Oligomer, Oligo selenophene, Coating film

Graphical abstract



References

- 1) Tagawa, R.; Masu, H.; Itoh, T.; Hoshino, K. *RSC Adv.* **2014**, *4*, 24053-24058.
- 2) Takashina, Y.; Mitogawa, T.; Saito, K.; Hoshino, K. *Langmuir* **2018**, *34*, 3049-3057.
- 3) Takashina, Y.; Hoshino, K. *Polym. J.* **2019**, *51*, 591-599.
- 4) Tachiki, M.; Tagawa, R.; Hoshino, K. *ACS Omega* **2020**, *5*, 24379-24388.
- 5) Kubo, M.; Doi, H.; Saito, R.; Horikoshi, K.; Tsukada, S.; Hoshino, K. *Polym. J.* **2021**, *53*, 1019-1029.
- 6) Kubo, M.; Tachiki, M.; Mitogawa, T.; Saito, K.; Saito, R.; Tsukada, S.; Hoshino, K. *Coatings* **2021**, *11*, 861.
- 7) Tachiki, M.; Tsukada, S.; Hoshino, K. *Dyes Pigm.* **2021**, *190*, 109302.
- 8) Tamura, R.; Miyamoto, K.; Tsukada, S.; Hoshino, K. *Mater. Adv.* **2022**, *3*, 3428-3437.
- 9) Sugiura, S.; Mitogawa, T.; Saito, R.; Tamura, R.; Tsukada, S.; Horiuchi, T.; Hoshino, K. *RSC Adv.* **2022**, *12*, 19965-19973.
- 10) Tsukada, S.; Saito, R.; Hoshino, K. *ACS Appl. Opt. Mater.* **2023**, *1*, 1847-1855.
- 11) Tsukada, S.; Doi, M.; Hoshino, K. *ACS Appl. Opt. Mater.* **2024**, Submitted.

Investigation of flotation behaviour of lepidolite using a novel mixed collector in terms of adsorption mechanism**B. Khandjamts¹, G. Margad-Erden¹, E. Otgonjargal^{1*}**¹ Mongolian Academy of Sciences, Institute of Chemistry and Chemical Technology, Ulaanbaatar 1330, Mongolia

* Correspondence: otgonjargale@mas.ac.mn; Tel.: +97699072135; khandaa_b@mas.ac.mn; Tel.: +97686076676

Abstract:

In the current century, the demand and supply of lithium are experiencing a significant boost. In the realm of lithium mining, Lepidolite plays a crucial role as one of the primary resources, alongside Spodumene. To effectively extract lithium, the concentration of Lepidolite is often achieved through flotation, a process that allows for the separation and concentration of this valuable mineral. However, the main collector of lithium ore is a monomeric surfactant with only one hydrophobic group and one hydrophilic group, which usually has low flotation separation efficiency. Therefore, in order to achieve better results in the flotation separation of lepidolite ore, in this work, amine-based combined surfactants, SDS+NaOL+ODA 3:1, HBDB+DDA 1:1, IM11+SDS 1:1 were combined and compared with the conventional single molecule collector BSA.

According to the test results, when the pH of flotation is pH 11.3, SDS+NaOL+ODA 3:1 and IM11+SDS 1:1 mixture of lepidolite ore enriched the pure lithium content to 4.9%. The results of zeta potential determined that the washed surface is more adsorbed than the main surface of lithium ore. It was observed that the SDS+NaOL+ODA and IM11+SDS combination reagents are more suitable for the main surface of lithium and are more adsorbed on the surface of lepidolite. The economic assessment of lepidolite and spodumene ores show that the use of a combination of SDS +IM11 can be more profitable than the use of the main single molecule BSA. Accordingly, this study describes a novel, high-efficiency collector mining mechanism for flotation beneficiation of lepidolite ore.

Keywords: Lepidolite, Spodumene, Mixed Collectors, Clay Minerals, Flotation, Adsorption**References**

1. Zhiqiang Huang,* Shiyong Zhang, Chen Cheng, Hongling Wang, Rukuan Liu, Yajing Hu, Guichun He, ACS Sustainable Chem. Eng. 2020, 8, 18206–18214.
2. Kemu Liu Kemu Liu (02 Aug 2023): Research Progress in Flotation Collectors for Lepidolite Mineral: An Overview, Mineral Processing and Extractive Metallurgy Review, DOI: 10.1080/08827508.2023.2243012.
3. Z. Huang, S. Shuai, H. Wang, R. Liu, S. Zhang, C. Cheng, Y. Hu, X. Yu, G. He, W. Fu, Froth flotation separation of lepidolite ore using a new Gemini surfactant as the flotation collector, Separation and Purification Technology (2021), doi: <https://doi.org/10.1016/j.seppur.2021.119122>

Photo-solubilization of Tunable Terpolyamides from Renewable Itaconic Acids

Mohammad Asif Ali^{1,2}, Maiko Okajima^{1,2}, Tatsuo Kaneko^{1,2*}

1 School of Chemical and Material Engineering, Jiangnan University

2 Graduate School of Advanced Science and Technology, JAIST

**Corresponding author: *tkaneko@jiangnan.edu.cn; asifali@jiangnan.edu.cn*

Abstract

The use of renewable biomass for conventional biopolyamides suffers from low thermal and mechanical performances. Conventional nylons such as polyamide 11 have diverse applications and are produced from renewable feedstocks with inferior mechanical properties due to a lack of rigid components [1]. The potential use of bioavailable itaconic acid (IA) derived from *Aspergillus terreus*, is in utilizing their functionalities that could make them a bridge between conventional polyamide 11 and Kevlar™. Here we report an approach to preparing sustainable ultra-strong N-substituted heterocyclic polyamide fibers from biomass-derived IA through an aza-Michael addition reaction with aliphatic diamines 1,9-nonanediamine and/or 2-methyl-1,8-octanediamine (NMDA/ MODA). Polyamides with molecular weights ranging over 52500 showed T_g values 51-65 °C, which were higher than conventional polyamides 11 (around 47 °C). The Young's modulus and mechanical strength of these polyamides ranged 49-104 MPa and 2.9-4.6 GPa, respectively. However, their processability were required to enhance by incorporation of an appropriate amount of terephthalic acid and the resulting copolymers showed T_{d10} values over 415 °C and Young's moduli ranging of 3.4–6.2 GPa. Besides, the copolymers became soluble in water and sea water under ultraviolet irradiation, which led to environmental corrosion. Other reasons associated with the photohydrophilization of polymer structure under ultraviolet irradiation in water, sea, and artificial sea salt water are associated with the ring opening of the pyrrolidone ring and expected to be disposed of at the end of their service life [2]

Keywords: Itaconic acid, Michael addition, BioNylons, Biodegradable plastics.

References

1. M. Ali, et al. Syntheses of High-Performance Biopolyamides Derived from Itaconic Acid and Their Environmental Corrosion. *Macromolecules*, 2013, 46: 3719-3725;
2. M. Ali, et al. High-performance BioNylons from Itaconic and Amino Acids with Pepsin Degradability. *Adv. Sus. Sys.* 2022, 6: 2270005.

Photosynthesis-Inspired Fiber-Optic Monitoring Network for Sustainable Civil Design

Rei Furukawa^{a,*}, Takafumi Sassa^b, and Nobuko Fukuda^c

^aThe University of Electro-Communications

^bInstitute of Physical and Chemical Research (RIKEN)

^cOkayama University

*Corresponding author: furukawa@ee.uec.ac.jp

Abstract

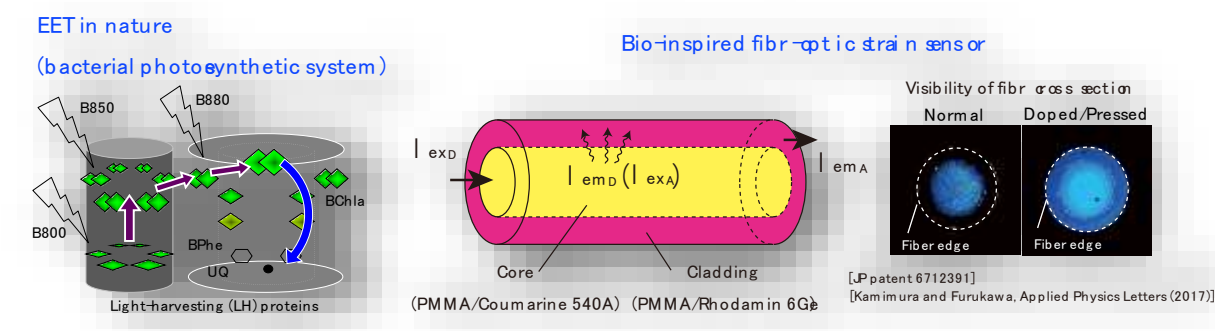
The efficiency and sophistication of excitation energy transfer (EET) that occurs in the surface membrane of purple bacteria has fascinated biochemists and physicists over years. Although the EET process involves only one dye, bacteriochlorophyll a, different configurations of bacteriochlorophyll a can absorb slightly different wavelengths. The resulting energy gradient across each pigment allows energy to flow to the reaction center.

The polymer optical fiber sensor presented here mimics natural EET by mimicking the cladding and core as two pigments through which energy flows in sequence[1,2]. Poly(methyl methacrylate) was used as the host, and the cladding and core were doped with Rhodamine 6G and Coumarin 540A, respectively. Rhodamine 6G and Coumarin 540A are specifically related synthetic dyes, with the emission of Rhodamine 6G matching closely with the absorption of Coumarin 540A. Plastic optical fibers are highly bendable, and deformation of the fiber causes light leakage from the core to the cladding, exciting the Coumarin 540A in the core. This mechanism makes it possible to monitor deformations in structures such as buildings and tunnels through a simple color change in the output cross-section of the fiber[3,4].

Worked with tunnel excavator, organic waveguide was developed towards specialized monitoring system which can detect alert during excavation. In addition, we developed an elastomer waveguide that achieves high elasticity[5].

Keywords: plastic optical fiber, light-harvesting pigments, excitation-energy transfer, fiber-optic strain sensing

Graphical abstract



References

1. S. Yajima, R. A. Furukawa, M. Nagata, S. Sakai, M. Kondo, K. Iida, T. Dewa, and M. Nango, *Appl. Phys. Lett.* 100, 233701 (2012)
2. R. Furukawa, M. Kondo, S. Yajima, and K. Harada, K.V.P. Nagashima, M. Nagata, K. Iida, T. Dewa, M. Nango, *MRS Communications* 8, 1124–1128 (2018)
3. Japanese patent # 6712391
4. S. Kamimura and R. Furukawa, *Applied Physics Letters* 111, 063301 (2017)
5. C. Hirose, N. Fukuda, T. Sassa, K. Ishibashi, T. Ochiai, and R. Furukawa, *Fibers*, 7, 37 (2019)

Dielectric Behavior of Plastic Crystal Based on Rod-shape Sulfonamide Derivatives

C. Sato,^{1*} S. Dekura,^{1,2} T. Sato,^{1,2} T. Takeda,³ T. Akutagawa.^{1,2}

^a Graduate School of Engineering, Tohoku University.

^b Institute of Multidisciplinary Research for Advanced Materials, Tohoku University.

^c Faculty of Science, Shinshu University.

*chisato.sato.s2@dc.tohoku.ac.jp

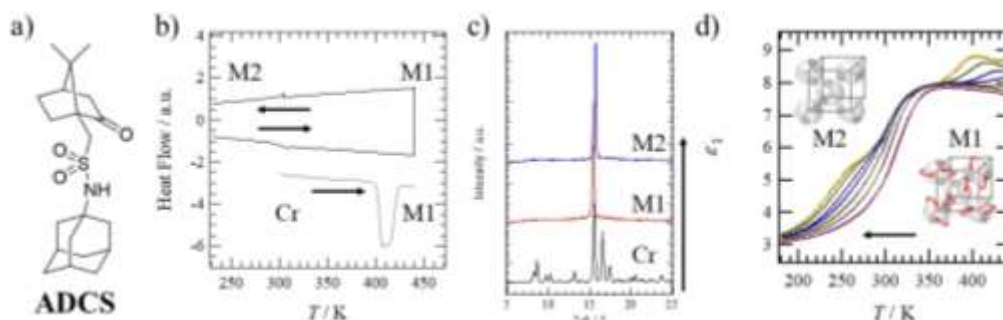
Abstract

Plastic crystalline phase is a mesophase between the solid and liquid phases, where molecules exhibit rotational motion while maintaining the crystal lattice. The use of globular molecules has been considered the major requirement for realization of plastic crystalline phase.¹ On the other hand, chemically connecting two different globular molecules may lead to unprecedented phase behavior and molecular dynamics. In this work, we synthesized a dual-rotator type molecule of *N*-adamantyl camphor sulfonamide (ADCS), where globular adamantane (AD) and chiral camphor (CS) were connected (Fig. 1a).²

The phase behavior of ADCS was evaluated using DSC, PXRD, and polarized optical microscopy (POM) images. The as-grown crystals of ADCS showed a phase transition from the crystal phase (Cr) to the solid-like mesophase (M1) around 400 K with transition entropy of $\Delta S = 61.6 \text{ J mol}^{-1} \text{ K}^{-1}$ (Fig. 1b). Upon cooling and re-heating process, a change in the DSC baseline was observed at ca. 300 K, leading to a glass-like M2 phase. The Cr phase showed many sharp diffraction peaks with a bright-field POM image (Fig. 1c). However, the disappearance of the birefringence in POM image and almost all the diffraction peaks except for only two peaks at ca. $2\theta = 15.5, 22.0^\circ$ were observed in M1 phase. Considering the *d*-spacing estimated from 2θ and the molecular length, the peaks were attributed to the 200 and 220 reflections of fcc structure, respectively. This structure and optically isotropic state were maintained in M2 phase.

The molecular dynamics were evaluated based on the temperature (*T*)- and frequency (*f*)-dependent real part of dielectric constants (ϵ_1) (Fig. 1d). During cooling ADCS from the M1 phase, a *f*-dependent broad peak was observed around 400–450 K, suggesting slow dipole dynamics in the molecular assemblies. Upon further cooling, the ϵ_1 value showed *T*/*f*-independent value down to ca. 330–273 K. This temperature range corresponds to the M1–M2 phase transition observed at ca. 300 K in DSC, indicating this transition involves freezing of the dynamics of polar molecule. In summary, the M1 and M2 phases are expected to be plastic crystalline and orientational glass phases, respectively.

Figure 1. a) Molecular structure, b) DSC chart, c) PXRD pattern and d) *T*- and *f*- dependent ϵ_1 behavior of ADCS.



Keywords: Camphor, Adamantane, Sulfonamide, Plastic Crystal, Molecular Dynamics

References

1. Das, S., Mondal, A., Reddy, C. M. *Chem. Soc. Rev.*, **49**, 8878 (2020).
2. Sato, C., et al., *Cryst. Growth Des.*, **23**, 5889 (2023).

Synthesis and Response Surface Method Based Optimization of Double-Network Hydrogel-Biochar Composites for Enhanced Water Absorption

Cindy Soo Yun Tan^{a*}, Dzureen Julaihi^a, Mohamad Izzat Arif Nordin^a, Nur Ellydia Mohamad Gustie Noorambia^a, Kaviraja Pandian Sambasevan^b, Suk-Fun Chin^c, Su Shiung Lam^d, Peter Nai Yuh Yek^e, Nazrizawati Ahmad Tajuddin^f, Margaret Abat^g

^aFaculty of Applied Sciences, Universiti Teknologi MARA, Cawangan Sarawak, 94300 Kota Samarahan, Sarawak, Malaysia.

^bAdvanced Materials for Environmental Remediation (AMER), Faculty of Applied Sciences, Universiti Teknologi MARA, Cawangan Negeri Sembilan, Kampus Kuala Pilah, 72000 Kuala Pilah, Negeri Sembilan, Malaysia.

^cFaculty of Resource Science and Technology, Universiti Malaysia Sarawak, 94300 Kota Samarahan, Sarawak, Malaysia.

^dHigher Institution Centre of Excellence (HiCoE), Institute of Tropical Aquaculture and Fisheries (AKUATROP), Universiti Malaysia Terengganu, 21030 Kuala Nerus, Terengganu, Malaysia.

^eCentre for Research of Innovation and Sustainable Development, University of Technology Sarawak, No.1, Jalan Universiti, Sarawak, Sib, 96000, Malaysia.

^fSchool of Chemistry & Environment, Faculty of Applied Sciences, Universiti Teknologi MARA, 40450 Shah Alam, Selangor, Malaysia.

^gAgriculture Research Centre Semonggok, P.O Box 977, 93720 Kuching, Sarawak.

*Corresponding author: cindytan@uitm.edu.my

Abstract

Water shortages for irrigated agriculture have become a serious concern, especially in arid and semi-arid regions. Moreover, agricultural sector is driven by the urgent need to address global challenges, including resource scarcity, environmental contamination and climate change. Beyond their traditional biological applications, superabsorbent hydrogels have emerged as appealing materials in addressing water scarcity, soil degradation and efficient nutrient delivery in modern agriculture. Superabsorbent double network hydrogel-biochar composites (DNHBC) based on potassium poly(acrylate-co-acrylamide) and poly(vinyl alcohol) (PVA) were fabricated as superabsorbent *N*-urea controlled release fertilizer (CRF) in a two-step reaction: free-radical random copolymerization and cyclic freeze-thaw. Response surface methodology integrated central composite design (RSM-CCD) was employed to evaluate the interactions of independent hydrogel composition parameters (methylene bisacrylamide (MBA) crosslinker, PVA and biochar (BC) concentrations) and derive a model to predict the hydrogel composition optimization for enhanced water absorption. Different DNHBC compositions showed deionized (DI) water absorption ranging between 44 – 480 g/g. Although the highest DI water absorption was recorded for DNHBC-R18 and DNHBC-R6 compositions, the structural fragility of swollen DNHBC-R18 and DNHBC-R6 make them less favourable as multi-functional CRFs. In contrast, DNHBC-R1 and DNHBC-R7 compositions exhibited superior structural integrity in swollen state and excellent DI water absorption (309 – 330 g/g), which are recommended as water reservoir and CRF for agricultural applications. From the equilibrium water absorption capacity studies of DNHBC in 0.9% NaCl solution and tap water, the DNHBC showed salt-solution-dependent swelling behaviour.

Keywords: Double-network, hydrogel, biochar, composite, synthesis, response surface method, water absorption

Cofacial Porphyrin Dimers Generated by Cooperative Ion Binding

Joe Otsuki^{a,*}

^aCollege of Science and Technology, Nihon University, Japan

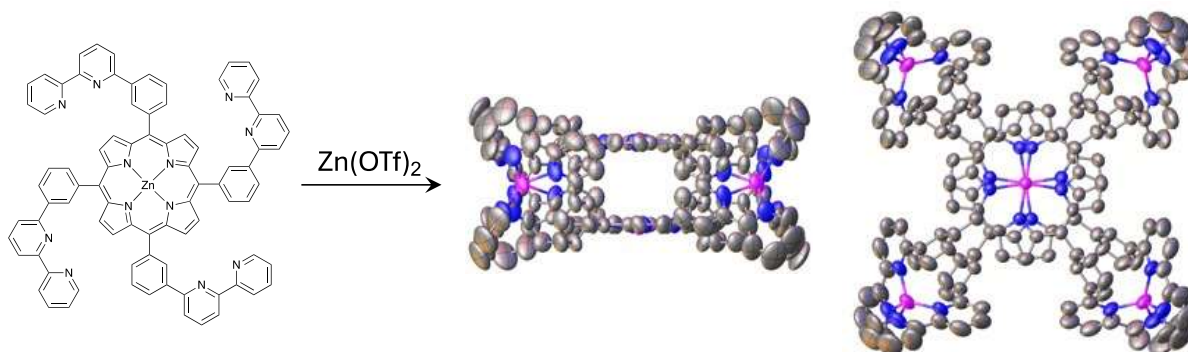
*Corresponding author: otsuki.joe@nihon-u.ac.jp

Abstract

Porphyrin assemblies have attracted the attention of chemists due to their potential applications as host compounds, sensors, catalysts, and molecular-scale devices, in which multiple porphyrin molecules play synergistic roles.¹ In this study, we introduce novel coordination-directed cofacial porphyrin dimers from *meso*-tetraphenylporphyrin derivatives modified with pyridine-based chelating moieties at the meta positions on the phenyl groups. For the derivative featuring 2,2'-bipyridine as the chelating sites, spectroscopic investigation has shed light on the binding processes of added metal ions and the structure of the resulting dimer in solution.² Initial Zn²⁺ ion binding to the porphyrin hinders the subsequent Zn²⁺ binding and the binding of the second porphyrin. However, once the dimer is formed, additional Zn²⁺ binding is notably enhanced, resulting in a pronounced S-shaped binding curve. The detailed structure of the dimer in solution was established based on UV-vis spectroscopy, various ¹H NMR spectroscopy techniques, and mass spectrometry. Simulations of ring-current-induced chemical shift changes provided evidence for the face-to-face porphyrin structure with tetrahedral coordination of the bipyridine ligands. The single crystal X-ray structure provided conclusive evidence for the structure of the face-to-face dimer, which remarkably resembles the model structure, which was deduced based on the ¹H NMR simulation. The stability of the dimer structure makes it promising for further exploration of this motif in developing new supramolecular structures and for their potential applications as host compounds and catalysts.

Keywords: coordination, cooperativity, face-to-face dimer, porphyrin, self-assembly

Graphical abstract (Optional)



References

1. Otsuki, J. *J. Mater. Chem. A* 2018, 6, 6710-6753.
2. Otsuki, J.; Sato, K.; K. Sugawa *Eur. J. Inorg. Chem.* in press.

Amino Acid-Functionalized Polyacrylamides: Evaluation of Protein Cleavage Activity

Takahiko Matsushita^{a,b,c}, Hinako Yamochi^a, Shinzo Omiya^a, Tetsuo Koyama^a, Ken Hatano^{a,b,c}, Koji Matsuoka^{a,b,c,*}

^aDivision of Material Science, Graduate School of Science & Engineering,

^bAdvanced Institute of Innovative Technology (AIIT),

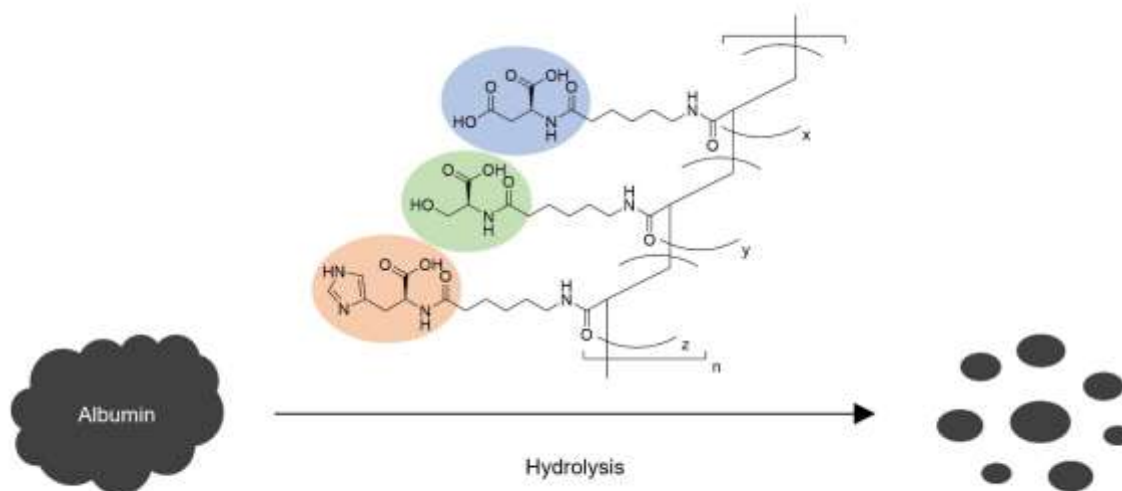
^cHealth Sciences and Technology Research Area, Strategic Research Center, Saitama University, Sakura, Saitama 338-8570, Japan.

*Corresponding author: koji@fms.saitama-u.ac.jp

Abstract

Research on artificial enzymes is a crucial field contributing to the realization of sustainable chemical processes. Our study focuses on the potential of amino acid-incorporated polymers to exhibit protein cleavage activity.¹⁾ Various compositions of polyacrylamides, including the catalytic triad of the natural serine protease chymotrypsin (serine, aspartic acid, histidine), were synthesized and investigated for their protein cleavage activity. SDS-PAGE analysis confirmed the cleavage activity of some synthesized ternary copolymers against bovine and human serum albumins. Furthermore, polyacrylamides incorporating a single type of amino acid also showed the ability to cleave protein substrates, exhibiting unique cleavage profiles and pH and temperature sensitivities distinct from α -chymotrypsin. These findings suggest the potential of amino acid-functionalized polymers as proteolytic artificial enzymes.

Keywords: Protease, Serine protease, Artificial enzyme, Polyacrylamide, Albumin, Radical polymerization



References

1. T. Matsushita, H. Yamochi, S. Omiya, T. Koyama, K. Hatano, and K. Matsuoka, *Bioorg. Med. Chem.* **92**, #117422, 2023.

Battery Performances of Organic Materials with One-dimensional Columnar Structures as Cathodes

Hirofumi Yoshikawa*

Department of Materials Science, Kwansei Gakuin University, Japan

*Corresponding author: yoshikawah@kwansei.ac.jp

Abstract

Organic cathode active materials for lithium-ion batteries (LIBs) have attracted considerable attention as viable alternatives to conventional cathode active materials based on rare element-containing transition metal oxides. Structural pores that efficiently intercalate Li^+ ions play an important role in a typical organic cathode active material in terms of battery performance. In this study, we investigated the correlation between packing structure and the charge/discharge properties of redox-active hexaazatriphenylene (HAT) derivatives composed of one-dimensional (1D) columnar structures. We synthesized 3,7,11-triethoxy-2,6,10-tricyano-1,4,5,8,9,12-hexaazatriphenylene (HATCNO₂), a single-component HAT derivative containing alternating electron-accepting nitrile ($-\text{CN}$) and electron donating ethoxy ($-\text{OC}_2\text{H}_5$) groups. Furthermore, HATCNO₂-poly, which was synthesized by the olefin metathesis of 3,7,11-tri(5-hexenyloxy)-2,6,10-tricyano-1,4,5,8,9,12-hexaazatriphenylene (HATCNO-hex) bearing 5-hexenyloxy side chains, exhibited improved structural stability. The testing of battery performance revealed that HATCNO₂ exhibits a fast charge/discharge performance ($353.5 \text{ mA h g}^{-1}$ at a current density of 500 mA g^{-1} in the first cycle) that originates from the rapid diffusion of Li^+ ions via the intercolumnar voids between its 1D columnar structures, whereas HATCNO₂-poly exhibits a slow charge/discharge performance ($188.5 \text{ mA h g}^{-1}$ at a current density of 500 mA g^{-1} in the first cycle) due to the absence of a 1D columnar structure and intercolumnar voids, thereby limiting any such diffusion process. This study provides clear structural insights into the design of organic-molecule-based cathode active material packing structures for LIBs.

Keywords: organic cathode materials, hexaazatriphenylene (HAT), one-dimensional (1D) columnar structures, lithium-ion batteries (LIBs)



ORGANIC SEMICONDUCTORS FOR OPTOELECTRONIC DEVICES AND OPTICAL SENSORS

Grazulevicius J.V

Department of Polymer Chemistry and Technology, Kaunas University of Technology, K. Barsausko g. 59,
51423 Kaunas, Lithuania

*Corresponding author: juozas.grazulevicius@ktu.lt

Abstract

Organic glass-forming semiconductors are used as emitters and hosts in OLEDs, as charge transporting materials (HTMs) in organic and hybrid solar cells. Organic emitters exhibiting long-living emission such as thermally activated delayed fluorescence or room-temperature phosphorescence (RTP) are widely studied as active materials of the sensors.

Compounds containing triphenylamine or 9-phenylcarbazole as donor moieties and pyrimidine-5-carbonitrile as electron-withdrawing unit were synthesized and studied [1]. Pure blue and greenish-blue fluorescent OLEDs with EQE reaching 7% and 6%, correspondingly, were obtained using the newly synthesized compounds as emitters. EQE of more than 20% and the operation time exceeding 20000 h were recorded for OLEDs with pyrimidine-5-carbonitriles as the hosts.

Sky-blue emitting derivatives of pyrimidine-5-carbonitrile and carbazole, tert-butylcarbazole or methoxy carbazole showed good performance both as emitters of OLEDs and as active materials of oxygen sensors [2]. Sky-blue OLED with EQE of 12.8% was fabricated using the newly synthesized emitter. The emitters were also used as oxygen probes.

Very sensitive probes for quantitative and organoleptic detection of oxygen based on conformer-induced RTP enhancement of the derivative of triazatruxene and phenothiazine were developed [3]. For 1% solid solution of the compound in Zeonex, the ratio of intensity of RTP observed under vacuum and fluorescence intensity recorded in air reached the value of 19.

Derivatives of dibenzothiophene with methoxyphenyl, trimethoxyphenyl, and carbazole moieties were synthesized as HTMs for perovskite solar cells (PSCs) [4]. Using the derivative of dibenzothiophene as HTM, power conversion efficiency (PCE) of 20.9% was achieved for additive-free PSC.

Indolo[3,2-b]carbazole-based HTMs also showed very good performance in dopant-free PSCs [5]. The devices demonstrated considerably higher stability and comparable efficiency as additives-containing reference PSCs with HTM spiro-OMeTAD.

Acknowledgment. This project has received funding from the Research Council of Lithuania (LMTLT), agreement No S-MIP-22-78

Keywords: organic semiconductor, organic light emitting diode, optical sensor of oxygen, perovskite solar cell.

References

1. Tsiko, U.; Volyniuk, D.; Andruleviciene V.; Leitonas, K.; Sych, G.; Bezikonny, O.; Jasinskas, V.; Gulbinas, V.; Stakhira, P.; Grazulevicius, J.V. *Mater. Today Chem.* 2022, 25, 100955.
2. Tsiko, U.; Bezikonny, O.; Sych, G.; Keruckiene, R.; Volyniuk, D.; Simokaitiene, J.; Danyliv, I.; Danyliv, Y.; Bucinskas, A.; Tan, X.F.; Grazulevicius, J.V. *J. Adv. Res.* 2021, 33, 41–51.
3. Skuodis, E.; Leitonas, K.; Panchenko, A.; Volyniuk, L.; Keruckiene, R.; Volyniuk, D.; Minaev, B.F.; Grazulevicius J.V. *Sens. Actuators B Chem.* 2022, 373, 132727.
4. Durgaryan, R.; Simokaitiene, J. Volyniuk, D.; Bezikonny, O.; Danyliv, Y.; Kim, B.J.; Woon, K.L.; Sini, G.; Boschloo, G.; Grazulevicius J.V. *Sol. RRL*, 2022, 6, 2200128.
5. Kim, Y.; Yang, B.W.; Suo, J.J.; Jatautiene, E.; Simokaitiene, J.; Durgaryan, R.; Volyniuk, D.; Hagfeldt, A.; Sini, G.; Grazulevicius, J.V. *Nano Energy* 2022, 101, 107618.

Anti-resonance stabilization for aromatic polybenzimidazoles superstable under extreme environments

**Tatsuo Kaneko^{a,b,*}, Xianzhu Zhong^b, Jiabei Zhou^b, Maiko Okajima^{a,b},
Mohammad Asif Ali^{a,b}**

^a School of Chemical and Material Engineering, Jiangnan University, China

^b Graduate School of Advanced Science and Technology, JAIST, Japan

*Corresponding author: tkaneko@jiangnan.edu.cn

Abstract

Conventional polybenzazoles showed ultrahigh thermoresistance among plastics owing to the aromatic π -conjugation along the polymer chain based on “resonance stabilization”. Polybenzimidazoles (PBI) showed the highest thermoresistance among these polymers, which was primarily attributed to interchain hydrogen bonding. However, we here proposed that extra effects of resonance stabilization from the monotonous aromatic repetition weakened hydrogen bonding, which was indicated by DFT calculations. For example, 10% mass-loss temperature, T_{d10} , of 2,5-PBI (poly(3,4-diaminobenzoic acid (DABA))) was 700 °C while T_{d10} for the copolymers of DABA and 4-aminobenzoic acid (4ABA) was 745 °C at a 4ABA composition of 15 % [1]. On the other hand, an excess amount of 4ABA remarkably decreased T_{d10} due to the intrinsic low thermostability of 4ABA homopolymer. A small amount of non-aromatic amide linkage cut the resonance continuity to enhance the interchain hydrogen bonding and thermostability, which is proposed as “anti-resonance stabilization”. The effects were investigated by changing the copolymer structures using polybenzoxazoles, polybenzthiazoles to show extremely high T_{d10} of 768 °C at maximum and flame retardancy (Fig) [2, 3]. Moreover, the films exhibited excellent insulating characteristics which can serve as strong substitutes for ceramic insulators for 6G wireless communication systems, efficient motors/turbines, etc.

Keywords: High-performance polymers, Imidazoles, Hydrogen bonding, Extreme circumstance

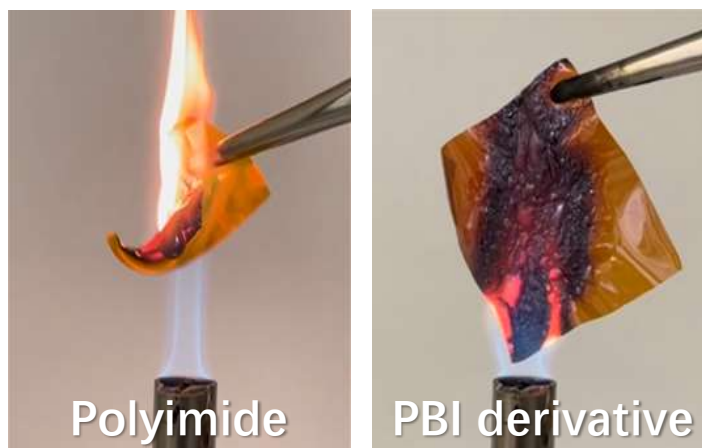


Fig. Flame-retardant test of PBI film stabilized by controlling resonance structures.

References

1. Nag, A. et al. *Adv.Sus.Sys.* 2020, 5:2000193
2. Zhong, X., et al., *Macromolecules*, 2024, 57, 356–363
3. Zhong, X., et al., *Macromolecules*, 2024, 57, 3328–3337

Crystal Structure and Property of Metal Endohedral [C₆₀] Fullerene

Eunsang Kwon^{a,*}, Rikizo Hatakeyama^b, Kazuhiko Kawachi^c, Yasuhiko Kasama^c,

^aResearch and Analytical Center for Giant Molecules, Graduate School of Science, Tohoku University, Sendai, Japan

^bNew Industry Creation Hatchery Center, Tohoku University, Japan

^cIdea International Co., Ltd., Sendai, Japan

*Corresponding author: ekwon@tohoku.ac.jp

Abstract

Since the synthesis and characterization of lithium cation endohedral metallofullerene (Li⁺@C₆₀, **1**),¹⁾ as the first metal endohedral C₆₀ fullerene, several investigations have explored its application in functional materials.²⁾ The essential structural feature of **1** is the presence of a lithium cation inside the spherical empty space of the C₆₀ fullerene. However, previous research faced limitations in obtaining detailed structural information on **1** due to the low electron density resulting from positional and dynamic disorder of the Li⁺.

In this study, we investigated the structure of **1** using powder neutron diffraction at low temperature (3.7 K).³⁾ The use of neutron diffraction allowed us to determine the precise structure of **1**. As shown in **Fig. a**), the nucleus of the Li⁺ was found to be closer to the inner wall of the fullerene cage than to the center. Additionally, we succeeded in synthesizing and isolating Na⁺@C₆₀ (**2**), the second example of the metal endohedral C₆₀ fullerene, and successfully elucidated its crystal structure using single-crystal X-ray crystallography (**Fig. b**)). Unlike in **1**, the encapsulated Na⁺ of **2** was positioned near the center of the fullerene.

Furthermore, we will introduce terahertz spectroscopy, solid-state NMR, and the energy storage characteristics of a capacitor with **1**.

Keywords: Endohedral Metallofullerene, Neutron Diffraction, Terahertz Spectroscopy, Energy Storage

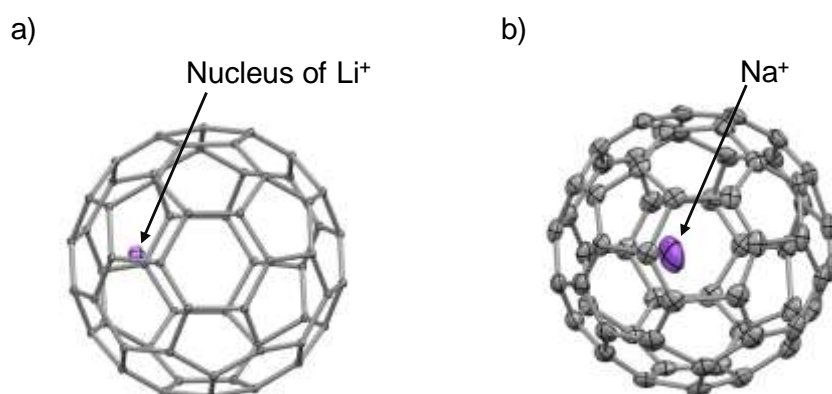


Fig. a) Molecular structure of Li⁺@C₆₀ determined by the neutron diffraction study at 3.7 K and **b)** ORTEP drawing of Na⁺@C₆₀ as determined by single-crystal X-ray diffraction analysis at 100 K (50% probability thermal ellipsoids).

References

1. Aoyagi, S. et al.; *Nature Chemistry*, 2012, 2, 678-683.
2. For recent reports, see: K. Ohkubo et al.; *Chem. Commun.*, 2013, 49, 7376-7378, K. Kokubo et al.; *Nanoscale*, 2013, 5, 2317-2321
3. E. Kwon et al.; *Chemical Physics Letters*, 2020, 801, 139678.

Solvent Dependence of Molecular Assembly Structures of Hexadecahydrotribenzo[12]annulene Derivatives with Alkylamide groups

Yotaro Kasahara^{a*}, Takashi Takeda^{a, b, c}, Shun Dekura^{a, b}, Atsuro Takai^d, Hayato Anetai^d, Ichiro Hisaki^e, Masayuki Takeuchi^d, Tomoyuki Akutagawa^{a, b}

^a Graduate School of Engineering, Tohoku University.

^b Institute of Multidisciplinary Research for Advanced Materials, Tohoku University.

^c Faculty of Science, Shinshu University.

^d National Institute for Materials Science

^e Graduate School of Engineering Science, Osaka University

*Corresponding author: yotaro@dc.tohoku.ac.jp

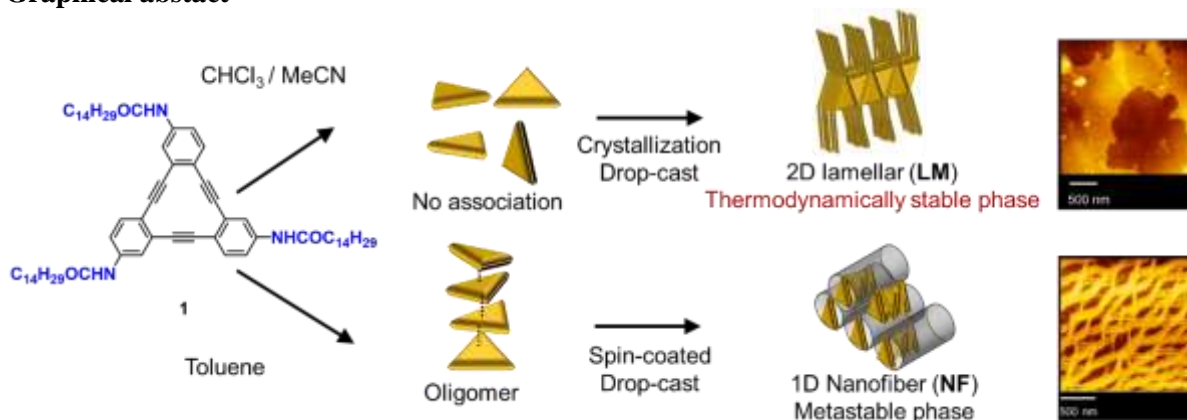
Abstract

In the organic material science, the molecular assembly structure is important factor to control the functions of materials even with the same molecule.¹ Few examples were reported to control the molecular assemblies, however, they utilized out-of-equilibrium conditions. Herein, to easier control of the molecular assembly structures, we designed the alkylamide-substituted hexadecahydrotribenzo[12]annulene ([12]DBA) derivative (**1**, in graphical abstract). [12]DBA is the planar molecule with triangular shape, which formed herringbone structure in single crystal.² The [12]DBA derivatives with various substituents formed different molecular assemblies such as crystal phase with dimer and glass.³ Alkylamide-substituted molecules formed supramolecular structures caused by intermolecular hydrogen bond of alkylamide units.⁴

Molecule **1** formed an organogel in toluene. AFM and PXRD measurements of the xerogel film from toluene revealed that the molecule **1** formed fibres with hexagonal columnar structure, which reticulately tangled each other. On the other hand, **1** formed crystalline powder from CHCl₃/MeCN without gelation, different from toluene. PXRD pattern of the crystalline powder and AFM of the cast film from CHCl₃/MeCN revealed that **1** formed 2D-sheets with lamellar structure. These results revealed that molecular assemblies of **1** exhibited significant solvent-dependence.

Keywords: Supramolecular Chemistry, Molecular Assembly, Dehydrobenzoannulene, Hydrogen-bond, Solvent-dependence

Graphical abstract



References

1. T. Fukui *et al.*, *Nat. Chem.* **2017**, 9, 493–499.
2. H. A. Staab, *et al.*, *Tetrahedron Lett.*, **1966**, 7, 751–757.
3. Y. Kasahara, *et al.*, *Chem. Commun.* **2021**, 57, 5374–5377.
4. Y. Matsunaga, *et al.*, *Mol. Cryst. Liq. Cryst.* **1986**, 141, 327–333.

Photo-induced water-dissolution of poly(ethylene terephthalate)s modified with pyrrolidone derivatives

Jixin Zheng^a, Keishin Yoshimitsu^b, Mohammad Asif Ali^{a,b*}, Maiko Okajima^{a,b}
Tatsuo Kaneko^{a,b*}

^a School of Chemical and Material Engineering, Jiangnan University

^b Graduate School of Advanced Science and Technology, JAIST

*tkaneko@jiangnan.edu.cn; asifali@jiangnan.edu.cn

Abstract

Poly(ethylene terephthalate) (PET), one of the most widely used plastics, has high mechanical properties and thermal tolerance but does not degrade in the natural environment¹. On the other hand, the conventional biodegradable polyesters are too degradable to use, and the polyesters durable during using but degradable after discarded and laid in environment are required in the sustainable future society. In the previous study, it was confirmed that itaconic acid (IA)-derived polyamides with pyrrolidone heterocycles were durable but became degradable by photo-irradiation using the artificial sun-light². Here we introduced the pyrrolidone ring to PET by polymer reactions with the amino acid monomer derived from IA and 1,10-diaminodecane (Scheme 1).

We obtained PET derivatives with the photo-induced water solubilization with the pyrrolidone ring which showed a photonic ring-opening reaction. PET was mixed with N-(10-aminodecyl)pyrrolidone-4-carboxylic acid, AC10A, which was derived by a reaction of itaconic acid and decamethylenediamine, and heated in the presence of catalysis. We confirmed AC10A incorporation into PET backbone by aminolysis and acidlysis by FT-IR and ¹H-NMR. The molecular weights of the resulting PET derivatives were increased by incorporation. The PET derivatives showed the solubility as low as PET and no decrease in heat tolerance. On the other hand, degradability was remarkably changed; PET derivatives showed a ultraviolet-induced disintegration in seawater by a test under ultraviolet irradiation to reproduce conditions similar to those found in marine.

Keywords: Poly(ethylene terephthalate), pyrrolidone, heterocycle, biodegradable, itaconic acid



Scheme 1. Syntheses of PET derivatives including pyrrolidone derived from 1, 10-diaminodecane.

References

1. Daubeny R P, et al. *Proceedings of the royal society of London. Series A. Mathematical and Physical Sciences*, 1954, 226, 531-542.
2. Ali M A, et al. *Macromolecules*, 2013, 46, 3719-3725.

High performance Nylon gels with pyrrolidone ring

Jie Liu ^a, Hayate Tomino ^b, Mohammad Asif Ali ^{a,b,*}, Maiko Okajima ^{a,b},
Tatsuo Kaneko ^{a,b,*}

^a School of Chemical and Material Engineering, Jiangnan University.

^b Graduate School of Advanced Science and Technology, JAIST.

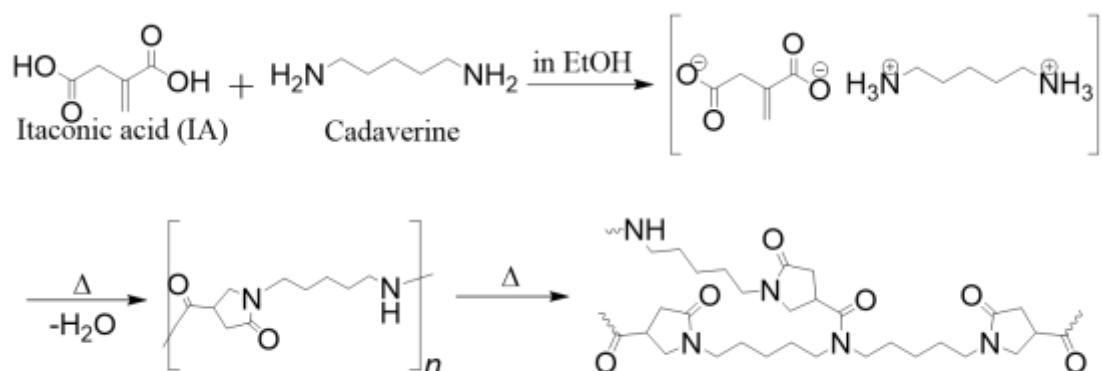
* asifali@jiangnan.edu.cn; tkaneko@jiangnan.edu.cn

Abstract

Itaconic acid is a microbial compound with two carboxyl groups and one vinyl group. It has been reported that a characteristic biopolyamide with pyrrolidone heterocycles in the main chain was synthesized by melt polycondensation from salt monomers of itaconic acid and diamines with great performance¹. Two amine end groups can connect through deamination reaction to form secondary amine which also can be reacted to form three-way branching. In this case, we propose the syntheses of cross-linked polyamides derived-from IA and cadaverine with the hydrophilicity to prepare hydrogels (Scheme 1).

Through ¹H-NMR and FT-IR measurement, we can confirm that the syntheses of polyamides from salt monomers of itaconic acid and cadaverine. As a result of polycondensation under different reaction conditions, the polyamides with the pyrrolidone rings cross-linked by annealing higher molecular weight prepolymers have a lower compression modulus about 65 kPa while those from the lower molecular weight prepolymers showed a higher modulus about 100 kPa. The higher number of the functional amino end groups are effective on inducing the higher cross-linking density and higher compression modulus. Moreover, the pyrrolidone ring of the preoligomers which can be used for hydrogelation can show photo-induced ring-opening reaction under UV-light inducing biodegradation². Furthermore, the BioNylon hydrogels have a great potential to be applied in the biomedical and agricultural fields.

Keywords: Polyamides, Hydrogels, High performance polymers, Heterocycles.



Scheme 1. Syntheses of cross-linking polyimides derived from itaconic acid and cadaverine

References

1. M. Ali, et al. *Macromolecules*, 2013, 46, 3719-3725;
2. M. Ali, et al. *Adv. Sus. Sys.* 2022, 6, 2270005.

Battery Performances of Organic Materials with One-dimensional Columnar Structures as Cathodes

Hirofumi Yoshikawa*

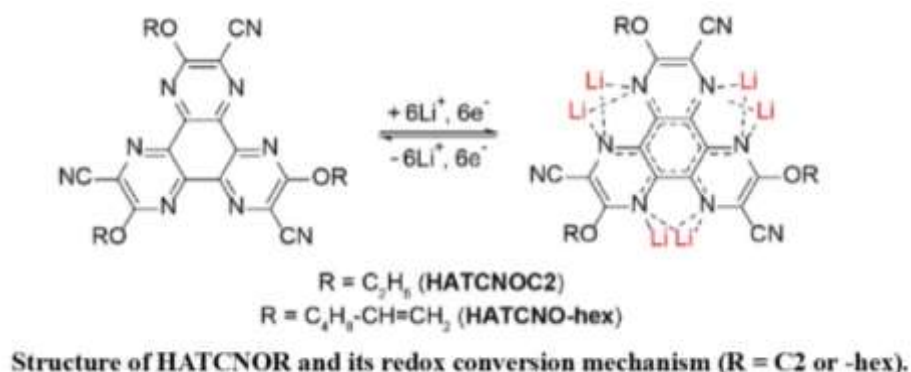
Department of Materials Science, Kwansei Gakuin University, Japan

*Corresponding author: yoshikawah@kwansei.ac.jp

Abstract

Organic cathode active materials for lithium-ion batteries (LIBs) have attracted considerable attention as viable alternatives to conventional cathode active materials based on rare element-containing transition metal oxides. Structural pores that efficiently intercalate Li^+ ions play an important role in a typical organic cathode active material in terms of battery performance. In this study, we investigated the correlation between packing structure and the charge/discharge properties of redox-active hexaazatriphenylene (HAT) derivatives composed of one-dimensional (1D) columnar structures. We synthesized 3,7,11-triethoxy-2,6,10-tricyano-1,4,5,8,9,12-hexaazatriphenylene (HATCNO_{C2}), a single-component HAT derivative containing alternating electron-accepting nitrile ($-\text{CN}$) and electron donating ethoxy ($-\text{OC}_2\text{H}_5$) groups. Furthermore, HATCNO_{C2}-poly, which was synthesized by the olefin metathesis of 3,7,11-tri(5-hexenyloxy)-2,6,10-tricyano-1,4,5,8,9,12-hexaazatriphenylene (HATCNO-hex) bearing 5-hexenyloxy side chains, exhibited improved structural stability. The testing of battery performance revealed that HATCNO_{C2} exhibits a fast charge/discharge performance ($353.5 \text{ mA h g}^{-1}$ at a current density of 500 mA g^{-1} in the first cycle) that originates from the rapid diffusion of Li^+ ions via the intercolumnar voids between its 1D columnar structures, whereas HATCNO_{C2}-poly exhibits a slow charge/discharge performance ($188.5 \text{ mA h g}^{-1}$ at a current density of 500 mA g^{-1} in the first cycle) due to the absence of a 1D columnar structure and intercolumnar voids, thereby limiting any such diffusion process. This study provides clear structural insights into the design of organic-molecule-based cathode active material packing structures for LIBs.

Keywords: organic cathode materials, hexaazatriphenylene (HAT), one-dimensional (1D) columnar structures, lithium-ion batteries (LIBs)



High-performance, water-soluble biopolyimides from aminocinnamoyl photodimers

**Boxin Zhou¹, Phruetchika Suvannasara², Sumant Dwivedi², Maiko Okajima^{1,2},
Mohammad Asif Ali^{1,2}, Tatsuo Kaneko^{1,2*}**

¹ School of Chemical and Material Engineering, Jiangnan University

² Graduate School of Advanced Science and Technology, JAIST

**Corresponding author: *tkaneko@jiangnan.edu.cn*

Abstract

Bio-based polymers are renewable and environmentally friendly, and their degraded compounds can be harmless. [1] The development of high-performance bio-based polymers, such as polyimides (PIs), is strongly demanded for a sustainable society. [2] Here the synthesis of PI based on renewable resources was carried out. The photodimer of 4-aminocinnamic acid (4ATA) which was derived from fermentation was used as bio-derived aromatic diamine and polycondensed with CBDA is also bioderived as fumarate photodimer, to give PI via poly(amic acid) precursors. The carboxyl side chains of the PI were ionized by potassium hydroxide to be water-soluble. By casting over the aqueous solution, an optically transparent film with extremely high clarity is obtained. This film exhibits a high T_{d10} value of up to 366 °C. Additionally, the fabricated polyimide film possesses superior ductility. A simple post-treatment with weak acid or multivalent metal ions such as calcium and aluminum can render the film back to insoluble in water. The reversible water-solubility is important to apply in actual society.

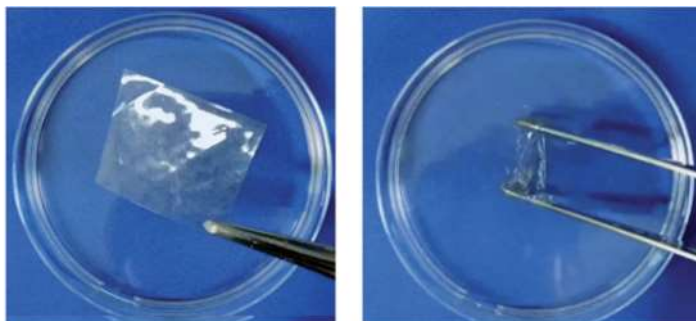


Fig. Water-solubilization of the polyimide film derived from 4,40-diamino-truxillate potassium salts. Left: transparent polyimide film, right: polyimides immersed in water.

Keywords: Biobased polymers, High-performance, polymers, Water-soluble polymers, Polyimides

References

1. P. Suvannasara. et al. Biobased Polyimides from 4-Aminocinnamic Acid Photodimer, *Macromolecules*, 2014, 47:1586–1593.
2. S. Dwivedi, et al. Molecular Design of Soluble Biopolyimide with High Rigidity, *Polymers*, 2018, 10:368.



INTERNATIONAL UNION OF
PURE AND APPLIED CHEMISTRY



MACRO 2026

51st IUPAC World Polymer Congress









5-9 July 2026

Kuching, Sarawak, Malaysia

<https://macro2026.org>



Scientific Sessions

- 1 Advances in Polymer Synthesis 
- 2 Polymer Physics & Polymer Characterisation 
- 3 Advances & Green Polymer Processing 
- 4 Advanced Functional Polymeric Materials & Membranes 
- 5 Biological, Biomedical & Environmental-friendly Polymers 
- 6 Polymeric Materials for Clean & Sustainable Energy 
- 7 Elastomers & Latexes 
- 8 Durability & Performance 

Supported by

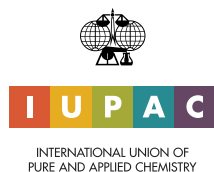


Venue



FIRST ANNOUNCEMENT

Under the Auspices of



Organised by



Co-organised by



Supported by



Meet in
Malaysia
BE Greater, Together.

Malaysia
Truly Asia

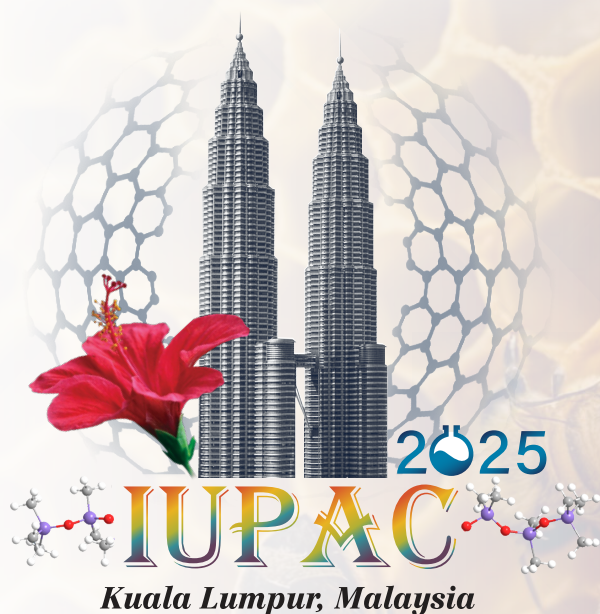
IUPAC2025

53rd IUPAC General Assembly (53GA)
12th - 15th July 2025

50th World Chemistry Congress (50WCC)
14th - 19th July 2025

Venue: Kuala Lumpur Convention Centre, Malaysia

Website: iupac2025.org



Chemistry for Sustainable Future